MCL-630/V

TRANSLATION

THEORY OF LIQUID-PROPELLANT ROCKET ENGINES

By A. V. Kvasnikov

Part I of II, Chapters I through IV, pages 1 through 274

October 1960

607 Pages

AD648037
TT61-19313

ACCESSION for
CFSTI WHITE SECTION
DDC BUFF SECTION
UNANNOUNCED
JUSTIFICATION
BY
DISTRIBUTION/AVAILABILITY
DIST. AVAIL.

DDC
RECEIVED
MAR 13 1967
B

PREPARED BY
LIAISON OFFICE
TECHNICAL INFORMATION CENTER
MCLTD
WRIGHT-PATTERSON AIR FORCE BASE, OHIO

ARCHIVE COPY

This translation was prepared under the auspices of the Liaison Office, Technical Information Center, Wright-Patterson AFB, Ohio. The fact of translation does not guarantee editorial accuracy, nor does it indicate USAF approval or disapproval of the material translated.

Comments pertaining to this translation should be addressed to:

Liaison Office
Technical Information Center
MCLTD
Wright-Patterson Air Force Base, Ohio

A. V. Kvasnikov

TEORIYA ZHIDKOSTNYKH RAKETNYKH DVIGATELEY

UAST' PERVAYA

Dopushcheno Ministerstvom Vysshego Obrazovaniya SSSR v Kachestve Uchebnogo Posobiya dlya Sodostroitel'nykh, Mashinostroitel'nykh i Aviatsionnykh Vuzov

GOSUDARSTVENNOE SOUIZNOYE IZDATEL'STVO SODOSTROITEL'NOI PROMYSHLENNOSTI
Leningrad, 1959
541 pages

MCL-630/V

THEORY OF LIQUID-PROPELLANT ROCKET ENGINES

by

Professor A.V.Kvasnikov

Part One

Approved by Ministry of Higher Education USSR
as a Textbook for Higher Educational Institutes
of Shipbuilding, Machine-Building, and Aviation

Sudprom

Giz

State Union Publishing House for the Shipbuilding Industry

Leningrad 1959

MCL-630/V

This book gives the principles of the theory of liquid-propellant rocket engines, compares them with other types of heat engines, and discusses their possible fields of application. Special reference is made to the working process in the combustion chamber and to its characteristics, as well as to the theory of chambers of liquid-propellant rocket engines with complex cycles.

The factual material and figures have been taken from unclassified USSR and foreign literature.

The author presents systems of coefficients to evaluate the internal losses in the chamber of the liquid-propellant rocket engine and of coefficients for evaluating such engines as thrust engines.

This book is intended as a text for students of higher educational aviation institutes who are specializing in rocket engines; it will also be of interest for engineers in the field of rocket engineering.

PREFACE

The rocket engine, which is a new type of heat engine, is a machine in which the engine itself is merged with the working machine (slave unit) in the design and working process. In operation, such an engine is not considered a device to do work, i.e., produce useful mechanical energy, but as a device to provide a power impulse, i.e., as a thrust engine.

The liquid-propellant rocket engine differs fundamentally from reaction engines operating in a medium, for example from the conventional air-breathing jet engine, in that it produces thrust by ejection of its own mass, thus creating the conditions for transportation outside the atmosphere.

This book is an exposition of the first part of the course, the theory of liquid-propellant rocket engines (LRE), and is based on the course of the working process of liquid-propellant rocket engines. Such important subjects as mixture formation, cooling, and stability of the process will be taken up in the second part of the course.

The students taking this course must be versed in thermodynamics, gas dynamics, and the theory of heat transfer, to the extent prescribed in the syllabi of university-grade technical schools of power engineering.

L.L.Klochkova, Senior Instructor of the Department at the Moscow Aviation Institute, had an important part in the preparation of this book, and the author expresses profound gratitude to her. She made the calculations, collected the reference materials, and worked directly on the basic content of the book, especially on

the Chapter "Thermodynamic Calculation of Liquid Rocket Engines".

The author is also grateful to Engineer V.V.Kuznetsov, who performed a considerable part of the calculations and handled the graphic layout of the book, as well as to Laboratory Assistant R.I.Gurevich and other members of the department.

ABBREVIATIONS AND PRINCIPAL SYMBOLS USED

Abbreviations

RE - Rocket engine

RE - p = c - Rocket engine operating at constant pressure

RE - V = c - Rocket engine operating at constant volume

LRE - Liquid-propellant rocket engine

GTE - Gas-turbine engine

TJE - Turbojet engine

TPE - Turboprop engine

RJE - Ramjet engine

PD - Piston engine

PA - Pneumatic accumulator

HA - Hydraulic accumulator

PPA - Powder pressure accumulator

GGG(GG) - Gas generator

SGG - Steam-gas generator

TPA - Turbo-pump unit

PVEDA - Electric double-action pneumatic valve

Principal Notation

P, P_t - Thrust; theoretical thrust

P_i, P_e, P_x, P_W, P_{st} - Following thrust components: internal, external, axial, dynamic, static

P_{sp}, $P_{sp\ t}$ - Specific thrust; theoretical specific thrust

$P_{sp\ i}$, $P_{sp\ e}$, $P_{sp\ W}$, $P_{sp\ st}$ - Following specific thrust components: internal, external, dynamic, static

V_{max}, V_o, V_{esc} - Rocket velocity at end of boost phase; at beginning of flight; necessary for escape of rocket from earth

V, V_h - Volume of chamber, working volume of chamber

v - Specific volume

v_k, v_{cr}, v_a, $v_{k\ o}$, $\bar{v}$ - Specific volumes respectively: of chamber; at critical cross section; at nozzle section; in chamber of RE - V = c at initial time; relative specific volume

γ, γ_p - Specific gravity; specific gravity of propellant

γ_k, γ_{cr}, γ_a, γ_{at} - Specific weight of gas as follows: in chamber; at critical cross section; at nozzle section; theoretical at nozzle section

p - Pressure

p_k, $p_{k\ t}$, p_{cr}, $p_{cr\ t}$, p_a, $p_{a\ t}$, $p_{k\ 1}$, $p_{k\ o}$, p_{ex}, $\bar{p}$, p_i - Pressure in chamber; theoretical pressure in chamber; pressure at critical cross section; at theoretical critical cross section; at nozzle section; at theoretical nozzle section; at initial cross section of velocity chamber; in chamber of RE - V = c at initial time; external pressure; relative pressure; partial pressure of ith gas in mixture.

T - Temperature, °K

T_k, $T_{k\ t}$, T_{cr}, T_a, $T_{a\ t}$, $T_{k\ 1}$, $T_{k\ o}$, T_h, T_{sg}, $\bar{T}$, T^*, $\bar{T}^*$ - Temperature as follows: in chamber; theoretical in chamber; at critical cross section; at nozzle section; theoretical at nozzle section; at initial cross section of velocity chamber; in chamber of RE - V = c at initial time; at head; in steam-gas generator; relative temperature; throttling temperature; relative throttling temperature

t - Temperature, °C

W - Velocity

W_k, W_{cr}, W_a, $W_{a\,t}$, $\bar{W}$ - Velocity of gas: in chamber; at critical cross section; at nozzle section; theoretical at nozzle section; relative velocity

a - Velocity of sound

a_k, a_{cr}, a_a Velocity of sound: in chamber; at critical cross section; at nozzle section

L - Specific work

L_{ad}, L_{iso}, L_n, L_{id}, L_i, L_e, $\bar{L}$ - Specific work: adiabatic; isothermal; polytropic; ideal (without losses); internal; effective; relative

L_{co}, L_R, L_{aft} - Work of cycle in presence of cooling; work of regenerative cycle; work afterburning

I, I_t - Total enthalpy; thermal enthalpy

I_o, I_f, I_p - Enthalpy: of oxidizer; fuel; propellant

I_k, $I_{k\,t}$, I_a, $I_{a\,t}$, I_i - Total enthalpy of gas: in chamber; theoretical in chamber; at nozzle section; theoretical at nozzle section; of i^{th} gas in mixture

S - Entropy

S_k, S_a, S_i - Entropy: in chamber; at nozzle section; of i^{th} gas in mixture

S_1 - Force of air resistance

S_ℓ - Length of arc of profile

C_p, C_v, C_n - Heat capacity of gas; at constant pressure; at constant volume; in polytropic process

$C_{p\,liq}$ - Heat capacity of liquid

C_x - Coefficient of drag

C_{sp} - Specific propellant consumption

Q_k, Q_n, Q_p, Q_v, $\bar{Q}$ - Quantity of heat imparted to gas: in chamber; during polytropic process; at constant pressure; at constant volume; relative

Q_{chem}, Q_ε, Q_β, Q_{fo} - Thermal energy: chemical; of dissociation; of ionization; of formation of substance

Q_{co}, Q_c, Q_h, Q_R - Losses of heat in cooling; in nozzle by cooling; in head by cooling; heat of regeneration

U - Internal energy of gas

U_k, U_a, U_c - Internal energy: of gas in chamber; of gas at nozzle section; of volume of gas enclosed in nozzle duct

G, G_t - Weight flow rate per second; theoretical weight flow rate per second

G_o, G_f, G_p - Weight flow rate per second: of oxidizer; of fuel; of propellant

g - Acceleration of gravity

g_i - Proportion by weight of i^{th} gas in mixture

r_i - Proportion by volume of i^{th} gas in mixture

r - Heat of evaporation

N_e, N_T - Power: effective and thrust

η - Efficiency

η_t, η_{ad}, η_i, $\eta_{o\ i}$, η_e, η_m, η_{To}, η_{fl} - Efficiency: thermal; adiabatic; internal; relative internal; effective; mechanical; thrust; flight

η_k, η_T, η_c, η_{feed}, η_y - Efficiency: total of chamber; internal of chamber; hydraulic of nozzle; of feed system; of power plant

η_{co}, η_R - Efficiency: of cycle with cooling; of regenerative cycle

ψ_c, ψ_{tot}, ψ_T, ψ_{c_i}, ψ_{c_e}, $\bar{\psi}_{tot}$, $\bar{\psi}_T$ - Indices: force; total; thrust; internal force; effective force; mean total on boost phase; mean thrust on boost phase.

$\psi_{c\ 1}$, ψ_{bo}, ψ_e, ψ_a - Coefficients of velocity (hydraulic) of nozzle; of burnout in nozzle; of external thrust; of losses due to nonparallel jets

φ_T, φ_c, φ_{tot} - Thrust coefficient of chamber; internal nozzle coefficient; relative total force factor

ζ - Experimental coefficient defining conditions of entry of shock wave into nozzle

ζ_p, ζ_g, ζ_{sp}, ζ_{abs} - Coefficients of completeness: of pressure; of flow; of specific thrust; of absolute thrust

F_k, F_{cr}, F_a - Cross-sectional areas: of chamber; of critical section; of nozzle section

$f = \frac{F}{G}$ - Specific cross-sectional area

f_k, $f_{k\,t}$, f_{cr}, $f_{cr\,t}$, f_a, $f_{a\,t}$, $\bar{f}$ - Specific cross-sectional area: of chamber; theoretical of chamber; critical section; theoretical critical section; section of nozzle; theoretical section of nozzle; relative

D_k, D_{cr}, D_a, $\bar{D}$ - Cross-sectional diameter: of chamber; of critical section; of nozzle section; relative

l, $\bar{l}$ - Length of duct; relative length of duct

R - Gas constant

R_k, R_{cr}, R_a, R_i - Gas constant: in chamber; in critical section; at nozzle section; of i^{th} gas in mixture

H - Altitude

H_I, H_{II}, H_p - Altitude of powered ascent; altitude of upward drift by momentum; design altitude

H_u - Heat value of propellant

$M = \frac{W}{a}$ - Mach number

M_k, M_{cr}, M_a - Mach number: in chamber; at critical section; at nozzle section

K_p, K_r - Chemical equilibrium constants: with respect to pressure; with respect to molar fraction

k - Adiabatic constant

n - Mean adiabatic constant or polytropic exponent

n_i - Number of moles of i^{th} gas in mixture

μ - Mass ratio of rocket

λ - Velocity coefficient

λ_k, λ_{cr}, λ_a - Velocity coefficient: in chamber; at critical cross section; at nozzle section

δ_k, δ_c, δ_e, $\delta_{e\,o}$ - Expansion ratio of gas: in chamber; in nozzle; in engine; in engine with V = c at initial time

δ - Wall thickness

α - Coefficient of excess oxidizer

α_1 - Coefficient of conversion of heat into kinetic energy

β - Deviation from design conditions

β_o - Degree of ionization of gas

ε - Degree of dissociation of gas

$\varkappa$ - Component ratio

$\varkappa_o$, $\varkappa_t$, $\varkappa_k$ - Component ratio: stoichiometric; in tank; in chamber

ν - Degree of nonequilibrium of process

j, j_{H_2O}, j_{feed} - Relative flow rate: of gas; of water; of working fluid in feed system

j_1 - Acceleration of rocket

ρ - Density

τ - Time

τ_z - Thermial

τ_W - Friction stress

q - Heat of solution

q_{f_k} - Thermal stress in chamber volume

σ_i - Concentration of i^{th} component

σ_1 - Stress at rupture

Ω - Rate of displacement of one system relative to the other

w - Humidity

CHAPTER I

CONDITIONS OF UTILIZATION OF ROCKET ENGINES

Section 1. Operating Principle of Rocket Engine

Modern engines are divided according to type of service into two main groups, stationary and mobile. Mobile engines are many times as powerful as stationary engines.

The source of motion in engines of any kind is the energy of the working fluid in its initial state, whose conversion process must be controlled.

In mobile engines, the working fluid in its initial state must possess high energy per unit weight; suitable energy carriers are chemical fuels whose energy is more concentrated than that of other substances, and in which it is easy to induce and regulate conversion of that energy. Owing to this fact, almost all mobile engines are chemical heat engines.

Means have recently been discovered to utilize a form of energy of matter that is still more complicated: nuclear energy.

There can be no doubt that mobile engines of the near future will use nuclear energy.

For the time being, the nuclear engine can be used only to produce thrust beyond the atmosphere, since only under these conditions can the products of nuclear reaction, ejected from the engine, be prevented from contaminating inhabited areas. The prospects for the use of nuclear energy in rockets are very favorable.

Figure 1 is a schematic diagram of the combustion chamber of a rocket engine. Until start of the combustion reaction, the working mass remains in the liquid or solid state. In the former case, the fluid is continuously fed to the chamber

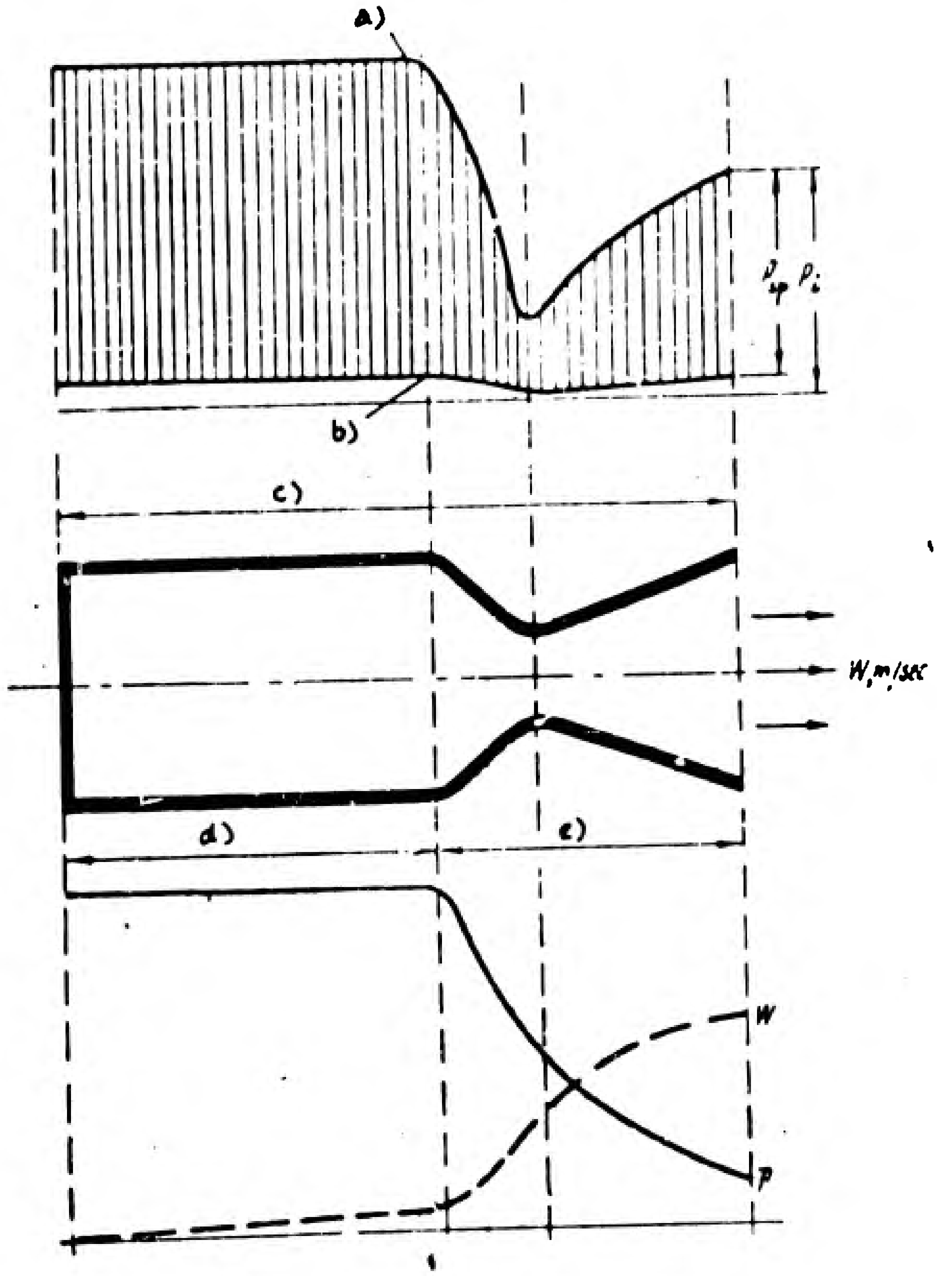

Fig.1 - Diagram of Combustion Chamber of Rocket Engine

a) Internal thrust component; b) External thrust component; c) Rocket engine chamber; d) Combustion chamber; e) Exhaust nozzle

where, as a result of combustion, it is converted into a gas at high temperature and pressure.

From the combustion chamber the gas flows to the duct of the exhaust nozzle, where it expands and gains in velocity. Generation of the highest possible exhaust velocity is the basic object of all the processes taking place in the chamber of a rocket engine.

The inner side of the chamber shell and exhaust nozzle absorbs the pressure of the gas. The axial component of the forces acting from the gas side on the chamber walls constitutes the so-called internal thrust; on combining with the forces acting on the outer walls of the chamber, this forms the total thrust, or engine thrust.

The thrust may also be determined on the basis of the law of conservation of momentum of the masses composing the power plant.

When the gas expands in the exhaust nozzle to exactly the ambient pressure, the engine thrust per 1 kg/sec gas flow rate, i.e., the specific thrust, will be

$$P_{sp} = \frac{W_a}{g}.$$

It is well known that the efficiency of an engine as an energy source is defined by its power. Power is a universal parameter permitting a direct correlation between a given engine and the working machine it is intended to actuate.

Transportation means such as automobiles, aircraft, ships, etc. require thrust. The source of thrust is a thrust unit, which consists of the engine as the source of motion together with a device to produce thrust power. On an aircraft, the propeller serves as such a device; on an automobile, this function is taken over by the wheel together with the transmission from the engine, etc.

It is more convenient to measure the efficiency of a thrust cylinder in units of power, i.e., of the magnitude of the thrust. In all rocket engines, the magnitude of the thrust obtained is determined by the character of the working process.

A rocket engine represents, at the same time, a device to produce thrust. Consequently, such an engine may be termed a thrust machine, and there is no need to determine its energetic power, since the thrust necessary for operation is known. For this reason, the power efficiencies or other constants which do not define the work losses but the thrust losses should be the basis for evaluating the economy of thrust engines.

Section 2. Fields of Application of Rocket Engines

It is not only to produce thrust that the process taking place in the chamber shown in Fig.1 is necessary. A high velocity gas flow may also be required under stationary conditions, and therefore the processes taking place in a rocket engine may be utilized to generate the thrust itself as well as to produce a high-velocity gas flow. A high-velocity flow is used in wind tunnels for model tests, in installations for investigating processes of heat transfer, heat protection and other thermal phenomena taking place on the surface of bodies around which a hot flow passes, in studying the processes of energy exchange between two gas flows in jet compressors, ejectors, and hydro-gas apparatus, and in many other cases.

The vehicles in which a rocket thrust machine is installed are conventionally divided into two main groups, those with stationary motion and those with accelerated motion. Aircraft belong to the former class, rockets to the latter.

Under steady (uniform) flight conditions of an aircraft, the thrust is exactly balanced by the resistance of the air.

The flight of a rocket during the engine operation is characterized by accelerated motion. The thrust work is expended to a lesser degree in overcoming ambient resistance, and to a greater degree in imparting kinetic energy to the mass of the rocket.

So long as the engine is operating, the rocket will accelerate and climb, during which time kinetic and potential energies accumulate. After burnout, the rocket becomes a body in free flight, and its mechanical energy is now expended in overcoming the resistance of the ambient medium.

The boost phase of the flight, i.e., the phase during which the engine operates, usually occupies only a small part of the total path of the rocket. On this portion

Table 1

Vehicles Served by Rocket Engines

Type of Vehicle	Purpose of Vehicle
Rockets for Peaceful Purposes	For flights in the atmosphere layer near the ground (usually powder rockets) - signal, illuminating, firework, rescue, postal.
	For scientific research - altitude, high speed, meteorological, etc: a) to study the structure of the atmosphere, cosmic radiation, motion in a vacuum, physical phenomena beyond the atmospheric shell, and biological processes; b) for photosurveys of the earth's surface
	Passenger and cargo winged and wingless rockets for long-range flights
	Takeoff assists for heavy and long-range rockets for launching and passage through the dense layers of the atmosphere
Military Rockets	Long-range rockets (surface-to-surface) for bombardment of distant ground targets
	Rocket mines for bombarding close-in targets
	Antiaircraft rockets (surface-to-air, air-to-surface), unguided and guided
	Aviation rockets (air-to-surface, air-to-air) unguided and guided, winged and simple
	Torpedo rockets (air-to-underwater, underwater-to-underwater, underwater-to-air) for aircraft, ships, and submarines
	Hand rockets and close-combat weapons as weapons for individual use
Aircraft	Rato units to facilitate the takeoff of heavy aircraft and ramjet aircraft
	Flight accelerators for accelerating an aircraft during a maneuver
	Self-contained engines for fighters, helicopters, etc.
Space Rockets	Short-range space rockets for placing artificial earth satellites into orbit for communication
	Interplanetary rockets for long-range space flights and flights between satellite orbits

the engine thrust is balanced, on the whole, by the inertial forces of the rocket mass rather than by the resistance of the ambient medium.

Today a rocket engine operates only during the boost phase of the path. After the process of re-entry has been mastered, conditions of hovering and of braking a rocket with operative engine will become acute.

Table 1 gives several designations of flight vehicles for various purposes, with rocket engines.

Section 3. Aircraft Installations

1. Boosters

The aircraft is a vehicle type for steady aerial flight, with entirely definite operating conditions of flight, with acceleration (in takeoff and in landing), cruising flight, maneuvers, and landing. Each of these four flight conditions makes its own demands on the power plant.

In the overwhelming majority of cases, takeoff is accomplished after the aircraft has made a takeoff run on the ground or on water. The shorter the takeoff run, the safer the takeoff. To decrease the required length of runway, an aircraft makes its takeoff run at maximum engine power. But even when this procedure is used, the takeoff of heavy aircraft still involves great difficulties; sometimes takeoff strips over 2 km in length are needed. Such aircraft take off somewhat more easily when equipped with takeoff assists or booster engines, operating only during the takeoff run, in addition to the main engines. A booster must be simple, cheap, develop a high thrust, and separate freely from the aircraft at the end of the takeoff run. These requirements are satisfied by powder rocket motors and by certain types of liquid rocket engines.

Additional boosters with high thrust are absolutely necessary to launch vehicles with a ramjet engine.

The action of takeoff assists (Fig.2) is sometimes combined with catapulting.

In such cases the large thrust of the booster is applied for only a short period of time.

The thrust of booster rockets varies over a wide range, from hundreds of kilo-

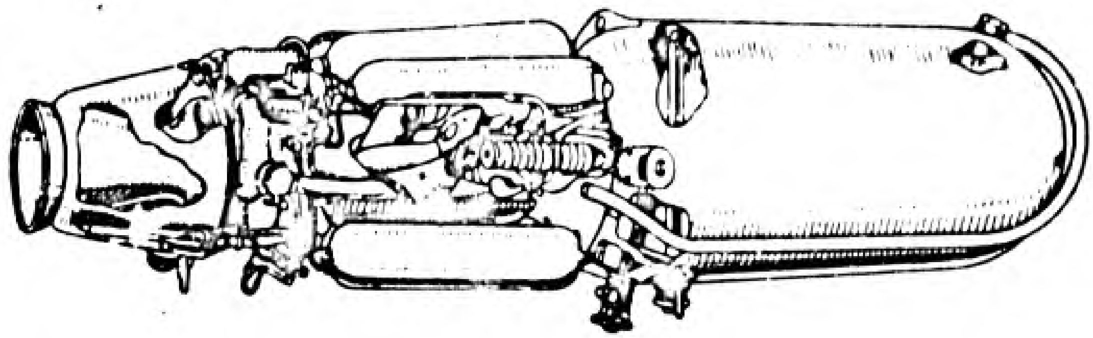

Fig.2 - General View of Takeoff Assist

grams to 20 tons, and the operating time from fractions of a second to 100 sec. The total impulse may reach 50,000 kg-sec.

Figure 3 shows the characteristic of a booster using hydrogen peroxide.

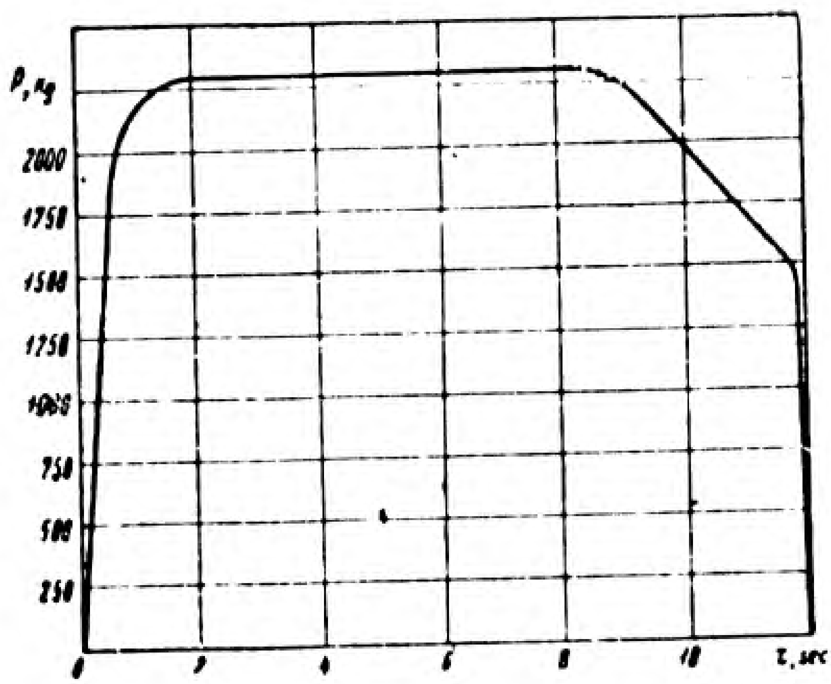

Fig.3 - Characteristic of Takeoff Assist

Takeoff assists must meet the following requirements:

1) Reliable operation and constant value of impulse even after prolonged 'storage;

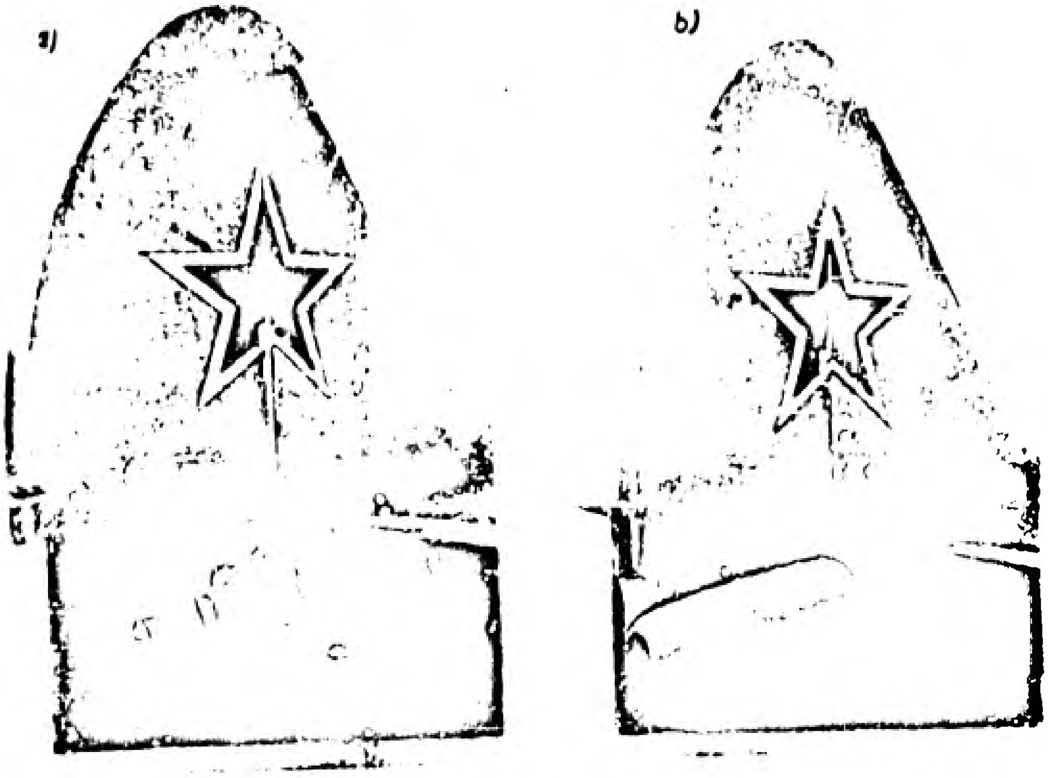

Fig.4 - Flight Booster RD-1KhZ:

a - With cowling removed; b - With cowling on

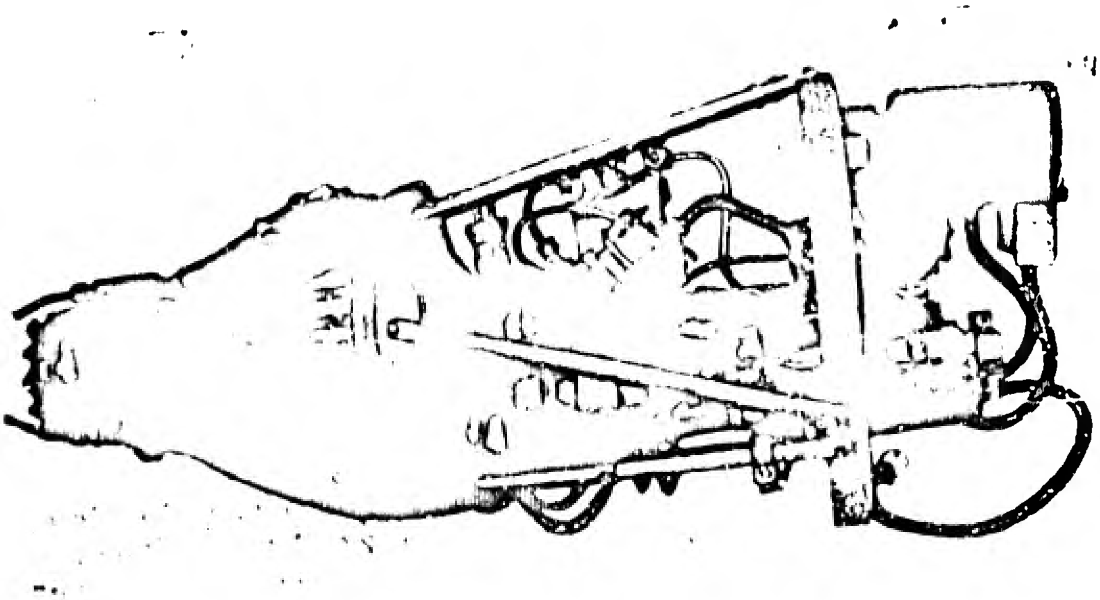

Fig.5 - General View of RD-1 Booster

2) Low cost;

3) Simple design and simple service at the airfield;

4) Maximum specific impulse (per unit dry weight of booster);

5) Rapidity and reliability of starting;

6) Maximum endurance after launching.

Flight boosters are designed to increase the power of the main aircraft engines in stunting and whenever a landing plan must be abandoned when already close to the ground. Since flight boosters are permanently installed on the aircraft, their size and thrust are appreciably less than those of takeoff assists.

Flight boosters must meet high requirements with respect to weight, dimensions, reliability of repeated starts, and safety of shutdown.

As an example, Fig.4 shows the RD-1KhZ flight booster installed in the tail section of the 120R aircraft. Figure 5 is an overall view of the RD-1 booster installed on a Pe-2 aircraft.

The use of rocket engines as boosters in air transportation is of great practical importance. In normal aircraft flight, such rocket boosters are considerably more economical than jet engines, and consume only a small fraction of the total working substance.

2. Self-Contained Rocket Engines

The steady flight of an aircraft is ensured by the main aircraft engine. If a rocket engine is used as the main engine, it is called self-contained.

Bearing in mind the operating conditions of an aircraft, its design, as well as the need for flight economy, safety, and convenience of the passengers, the engine must meet the following requirements:

1) Engine thrust between 300 kg and 10 tons, or more;

2) Low specific weight per unit thrust;

3) Small frontal area, i.e., small cross-sectional dimensions;

4) Complete uniformity of thrust and absence of vibration;

5) Low specific fuel consumption, i.e., high specific thrust;

6) Good pickup, i.e., rapid transition to high-thrust conditions;

7) Possibility of regulating the thrust over a wide range, from 0.1 up to normal;

8) Possibility of brief forcing of thrust during takeoff and under other aircraft operating conditions;

9) Reliable and repeated starting under conditions of change of altitude and ambient temperature;

10) Sufficiently long life;

11) Reliable operation in maneuvers;

12) Fire and explosion safety;

13) Reliable protection from injurious or toxic working fluids;

14) Altitude control of thrust.

Depending on the purpose of the aircraft, not all of these requirements must be satisfied to the same extent, the more so since some of them are mutually exclusive. In each specific case, it is necessary to establish the most important requirements and, after satisfying them to the maximum possible degree, meet average standards for the others.

An aircraft power plant must meet the following additional requirements:

1) Low vulnerability if hit by bullets or fragments;

2) Maximum concealment, electrical, optical, and acoustic;

3) Design permitting mass production of the engine;

4) Design consistent with rapid engine repair and engine unit replacement under operating conditions;

5) Minimum use of high-priority materials in engine production and operation.

The use of rocket aircraft in the dense layers of the atmosphere is justified only in special cases usually connected with a combat mission.

The practical limit of use of air-breathing aircraft engines may be considered an altitude of 20 - 30 km. Rocket engines or rocket motors must be used for flights

Fig.6 - Self-Contained Three-Chamber Engine

at greater altitudes. Consequently, self-contained rocket engines are designed for aircraft for flights at very high altitudes.

Figure 6 gives an overall view of a self-contained three-chamber aircraft engine. Its characteristics in brief are: sea-level thrust, 900 kg; propellant, nitric acid and kerosene; fuel feed system, turbo-pump.

Section 4. Rockets and their Characteristics

1. Classification of Rockets and Basis for General Engine Specifications

We have already mentioned the classification of rockets in accordance with practical uses (Table 1). The ultimate purpose of a rocket flight is to reach a certain altitude above sea level. to transport cargo from one point of the earth's surface to another, or to develop a specified velocity. Accordingly, three groups of rockets may be considered: altitude, long-range, and high-speed.

In a specific assignment, the above three tasks are combined into a definite flight program, but one of them is always the major element.

If the fields of resistance, dimensions of the rocket, and engine characteristics are known, then the ultimate flight parameters, i.e., the altitude, range, or speed, are determined by calculation. If, however, the principal parameter is specified in advance, the requirements for the rocket and engine are found by calculation.

The principal requirements that an engine must meet may be formulated for some typical flight variant, for example rocket travel in free space. In this case, the figure of merit of engine operation will be the rate of acceleration of the rocket V_{max} developed by the instant engine operation ceases.

The requirements for an engine in connection with the need for obtaining V_{max} are the same, or almost the same, as the requirements that ensure the optimum result of the flight as a whole.

The conditions for obtaining V_{max} were formulated as long ago as 1897 by Professor I.V.Meshcherskiy, and in 1903 by K.E.Tsiolkovskiy.

Let $\mu = \frac{M_0}{M_k}$ be the mass ratio of the rocket.

Obviously,

$$M_0 = M_k + M_T \text{ and } dM = dM_T.$$

Considering the motion of the gas with respect to the chamber, let us write an equation showing the change in momentum of the gas to be equal to the impulse of the forces of interaction between gas and chamber walls (assuming the exhaust velocity to be constant):

$$P\,d\tau = -W_a\,dM_T,$$

whence

$$P = -W_a \frac{dM}{d\tau} = -W_a m_{sec}. \tag{1}$$

If the weight rate of propellant flow is 1 kg/sec, the specific thrust, i.e., the force exerted by the gas on the chamber walls will be

$$P_{sp} = \frac{W_a}{g}. \tag{2}$$

The direction of P_{sp} is opposite that of the force P defined by eq.(1). It will give the total thrust if the pressure is the same along the entire external contour of the chamber and of the exhaust nozzle, i.e., if the static forces acting on the chamber from without are in equilibrium. Such a phenomenon takes place on the expansion of a gas to the ambient pressure. Let us assume that this is so in our case.

In free flight without resistance, the acting force is in equilibrium with the forces of inertia of the rocket body. Consequently,

$$P = Mj_1 \quad M\frac{dV}{d\tau}.$$

Bearing eq.(1) in mind, and taking into account that dM is a negative quantity, we get

$$M\frac{dV}{d\tau} = \quad W_a\frac{dM}{d\tau}.$$

On dividing the variables, we find

$$dV = \quad W_a\frac{dM}{M}.$$

On integrating, we find

$$V - V_0 = -W_a \ln\frac{M}{M_0} = W_a \ln\frac{M_0}{M}.$$

Assuming that $V_0 = 0$ at the beginning of flight and that the final mass is M_k, we get

$$V_{max} = W \ln\frac{M_0}{M_k} = W \ln \mu. \qquad (3)$$

Equation (3), which is often called the Tsiolkovskiy equation, is also given in the following form:

$$\mu = e^{\frac{V_{max}}{W}} \qquad (4)$$

At very high exhaust and flight velocities, the laws of the theory of relativity must be taken into account. In this case, instead of eqs.(3) and (4), we get

$$\frac{V_{max}}{c_1} = \frac{\mu^{\frac{2W}{c_1}} - 1}{\mu^{\frac{2W}{c_1}} + 1}, \tag{5}$$

where c_1 is the velocity of flight.

Figure 7 shows the variation in $\frac{V_{max}}{c_1}$ with the mass ratio of the rocket for the two exhaust velocities $W_a = \frac{c_1}{2}$ and $W_a = \frac{c_1}{10}$. The exhaust velocities have

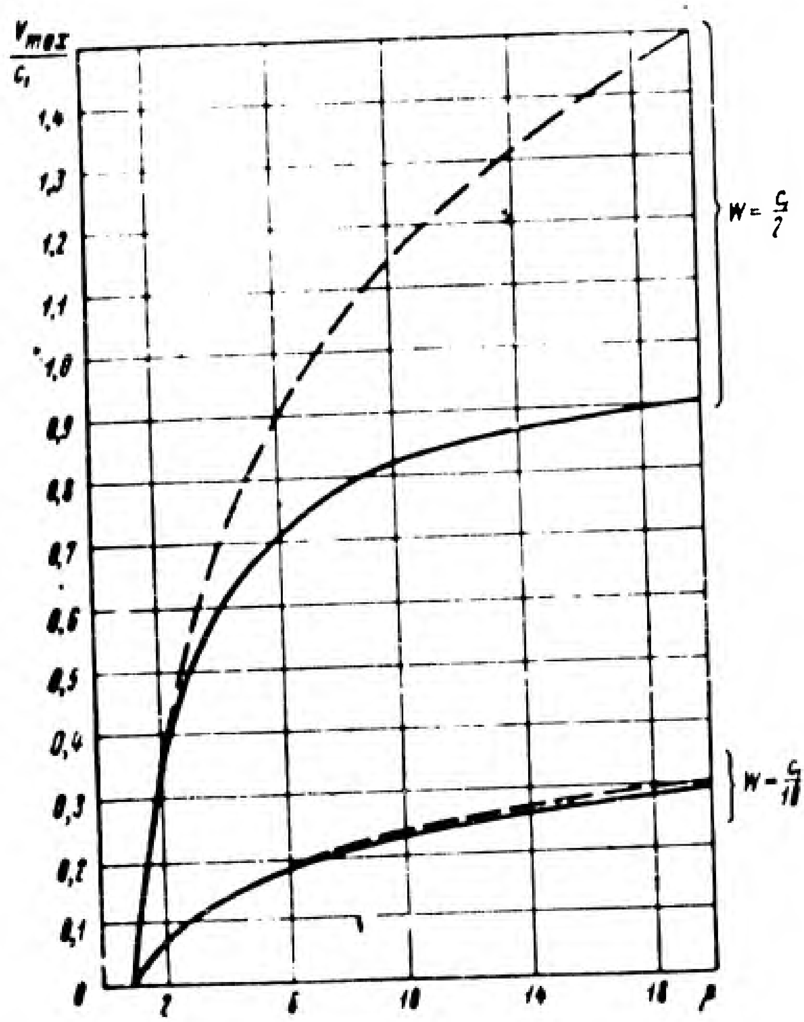

Fig.7 - Influence of the Mass Ratio of the Rocket and of the Exhaust Velocity on the Rate of Acceleration of the Rocket

——— according to the formula $\frac{V_{max}}{c_1} = \frac{\mu^{\frac{2W}{c_1}} - 1}{\mu^{\frac{2W}{c_1}} + 1}$;

\- - - according to the formula $V_{max} = W \ln \mu$.

been calculated by the formulas of classical and relativistic mechanics. The discrepancy in the results increases with the exhaust velocity and with the mass ratio of the rocket μ.

When a rocket moves in a dense medium, it may trap some of the surrounding mass. As will be seen later, such a capture of external mass may prove useful, since it might increase the total engine thrust during the boost phase without increasing the fuel consumption.

Assume that

m' and m'' is the respective masses of the propellant and the inert medium being trapped;

$\lambda_1 = \frac{m''}{m' + m''}$ is the relative inert mass.

Obviously,

$$P\,d\tau = W\,dm - V\,dm''.$$

But since

$$\frac{dm}{dm'} = \frac{1}{1-\lambda_1} \text{ and } \frac{dm''}{dm'} = \frac{\lambda_1}{1-\lambda_1},$$

then

$$P\,d\tau = \frac{W - V\lambda_1}{1-\lambda_1}\,dm'.$$

On the other hand, if M is the mass of the rocket, it follows that

$$P = M\frac{dV}{d\tau} = \frac{W - V\lambda_1}{1-\lambda_1}\,\frac{dm'}{d\tau}.$$

Dividing the variables, we get

$$(1-\lambda_1)\frac{dV}{W - V\lambda_1} = -\frac{dm'}{M} = -\frac{dM}{M}.$$

Integration leads to the formula

$$V_{max} = \frac{W}{\lambda_1}\left[1 - \left(\frac{M_k}{M_0}\right)^{\frac{\lambda_1}{1-\lambda_1}}\right]. \tag{6}$$

At $\lambda_1 = 0$, eq.(6) changes into the Tsiolkovskiy formula.

In Fig.8, the relative rate of acceleration for rockets of mass ratio $\mu = 2 - 10$, is plotted against the relative inert mass.

Before formulating the requirements to be met by the engine, let us find

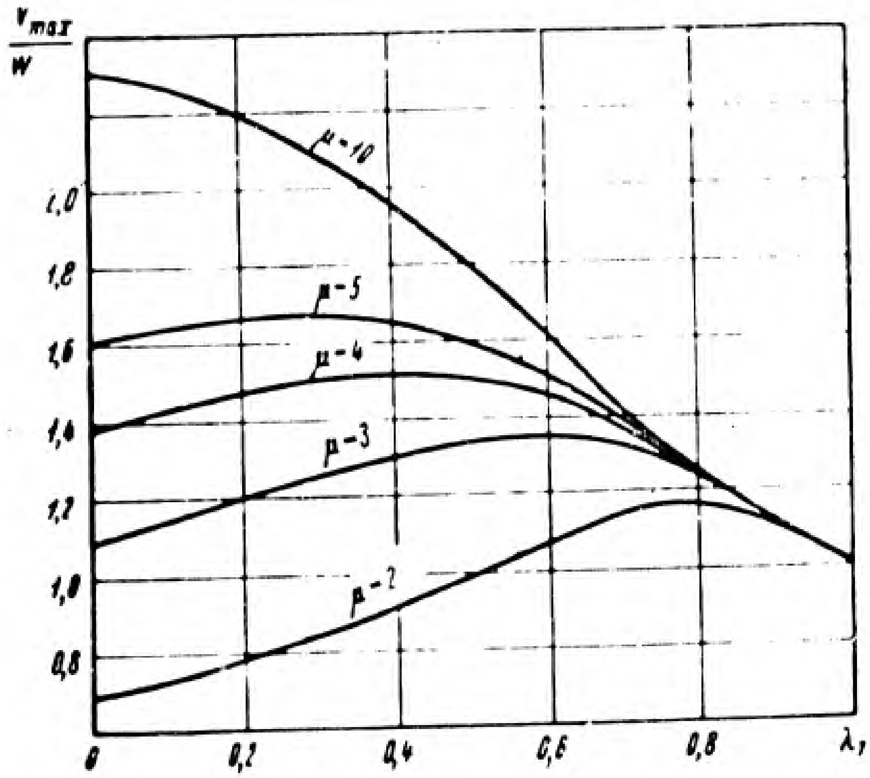

Fig.8 - Effect of Relative Quantity of Admixed Inert Mass on the Rate of Acceleration of the Rocket

expressions for the altitude of vertical ascent of the rocket under the conditions that

1) There is no air resistance;

2) The exhaust is characterized by the constant velocity W_a and the constant thrust P;

3) The acceleration of gravity is constant.

Under these conditions, the rocket will move under acceleration, and

$$\frac{dV}{d\tau} = j_1 - g,$$

where j_1 is the rocket acceleration in the absence of gravity.

Consequently, the velocity at the end of the boost phase may be represented in the form of two components:

$$V_1 = \int j_1 \, d\tau - \int g \, d\tau = V_{max\,0} - g\tau_1 = V_{max\,0} - V_g.$$

According to eq.(3),

$$V_1 = W_a \ln \frac{M_0}{M_k} - g\tau_1. \tag{7}$$

The engine operating time depends on the weight of propellant carried M_T and on its flow rate m_{sec}, i.e.,

$$\tau_1 = \frac{M_T}{m_{sec}} = \frac{M_T}{P} W_a.$$

Then, instead of eq.(7), we may write

$$V_1 = W_a \left(\ln \frac{M_0}{M_k} - \frac{M_T g}{P} \right). \tag{8}$$

The burnout altitude H_1 is determined from the equation

$$dH = V \, d\tau = W_a \ln \frac{M_0}{M_k + M_x} \, d\tau - g\tau \, d\tau,$$

where M_x is the mass of the propellant remaining in the rocket at any arbitrary instant during engine operation.

Just like the velocity, the burnout altitude may be represented as consisting of two parts:

$$H_1 = H_{max\,0} - H_g.$$

Let us calculate $H_{max\,0}$:

$$H_{max\,0} = W_a \int \ln \frac{M_1}{M_k + M_x} \, d\tau.$$

However,

$$\tau = \frac{M_T - M_x}{m_{sec}} \text{ and } d\tau = -\frac{dM_x}{m_{sec}},$$

and, therefore,

$$H_{max\,0} = -\frac{W_a}{m_{sec}} \int_{M_1}^{0} \ln \frac{M_1}{M_k + M_x} \, dM_x.$$

and, finally,

$$H_{max\,0} = W'_a \tau_1 \left(1 - \frac{M_k}{M_1} \ln \frac{M_1}{M_k}\right)$$

or

$$H_{max\,0} = W'_a \tau_1 \left(1 - \frac{\ln \mu}{\mu - 1}\right).$$

We find the second component from the equation

$$H_g = \frac{g \tau_1^2}{2}.$$

The burnout altitude will now be

$$H_1 = H_{max\,0} - H_g = W'_a \tau_1 \left(1 - \frac{\ln \mu}{\mu - 1}\right) - \frac{g \tau_1^2}{2}. \qquad (9)$$

Figure 9 shows patterns of vertical flight.

On the boost phase H_I for τ_I sec, the engine is operative, and the rocket is

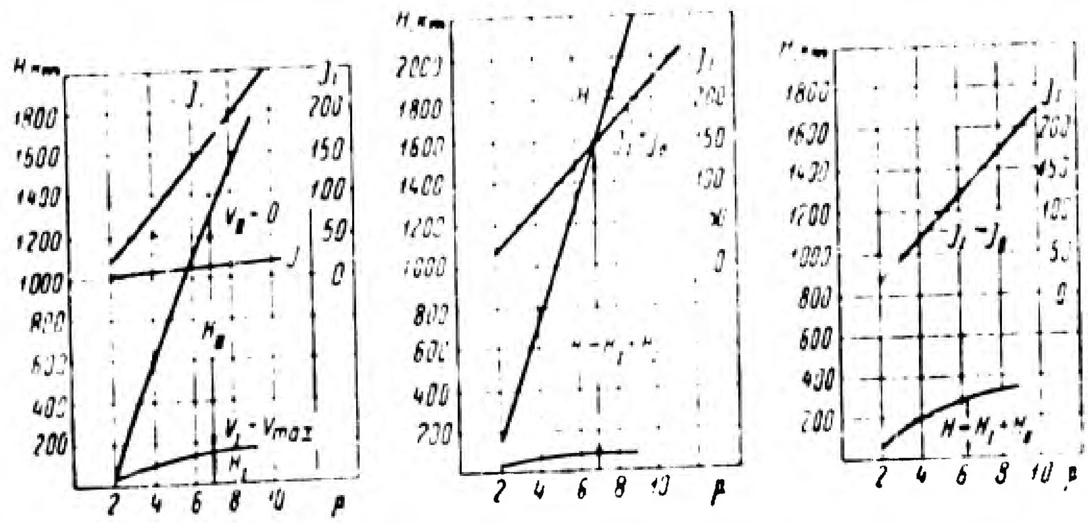

Fig.9 - Versions of Vertical Ascent of Rocket

Version I	Version II	Version III
P = const; W ; const; $j_1 \neq$ const	$j_1 = j_I$ = const; W = const; $m_{sec} \neq$ const	$j_1 = j_I$ = const; m_{sec} = = const; $W \neq$ const

accelerated to the velocity V_I, which is the maximum during its flight. The rocket subsequently still continues to climb, using up its kinetic energy like a free body.

The magnitude of the second phase of the path is determined by the well-known formula for the vertical motion of a body hurled upward at an initial velocity V_1.

Making use of eq.(7), we get

$$H_{II} = \frac{(W'_a \ln \mu - g\tau_1)^2}{2g}. \tag{10}$$

Adding H_I and H_{II}, we find the total altitude of ascent of the rocket:

$$H = W'_a \tau_1 \left(1 - \frac{\mu}{\mu - 1} \ln \mu\right) + \frac{W'^2_a}{2g} (\ln \mu)^2 \tag{11}$$

or

$$H = W'_a \tau_1 - \frac{\mu \tau_1}{\mu - 1} V'_{\max 0} + \frac{V^2_{\max 0}}{2g}. \tag{12}$$

The value of the binomial in the parentheses in eq.(11) is negative. This means that

$$H < \frac{V^2_{\max 0}}{2g}.$$

will always be valid.

If all the propellant is instantaneously consumed, which corresponds to $\tau_1 = 0$, the maximum value of the altitude will be

$$H_{\max} = \frac{V^2_{\max 0}}{2g}.$$

The reserve of kinetic energy in the rocket at instantaneous expenditure of the propellant is the same as in the rocket with acceleration in free space, which is explained by the fact that no work is done in overcoming the force of gravity.

The time of ascent during the second phase is determined from the equation

$$\tau_{II} = \frac{V_I}{g}.$$

Substituting the value of V_I from eq.(8), we get

$$\tau_{II} + \tau_I = \tau = \frac{W_a}{g} \ln \mu. \tag{13}$$

A different model of vertical motion of the rocket, with constant acceleration, is also conceivable.

Constant acceleration provides both cargo and passengers with a constant dynamic load within the allowable limits. During the boost phase, the acceleration will be $j_I - g$, where j_I is the acceleration that would be obtained under the action of the same thrust in a medium without gravitation.

The acceleration may be held constant by varying either the propellant flow rate per sec, m_{sec}, or the exhaust velocity W_a.

Setting the flow rate as constant, we get the following formulas:

The flight times during the first or boost phase and during the second phase, when the rocket ascends only on account of the accumulated kinetic energy, are respectively equal to

$$\tau_I = \frac{W_a \ln \mu}{j_I}; \quad \tau_{II} = \frac{j_I - g}{j_I} \cdot \frac{W_a}{g} \ln \mu.$$

The velocity of the rocket at the end of the boost phase is

$$V_I = \frac{j_I - g}{j_I} W_a \ln \mu.$$

The altitude is calculated from the formulas

$$H_I = \frac{j_I - g}{j_I^2} \frac{W_a^2}{2} (\ln \mu)^2 \text{ and } H_{II} = \frac{(j_I - g)^2}{j_I^2} \frac{W_a^2}{2g} (\ln \mu)^2.$$

The peak altitude and the total time of ascent to that altitude are, respectively,

$$H = \frac{j_I - g}{j_I} \frac{W_a^2}{2g} (\ln \mu)^2 \text{ and } \tau = \frac{2j_I - g}{j_I} \frac{W_a \ln \mu}{g}. \quad (14)$$

The ejection of mass, varying in accordance with the law

$$m_{sec} = m_{sec\,0} \frac{M}{M_0},$$

decreases in proportion to the mass of the rocket.

If, however, we consider the flow rate m_{sec} to be constant and the exhaust velocity W_a to be variable, then this velocity, if the acceleration of the rocket is held constant, must vary in accordance with the law

$$W_a = W_{a0}\frac{M}{M_1}.$$

As the rocket ascends, its velocity decreases proportionally to the mass of the rocket, and at the end of the boost phase will be equal to

$$W_{a1} = \frac{W_{a0}}{\mu}.$$

The corresponding time intervals are

$$\tau_I = \frac{\mu - 1}{\mu}\frac{W_{a0}}{j_1}; \quad \tau_{II} = \frac{\mu - 1}{\mu}\frac{j_1 - g}{j_1}\frac{W_{a0}}{g}; \quad \tau = \frac{2j_1 - g}{j_1}\frac{\mu - 1}{\mu}\frac{W_{a0}}{g}.$$

The velocity of the rocket at the end of the boost phase is determined from the formula

$$V_1 = \frac{\mu - 1}{\mu}\frac{j_1 - g}{j_1}W_{a0}.$$

The altitude, by segments of the path, is determined from the formulas

$$H_I = \frac{(j_1 - g)\tau_I^2}{2}; \quad H_{II} = \frac{(j_1 - g)^2\tau_I^2}{2g}.$$

The peak altitude will be

$$H = \left(\frac{\mu - 1}{\mu}\right)^2 \frac{j_1 - g}{j_1}\frac{W_{a0}^2}{2g}. \tag{15}$$

In a climb at constant acceleration, in both cases, the ratio of peak altitude to burnout altitude is the same:

$$\frac{H}{H_1} = \frac{j_1}{g},$$

while the peak altitude is similarly connected with the maximum rate of acceleration

Table 2

Results of Altitude Calculation for Three Versions of Vertical Rocket Flight

Version	I					II					III				
Conditions of Vertical Flight	$W_{a0} = W_{a1} = 3000$ m/sec; m_{sec} = const; $j_1 \neq$ const					$W_{a0} = W_{a1} = 3000$ m/sec; $m_{sec} \neq$ const; j_1 = const					$W_{a0} = 3000$ m/sec; W_a = const; m_{sec} = const; j_1 = const				
μ	2	4	6	8	9	2	4	6	8	9	2	4	6	8	9
H_I, km	42	95	130	160	170	42	70	80	85	90	20	22	24	26	28
H_{II} "	48	505	970	1370	1560	108	640	1220	1615	2130	50	178	266	314	322
H "	90	600	1100	1530	1730	150	710	1300	1700	2220	70	200	290	340	350

of the rocket in gravity-free space:

$$H = \frac{j_1 - g}{j_1} \frac{V_{max}^2}{2g}.$$

It must also be borne in mind that, in the case W_a = const,

$$V_{max} = W_a \ln \mu.$$

If, however, m_{sec} = const and $W_a \neq$ const, then

$$V_{max} = \frac{\mu - 1}{\mu} W'_{av}.$$

The results of calculation of the altitude of flight of a rocket for these versions are given in Table 2. The mass ratio μ, the maximum acceleration, and the initial mass of the rocket are taken as being the same for all these versions.

Equations (3), (11), and (15) establish the final performance parameters of rocket flight under idealized conditions. Under these conditions, the principal requirements for an engine still remain in force.

In exact calculations for space rockets, and especially for high-altitude rockets, allowance is also made for the force of air resistance S_1, the inclination of the trajectory to the horizon, and the variation in terrestrial acceleration with distance from the center of the earth, in accordance with the law:

$$g = g_0\left(\frac{r_0}{r}\right)^2,$$

where r_0 and r are the respective distance from the center of the earth to sea level and to the altitude in question.

The equation of vertical motion of the rocket has the following general form:

$$M\frac{dV}{d\tau} = P - Mg_0\left(\frac{r_0}{r}\right)^2 - S_1.$$

Dividing all terms by M and bearing in mind that

$$S_1 = f(V, H),$$

we get

$$\frac{dV}{d\tau} + \frac{W_a}{M}\frac{dM}{d\tau} + g_0\left(\frac{r_0}{r}\right)^2 + \frac{f(V, H)}{M} = 0. \qquad (16)$$

The solution of this equation is highly complex. We shall give here only one of the approximate solutions for the case where the exhaust velocity W_a and the acceleration j_1 of the rocket on the boost phase are both constant.

Let F be the maximum cross section of the rocket, $\bar{c}_x$ the mean value of the coefficient of drag during the boost phase, $\bar{\rho}$ the mean density during the same phase, and k_1 the ratio of rocket acceleration to exhaust velocity;

Then,

$$V_{max} = V_{max\,0} - (\Delta V)_g - (\Delta V)_f =$$

$$= W_a \ln\mu - g_0\left[\frac{1}{2 + \frac{j_1}{r_0}\tau_1^2} + \frac{\sqrt{\frac{r_0}{2j_1}}}{\operatorname{tg}\left(\tau_1\sqrt{\frac{j_1}{2r_0}}\right)}\right] - \frac{\bar{c}_x F\bar{\rho} j_1^2}{2M_0}\left[\frac{1}{k}e^{k_1\tau_1}\left(\tau_1^2 - \frac{2\tau_1}{k_1} + \frac{2}{k_1^2}\right) - \frac{2}{k_1^3}\right],$$

where $(\Delta V)_g$ are the velocity losses due to the influence of the earth's gravity;

$(\Delta V)_F$ are the velocity losses due to the air resistance.

Figure 10 shows the characteristic of rocket ascent in the presence of air resistance. If the flight takes place at an altitude of $H \leq 100$ km, the air resistance will have a substantial effect on the final flight characteristics. The air resistance exerts a slight influence on the performance characteristics of high-altitude rockets, especially of space rockets. This influence may sometimes be neglected.

Figure 11 shows the variation in maximum velocities when the rocket moves vertically at constant accelerations g_o, $3\ g_o$ and $5\ g_o$, depending on the altitude reached. The higher the rocket ascends, the less will be the velocity V_{esc} necessary for escape from the earth.

The intersection of the curve V_{esc} with the velocity curves of the rocket in-

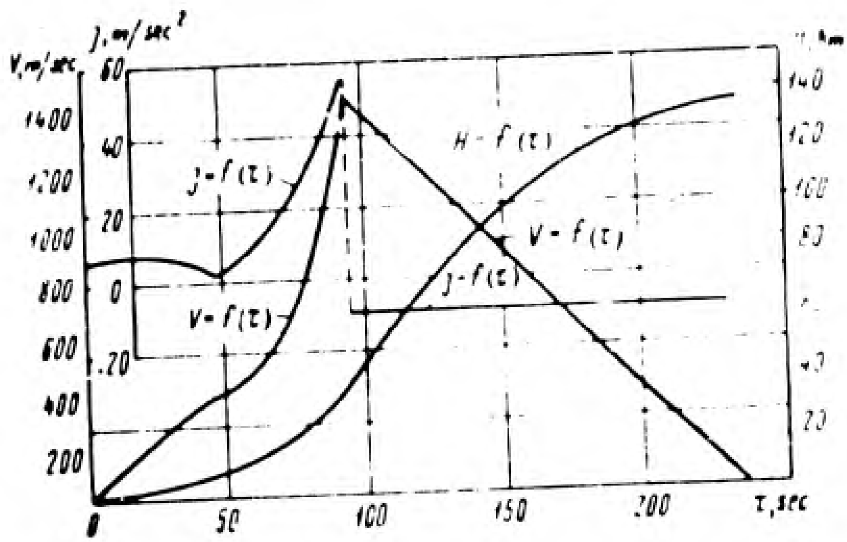

Fig.10 - Characteristic of Vertical Ascent of Rocket, Allowing for Air Resistance

$H = 133$ km; $\tau = 233$ sec; $V_{max} = 1340$ m/sec; $j_{max} = 50.4$ m/sec^2

dicate the altitudes at which engine operation will stop, since the rate of climb attained is already sufficient for the rocket to overcome the force of gravity of the earth.

Equations (3), (11), (13), (14), and (15) show with sufficient clarity the requirements for the rocket engine.

The principal performance characteristics of rockets, besides the payload, are

V_{max} and H. To increase these, it is necessary to:

1) Have the greatest possible exhaust velocity W_a. This is a particularly important factor of all characteristics determining the quality of rocket flight and relates directly to the process in the engine. The attainable velocity of a rocket is directly proportional to the exhaust velocity, while the altitude of ascent is proportional to the square of this velocity. Consequently, to improve the exhaust velocity, all available possibilities must be utilized.

2) Increase the mass ratio μ of the rocket. This requirement means to minimize structural weight and maximize propellant weight. This may be accomplished in various ways. Imagine, for instance, that many of the structural parts were made of solid fuel components. In this case, the ratio μ would be considerably increased.

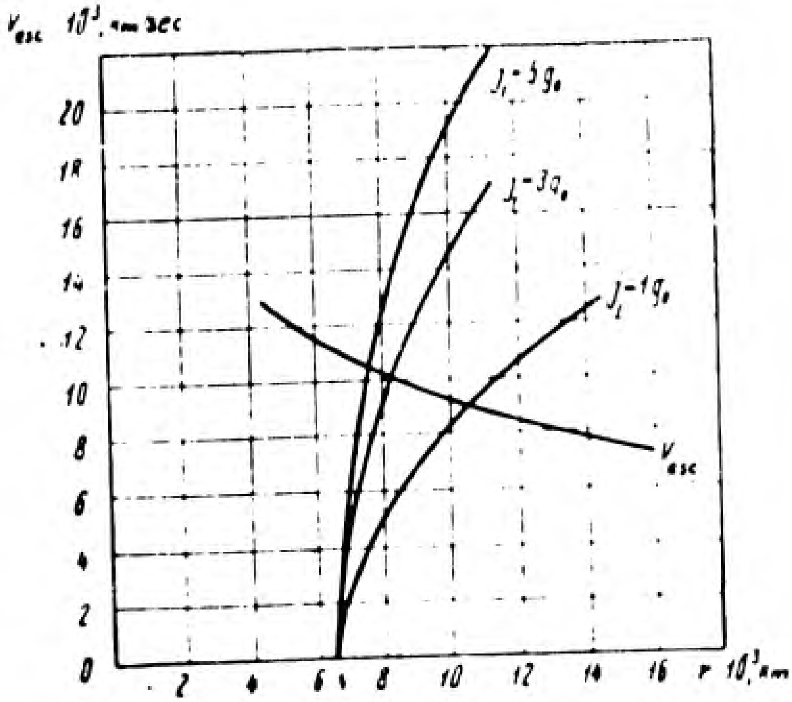

Fig.11 - Velocity Variation of a Space Rocket at Constant Acceleration, with Distance from the Center of the Earth. Graph of escape velocity

A.F.Tsander's suggestion that certain portions of the metal structural elements could be burned as fuel in the combustion chamber follows this same aim. The ratio μ may be increased by an appropriate choice of propellant. At equal heat values of equal exhaust velocities the propellant with the higher specific gravity should be given preference.

3) To minimize the fuel-consumption time or maximize the acceleration of the rocket. It is important to shorten the time of propellant consumption when the rocket traverses a field of any resistance, for example, a field of gravitational forces. It will be seen from eqs.(11) and (14) that instantaneous consumption of the entire propellant supply gives the maximum peak altitude. However, the acceleration is limited by the need to protect the passengers, instruments, and structure from possible mechanical destruction due to the high acceleration forces. Moreover, an increase in the flow rate per second would involve enlarging the combustion chamber and ducts, or increasing the pressure in these. Either option would tend to increase the weight of the engine piping, which from a certain instant on, might adversely affect the flight indices of the rocket. In specific cases, it is necessary to take account of many circumstances and find the optimum solution, striving to obtain the maximum permissible acceleration.

4) Obtain the lowest drag of the vehicle.

In this connection several requirements are imposed on the shape of the rocket and its outside dimensions. The power plant must be such that its dimensions, the shape of its parts, and its layout shall not have an adverse effect on the aerodynamic qualities of the rocket.

It is well known that, depending on the manufacturing, storage and operating conditions of a rocket and on its purpose, rockets and engines must meet many requirements in addition to those given above.

The basic requirements to be met by engines designed for rockets coincide in many respects with the requirements for self-contained rocket engines (points 2 - 7 on pp.9 - 10, and points 2 and 5 on p.10). Rocket engines, however, must meet more severe requirements as to specific thrust and low specific weight, while the requirements as to uniform thrust are less strict.

Moreover, such engines must meet the following requirements:

1) The thrust developed by a single-chamber (unit) engine must range from the very lowest values up to 40 - 100 tons or even more;

2) It must be possible to realize at least two thrust conditions for high-altitude, long-range, and heavy rockets;

3) The engine must start reliably and exactly on time at any atmospheric temperature;

4) The operating time must be as long as several minutes;

5) Permanent storage, in the charged state (without compressed gases), must be possible for prolonged periods of time under normal climatic conditions.

All measures to increase the specific thrust and decrease the specific weight of the engine and its units lead to an increase in rocket acceleration.

The quantitative characteristics for the respective categories of requirements are usually determined by the specifications for the typical groups of rockets.

Mass combat use of rockets places special emphasis on the problem of their cost, since all such rockets are expendable and nonrecoverable. For this reason, the requirements of points 3 and 5 (p.10) given for engines of military aircraft are also of great importance for rockets.

For heavy scientific rockets, it is absolutely essential to develop means of recovering the rocket structure after accomplishment of the flight program.

2. Features of Space Rockets

The rocket engine, as the source of a high-power impulse independent of the ambient medium, is still the most suitable means for flight into interplanetary space. Nevertheless, there are considerable difficulties to be overcome before such flight will have been mastered.

A space rocket in the full sense of the word is a vehicle moving in cosmic space under the action of the local fields of gravity and of the thrust of its own engine. Today the problem of practical design and planning of short-range cosmic rockets, serving the area of earth satellites, has already been solved. This first stage in the conquest of space will probably be completed by the construction of close-in space stations for long-range space ships.

The availability of nuclear fuel will allow the placement of large energy reserves on a rocket. But the supply of active mass will be limited, and the operating period of the rocket engine will be short. In all probability, there will be stations in cosmic space to replenish the supply of working fluid, and if this should prove difficult, the role of the engine will be reduced to correcting flight during the program representing optimum utilization of the gravitational fields. The consumption of mass must be economical, and the engine must be cut in for short intervals of time, at instants suitable for changing the course or the flying speed.

Thermal rocket engines, to which the present book is devoted, are essentially intended for use near the ground (near the planet); for their operation, the reserve of mass is most essential.

Bearing in mind that the reserve of mass on a flight vehicle is limited, the area of operation of the engines must remain in the immediate proximity of the source of working fluid, i.e., of the planet.

To economize the working fluid or substance, especially high exhaust velocities, i.e., especially high specific thrusts, will be needed. The absence of an ambient medium in interplanetary space will promote excessive expansion of the gas in the exhaust nozzle and lead to a corresponding increase in velocity. The conditions for utilization of nuclear energy in a rocket engine are favorable, since there is no need to worry about the harmful effect of radiations from the ejected mass. Consequently, the engine of a future space rocket will probably be a high-yield nuclear engine with a high expansion ratio in the nozzle.

At very high flying speeds, comparable to the velocities of nuclear reaction products, it will be possible to use rocket engines in which the active mass consists of a mass of reaction debris, ions, photons, and other particles.

The quantity of matter serving as the carrier of nuclear energy will be negligible by comparison with the mass of the rocket, although it will contain immense reserves of energy, utterly incomparable with the energy reserves provided by thermal rocket engines. If we assume that the ratio of the available energy to the kinetic energy of a space rocket would be approximately the same as in modern rockets, then the speed of cosmic rockets would correspond to the times acceptable for human travel over distances measured in light years (9.4727×10^{12} km).

Besides gravitational fields, outer space also has other fields of variable potential. Obviously, such peculiar types of "cosmic currents" may be utilized to obtained motion in the desired direction.

The takeoff from a planet and landing on it must be considered difficult instants in the operation of a space rocket. To escape from the earth's gravitational attraction, the velocity of a rocket must theoretically be 11.2 km/sec; in practice, however, allowing for the resistance of the atmosphere, this escape velocity is still higher.

The exhaust velocity in modern liquid-propellant rocket engines averages 2 km/sec. Let us assume V_{max} = 12 km/sec. Then, according to eq.(3), we have

$$\ln \mu = \frac{12}{2} = 6 \text{ and } \mu = 402.$$

Surveying actually constructed rockets, we find that, in modern designs, $\mu = 2 - 5$. Consequently, the conventional designs of present-day rockets are entirely unsuitable for use as space ships.

Bearing in mind that the velocity V_{max} must provide a certain margin, and that the payload would be appreciably less than the dry weight of the rocket, we reach the conclusion that the ratio of the takeoff weight of a space rocket to the payload must reach several thousand, which is impossible to realize in practice. Change-over to a propellant with higher heat value will increase the exhaust velocity.

A survey of chemical fuels permits the conclusion that the maximum exhaust velocity of the products of a chemical reaction would be about 6000 m/sec. The use of nuclear fuel to heat the active mass will permit a considerable increase in the exhaust velocity whose value will be limited by the permissible combustion-chamber temperature.

Table 3 gives the mass ratios of single-stage space rockets for three interplanetary routes, with propellant consumption only during takeoff and landing. The exhaust velocities given in the Table for chemical and thermonuclear propellants cannot be as yet attained, but there is definite reason to assume that such will be ultimately the case.

Table 3 demonstrates the immense importance of further efforts to increase the exhaust velocity of the gases issuing from the engine. Among the steps necessary for interplanetary travel, the most important is the development of an engine with an exhaust velocity at least eight times that of present-day rocket engines.

Table 3

Mass Ratios of Single-Stage Interplanetary Rockets

Flight	Mass Ratio, $\mu = \frac{M_0}{M_k}$	
	Propellant	
	Chemical $W_{max} \approx 6400$ m/sec	Thermonuclear $W = 15,250$ m/sec
Earth-Moon (with landing) - Earth (with landing)	36,1	3,55
Earth-Mars (with landing) - Earth (with landing)	82	4,51
Earth-Venus (with landing) - Earth (with landing)	458	13,1

The conditions of launching a space rocket will be greatly simplified if the consumption of energy on accelerating the mass of the structure can be minimized.

There are many methods of decreasing the influence of the structural weight. Methods of stepwise lightening of a rocket and methods of refueling in flight deserve the most attention.

Stepwise lightening of the structure is accomplished by the use of step rockets (Fig.12), consisting of several rockets operating either simultaneously (in parallel) or alternately (in series). A parallel group of rockets is sometimes called a cluster or bundle. In a step rocket, only one of the component rockets reaches the

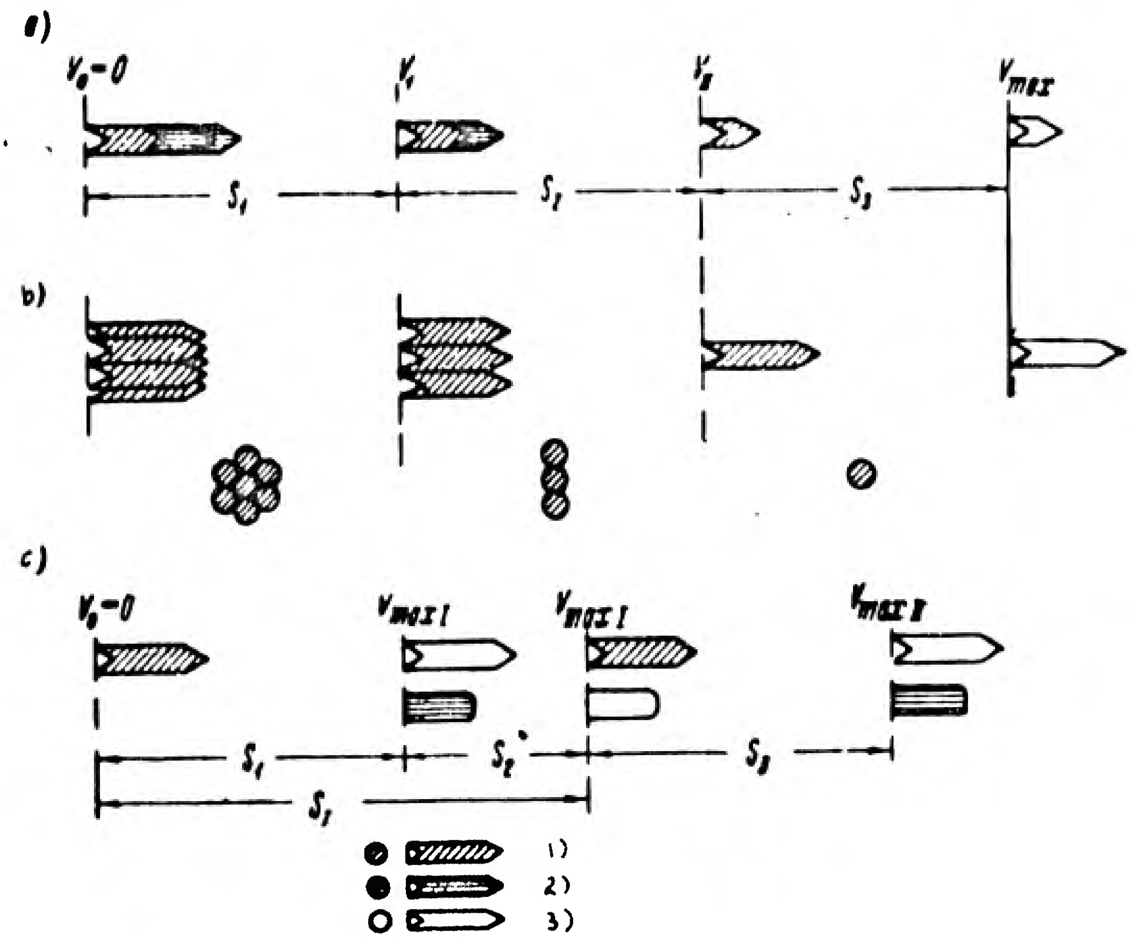

Fig.12 - Schematic Diagrams of Free Acceleration of Step Rockets and Stepwise Fuel Feed

a - Series coupling; b - Parallel coupling; c - Stepwise fuel feed

1) Operative rocket; 2) Nonoperative rocket; 3) Dry rocket

objective, while the others are accelerated and are jettisoned at velocities below the maximum velocity of the final rocket. Consequently, the energy of the fuel will not be expended (as is the case in the single-stage rocket) on accelerating the entire mass of the structure to the maximum velocity.

Consider the motion of a multistage rocket, with the stages connected in sequence. Operation of the first stage of the step rocket ends on the first phase of flight S_1, and this stage is dropped. The increase in velocity is determined by the conventional formula

$$\Delta V_1 = V_1 = W_1 \ln \mu_1 \quad W_1 \ln \frac{M_0}{M_{k1} + M_2 + M_3 + \ldots},$$

where M_0 is the initial weight of an n-stage rocket, equal to

$$M_0 = M_1 + M_2 + M_3 + \ldots + M_n.$$

For the second phase we find, respectively,

$$\Delta V_{II} = W_{II} \ln \mu_{II} = W_{II} \ln \frac{M_2 + M_3 + \ldots}{M_{k2} + M_3 + M_4 + \ldots} = W_{II} \ln \frac{M_0'}{M_{k2} + M_3 + M_4 + \ldots}$$

or, in the general case,

$$\Delta V_k = W_k \ln \mu_k = W_k \ln \frac{\sum_{k}^{n} M_i}{\sum_{k+1}^{n} M_i + M_{kk}}.$$

If the initial velocity is zero, then, adding the velocity increments, we get

$$V_{max} = \sum_{1}^{n} W_a \ln \mu.$$

Let us assume, for simplicity of derivation, that the exhaust velocities and mass ratios of the individual stages are the same. Then the terminal rate of acceleration of the final stage will be

$$V_{max} = W_a \ln \frac{M_0}{M_{kn}} = W_a n_1 \ln \mu_1, \tag{17}$$

where M_{kn} is the mass of the structure of the final stage of the rocket plus the payload.

Consequently, an n_1-stage rocket is equivalent to a hypothetical single-stage rocket, having, at the same exhaust velocities, would have a considerably more favorable mass ratio:

$$\mu = \mu_1^{n_1}.$$

or equivalent to a single-stage rocket in which, at the same value of μ, the exhaust velocity would be n_1 times as great. A similar conclusion may be drawn for a cluster of rockets.

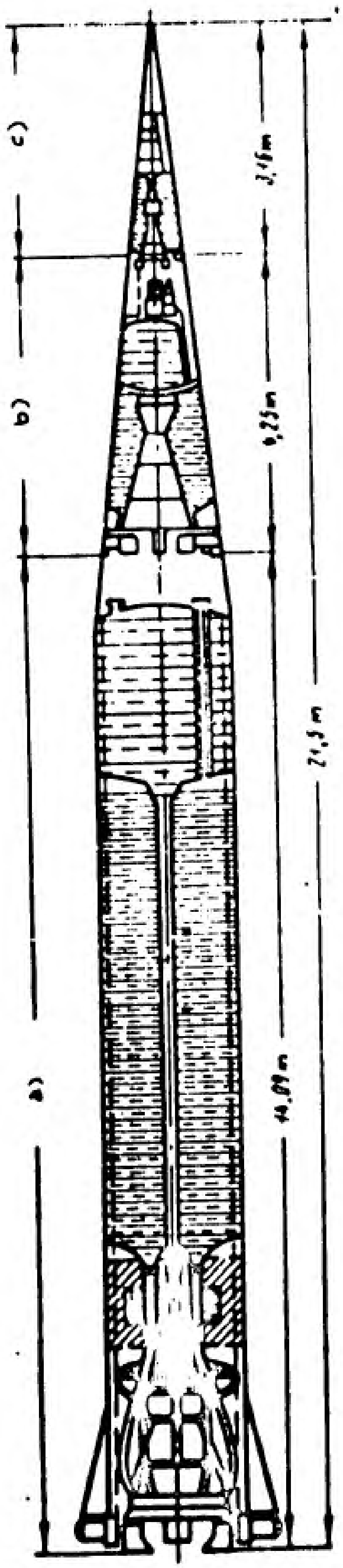

Fig.13 - Schematic Diagram of Three-Stage Space Rocket

a) First stage; b) Second stage; c) Third stage

Each variant of rocket coupling has its own advantages and disadvantages. These will not be discussed here. We note merely that in a rocket cluster all engines must be able to operate simultaneously, and that the propellant of a rocket group, ejected in turn, can be consumed very rapidly directing it into all engines. Both these facts favor an increase in acceleration j_1 and an earlier jettisoning of excess mass.

Figure 12 also shows a schematic diagram of a rocket with stepwise fuel feed. A single-stage or multistage rocket is accelerated to the velocity $V_{max\ I}$ on the segment S_1 of the path until it catches up with a flying fuel tank, moving at about the same velocity. After equalization of the velocities, the fuel is transferred to the rocket on the flight segment S_2. The second acceleration to $V_{max\ II}$, etc. then takes place.

Let us consider, as an example for illustrating the essence of the idea, the simplest version in which the velocities of the flying fuel tanks at each point of encounter are equal to the accelerated velocities of the rocket. In this case, during each acceleration stage, the velocity will increase by one and the same quantity:

$$\Delta V = W \ln \mu.$$

For the case of n stages of fuel feed, we have

$$V_{max} = \sum_{1}^{n} W \ln \mu = W \ln \mu^{n} = W n \ln \mu,$$

i.e., the same result as for a multistage rocket connected in series.

Such "refueling stations" must be outside the earth's atmosphere and move like its satellites on suitable orbits. Undoubtedly intermediate stations of this type will be an important item in the equipment of short-range routes for interplanetary travel. But their installation and the stockpiling of fuel supplies by means of the same chemical rockets involves great difficulties and immense expenditure of materials. Ways and means of facilitating the solution of this problem must be devised by improving the processes in the engine and decreasing the structural weight of the rocket, and also by finding possibilities of obtaining material for the working fluid during the trip, i.e., in interplanetary space, with easy delivery of such substances to the orbit of the station.

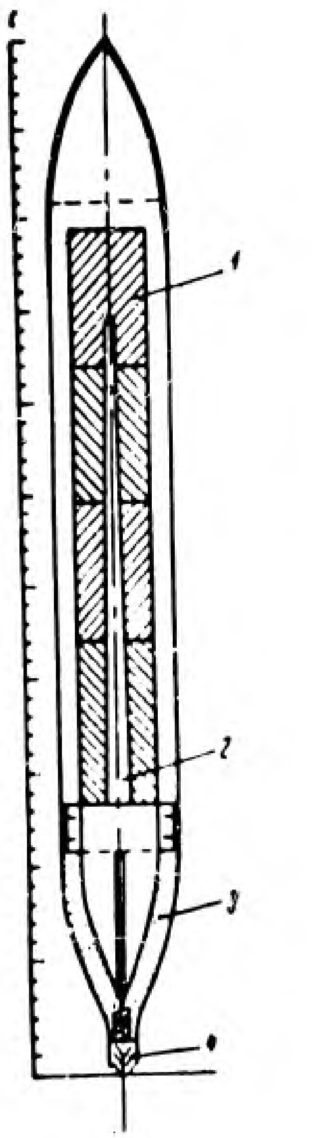

Fig.14 - Schematic Diagram of Rescue Rocket

1 - Powder;
2 - Conical depression; 3 - Fork;
4 - Wooden rod

One of the variants of a three-stage space rocket with a payload of 10 kg is shown in Fig.13. Such a load can be delivered to the moon if the initial weight of the rocket is 50,000 kg, the propellant consists of tetranitromethane $C(NO_2)_4$ plus gas oil, and the thrust of the successive stages is 100, 10, and 1 ton.

For a successful trip with a 10 kg payload, with subsequent re-entry into the atmosphere, the takeoff weight would have to be approximately 2.5×10^8 kg.

This example shows that even a multistage chemical rocket is unsuitable as a space ship.

Let us consider several engine types for the rocket vehicles mentioned in Table 1.

The first four types of unmanned rockets (Fig.14) are used at low altitudes, usually near sea level. Their distinctive features are brief operation and simple layout, attainable by using powder as the monopropellant filling the space of the combustion chamber. The average burning time of the powder is short, from 0.005 to 5 - 10 sec. The main body is made of light metal, compressed cardboard, and other metal substitutes. Such rockets are cheap and convenient for prolonged storage, transportation, and operation.

Rockets for research at great altitudes are of great importance. The upper layers of the atmosphere are usually studied by ground observation, and also from records of instruments carried aloft by pilot balloons.

The low altitude ceiling of pilot balloons (40 km), and their lack of direct contact with high-altitude space, prevents the solution of many scientific problems.

The literature contains references to rockets that have been built, and are being built, for high-altitude research. We present the data of one of the large rockets of this kind:

Length of rocket, m	13.8
Maximum diameter of shell, m	0.81
Propellant weight, kg	3240
Thrust at sea level, kg	9100
Engine operating time, sec	75
Payload, kg	454
Takeoff weight, kg	4740
Maximum velocity of rocket, m/sec	1850

Maximum acceleration . . . . 7.3 g

Burnout altitude, km 46

Altitude ceiling, km 224

High-altitude rockets are also made in multistage versions (Fig.15).

Military rockets have reached the highest development stage, especially short-range powder rockets with short engine operating period. Such rockets are much simpler than the other types, but their mass ratio is unfavorable for prolonged flights. Powder rockets are used as antiaircraft, aircraft, and torpedo rockets, and as rocket mines. Powder rocket grenades are also suitable for close combat (Fig.16).

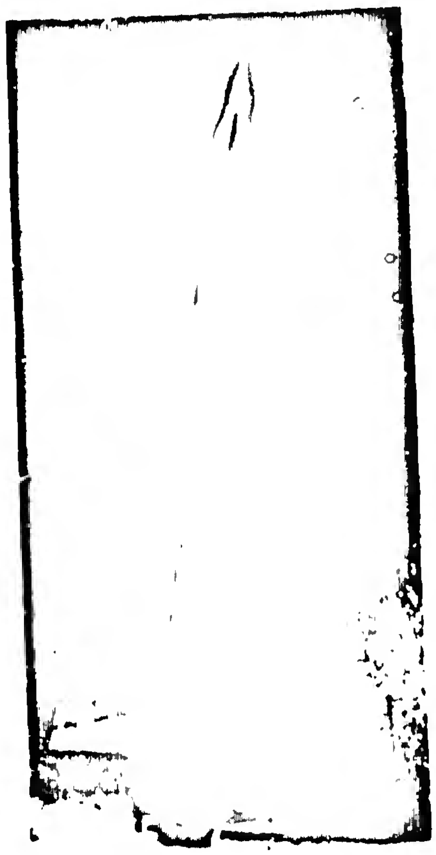

Fig.15 - Two-Stage "Nike-Ajax" Experimental Rocket in Flight (United States)

Today most large rocket missiles are of the target-seeking or guided type.

In most case, powerful rockets are served by liquid-propellant rocket engines. These include long-range rockets, antiaircraft rockets, and also some aircraft rockets, i.e., winged rockets. At the end of World War II, Germany used the heavy V-2 rocket to bombard London from the northern coast of Europe (Fig.17). The rocket carried a warhead weighing about one ton. The propellant consisted of 3500 kg of a 75% aqueous solution of ethanol (C_2H_5OH) and 5000 kg of liquid oxygen. Figure 18 shows the calculated path of this rocket. At first, the rocket ascended vertically, but soon began to incline under the action of automatically deflected control surfaces. At an altitude of 20 km, the rocket axis made an angle of about 40° with horizon, and the fuel was completely consumed. At this instant, the power of the rocket was 680,000 hp, the engine thrust 30 tons, the velocity 1700 m/sec, and the acceleration 8 G. The burnout occurred in about 67 sec; the total flying time was 5 min. The flight continued by inertia after burnout, after which the rocket described a parabolic curve reaching an altitude of 80 km, and then dropped to the ground 270 - 300 km from the

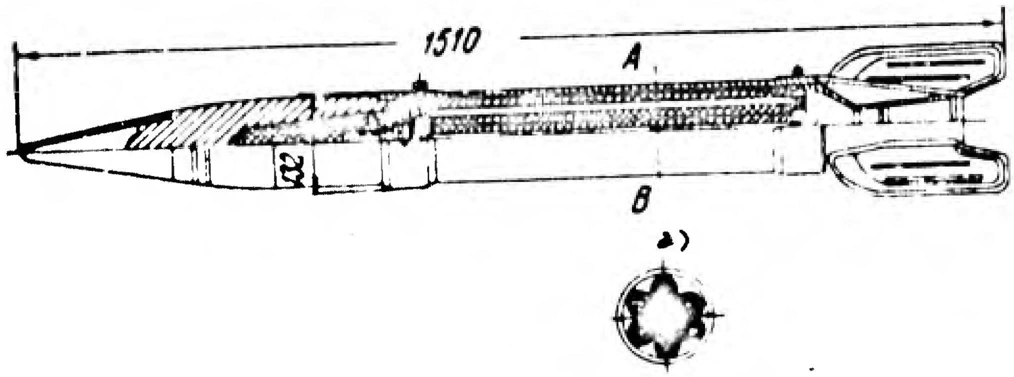

Fig.16 - Antitank Rocket Missile, 132-mm Caliber

a) Section through A-B

launching site. The initial weight was about 13 tons, and the mass ratio was in the range of $\mu = 2.9 - 3.25$.

As a result of the postwar development of long-range rockets in the USSR, intercontinental rockets and earth-satellite rockets have been designed and built. The range of rockets over the earth's surface today is unlimited.

To illustrate, let us consider several models of aircraft rocket engines.

The principal data of a typical rato unit are:

Initial weight, kg	93
Final weight, kg	52
Average thrust P_{av} at $\tau = 12$ sec, kg	453
Thrust power at velocity V = 145 km/hr, hp	331
Takeoff run of aircraft weighing 11.4 tons without rato unit, m	1200
Takeoff run with rato unit, m	750

Obviously, the use of a rato unit considerably improves the takeoff conditions.

Liquid-fuel rato units are most often used for heavy aircraft. A relatively low power rato has the following characteristics:

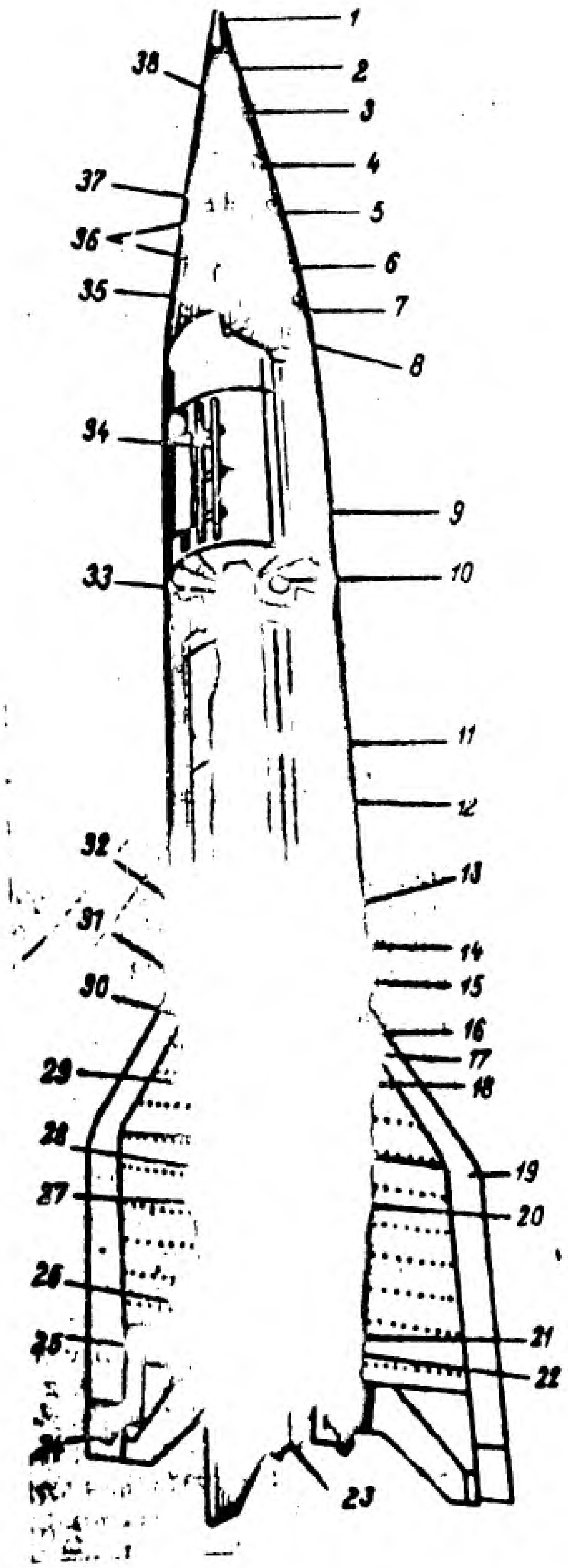

Fig.17 - V-2 Long-Range Ballistic Rocket

1 - Nose cone with warhead fuze; 2 - Conduit with wires; 3 - Central exploder tube; 4 - Electric fuze; 5 - Plywood frame; 6 - Nitrogen bottles; 7 - Front joint ring; 8 - Pitch and azimuth gyros; 9 - Alcohol tank; 10 - Alcohol filling nipple; 11 - Double-walled alcohol delivery pipe to pump; 12 - Liquid oxygen tank; 13 - Liquid-oxygen filling nipple; 14 - Concertina connections; 15 - Hydrogen peroxide tank; 16 - Tubular frame, holding turbo-pump assembly; 17 - Permanganate tank (gas generator behind this tank); 18 - Oxygen distributor; 19 - Stabilizing fins; 20 - Alcohol pipes for subsidiary cooling; 21 - Alcohol inlet orifice; 22 - Electro-hydraulic servo-motors; 23 - Jet vanes; 24 - Air vanes; 25 - Chain drive to air vanes; 26 - Electric motor; 27 - Combustion chamber and venturi; 28 - Burner cups; 29 - Alcohol supply pipe; 30 - Turbopump assembly; 31 - Compressed air bottles; 32 - Rear joint ring; 33 - Servo-operated alcohol outlet valve; 34 - Rocket shell construction; 35 - Control compartment; 36 - Radio equipment; 37 - Pipe from alcohol tank to warhead; 38 - Warhead

Thrust, kg	$P = 650$
Operating time, sec	$\tau = 38$
Exhaust velocity, m/sec	$W_a = 1870$
Propellant	hypergolic: nitric acid + + aniline (C_6H_7N)
Fuel-feed system	pressure-feed

The thrust of aircraft rato units may reach 20 tons;

The rocket aircraft engine was developed as a logical consequence of air defense requirements. Modern bombers operate at altitudes of 12 - 18 km and above.

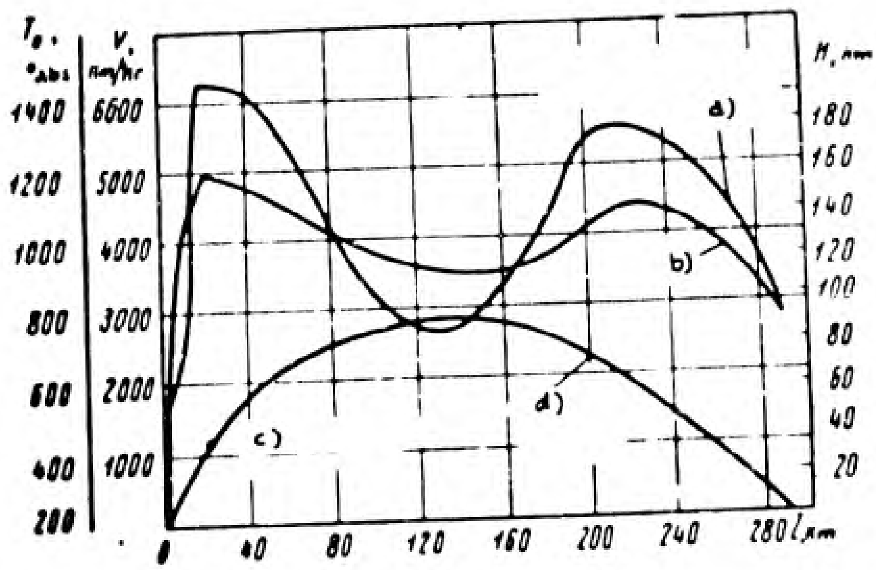

Fig.18 - Flight Characteristics of V-2 Rocket

a) Deceleration temperature; b) Speed;

c) Thrust cutoff; d) Rocket path

Artillery fire is almost ineffective at such altitudes. Fighter planes with air-breathing engines do not provide rapid and reliable defense organization of a target, owing to their low rate of climb and to the decrease in engine power at great altitudes.

The first flight of the rocket plane designed by S.P.Korolev, equipped with an engine having a thrust of P = 300 kg, was made on 28 February 1940. A conventional aircraft carried the rocket plane to an altitude of H = 2000 m. After release from the parent plane and a glide, the rocket engine was started.

In May 1942, the first USSR flight of a rocket ship, designed by V.F.Bolkhovitinov, took place. The thrust was P = 1100 kg.

As shown by even the brief experience in World War II, rocket aircraft are suitable for defense against surprise attack. For example, a Messerschmidt-163 aircraft with an engine thrust of 2 tons climbed to an altitude of 14 km in 2 min. The propellant used was 80% hydrogen peroxide plus a 50% mixture of hydrazine hydrate (N_2H_5(?) and methanol (CH_3OH), with an addition of an 0.?4% solution of copper-potassium cyanide as catalyst. In 1944 - 1945, these aircraft operated with fair success against American bombers.

As an example of an aircraft rocket engine, we may mention the "Screamer" produced by the Armstrong Siddeley Co. This engine has the following data:

Propellant components, %:	
Liquid oxygen	60
Wide-cut aviation gasoline	23
Filtered water	17
Static thrust at sea level, kg	454-3630
Maximum thrust at altitude 12,200 m, kg	about 4080
Flow rate through steam-gas generator at full thrust, kg/sec	0.68-0.91
Pressure in steam-gas generator at full thrust, kg/cm^2	28
Temperature in steam-gas generator, °C	625
Pressure in combustion chamber at full thrust, kg/cm^2	42
Temperature in combustion chamber, °C	3200
Flow rate per second through combustion chamber at full thrust, kg/sec	16.73
Specific thrust at sea level, kg-sec/kg	217
Exhaust velocity, m/sec	2130

Figure 19 is a schematic diagram of the "Screamer" rocket engine. The principal parts are the steam-gas generator (SGG), the turbopump unit, and the combustion chamber.

The steam-gas generator operates on the same propellant components as the main combustion chamber and is fired by the electric system of the burner cups. The coolant used is water which, after passing through the cooled zone, is partially injected into the nozzle part of the steam-gas generator, thus reducing the temperature of the combustion products to tolerable levels (625°C). During the starting period, the steam-gas generator is fed from auxiliary primer tanks from which the propellant components are ejected by nitrogen gas. After each start, the primer tanks are automatically refilled.

From the steam-gas generator the steam gas is fed to the turbine of the turbopump assembly through three nozzle orifices. At 20,000 rpm, the turbine delivers about 350 hp, which is entirely sufficient to drive the three pumps pumping the propellant components from the main tanks, and to run the fuel-feed and automatic units.

All three pumps of the turbopump assembly are designed for a maximum speed of the order of 20,000 rpm. At this speed, they yield a lox pressure of 63 kg/cm^2 and a water and gasoline pressure of about 60 kg/cm^2. To prevent cavitation in the lox pump, a screw pump is installed.

Figure 20 is a diagram of the main combustion chamber, designed on the principle of a semithermal nozzle. Despite the fact that the specific thrust is lower than in a chamber with p = const, the semithermal nozzle permitted simple chamber design, stable operation, and good weight characteristics. The rated altitude for the combustion chamber at full thrust conditions is 6000 m. The chamber is water-cooled; the water passes through the cooling jacket and is then injected into the combustion chamber, forming a continuous protective film on its inner wall. The losses in specific thrust due to the lowered combustion temperature as a result of the water injection are partially compensated by the water-induced decrease in the average molecular weight of the combustion products. The combustion chamber, like the steam-gas generator, is fired by the electric system of the burner cups. All

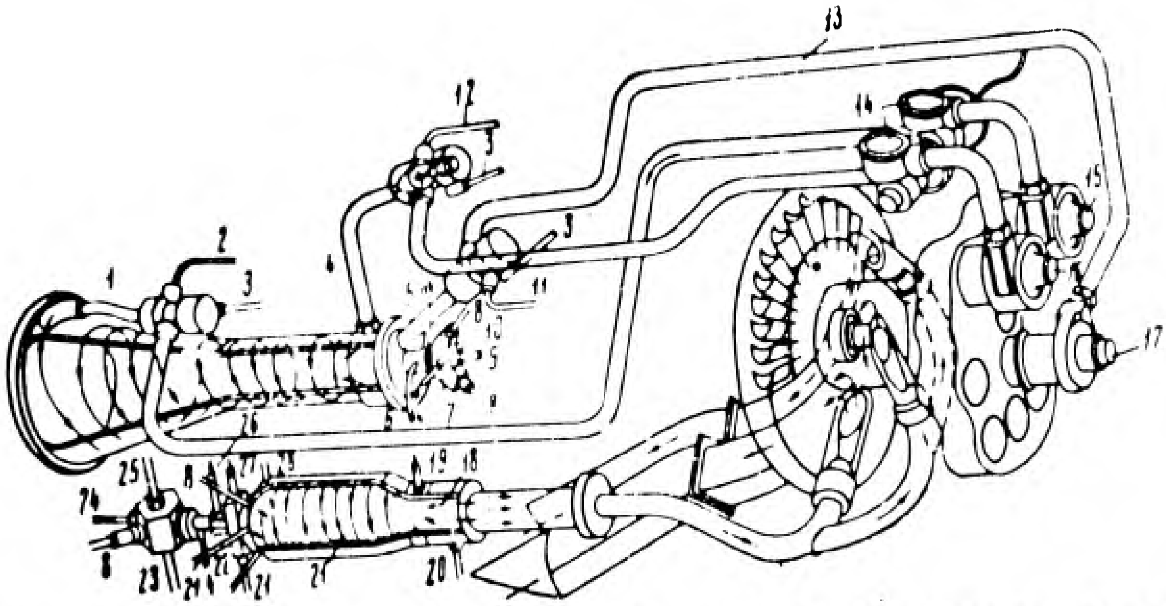

Fig.19 - Schematic Diagram of the Liquid-Propellant Rocket Engine "Screamer"

1 - Water supply to main chamber; 2 - Water valve; 3 - Delivery of nitrogen pressure to control system; 4 - Fuel to main chamber; 5 - Water supply to ignition system; 6 - Water discharge from ignition system; 7 - Fuel supply to main chamber ignition system; 8 - Ignition-system sparkplugs; 9 - Liquid oxygen feed to main-chamber ignition system; 10 - Gas pressure; 11 - Liquid-oxygen valve; 12 - Fuel valve; 13 - Liquid-oxygen feed to main chamber; 14 - Main flow regulators; 15 - Water pump; 16 - Fuel pump; 17 - Liquid-oxygen pump; 18 - Water injection into chamber; 19 - Coolant-water discharge; 20 - Feed of water for injection into steam-gas generator; 21 - Feed of liquid oxygen to steam-gas generator; 22 - Water inlet for ignition system of steam-gas generator; 23 - Gas pressure; 24 - Oxygen feed to ignition system of steam-gas generator; 25 - Fuel feed to steam-gas generator ignition system; 26 - Water outlet from ignition system of steam-gas generator; 27 - Coolant-water supply; 28 - Fuel injectors

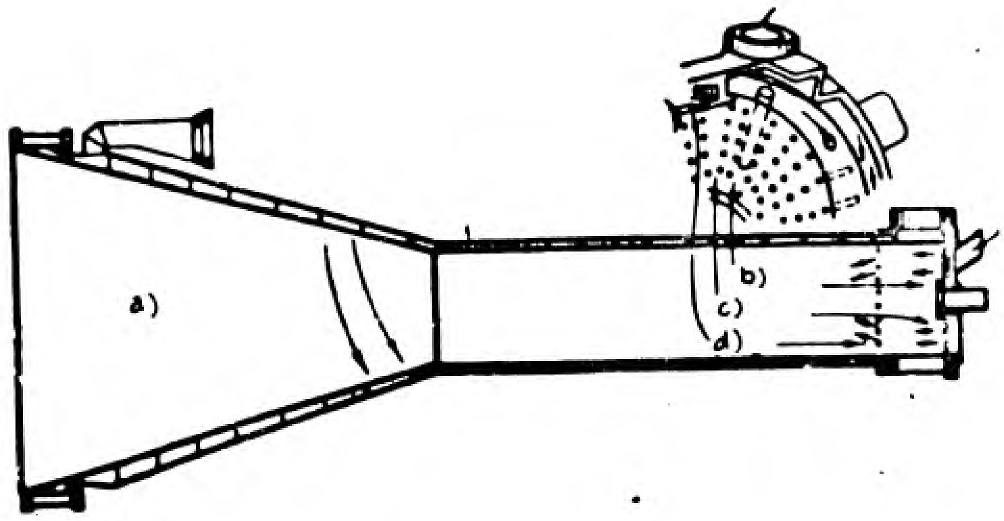

Fig.20 - Schematic Diagram of Combustion Chamber of Liquid Rocket Engine "Screamer"

a) Water circulation; b) Fuel; c) Oxygen; d) Water atomizers of the head are of the jet type.

The rated life of the engine is 25 hrs. A life of about 36 hrs was attained on the test stand, corresponding to over 1350 starts.

In connection with the improvement in the altitude properties of air-breathing engines, a rocket-powered fighter with a rocket engine would probably have a ceiling of 20 - 40 km or, in some cases, of 70 - 80 km.

Rocket aircraft have the following advantages over short-range fighters equipped with air-breathing engines:

1) Increase in engine thrust and aircraft speed with increasing altitude;

2) Exceptionally high rate of climb, which increases with altitude;

3) Possibility of obtaining particularly high thrust at small dimensions;

4) Excellent pickup and practically instantaneous starting;

5) At equal thrust, especially at high altitudes, considerably smaller frontal area and lower weight.

CHAPTER II

THE ROCKET ENGINE AS A HEAT ENGINE

Section 5. Heat Engines and their Classification

An operating machine assembly, consisting of a group of machines, performs all operations necessary to produce the finished product from the object or workpiece. The engine serves as the prime mover, and its force acts on those parts of the assembly which must transmit this action to the object of work.

The object of work, or workpiece, is converted into a finished product in a working machine, which exerts direct mechanical action on the workpiece. The engine and working machine are the two necessary and principal parts of a machine assembly. These are often coupled by a transmission mechanism, designed to transmit the motion, change its form, and regulate it.

An operator controls the operating conditions under which an article is processed by varying the action of the working machine. Such variation is obtained by manipulating the control elements of the working machine, of the prime mover and sometimes also of the transmission mechanism.

In certain modern and highly perfected machines, the process control is automatic, and the operator merely starts and stops the machine, or only starts it as is the case in most rocket engines.

A system of automatic program control of the processes must be considered a fourth important part of modern machine assemblies, characterizing its structure.

In rocket engines, this part is outstanding in its importance.

Table 4 gives the characteristics of the prime mover and the working machine.

If the movable and fixed parts of the engine and working machine are, to some extent, combined into a single integral unit, the machine assembly, under operating conditions, will have a generic name, reflecting some important feature of its operation or layout.

Table 4

Characteristics of Prime Mover and Performer

Type	Characteristics
Prime Mover	Generator of motion. Combination of interrelated bodies in which, by transformation of a body with a high initial energy concentration, motion is generated in a form useful for utilization in the performing machine.
Performer	Consumer machine, relative to the prime mover. An assembly of interrelated bodies which, by their motion, ensure performance of the specified technological process, consisting in the mechanical modification of the workpiece, its displacement in a field of force, or in a modification of its energetic state.

In an operating machine assembly or in an individual machine, for example a prime mover, two groups of bodies may be distinguished: a mechanism whose elements periodically convert motion into energy, and the working bodies or substances between which the exchange of energy takes place.

The first working body or working substance is the carrier of the natural energy utilized to generate motion. That element of the mechanism or that part of the element with which the working body interacts, is called the first working element of the machine. Thus, in an assembly with a piston engine, the working body (or working substance) is the gas mixture and the working element is the piston.

The body that is modified under the action of the working machine (or performer) must be considered the second working body. The part of the working machine which is in direct contact with the working body and which changes the state or form of that working body, is the second working element of the assembly. Such pairs may be the cutter plus the workpiece, the compressor piston plus the air, the propeller plus the air, etc.

Two working elements, two working bodies, and the transfer of energy and force between the two working bodies, represent a scheme which is entirely applicable to a prime mover or working machine taken separately. Figure 21 shows the general scheme of the classical machine assembly.

In addition to the principal working bodies, between which the intentional exchange of energy takes place, the machine system also includes other bodies of auxiliary importance for its operation. These include the cooling water, the lubricant, the atmospheric air surrounding the machine, etc. The lost portion of the energy usually is transferred to these bodies.

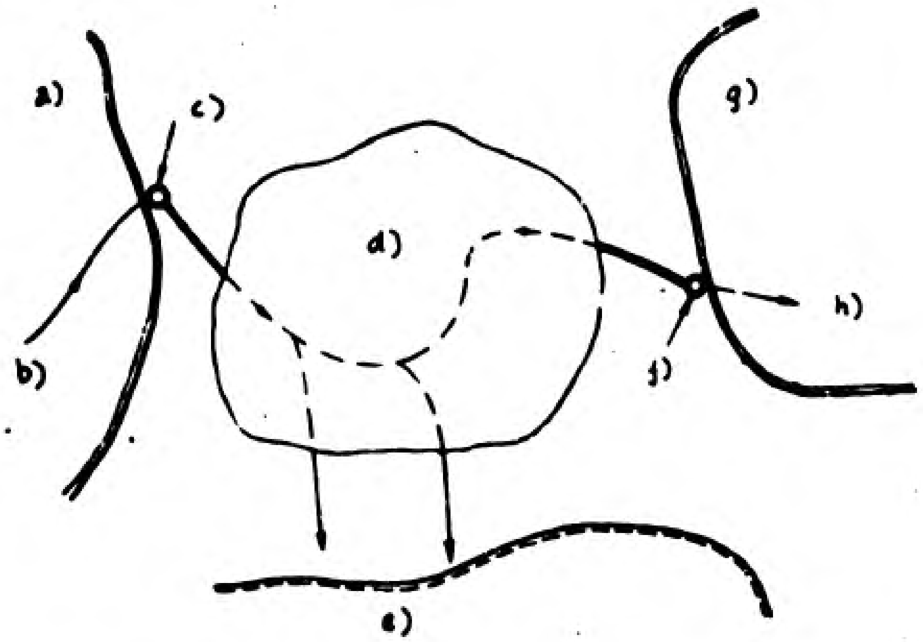

Fig.21 - Structural Schematic Diagram of a Machine Assembly

a) First working body (body - source); b) Energy being expended; c) First working element; d) Mechanism; e) Bodies to which the lost energy is transferred (surrounding medium); f) Second working element; g) Second working body (consumer - body); h) Energy usefully transferred (useful work)

The scheme of the classical machine may be greatly modified in specific cases. The working elements, for example, may be connected with each other, or separately with the working bodies, or the working bodies may be interconnected. The mechanism may be simplified to such a degree that only the working elements remain.

Table 5 shows the basic features of a machine, by which we may understand a prime mover, a working machine, or a complex group of machines designed to perform a definite technological process. Two working bodies, considered as the source of energy and its consumer, are necessary for any operating machine.

Table 5

Principal Technological Criteria of a Machine

Principle of Classification	Technological Criteria	Remarks
Machine structure	1. Presence of a mechanism (including the extreme case of the presence only of a working element). 2. Presence of two or more working bodies between which there is a useful transfer of energy caused by operation of the machine. 3. Presence of two or more working elements of the machine, representing parts of the mechanism adapted by design to absorb forces applied by the working substance.	1. Working elements in which the working bodies of the prime mover and working machine may be merged in a single physical body. 2. The working element and the working body may constitute an integral physical body.
Machine processes	1. Periodic operation. 2. Force interaction between the members of the machine mechanism and the working substance. 3. Utilization of natural energy in its natural or converted form. 4. Transfer of energy, usually with a change of form, from one body to another	The frequency of the periods may be infinite

As a technical device, a machine may also be considered without the working bodies, which is often done during its initial study. In this case, the action of the working bodies on the machine parts is replaced by the action of abstract factors, whose potential is expressed in physical units of measurement (for instance, in force).

The quantity of energy usefully transferred is generally termed the work and is measured in mechanical units, calculated from such indices of motion of the point of application of force to the second working body, as force and translation. In the vast majority of cases, a prime mover and a working machine are independent of each other, in the sense that one of the machines may be replaced by another one of the same type, without affecting the process in the first. Prime movers and working machines of this type are termed independent. Not all elements constituting the power plant are distinctly separate. In a simplified mechanism, it may be that only working machines are retained, as, for instance, in a motor compressor with free pistons. In the extreme case, for example in some reaction engines, the working elements are the only parts acting on the working substance in the same way.

Let us consider the operation of the ramjet engine shown in Fig.22, from the point of an observer on an aircraft.

The purpose of operating the assembly is to transfer the energy of the first working body, received in the chamber as thermal energy, in the optimum manner to a gas issuing from the exhaust nozzle as a high-velocity jet. Consequently, in terms of the definition of the conventional engine, in this case the working elements are merged into an integral whole, which is represented by a duct of variable cross section, whose inside walls exert a mechanical action on the working body.

The prime mover and the working machine are, in this case, physically represented by one and the same body.

The situation is different when the ramjet engine is viewed from the position of a ground observer. For him, the assembly also includes the aircraft, in which the ramjet engine is the thrust generator. In this case, the aircraft acts as the working machine or performer. Somewhere on the aircraft, there is a transfer of

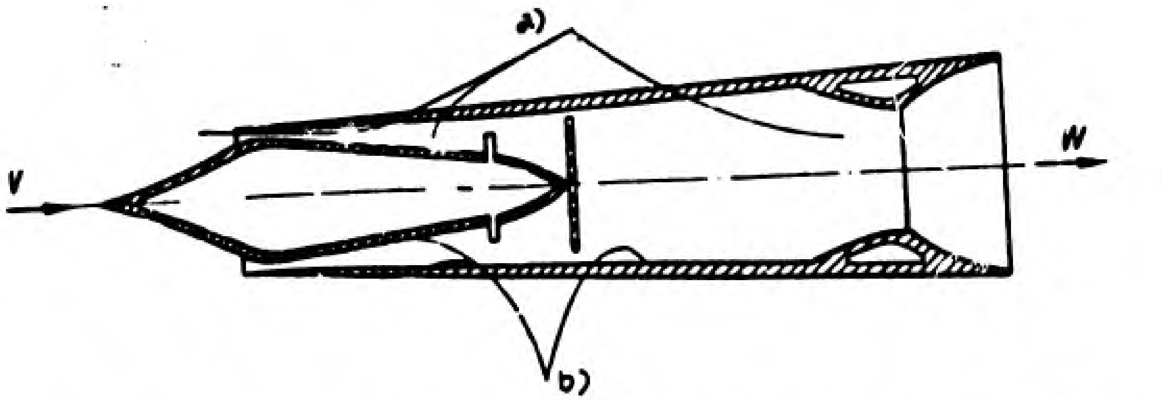

Fig.22 - Structural Schematic Diagram of Ramjet Engine, Seen by an Observer on the Aircraft

a) First and second working bodies; b) First and second working elements

force from the prime mover to the working machine and to the second working element of the engine or to the first working element of the aircraft (Fig.23).

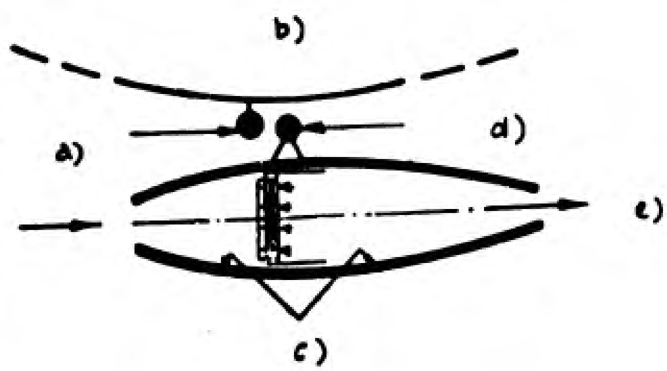

Fig.23 - Schematic Diagram of a Thrust Ramjet Engine

a) Second working body of prime mover; b) Aircraft - consumer; c) First working element of prime mover; d) Second working element of prime mover; e) First working body of prime mover

Consequently, in this case the working bodies, like the working elements, are separate.

Figure 24 shows a schematic diagram of an assembly with a rocket engine, which in totality constitutes a power plant. The line a-a arbitrarily separates the system of bodies belonging to the engine from the rest of the rocket, considered as the crew.

The engines schematically shown in Figs.23 and 24 are known as jet engines, and are considered prime movers without a mechanism.

The prime movers and performers include a large group of thrust producers, which group, in turn, includes reaction engines.

The purpose of a thrust generator is the direct production of the thrust necessary to move the vehicle (the working machine or performer). The primary factor in

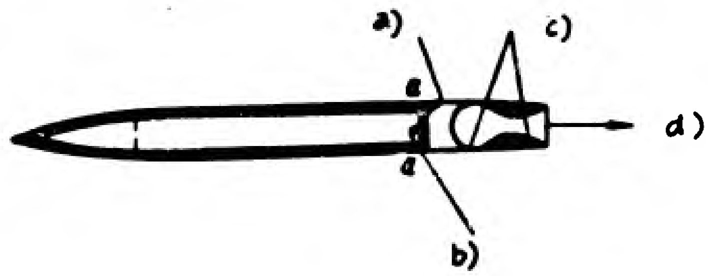

Fig.24 - Structural Schematic Diagram of a Rocket Thrust Engine

a) Second working element of prime mover; b) Second working body of prime mover; c) First working element of prime mover; d) First working body of prime mover

the operation of a thrust machine is that the thrust is produced by its working body.

The universal index of efficiency of an independent prime mover (i.e., the power), as noted in Chapter I, is unsuitable to evaluate the operation of a thrust machine; the principal quantity characterizing the quantitative aspects of its operation is the thrust.

Table 6 gives the designations of the principal groups of engines according to conditions of their availability and utilization.

In primary engines, energy is utilized in its natural form - chemical, nuclear, or mechanical; in secondary engines, the energy used is obtained artificially, for instance electric energy.

A steam engine using steam from an electric boiler, which in turn is fed by current from a hydroelectric power station, is a secondary engine.

When the working body itself contains energy in the active form, i.e., thermal,

Table 6

Principal Groups of Engines

Characteristics of Group	Type of Engine Group
Form or type of energy utilized	Chemical, Heat } Heat Electrical Mechanical (hydraulic, wind-powered, etc.) Radiation (solar, etc.) Nuclear Compound type
Degree of utilization of natural energy	Primary Secondary
Character of utilization of natural energy	Engines of direct utilization Conversion engines
Source of working body	Medium (atmospheric, water, solar, etc.), i.e., engines with an external source of working substance. Engines carrying a supply of working substance, i.e., with an internal source
Connection with working machine	Independent engines Working-machine engines

electrical or mechanical energy, the action of force on the working element of the engine will be direct, and the working process will not be accompanied by any change in the form of that energy. Direct-utilization engines operate under such conditions.

The greatest supplies of natural energy, however, exist in the potential form only (chemical, nuclear), so that in most cases the energy introduced must first be converted into a different form in engines, and in this converted form the energy is utilized for its direct purpose.

The class of conversion engines includes steam engines, internal combustion engines, and various nuclear engines.

Figure 25 shows several schemes of engines and assemblies which may be utilized

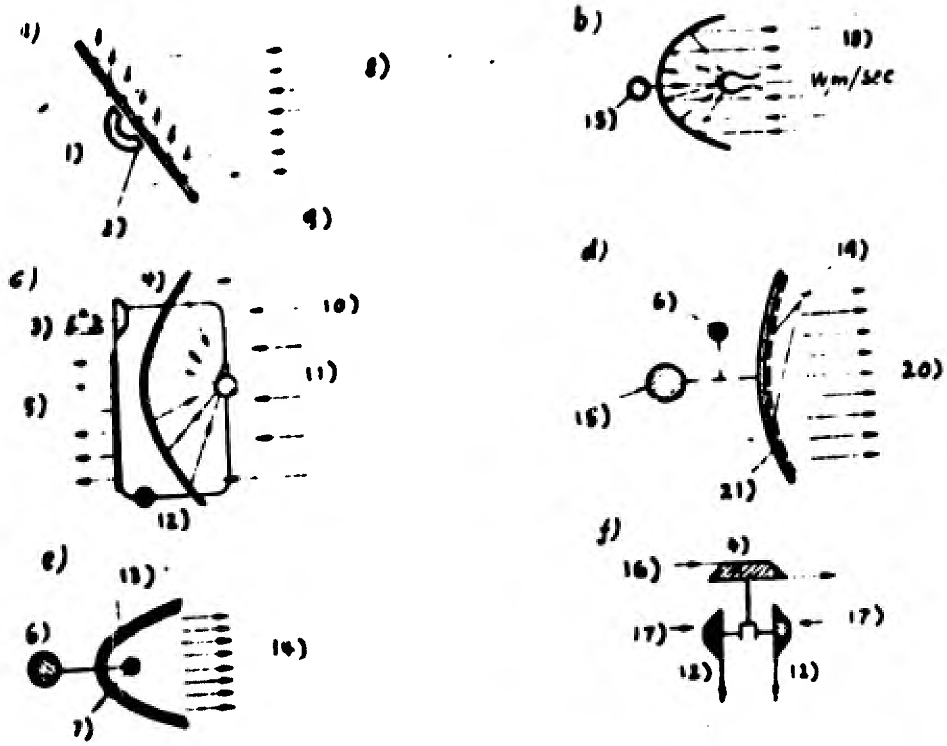

Fig.25 - Several Schemes of Prime Movers and Assemblies

a - Structural scheme of solar cosmic unit (primary direct-utilization solar engine); b - Scheme of thermosolar reaction engine (secondary solar reaction engine-transformer with its own supply of mass); c - Scheme of independent secondary thermal engine-transformer with constant supply of working substance; d - Primary nuclear engine and working machine-transformer, with its own supply of mass; e - Primary nuclear engine and working machine-transformer utilizing only the mass of the fuel; f - Scheme of turbopump unit (machine assembly)

1) Second working body (mass of ship); 2) Second working element; 3) Dynamo; 4) Turbine; 5) Light condenser; 6) Nuclear fuel; 7) Source and site of nuclear reaction; 8) First working body (protons); 9) First working element; 10) Photons; 11) Steam generator; 12) Pump; 13) Reflector; 14) Reaction products (photons, nuclear fission fragments, etc.); 15) Supply of mass; 16) First working body; 17) Second working body; 18) Rays; 19) Nuclear explosion in medium of inert mass; 20) Products of working body; 21) Screen

primarily as rocket engines. The inscriptions beneath the diagrams correspond to the definitions of Table 6.

In selecting a generic name for engines, the general rule is usually to reflect one specific principal feature, such as the purpose, or some peculiarity of the process, the working body, or the design. For this reason, many engines have been given designations that are not particularly fortunate. Such misnomers include liquid jet engine, turboprop engine, etc.

According to Table 6, heat engines include chemical engines and pure heat engines. In heat engines, the principal working process consists of a cycle of alternating thermal phenomena. In chemical engines, the energy in its original state is in the chemical form and is converted into heat during operation of the engine. In both cases, the working substance entering into direct interaction with the parts of the engine possesses energy in the thermal form; and the most important processes determining the efficiency of engine operation are thermal processes.

A heat engine has numerous and diverse characteristics, especially in view of its rich historical past and widely varying interrelation with human activity. For this reason, the concepts used as basis for the classification of engines may also vary widely.

Figure 26 shows the classification of the principal types of heat engine-converters. According to this classification, engines in which two or more working bodies interact and in which an intermediate mechanism is used belong to one of the two groups; these are, as a rule, self-contained engines.

The second group includes working machines, being mostly thrust machines, as well as engines whose working bodies markedly differ from each other (motor compressor with free pistons, Humphrey pumps, etc.), and working machines characterized by partial or total merger of the working bodies and the working elements (reaction engines); in the latter, the reactions of the second working body whose kinetic energy is increased determine the useful work transferred to the working machine.

Some reaction engines are simple, since all their parts are fixed and only have to absorb the reaction of a flowing jet of the working substance (jet engines); others are complex, since they also have machine plants to improve the process (gas-turbine engines)

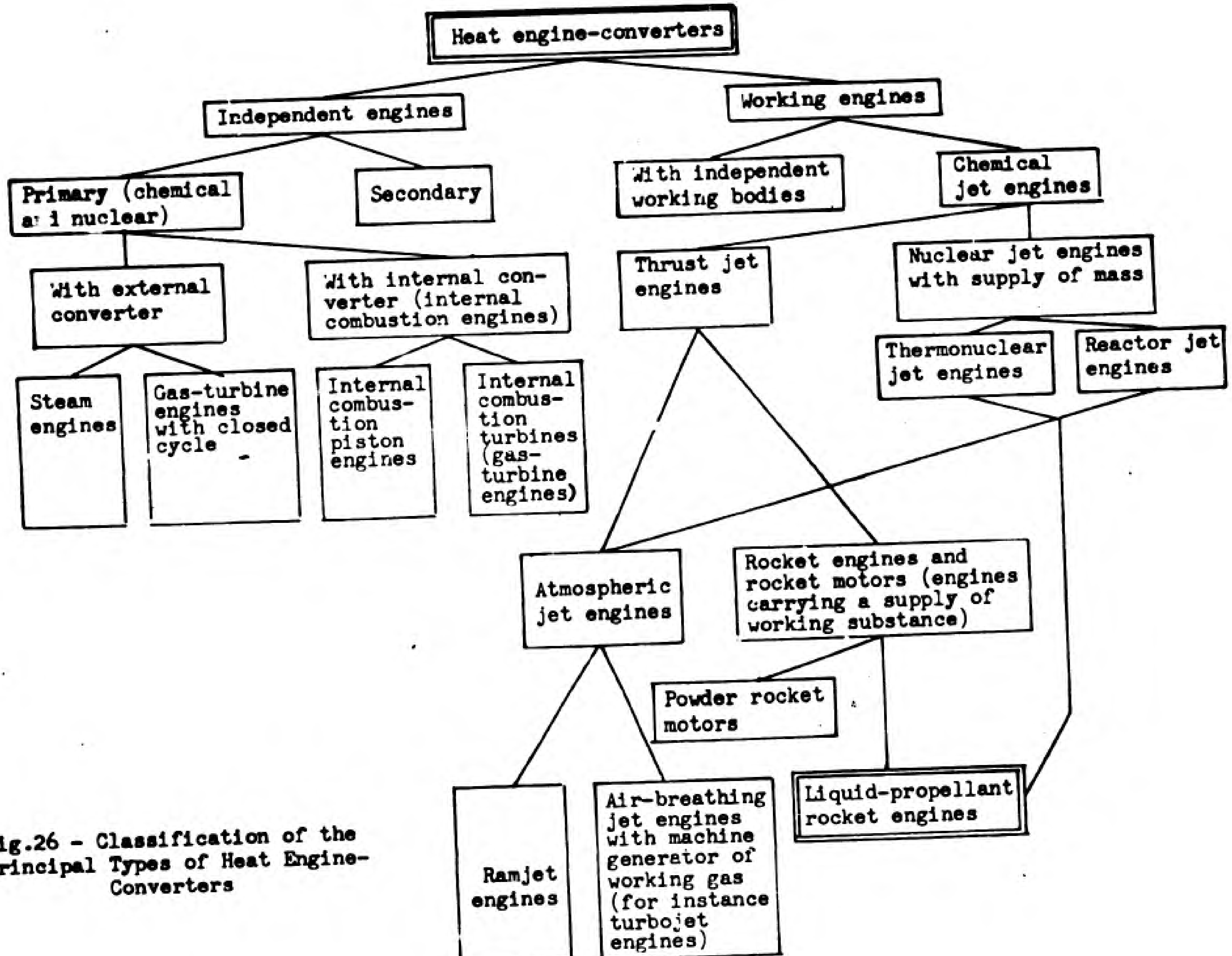

Fig.26 - Classification of the Principal Types of Heat Engine-Converters

In reaction engines, the thermal processes are so intimately connected with gas-dynamic processes and the significance of the gas-dynamic processes is so great, that the term heat engine does not reflect the most important factors in the working process. In order to cover the important role played by the conversion of thermal energy into the velocity-energy of the working substance, such engines would have to be called heat-jet engines.

The chemical-reaction engines in widest use today are subdivided within the general scheme into two forms: those making use of the ambient medium - for example, air-bre g jet engines - and rocket engines carrying their own supply of working substance.

In air-breathing jet engines, the atmosphere serves as the source of working fluid. The fuel itself (the supply proper) constitutes only 1/20 to 1/50 of the oxidizer in the working mixture, i.e., in the atmospheric air that source is inexhaustible. The rocket engine may be defined as follows: a modern rocket engine being a thrust heat-jet working machine, independent of the ambient medium.

Section 6. Rocket Engines

Any classification is usually based on an effort to bring out the differences of the object by means of some group of characteristic criteria. An engine classification can be based, for instance, on such criteria as purpose, design, working process, features of the fuel-feed system, and control.

We shall now present a classification of rocket engines, based on the operating requirements, according to the energy sources used, since the physical and chemical properties of the propellant, the carrier of energy, largely determine the layout of the engine assembly, the design of its important units, and some of the important features of the working process in the chamber. This fundamental criterion is supplemented in the classification by certain other important properties of the engine.

The classification includes nuclear rocket engines carrying their own supply of mass; for brevity, we shall term these gas-nuclear rocket engines.

In Fig.27 we give the designations for the groups of rocket engines and the

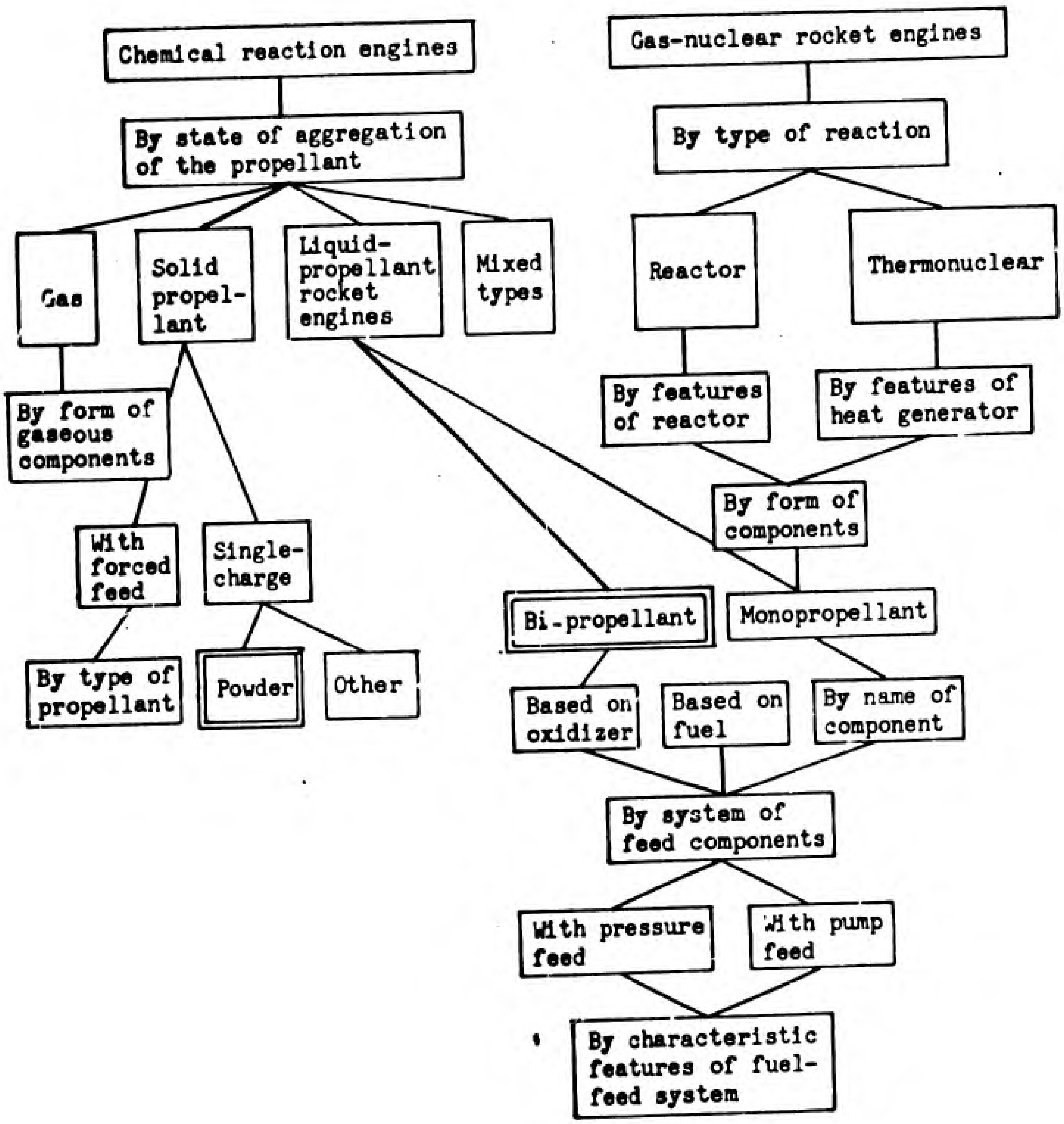

Fig.27 - Classification of Rocket Heat Engines

criteria according to which the specialized definitions are established. The double lines in the flow sheet separate the two-component liquid rocket engines and powder rocket motors, which are widely used in operation.

The criteria for the substantial difference between various types of chemical rocket engines are listed in Table 7. The type of propellant and the method of feeding it to the chamber have a substantial influence on the layout of the propellant-feed system which, in rocket engines, is considerably more complex than in other types of heat engines, and likewise affect the design of the power plant and its operating characteristics.

Several typical schemes of rocket engines, to illustrate the data in Figs.26 and 27 and Table 7, are described below. The fuel-feed systems are considered in the description in simplified form, and the control systems and automatic systems

Table 7

Classification of Chemical Liquid-Propellant Rocket Engines

Criterion of Classification	General Definition of Engine Group	Specialized Features of Definition
Form of propellant used	Single (monopropellant)	By type of fuel (peroxide, etc.)
	Bipropellant	By type of oxidizer (oxygen, nitric acid) By peculiarities of fuel
Method of feeding	With pressure feed	Gas-generator feed system Powder pressure-storage feed system Hydraulic storage feed system
	With pump feed	Turbopump assembly (TPA) named after the principal components: Turbopump assembly using monopropellant Turbopump assembly pumping coolant for liquid rocket engine By features of pumps and turbines

are disregarded. The notation for the schematic diagrams is given in Table 8.

One of the forms of a mixed bipropellant rocket engine is shown in Fig.28. Solid fuel is applied to the chamber walls and liquid oxidizer is fed from a separa

Table 8

Notation used in the Rocket Engine Diagrams

Notation	Form
Main-component tanks:	
Systems with loaded tanks	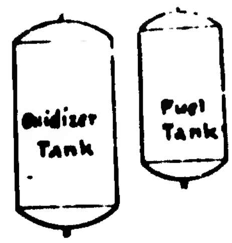
Systems with unloaded tanks	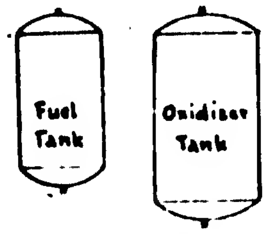
Auxiliary-component tanks	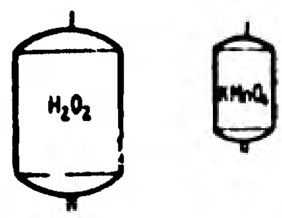
Combustion chambers:	
cooled	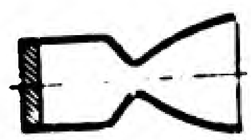
uncooled	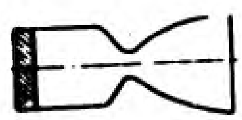
powder	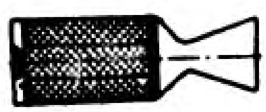

(Continued)

Table 8 (Cont'd)

Notation	Form
Gas-generators	
Pressure accumulators: pneumatic (VAD)	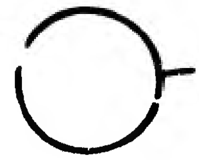
powder (PAD)	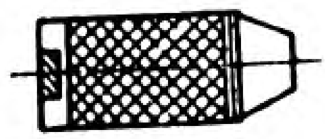
Liquid gas generators:	
generator in which the gas is the reaction product of decomposition of the components (hydrogen peroxide + + potassium permanganate, etc.)	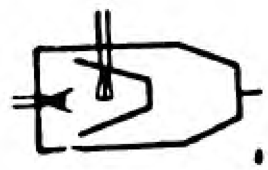
generator in which the gas is the product of the oxidation reaction of the main or auxiliary components	
Atomizers	
oxidizer	
fuel	
bipropellant (or atomizer of monopropellant)	
Piping:	
with gas	
with liquid	
Units:	
turbine	

(Continued)

Table 8 (Cont'd)

Notation	Form
pump	
gas reducer	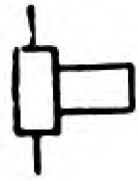
gas reducer combined with pyrotechnic cartridge	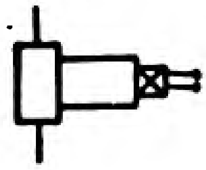
electrohydraulic valve (EHV)	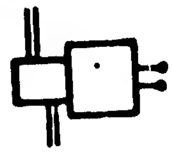
electropneumatic valve (EPV)	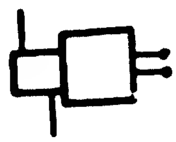
hydraulic valve controlled by air	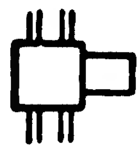
burst diaphragm	
relief valve	
pressure relay	
cock or valve	

tank; compressed gas, neutral to the oxidizer, is supplied from a separate bottle to feed the oxidizer. In 1933 - 1934, such an engine and the rocket in which it was installed were tested by M.I.Tikhonravov. Gasoline jelly was used as the fuel and liquid oxygen as the oxidizer.

In Germany in 1943 - 1945 work was also done on such a rocket, using graphite

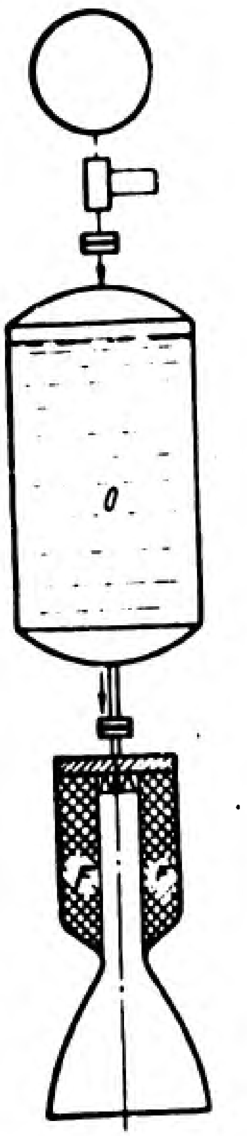

Fig.28 - Schematic Diagram of Bipropellant Rocket Engine with Solid Fuel Housed in Chamber

0 - Oxidizer; F - Fuel

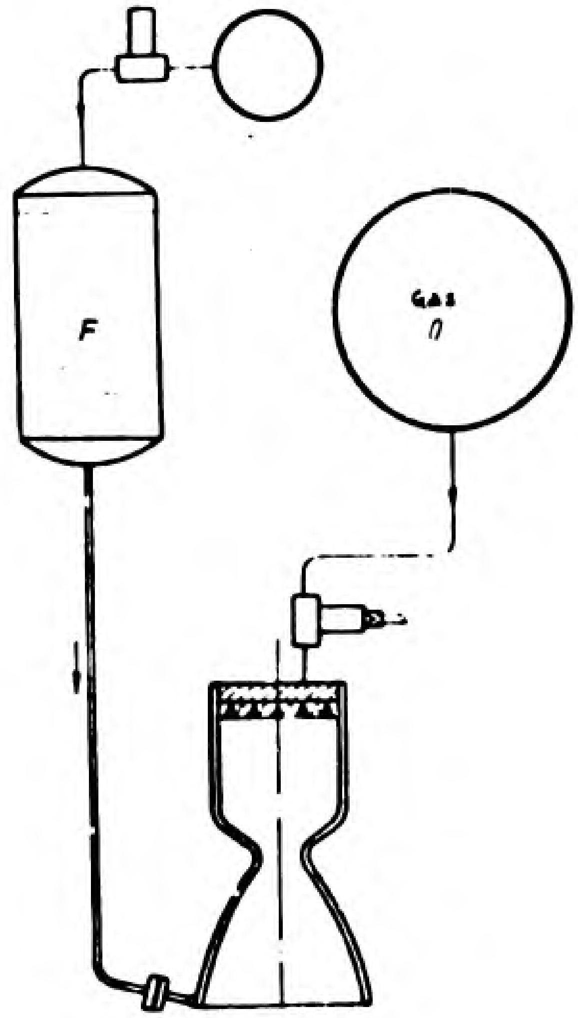

Fig.29 - Schematic Diagram of Bipropellant Rocket Engine with Gaseous Oxidizer

0 - Oxidizer; F - Fuel

and liquid nitrogen dioxide as components. Figure 29 shows an example of the system of a bipropellant mixed engine with one of the components being a gas.

The Schmidding rocket, in which the components were oxygen compressed to 220 atm and an 88% solution of methanol in water (P_{sp} = 180 kg/kg-sec) is well known.

Mixed engines in many cases are convenient for research and laboratory work.

Figure 30 shows a schematic diagram of a powder rocket motor. In this motor, the chamber walls are usually not cooled, the pressure in the powder chamber is considerably higher than in liquid engines, and the ratio between critical cross sec-

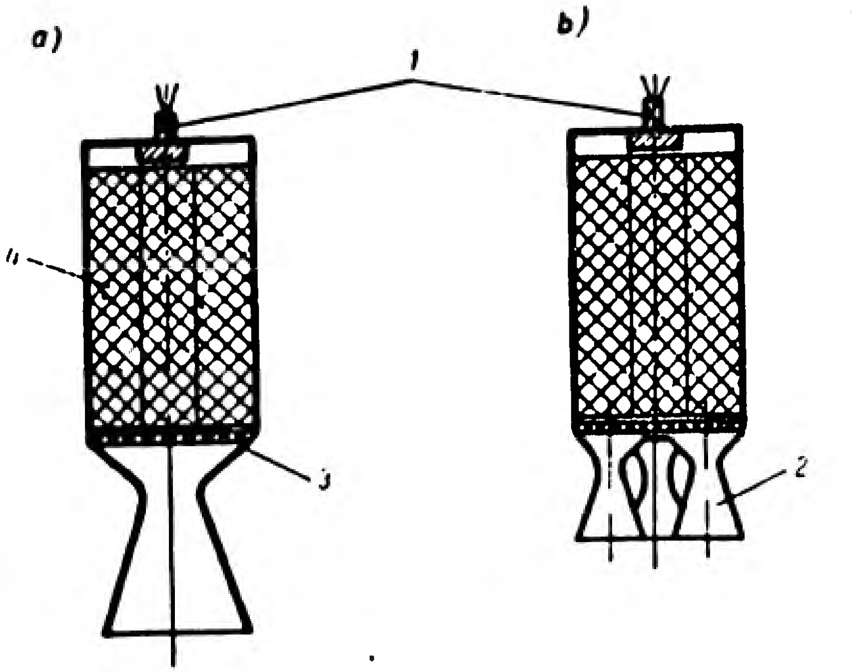

Fig.30 - Schematic Diagram of Powder Rocket Motor

a - With a single nozzle; b - With four nozzles

1 - Ignition; 2 - Four nozzles; 3 - Diaphragm; 4 - Powder

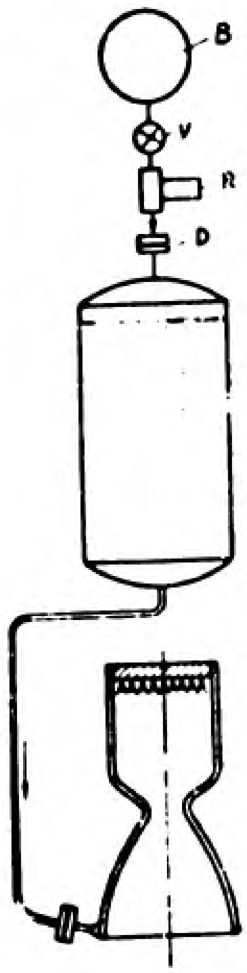

Fig.31 - Arrangement of Liquid Rocket Engine with Monopropellant and Pneumatic Pressure Storage

tion and chamber cross section is smaller, while the relative length of the chamber is greater.

A different mass burning velocity of a powder may be obtained by changing its type, or the shape of the grains, or by controlling the burning surface with the aid of a protective layer.

Among liquid rocket engines, monopropellant engines are the simplest. In the engine shown in Fig.31, the fuel, forced from the tank into the chamber by the air stored under high pressure in the bottle B, first flows into the jacket surrounding the chamber and then enters the atomizers in the chamber head.

On the way to the propellant tank B, the air passes the shutoff valve V, the reducer R, and the burst diaphragm D.

In the USSR, experiments have been made on a liquid monopropellant (60% nitrobenzene and 40% nitrogen tetroxide) by Engineer V.A.Shtokolov.

A monopropellant has a low heat value. Of all the forms of monopropellants, the best known is hydrogen peroxide, with which a large number of rato units are fired, (80% H_2O_2 solution in water).

The advantage of a bipropellant fuel system over the monopropellant system primarily is the considerably higher heat value that can be obtained with two components. A particular shortcoming of this system is its failure to consume a certain portion of the propellant.

Owing to the unavoidable fluctuations in the technology of manufacture and the assembly of the feed system, the discharge conditions from the propellant tanks differ from the rated values.

As a result, one of the components is consumed somewhat earlier than the other, and the residue of the second component is an addition to the structural mass of the rocket M_k. Moreover, in order to avoid repeated flash at burnout, and to obtain a reliable full combustion of the fuel in the chamber, one of the components must be present in somewhat greater quantity than required by calculation, thus diminishing the actual mass ratio μ of the rocket.

The system of the bipropellant engine with pressure feed is widely used today (Fig.32). The oxidizer O and the fuel G are stored in separate tanks. One of the components (less often, both) is used for external cooling of the nozzle and chamber walls. The components are expelled from their tanks by air or an inert gas (nitrogen) stored in a cylinder (Fig.32 a); by air preheated in a special chamber and possessing high specific volume (Fig.32 b) or by gas formed in the liquid pressure accumulator (LPA), to which the liquid propellant flows (Fig.33), or by gas

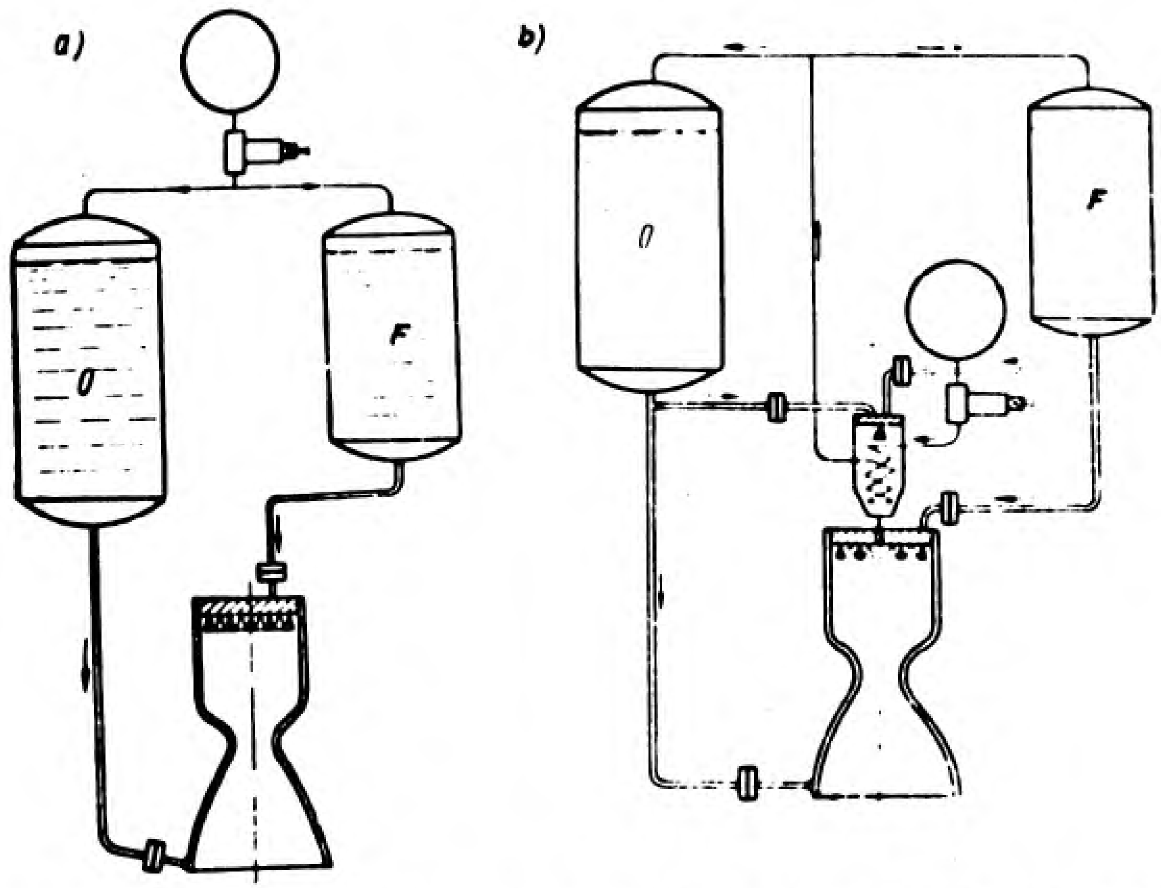

Fig.32 - Schematic Diagram of Bipropellant Liquid Rocket Engine with Pressure Feed

a - Pneumatic pressure accumulator; b - Preheated pneumatic pressure accumulator

from a small powder chamber, a powder pressure accumulator (PPA), shown in Fig.34. Such systems are suitable for expendable rockets. The repeated starting necessary for an aircraft engine is ensured by more complex feed systems. Figure 35 is an example of a bipropellant rocket engine with gas-bottle feed, permitting the engine to be started and stopped several times; to start and stop it, there is a cutoff hydropneumatic valve (1), controlled by the double-action electropneumatic valve (2). When the pressure in the feed system and the chamber reaches a certain level, the two pressure relays (4) switch on signal lamps in the control cabin. The throttle cock (3) may be used to decrease the feed pressure and thrust of the chamber.

Some rockets used a piston propellant feed system (Fig.36). The need for

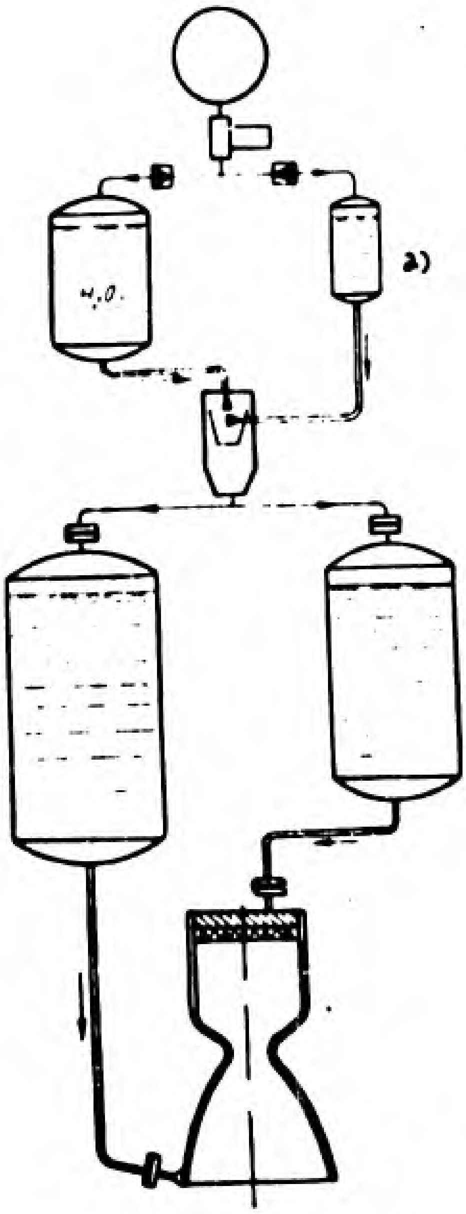

Fig.33 - Schematic Diagram of Bipropellant Liquid Rocket Engine with Pressure Feed (Chemical Pressure Accumulator)

a) Potassium permanganate ($KMnO_4$)

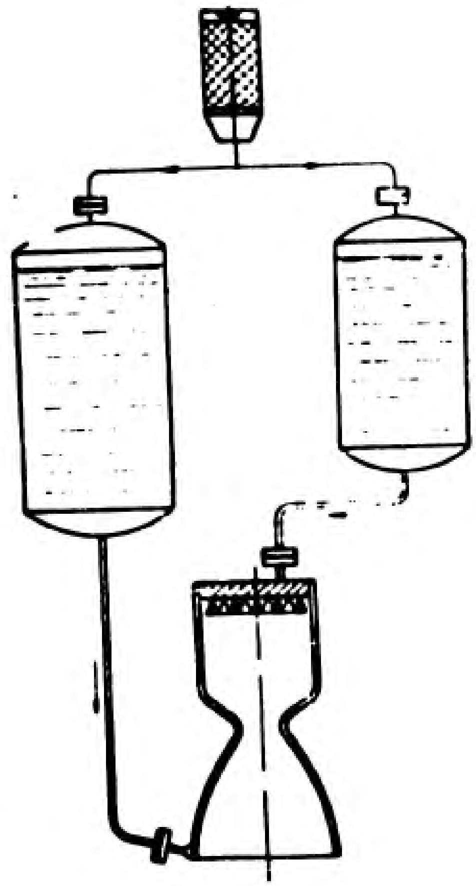

Fig.34 - Schematic Diagram of Bipropellant Liquid Rocket Engine with Pressure Feed (Powder Pressure Accumulator)

packing the piston along its circumference and protecting it from pitting complicates such a system and makes it less reliable than other pressure systems.

The main working body may also serve as the source of energy for the displacing gas. In this case the displacing substance, for example nitrogen, is charged into a gas generator in the liquid state. A small quantity of gas is withdrawn from the chamber into the gas generator, where evaporation takes place at elevated pressure. The evaporation products are fed to the propellant tanks. Figure 37 gives a schematic diagram of the oxygen evaporators used in the power plant of the V-2 rocket to

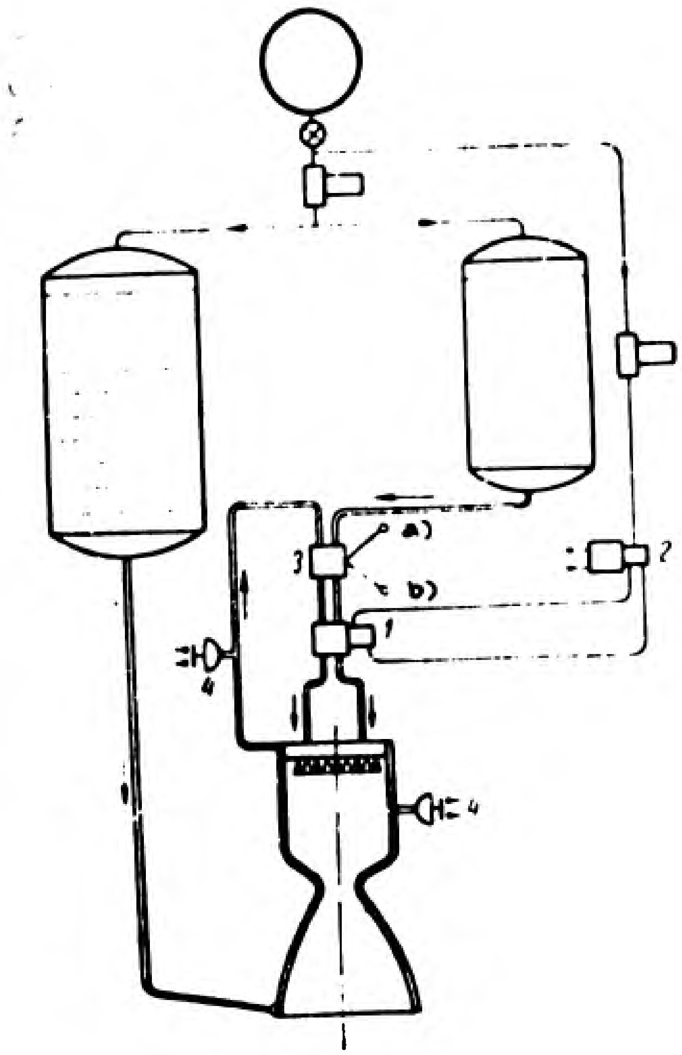

Fig.35 - Schematic Diagram of Bipropellant Liquid Rocket Engine with Pressure Feed and Repeated Starting

a) Regime I; b) Regime II

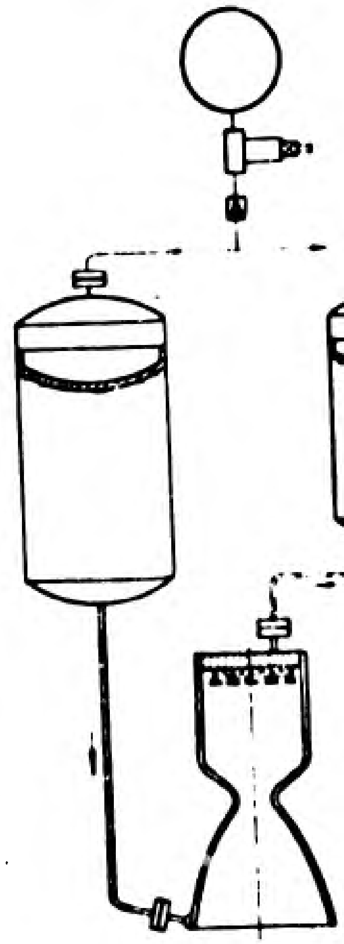

Fig.36 - Schematic Diagram of Bipropellant Liquid Rocket Engine with Piston Feed of Propellant

produce a slight head in the oxygen tank. The tanks in the pressure feed system are under a higher pressure than exists in the chamber.

An increase in the size of the tanks and an increase in the combustion-chamber pressure increases the weight of these units, and therefore pump feed of the propellant is preferred in large rockets (Fig.38). Here each component is fed to a pump (usually of the centrifugal type) from its own tank, and then enters the chamber. The pumps are driven by an engine, usually a turbine engine, using a working fluid consisting of either the decomposition products of hydrogen peroxide or other substances with a high heat of decomposition, the combustion products of

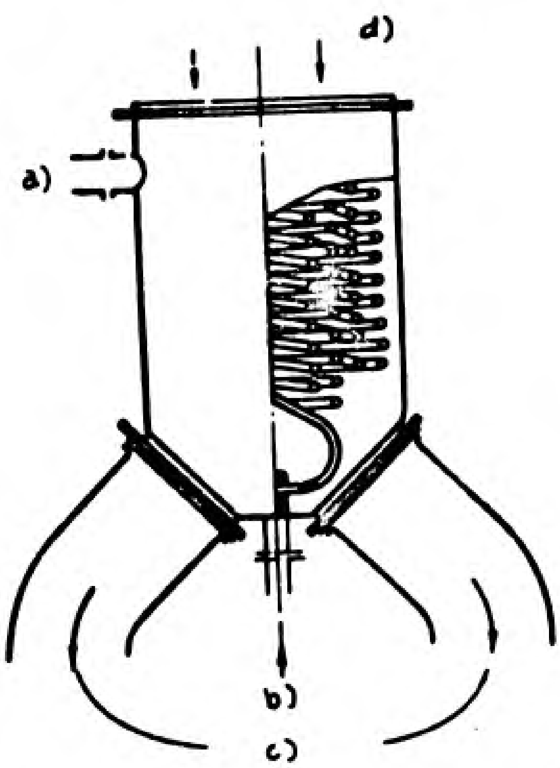

Fig.37 - Evaporator for Pressurizing the Oxygen Tank in the V-2 Rocket Engine

a) Oxygen gas in drainage pipe and tank for oxygen pressurizing;
b) Liquid oxygen; c) In atmosphere;
d) Spent steam gas from turbine

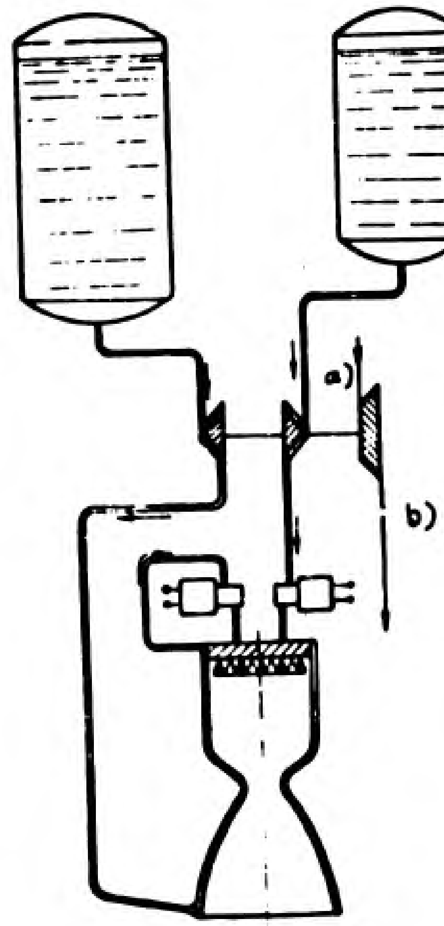

Fig.38 - Schematic Diagram of Bipropellant Liquid Rocket Engine with Pump Feed of Propellant

a) From steam-gas generator;
b) To exhaust nozzle or to tank pressurization

powder, gases withdrawn from the main chamber or produced from the main components in a separate generator, or else vapor of the substance used for cooling the chamber walls. The additional weight of the turbopump assembly and its feed system should be considerably less than the saving in tank weight when pressure is no longer used in them. To avoid cavitation in the high-speed pumps of the turbopump assembly, the tanks are pressurized.

The greatest range, velocity, thrust, and altitude have been obtained by using a liquid rocket engine (LRE) with a turbopump assembly (TPA).

In a nuclear heat engine, the reactor is of great importance. In it the working fluid of the engine receives the heat from the disintegration products of the nuclear fuel.

Figure 39 gives the schematic diagram of a nuclear rocket engine, utilizing the disintegration of nuclear fuel. The working substance in the heat-exchanger

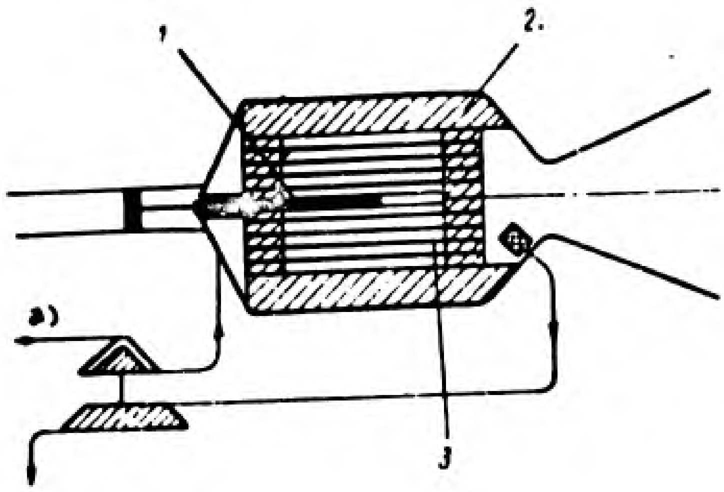

Fig.39 - Schematic Diagram of Nuclear Rocket Engine with Heat-Exchanger Reactor

1 - Control rod; 2 - Neutron reflector; 3 - Reactor

a) From tank

reactor receives the heat from the surface of the solid substance enclosing the fuel As in modern atomic reactors, the disintegration is controlled by means of a control rod. Figure 40 is a schematic diagram of a hypothetical thermonuclear rocket engine The working substance enters the chamber along all wall surfaces, thus protecting them from overheating. Since the temperature of the plasma along the axis of the chamber is measured in millions of degrees, the temperature of the gas in its cross section must vary sharply. Gas-dynamically, the heat-transfer chamber is a heat co sumer. If the gas in the chamber is accelerated to sonic velocity, no constriction in the exhaust nozzle is needed.

The working process of the propellant feed system with turbopump assembly is frequently, directly or indirectly, connected with the main process in the chamber. Table 7 shows the principal versions of pump-fed systems. The consumption of energy or propellant in the pump system is always taken into account in estimating the economy of a rocket engine.

Let us consider the most widely used and most interesting systems of propellant feed by a turbopump assembly. Figure 41 gives a typical schematic diagram of an

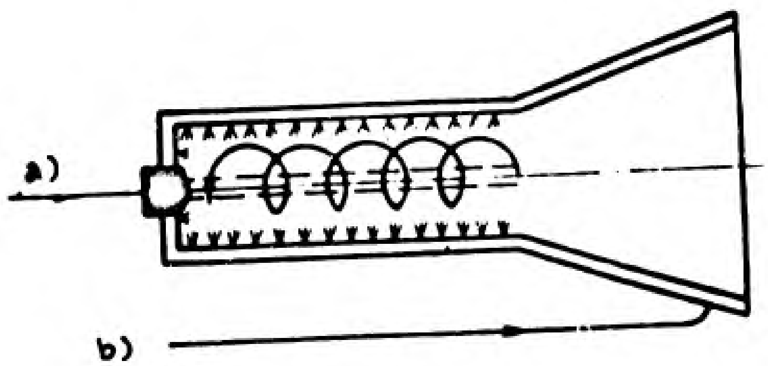

Fig.40 - Schematic Diagram of Thermonuclear Rocket Engine with Ejection of Active Mass

a) From energy source; b) From pump

independent turbopump assembly with hydrogen peroxide which is widely used today in systems of this type in rockets made in other countries. The desire to give the rocket a minimum quantity of working fluid is natural; therefore, gas generators using the principal components of the rocket propellant are becoming increasingly popular. As far back as 1937 it was shown that a gas generator could operate on nitric acid and kerosene, at a moderate gas temperature, provided water was also introduced. The gas temperature may also be decreased to the levels permitted by the heat resistance of the turbine blades, by using extremely rich or extremely lean mixtures in the gas generator.

Figure 42 gives a schematic diagram of a turbopump assembly, using the main propellant components. The necessary gas temperature is established by selecting the component ratio for the gas generator. The exhaust gases from the gas generator are discharged to the outside through the exhaust nozzle but, more often, are fed in part to the tanks to pressurize them. Figures 43 and 44 show versions of chamber-gas utilization in the turbine. In the first case, the gases withdrawn from the

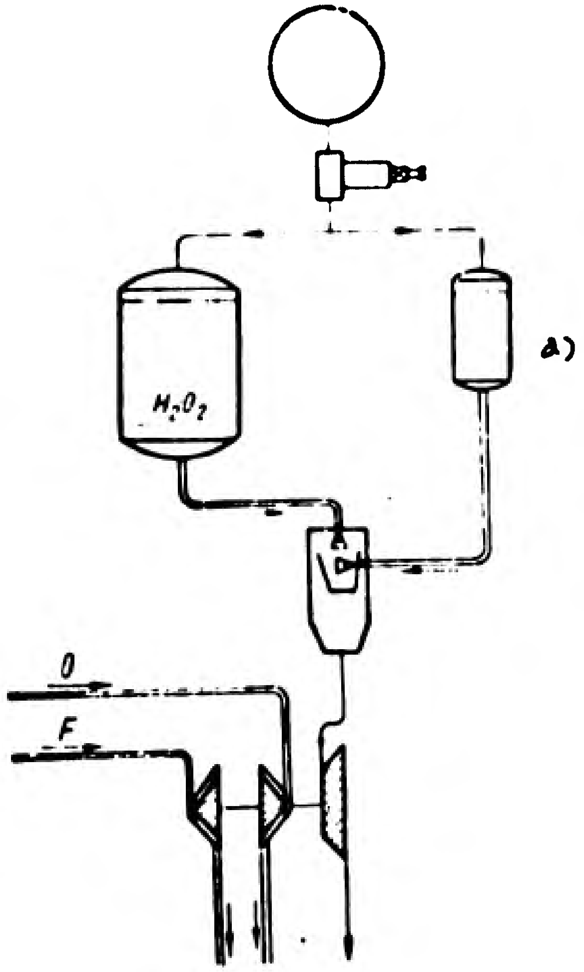

Fig.41 - Schematic Diagram of Gas Generator for Turbopump Assembly, Using Hydrogen Peroxide

a) Potassium permanganate ($KMnO_4$)

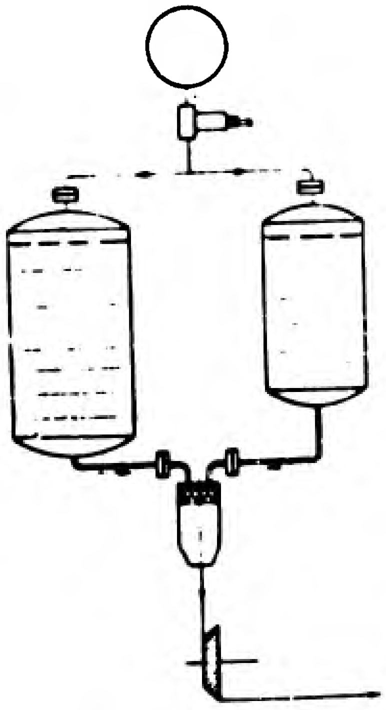

Fig.42 - Schematic Diagram of Chemical Gas Generator with Pressure Feed, Using Main Propellant Components

chamber enter the steam generator, where the working fluid of the turbine is evaporated; in the second case, the gas is passed through a turbine, eliminating the need for additional working fluid. Consequently, the chamber acts as the gas generator in this case, which simplifies the feed system as a whole.

Such a system, however, requires high-temperature turbines. A coolant injected between chamber and turbine, or injection of fuel into the tapped gas, will lower the temperature of the gases entering the turbine.

Figure 45 shows a system in which the greater part of the working fluid passes successively through the turbine and the chamber. First, with an excess quantity of one of the components, gas formation takes place in the gas generator. The working substance then enters the turbine at moderate temperature, and goes from there

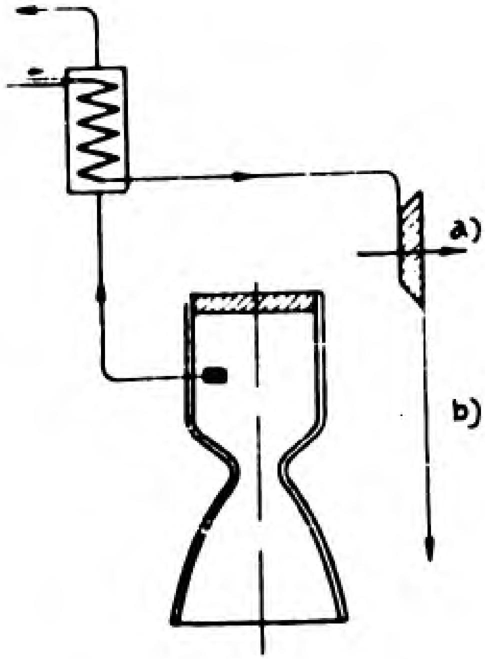

Fig.43 - Schematic Diagram of Turbopump Assembly, with Withdrawal of Gas from the Chamber

a) To pump, b) To exhaust nozzle or to tank pressurization

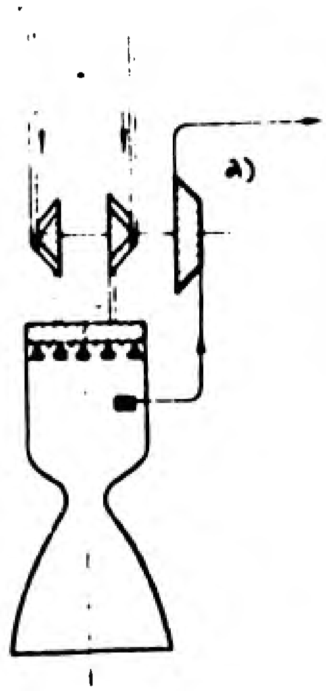

Fig.44 - Schematic Diagram of Steam Generator, Using Gas Withdrawn from the Chamber

a) To exhaust nozzle or to tank pressurization

to the chamber. The component not utilized in the gas generator is fed for cooling into the chamber jacket and then into the chamber itself into the gas jet issuing from the turbine. An additional reaction between the components raises the temperature of the gases in the chamber, which in this case is supplied with components in the gas and in the liquid phase. If one of the components is liquified gas which is evaporated in the gas generator while feeding a small quantity of the second component to the generator (internal-combustion gas generator), then the turbine may be "cold", i.e., operate at a gas temperature of about 50 - 100°C.

The working fluid of the turbopump assembly may also be heated in the cooling jacket of the chamber (Fig.46). In this case, the water heated in the jacket under high pressure will serve as the working fluid of the turbopump unit. In the separator, the condensate is separated from the steam. The separated steam is routed to the turbine and then into a condenser cooled by the cold component, for instance oxygen. The condensate enters a low-pressure pump. On leaving the pump, it is mixed with the liquid separated in the separator and cooled in its own heat exchanger. The liquid is supplied to the high-pressure pump and is directed under high pressure into the cooling jacket of the chamber. For reliable cooling of the chamber, it is preferable not to produce the steam in the cooling jacket but by throttling the liquid where it leaves the jacket.

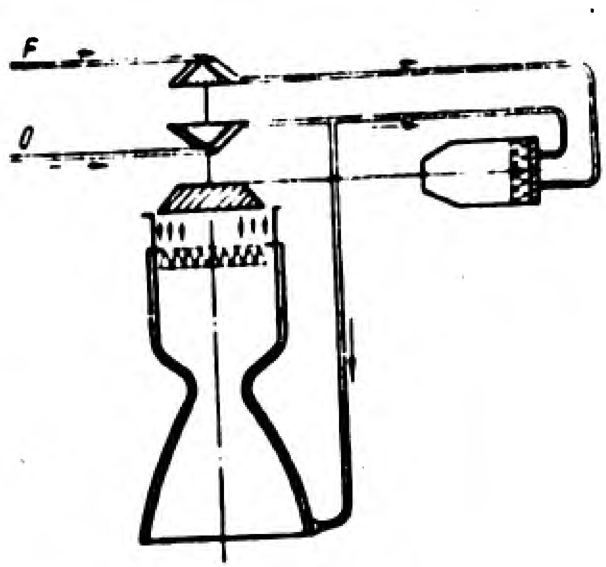

Fig.45 - Successive Coupling of Turbopump Assembly with Combustion Chamber of Rocket Engine

In this system, the turbine operates on saturated steam. Superheated steam, however, may also be used, including the vapor of one of the main components if it is suitable for this purpose (for example, ammonia, methane, and other fuels). Systems of this kind are complicated, and their use is justified only in high-power rocket engines.

It is entirely possible that an electric drive will be used for the pump in large power plants (Fig.47). In this case, a turbodynamo serves as the source of electric power. High-power and lightweight equipment for the machineless production of electric current has not yet been developed.

Section 7. Aircraft and Rocket Engines

Rocket engines, like air-breathing aircraft engines, are heat engines which are in particularly wide use as transport engines.

In air-breathing engines which use air as the oxidizer, the fuel consists of a liquid prepared mainly from petroleum.

Artificial propellant components are also used for rocket engines (nitric acid,

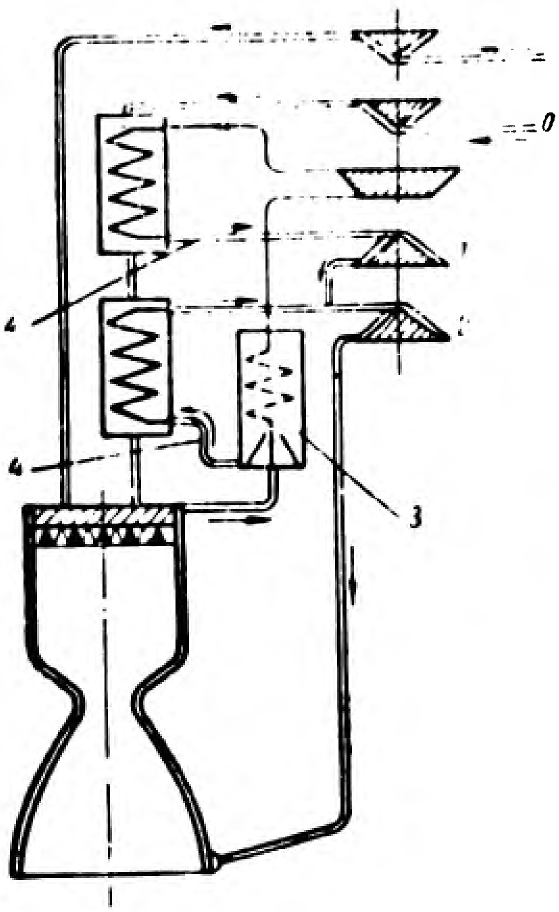

Fig.46 - Schematic Diagram of Separator Steam Generator for Turbopump Assembly, Using Heat from the Cooling Jacket of the Chamber

1 - Low-pressure pump; 2 - High-pressure pump; 3 - Separator; 4 - Condensate

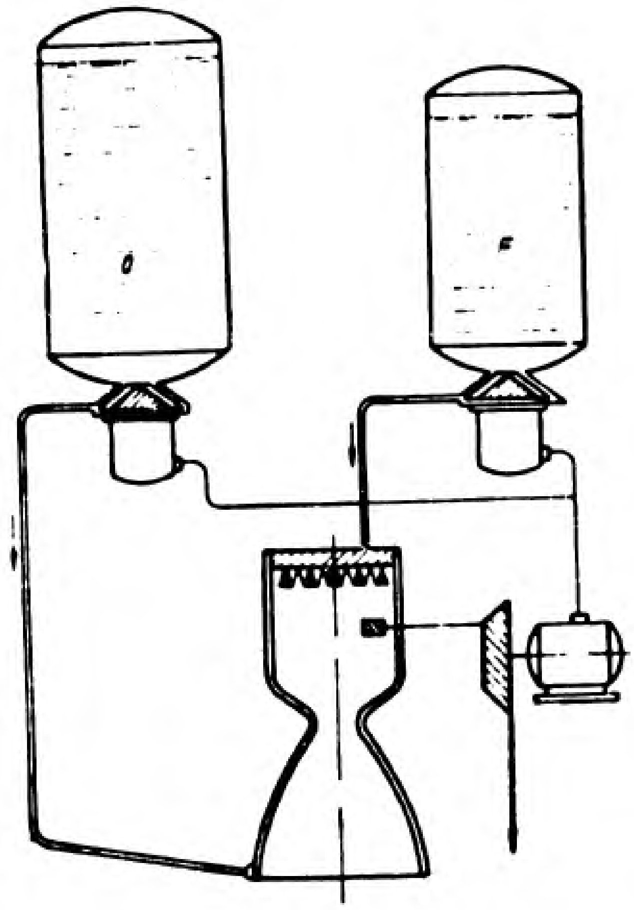

Fig.47 - Schematic Diagram of Electrified Pump Feed

alcohol, hydrogen peroxide, fluorine oxide, powder, etc.) but their production requires rather complex industrial plant processes.

The engines used in aircraft are customarily divided, in aviation engineering, into the following groups:

1) piston engines (PD);

2) gas-turbine (GTE), turboprop (TPE), and turbojet engines (TJE);

3) ramjet engines (RJE);

4) rocket engines (RE).

The first three of these groups are air-breathing engines. Representatives of the individual groups may be combined in a single engine, which is usually called a compound engine.

Let us briefly discuss the comparative characteristics of the engines.

The exclusive supremacy of the piston engine in aviation lasted about forty years. But, as in stationary heat engineering, the progressive development of aviation finally led to requirements that were very difficult or even impossible to meet if the earlier piston engines, or even modified versions, were used.

In turn, the development of heat engineering, under the influence of the demands made on aviation, created the possibility of the practical use of turbine and jet engines, which could, without trouble, develop high unit power and allow operation of aircraft at particularly high speeds.

Among atmospheric aircraft engines, piston engines are most economical at speeds up to M = 1.0. In specific cases, the fuel consumption was 115 - 140 gm/hp-hr, at a heat value of H_u = 11,000 kcal/kg. The power reached 3000 - 4000 hp.

Figure 48 gives an idea of the changes in maximum power, mean effective pressure, engine speed, and working cylinder volume in the most common types of piston aircraft engines from 1935 to 1949.

It took about 15 years to solve the fundamental questions of gas-turbine building in aviation. Today chemical gas-turbine engines are in the last stage of the ascending line of their development, and are used primarily as high-power engines. There are definite prospects for improving their economy, connected with the advances in the following technical fields:

1) Improvement in the heat resistance and refractory properties of the materials used in the jet-exposed parts of the turbine, primarily the blades;
2) Development of reliable systems for blade cooling;
3) Decrease in the internal losses in both turbine and compressor;

4) Use of regenerative cycles, which will become feasible as soon as notable improvement in heat transfer within the regenerator can be achieved.

Gas-turbine engines are used to power aircraft at high subsonic and supersonic

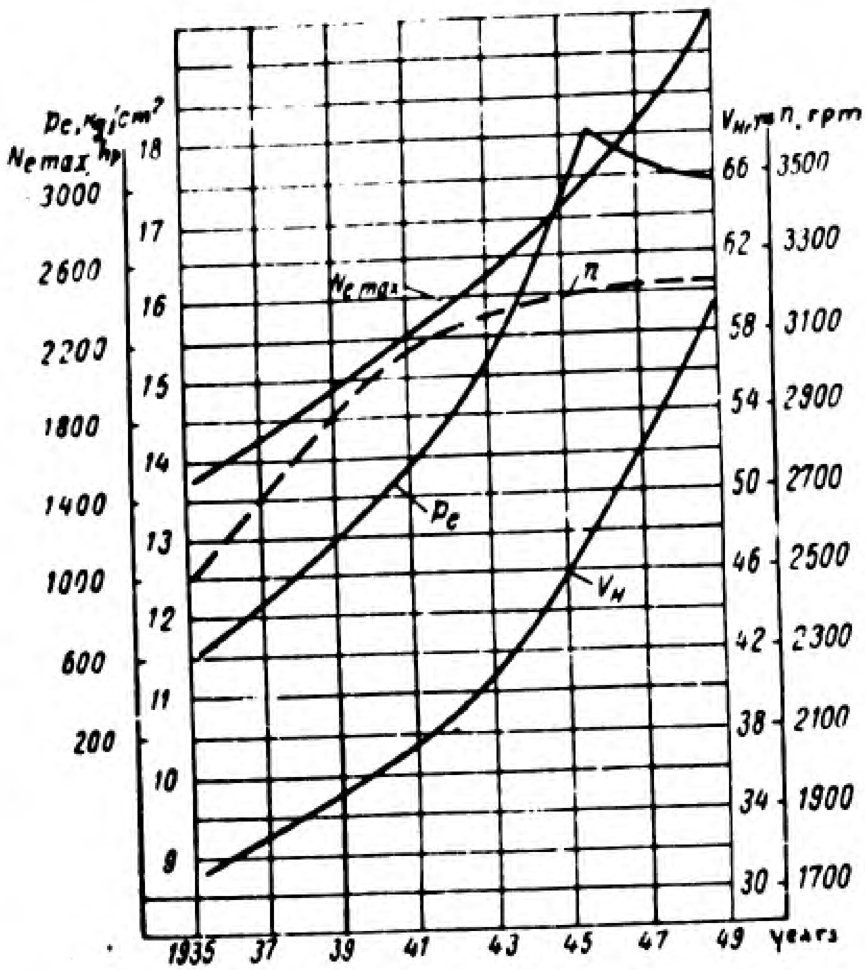

Fig.48 - Changes in Principal Data of Piston Engine from 1935 to 1949 (according to M.P.Pal'nikov)

speeds and, to some extent, are useful for the same purposes as piston engines.

The continuity of flow, the high velocity of the working fluid inside the machine, and the large ratio of exit cross section to center cross section of the engine permitted a quantitative jump in the gas-turbine engine with respect to fuel consumption, by comparison with the piston engine. In the gas-turbine engine, the air-flow rate is measured in tens of kilograms a second, which is reflected in its power. The extreme power of a gas-turbine aircraft engine has not as yet been established.

High-altitude flights bring out one favorable feature of a plant with a gas-turbine engine, which will be clear from Table 9. Heat exchangers in which the heat is transferred to the ambient air are undesirable in aircraft power plants since, with increasing altitude, the coefficient of heat transfer ..om the walls of the heat exchanger sharply drops as a result of the decreased air density, and with increased flying speed the heat transfer is made difficult by the increasing external ram temperature. Consequently, the increase in altitude and speed in a power plant with a large heat exchange in the direction of the ambient medium has an unfavorable effect on engine performance, since the weight of the power plant increases and the additional drag of the heat exchangers also increases.

Table 9

Heat Exchange with the Ambient Medium by Engines of Various Types

Engine Type	Brake Horsepower Efficiency, %	Heat Exchange, %	
		Through Heat Exchanger to Atmosphere	Of Working Fluid with Atmosphere
Aircraft steam engine	18 - 24 (up to 45 possible)	82 - 75 (up to 55 possible)	no heat exchange
Piston aircraft engine	25 - 35 (up to 45 - 50 possible)	water and oil radiators 14 - 18, air radiator 1 - 6	45 - 60
Gas-turbine aircraft engine	16 - 22 (up to 24 - 35 possible)	oil radiator 0.4 - 1.0	77 - 88
Ramjet aircraft engine	5.0 - 10.0(up to 45 - 50 or more possible)	no heat exchangers	90 - 95
Rocket engine	30 - 45 (up to 50 - 60 or more possible)	no heat exchangers	55 - 70

It is clear from Table 9 that steam turbines are the heaviest engines with heat exchangers, and require condensers for transfer of up to 82% of the heat of the fuel across their surface. The dissipation of heat in piston engines is considerably less difficult, and there is practically no trouble of this kind in gas turbine engines and jet engines.

The ramjet engine develops even more power than the gas-turbine engine. Whereas gas-turbine engines develop tens of thousands of horsepower and sometimes hundreds of thousands, the ramjet engine, even at present flying speeds, can develop several hundred thousand horsepower.

An advantage of the ramjet engine is the simple design of its working part, which consists of a duct of variable cross section. Another advantage is the good utilization of the center cross section for air intake. A drawback is the difficulty of regulating the thrust and the absence of thrust on takeoff, when the airflow is stationary with respect to the aircraft. The ramjet engine is therefore started by means of extrinsic starters, which complicates operation of the equipment, or by the aid of auxiliary mechanisms in the engine, which cancels its simplicity. The initial acceleration of flight vehicles with ramjet engines is often obtained by using other engines, most often rocket units. Because of this shortcoming of ramjet engines, compound engines will probably become of practical importance. The most probable are combinations of a ramjet engine with rocket engines for nonrecoverable vehicles, and with gas-turbine engines for aircraft.

The combination of a ramjet engine with a gas-turbine engine may be useful in utilizing nuclear fuel, when the resistance in the reactor (or other heat exchangers through which atmospheric air flows) is a considerable fraction of the velocity head. The thermal and hydraulic resistances in such cases are overcome by the aid of a turbocompressor unit.

In general, the field of application of the ramjet engine is for atmospheric vehicles, with a power and speed that has not yet been mastered. The high specific power, computed from the weight and center cross section of the engine, by comparison with other atmospheric engines, permits us to consider the ramjet engine as suitable for long-range missiles, and also for carrying an extra-atmospheric engine beyond the boundaries of the dense atmosphere.

The rocket engine, like the ramjet engine, belongs to the group of jet engines. Like the ramjet engine, a rocket engine can develop great thrust and power. The important features of its design and use, listed in Table 10, are due to the fact that the entire weight of the working substance lies in the rocket-consumer of the engine work. The rocket engine is a highly perfected machine, whose cycle is characterized by greater brake horsepower efficiencies than that of piston engines. At its present utilization for transportation near the ground, the total efficiency of a rocket engine is low, because of the relatively low flying speeds by comparison with the exhaust velocity of the gas from the engine. In long-range rockets, the total efficiency already begins to approach values close to those for atmospheric engines. We recall that for rocket engines with constant flying speed, the total efficiency must be determined only in the case where the engine is installed on an aircraft.

In installation on a rocket, the total efficiency must be calculated as the mean value for the entire flight.

Figure 49 shows pv-diagrams of the following engines: a piston engine with a driven compressor, a supersonic gas-turbine engine, a supersonic ramjet engine, and a rocket engine. Each diagram shows the rough values of the maximum temperature and pressure in the cycle. The diagrams show that the specific volume of the gases issuing from the rocket engine is about twice as large as that of gases from the gas-turbine engine. This should be reflected in the relative dimensions of the nozzle exit cross section. However, the exhaust velocity in the rocket engine is about three times as great, meaning that, at the same exit cross section, the weight flow rate of gas in the rocket engine will be 1.5 times as great.

The principal performance data of aircraft and rocket engines are given in Tables 11 and 12. The maximum values of thrust, power, and efficiency in individual cases have not yet been attained but are entirely realistic with the existing

Table 10

Performance Characteristics of Rocket Engines

Criteria of Engine Quality	Internal Criteria	External Criteria	
Simple shape of flow area and working element of engine, possibility of cooling the walls of the working element	Realization of cycles at higher pressure and temperature than in atmospheric engines	Higher brake horsepower efficiencies. High exhaust velocity and specific thrust	Possibility of obtaining high-speed flight at high economic indices
All the propellant is in the feed system	Use of fuel of higher heat value than in atmospheric engines	High specific fuel consumption	Independence from ambient medium as source of working fluid. Possibility of use for space flights. Possibility of use for underwater missiles. Maximum propellant charge of rocket
High speed and density of gas in cross sections, determining the ejection and feed of the working substance in liquid and solid states	High handling capacity	Especially high thrust and power. Especially low specific weight and small dimensions	Serves particularly high-power flying missiles and aircraft
Brief operation, due to limited propellant supply	Tendency to utilize material of power plant as propellant		Flight at variable speeds and high accelerations. Peculiarity in the exchange of useful energy between engine and consumer, consisting in an accumulation of kinetic energy in the missile. Subsidiary use as a booster. Used in conjunction with ramjet engine

Table 11

Rough Performance Characteristics of Heat Engines in Flight Vehicles

Designation of Engine	Specific Work L_e, kg-m/kg	Brake Horsepower Efficiency, η_e, %	$\frac{L_e}{L_{e\ pist}}$	$\frac{\eta_e}{\eta_{e\ pist}}$	Weight flow rate G, kg/sec	Effective Power, N_e, Brake Horsepower
Subsonic ramjet engine ($M = 0.5 - 0.9$; $H = 0$; center cross section 1 m^2)	6 000—20 000	3—9	0,13	0,17	3,0—70	300—20 000
Gas-turbine engine ($H = 0$; $M = 1.0$)	16 000—35 000	16—32	0,2—0,3	0,7—0,8	3,0—1000	1000—45 000
Piston engine	90 000—100 000	24—25	1,0	1,0	0,05—4,0	50—4000
Rocket engine	20 000—250 000	24—45	2,0—2,5	1,0	To 200	To 700 000
Supersonic ramjet engine ($M = 3.5 - 4.0$; center cross section 1 m^2; $H = 11$ km)	250 000—320 000	50—65	2,5—3,2	1,4—2,2	To 300	To 500 000
Rocket engine, $V_{max} = 3 - 5$ km/sec	Up to 600,000 (millions in nuclear rocket engines)	35—60	To 6	1,5	To 500	Up to tens of millions

Table 12

Approximate Performance Characteristics of Thrust Engines for Flight Vehicles

Designation of Engine	Specific Thrust P_{sp}, kg/kg-sec	$\frac{P_{sp}}{P_{sp \cdot pist}}$	Total Thrust P, tons	Specific Weight λ, kg/kg of Thrust	Specific Fuel Consumption C_{sp} kg/kg of Thrust	Thrust Power N_T, hp
Subsonic ramjet engine ($M = 0.5 - 0.9$, $H = 0$; center cross section 1 m^2)	20—35	0,05	0,1—2,5	0,035—0,15	4,0—9,0	200—10 000
Gas-turbine engine ($H = 0$; $M = 1.0$)	40—70	0,20	0,2—10,0	0.2 - 0.3 (to 0.60 in turboprop engine)	0.75 - 0.9 (to 0.3 - 0.5 in turboprop engine	800—40 000
Piston aircraft engine	350—450	1,0	0,02—1,5	1.2 - 2.0 (in flight)	0,25—0,5	40—3500
Rocket engine	190—300	0,5	to 50 and higher in clusters	0.04 - 0.12 (in powder rocket motors, to 0.005)	14—18	to 1,000,000 (at end of boost)
Supersonic ramjet engine ($M = 3.5 - 4$; center cross section 1.0 m^2; $H = 11$ km; T_{max} up to 2500°K)	55—75	0,16	o 25	—	2,0—3,0	o 300 000
Rocket engine $V = 3 - 5$ km/sec	250-400 in chemical engines and more in nuclear engines (up to 10,000)	1,0	o 200	—	4,5—8,0	to tens of millions (at end of boost)

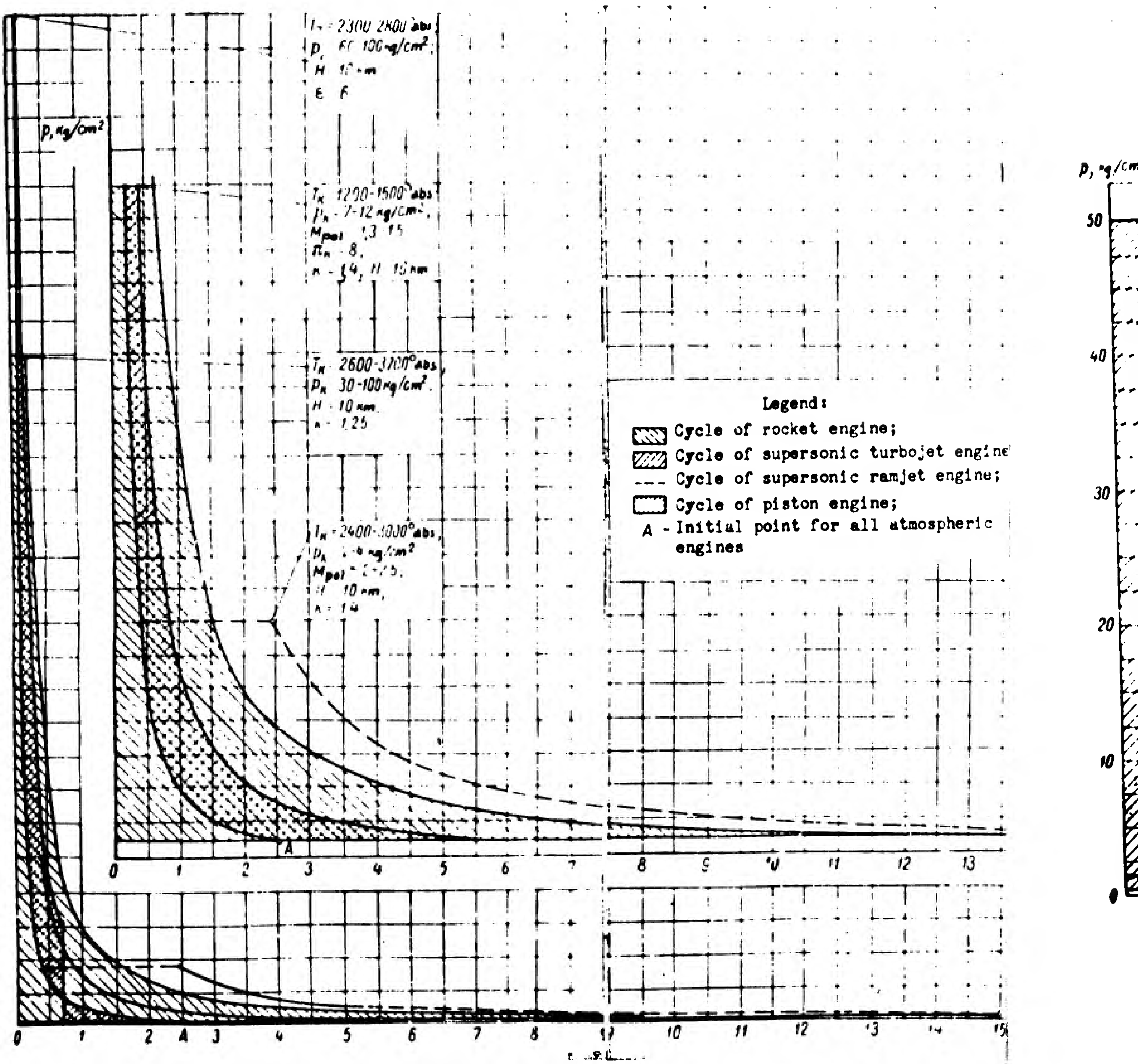

Fig.49 - pv-Diagrams of Four Cycle Engines Used in Aviation

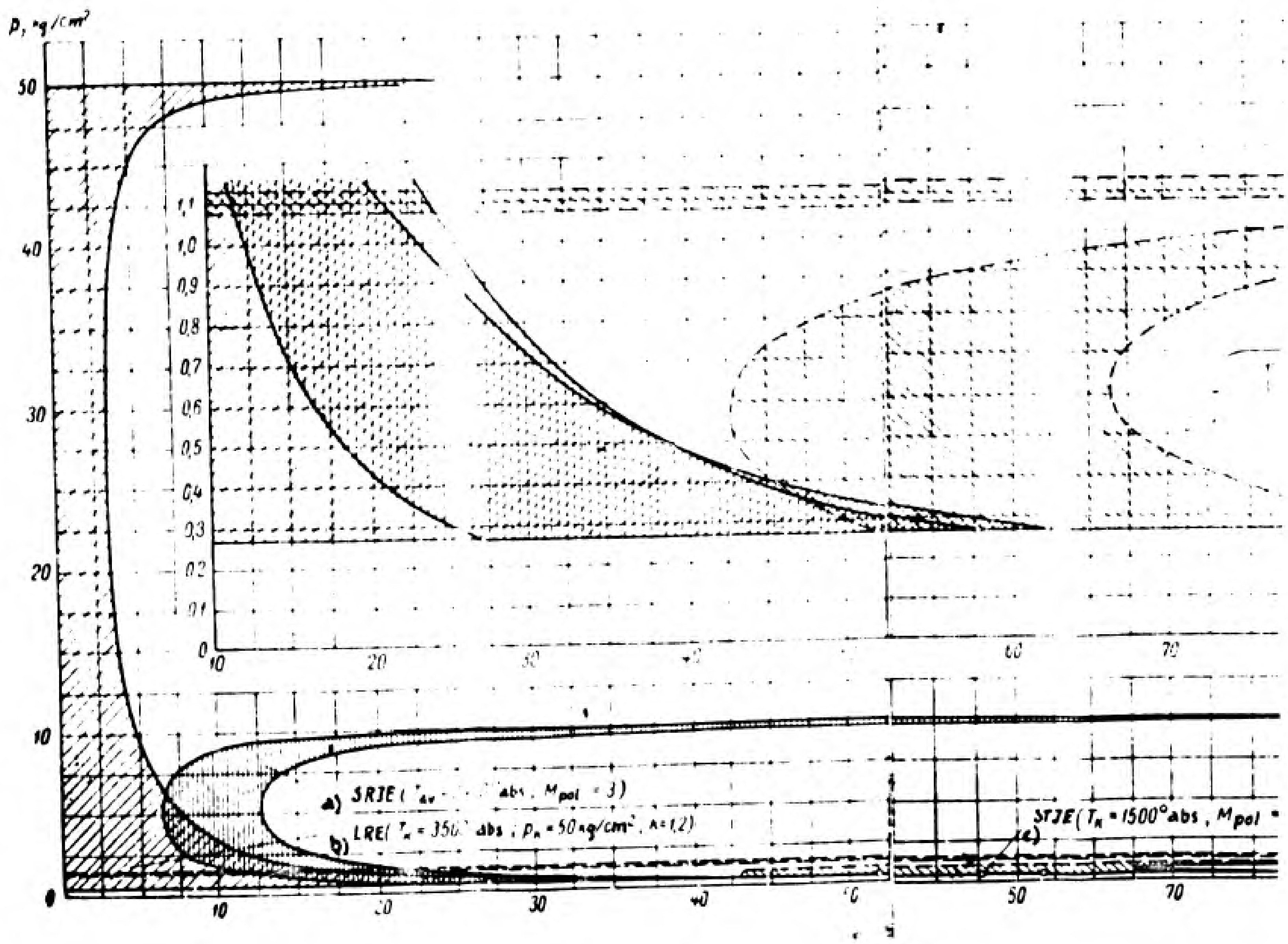

Fig.50 - pf-Diagrams for Three Engines at Altitude H = 10,000 m

a) Supersonic ramjet engine (T_{av} = 2450°K; M_{pol} = 3); b) Liquid rocket engine (T_k = 3500°K; p_k = 50 kg/cm²; K = 1.2); c) Supersonic turbojet engine (T_k = 1500°K; M_{pol} = 1.56; π_k = 9.3) possibilities.

As will be seen from the Tables, the working substance is most fully utilized in piston and rocket engines, which have the highest specific work and specific thrust. Even in its present state of development, a rocket engine is most highly stressed in its thermal process; its specific work is 2 - 2.5 times as great as that of a piston engine and 10 times as great as that of a gas-turbine engine. In total thrust, the rocket engine differs sharply from other engines. Whereas the maximum thrust in the most powerful of these engines is 5 - 10 tons, it reaches several tens of tons in the rocket engine.

The ramjet engine is also very powerful at speeds of M = 2 - 3. Flight at particularly high speeds in the atmosphere takes place at great altitudes, for which reason the data for the ramjet engine are given for an altitude of 11 km at a speed of M = 2 - 3. Both power and thrust depend on the quantity of working fluid and thus also on the dimensions of the cross sections of the flow area. Tables 11 and

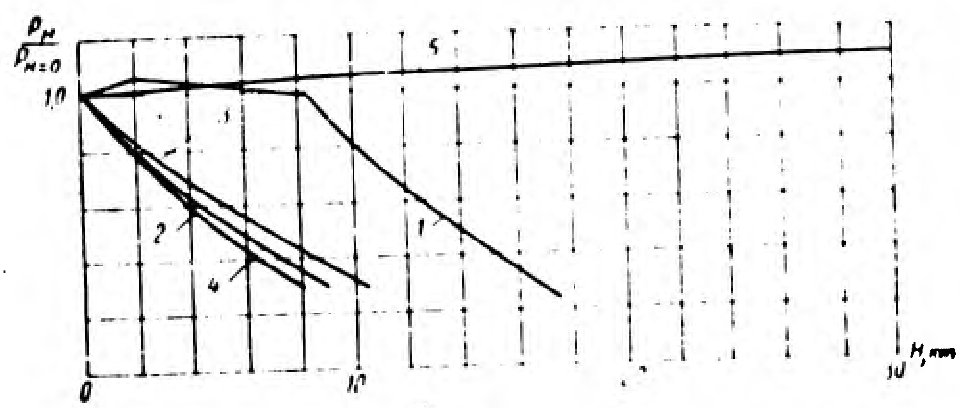

Fig.51 - Altitude Characteristics of Aircraft Engines

1 - High-altitude piston engine; 2 - Simple piston engine; 3 - Turbojet engine ($\pi_k = 6$; M = 0.75; $T_k = 1200^oK$); 4 - Ramjet engine ($H \approx 11$; $T_k = 2500^oK$); 5 - Rocket engine

12 give the values of power and thrust for the ramjet engine with a center cross section of 1 m^2.

Taking cognizance of the fact that the speed and thrust of a ramjet engine and a rocket engine are almost the same, a combination of these engines will evidently yield good practical results. Figure 50 shows the power diagrams of a rocket engine, a supersonic turbojet engine, and a supersonic ramjet engine. The specific cross sections in the flow area of the engine f are plotted on the abscissa against the pressure p on the ordinate. The areas inside each curve, as will be shown in Chapter III, correspond to the values of the specific thrust. It will be clear from

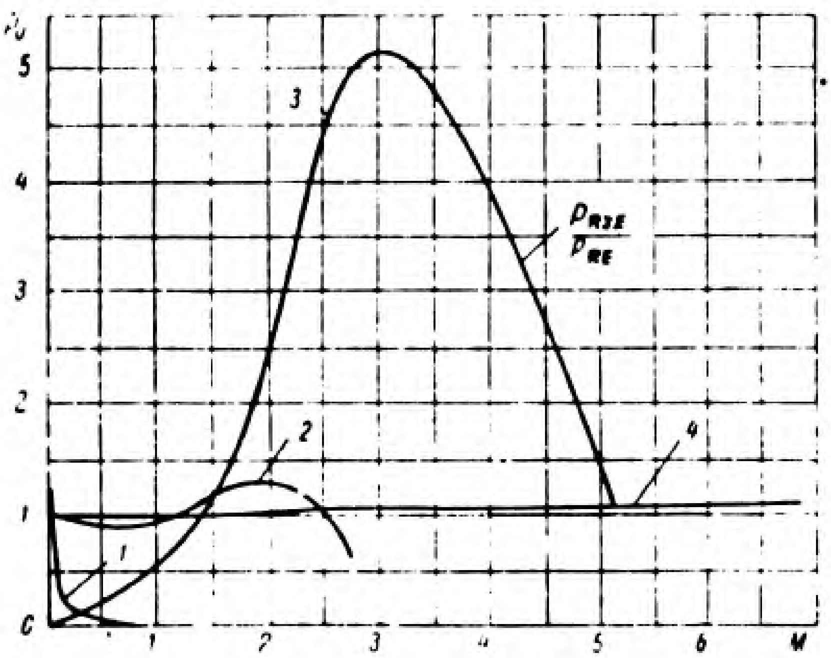

Fig.52 - Altitude Characteristics of Aircraft Engines

1 - Piston engine; 2 - Turbojet engine (T_k = 1200°K; π_k = 12); 3 - Ramjet engine (T_k = 2400°K); 4 - Rocket engine (T_k = 3000°K; p_k = 100 kg/cm); P_o - Takeoff thrust

these diagrams that the performance characteristics of the rocket engine and the supersonic ramjet engines are close together in the zone of application of the ramjet engine.

The drawbacks of the rocket engine include its high specific fuel consumption, which prevents its use on civil aircraft. In turn, atmospheric engines are entirely unsuitable for performing the functions of rocket engines, especially for flights beyond the atmosphere - or, in practice, at altitudes above 30 km. Under atmospheric conditions, the rocket engine cannot be replaced as a means of developing a very high frontal thrust for short time intervals. Such an engine differs sharply from an atmospheric engine in the number of times it can be used. In nonrecoverable rockets, the operating time of a liquid-propellant rocket engine ranges from 5 sec to 2 - 3 min, while that of a powder rocket motor goes down to fractions of a second (lower limit). In aircraft, the total operating time of a liquid rocket engine is measured in hours. There is no doubt that, in the future, the operating time of rocket motors and aircraft liquid rocket engines will be increased further.

Figure 51 shows the altitude characteristics of comparable standard aircraft engines. The decreased air density with increasing altitude leads, in atmospheric engines, to a lowered consumption of the working substance and a sharp decrease in thrust. In a rocket engine with a constant gas flow rate, there is an appreciable improvement in thrust with increasing flight altitude.

At altitudes above 30 km, atmospheric engines have practically no more air available, although air is the principal source of their working fluid.

Figure 52 shows the velocity characteristics of aircraft engines. A particularly favorable effect of flying speed on engine thrust is noted in the ramjet engine. At low flying speeds, the thrust of a rocket engine is independent of the speed, but at high speeds ($M > 1.5 - 2.2$) the thrust increases owing to rarefaction on the underside and approaches the thrust in vacuum.

CHAPTER III

THEORY OF IDEAL ROCKET ENGINES OF CONSTANT PRESSURE AND VOLUME

Section 8. Determination of the Work and Thrust in a Constant-Pressure Rocket Engine

1. Principal Data of a Rocket Engine and Features of their Determination

As already pointed out, the rocket engine may be considered a heat engine in which the typical processes of the thermodynamic cycle are accomplished. The principal performance characteristic of a heat engine is the work, while its economy is evaluated by the energetic efficiency, the thermodynamic efficiency, etc.

At the same time, the rocket engine is also a thrust machine in which, as a result of the change of state of the mass carrier, an impulse is produced which is utilized directly by the consumer (the flight vehicle). From the viewpoint of the consumer, the reserve of performance of a rocket thrust machine is determined by thrust and the duration of its action, i.e., by the total impulse during the engine operating time.

Like the heat value, which determines the amount of energy liberated on combustion of 1 kg of fuel, the term "impulse value" is used for the momentum obtained after combustion of 1 kg of fuel and subsequent expansion of the gases to absolute vacuum. In that case, the available momentum exerted on the vehicle will be measured by the product of the impulse value and the amount of fuel consumed.

To evaluate the economy of a rocket thrust engine, it is expedient to establish a system of impulse or power parameters, representing the ratio of the true impulses (to thrust) to the ideally available impulses (to the ideal thrust).

In analyzing the processes taking place in an engine, all the energetic transformations of the mass carrier must be studied, since, the more perfect these are, the higher will be the thrust parameters of the engine. The technique of evaluating the energetic transformations, well developed in the theory of heat engines, can be completely taken over in studying the rocket engine. We shall use it hereafter when considering ideal rocket engines.

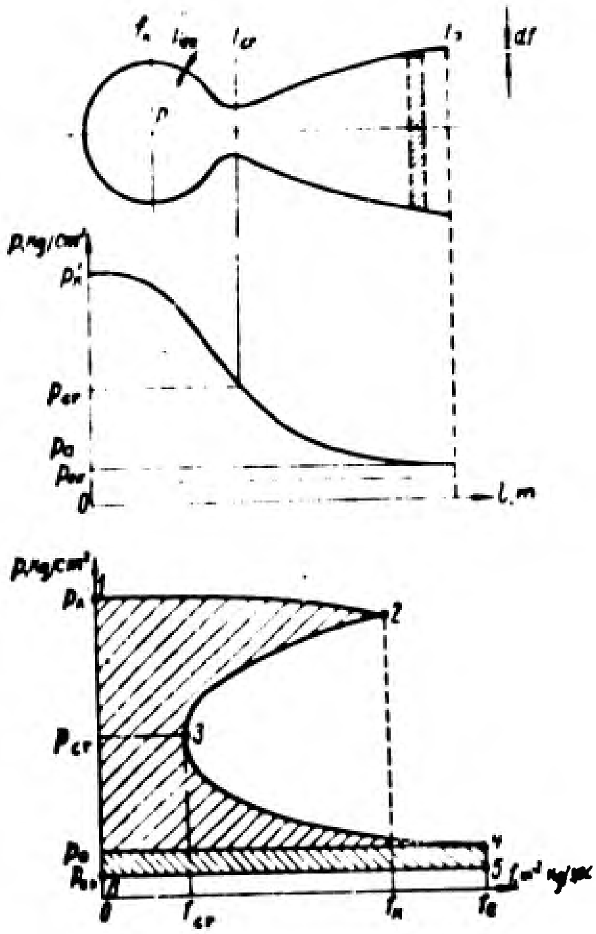

Fig.53 - Example of Power Cycle of Rocket Engine under Conditions of Incomplete Expansion

An analysis of the actual process and an evaluation of the losses in the engine may likewise be based on the classical theory of heat engines. At the same time, the losses must also be determined in units of lost impulse. This is justified by the need to know the quantitative measure of the influence of some special phenomenon taking place inside the engine, on its most important parameter - the impulse of the exhaust jet. Moreover, a direct experimental study of a thrust engine more often and more readily permits determination of the loss of impulse, but not of the energy.

Henceforth, in considering the working process of a rocket engine, we shall determine the relative value of the losses in the impulse system and in the energetic system.

2. The Power Cycle of a Rocket Engine at p = c

In determining the thrust of jet engines, one may use a pf-diagram, whose role is analogous to that of the pv-diagram in determining the work. Figure 53 shows a power cycle for the chamber of a liquid rocket engine of arbitrary shape.

The thrust P is composed of the sum of the forces acting on the inside and outside of the chamber walls and directed along the axis of the chamber. In an elementary area, therefore, the applied force will be

$$dP=p\,df,$$

where:

p is the pressure on the wall;

f is the specific cross section of the chamber, $f = \frac{F}{G}$.

For the case in question, G = 1 kg/sec, f = F, $P = P_{sp}$.

The total force acting on the entire inside surface of the chamber is

$$P_i = \int_0^{f_a} p\,df = \int_0^{f_a} \varphi(f)\,df.$$

This force is termed the internal thrust of a rocket engine. On the diagram of Fig.53, P_i is measured from the area 1-2-3-4-f_a-0-1. The force acting on the outer surface is

$$P_{ex} = -\int_0^{f_a} p_{ex}\,df = -p_{ex}\int_0^{f_a} df = -p_{ex} f_a.$$

This force, corresponding on the pf-diagram to the area under the straight line 5 - 6, is always negative, i.e., it is directed opposite to the motion of the rocket. The sum of the internal and external forces represents the total engine thrust:

$$P = P_i + P_{ex} = \int_0^{f_a} p\,df - p_h f_a. \tag{18}$$

Section 9. The Ideal Constant-Pressure Rocket Engine

1. Determination of the Work and Thermodynamic Efficiency of a Rocket Engine at $p = c$

Figure 54 shows the simplest possible scheme of a liquid rocket engine. Compressed air from the bottle enters the propellant tank and forces the propellant into the combustion chamber, where the working fluid is heated at constant pressure. The actual cause of the temperature rise of the working fluid may be a chemical reaction, the presence of high-temperature surfaces in the chamber, or the gaseous product of a nuclear reaction.

From the chamber, the gas passes into the exhaust-nozzle duct and expands there to the external pressure p_{ex}. The work performed during this process is transferred to the working fluid, causing its kinetic energy to increase.

The operating conditions of an ideal constant-pressure rocket engine are determined by the following criteria:

1) The sources of the working substance and the heat (i.e., two sources) are the sources of the constant pressure;
2) The work of compression in the thermodynamic cycle is zero;
3) The working fluid is an ideal gas. At all instants of the cycle it is characterized by chemical, thermal, and mechanical uniformity;
4) The transverse dimensions of the chamber are so great that the velocity of the gas, on entering the nozzle duct, will be zero;
5) The processes composing the cycle take place reversibly inside the engine, i.e., without chemical, thermal, or gas-dynamic losses.

These criteria which determine whether a given cycle is ideal are the usual ones, except for the second and fourth.

The compression of the working fluid takes place outside the chamber, in the pumps or in the propellant tank. During the compression, the working fluid is in the liquid state, the work of compression is negligible by comparison with the work of expansion, and therefore, in determining the work and efficiency of an engine, the work expended on compression is not taken into account. In an actual engine, the work losses on compression are more marked, and are in fact taken into account in calculating a specific engine.

Neglecting the velocity of the gas in the chamber is justified by the fact that its actual magnitude in most engines is small, and exerts practically no influence on the specific thrust. Moreover, in considering engines with velocity chambers, we shall show that the thrust must be determined when the gas is accelerated, and in the chamber.

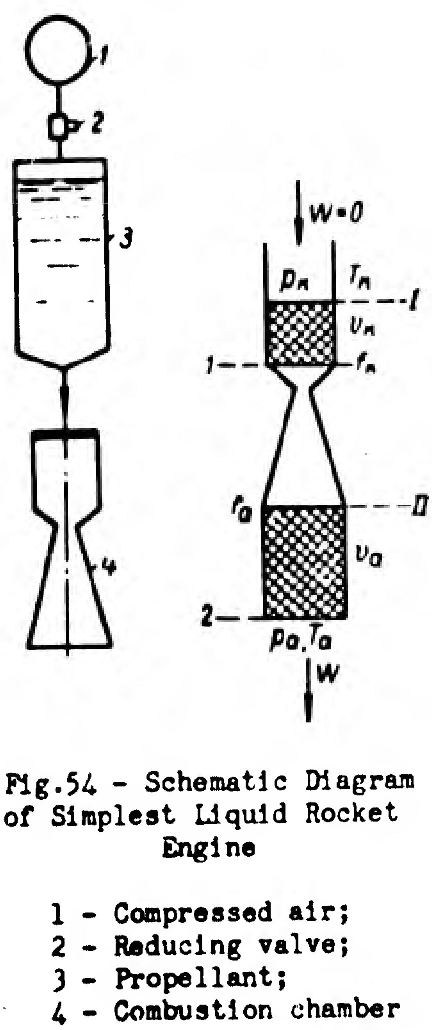

Fig.54 - Schematic Diagram of Simplest Liquid Rocket Engine

1 - Compressed air;
2 - Reducing valve;
3 - Propellant;
4 - Combustion chamber

In a jet engine, the conditions of encounter of the working fluid with the lower source are different from those in a piston engine. Thus, if the ratio of the pressure in the chamber to that in the atmosphere is higher than the critical value, the pressure p_a at the end of expansion will be determined only by the expansion ratio, i.e., by the ratio of the areas $\frac{f_a}{f_{cr}}$, and by the magnitude of pressure in the chamber. When the ratio $\frac{f_a}{f_{cr}}$ equals unity (convergent nozzle), the pressure of the working fluid on discharge into the atmosphere equals the critical pressure calculated by the formula

$$p_a = p_{cr} = p_k \left(\frac{2}{1+k}\right)^{\frac{k}{k-1}}.$$

With increasing divergence of the nozzle, the pressure p_a decreases, at first reaching atmospheric pressure and then, at the instant of disturbance of the normal flow on entrance of a shock wave into the nozzle, reaching a minimum value.

In all cases, the work of gas expansion in the nozzle duct between the pressures p_k and p_a is stored in the working fluid as its kinetic energy.

The further transfer of energy takes place outside the engine, in the atmosphere, and has no effect whatever on the extent of the work of expansion. However, this transfer should be further studied since it governs the maximum overexpansion or the minimum pressure p_a.

Consequently, the cycle of a jet expansion machine differs from the cycle of a static machine (piston machine) by the fact that the work of expulsion depends not on the atmospheric pressure but on the pressure in the nozzle section. This means that the work of an ideal engine with a fixed nozzle, within certain limits of variation in the external pressure, will be constant.

Figure 55 shows a cycle for which the design conditions are determined by the

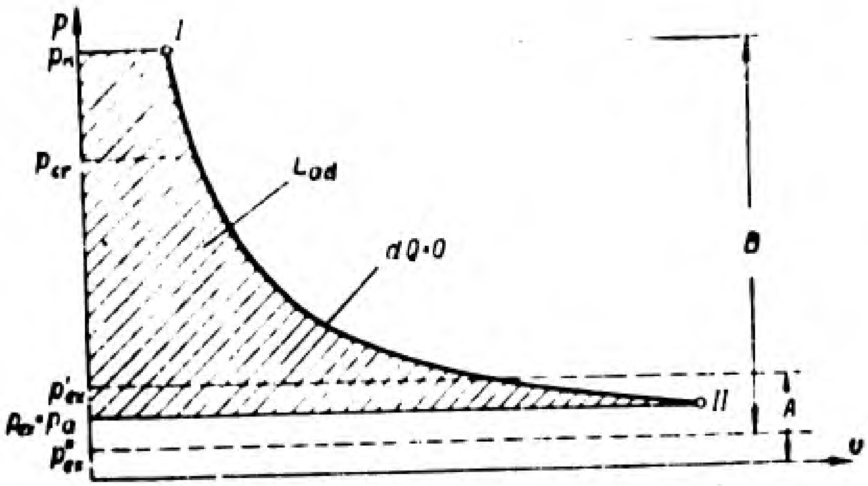

Fig.55 - Cycle of Liquid Rocket Engine and Limits of its Subsistence

A- At assigned values of p_k and δ_c $0 < p_a < p'_{ex}$; B - At assigned values of p_k and p_{ex}, $p_{ex} < p_a < p_k$

external pressure $p_{ex} = p_a$. The cycle does not change its form if the external pressure drops below the rated pressure $p_{ex} < p_a$. With increasing external pressure, the cycle remains unchanged up to a certain pressure p'_{ex}, determined by the entrance of a shock wave into the nozzle exit.

To determine the work of the cycle of an ideal rocket engine, consider the transition of the system from the position I-II to the position 1-2 (Fig.54). In the absence of heat losses, the expression of the first law of thermodynamics in this case will be of the following form:

$$U_a - U_k + L + \frac{W_a^2 - W_k^2}{2g} = 0. \tag{19}$$

Here and later in the text, we shall express the value of energy of any form in mechanical units.

Obviously,

$$U_a = C_v T_a + U_c$$

and, accordingly,

$$U_k = C_v T_k + U_c,$$

where U_c is the external energy of the gas within the nozzle duct.

The work L must be determined along the boundaries of displacement of the gas at the nozzle mouth and at the nozzle exit. Considering, as usual, that work accompanied by an increase in volume of the system is positive, and work accompanied by a decrease in its volume is negative, we may write:

$$L = p_a v_a - p_k v_k = RT_a - RT_k.$$

Then, instead of eq.(19), considering the velocities of the gas at the nozzle mouth as $w_k = 0$, we get

$$C_v T_a - C_v T_k + RT_a - RT_k + \frac{W_a^2}{2g} = 0.$$

Let us define the value of the useful work:

$$\frac{w_a^2}{2g} = L_{ad} = I_k - I_a = C_p (T_k - T_a) = C_p T_k \left(1 - \frac{T_a}{T_k}\right). \tag{20}$$

The source of the working fluid for the nozzle is the generator of this substance, namely the chamber and the ambient medium.

Substituting the pressure ratio obtained from the adiabatic equation for the temperature ratio in the last formula, we get the following expression for the specific work of the cycle:

$$L_{ad} = \frac{k}{k-1} RT_k \left[1 - \left(\frac{p_a}{p_k} \right)^{\frac{k-1}{k}} \right] = \frac{k}{k-1} RT_k \left(1 - \frac{1}{\delta_c^a} \right), \tag{21}$$

where

$$a = \frac{k-1}{k}.$$

The work is determined in the entropy diagrams TS and IS, as shown in Fig.56. The quantity of heat consumed in the ideal cycle is measured in this case by the

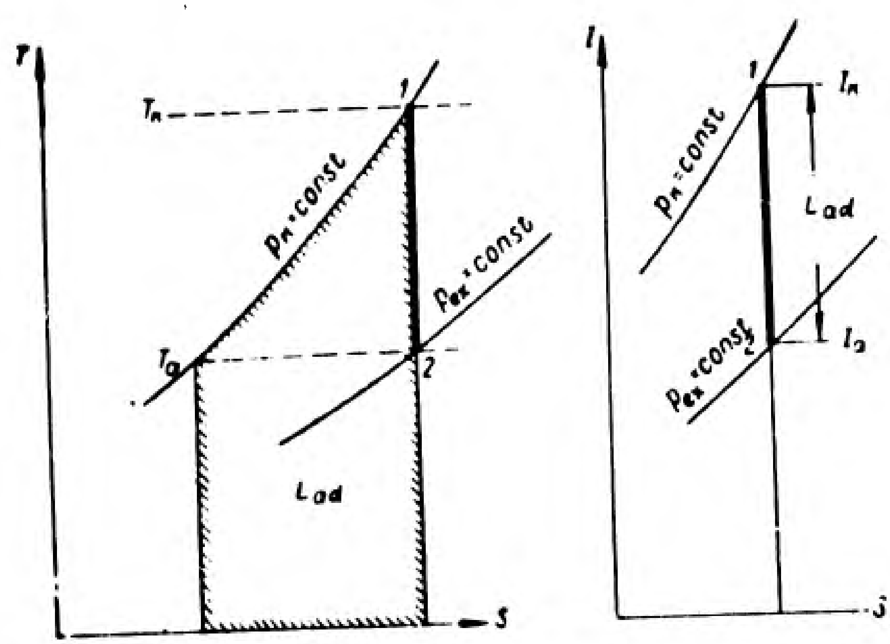

Fig.56 - Entropy Diagrams of an Ideal Rocket Engine at p = c

enthalpy of the gas at the end of the heat-transfer process. At the beginning of the heat transfer to the volume, the temperature and the enthalpy of the ideal gas are zero. Consequently,

$$Q_1 = I_k = C_p T_k = \frac{k}{k-1} RT_k.$$

We now determine the thermal efficiency from the equation

$$\eta_t = \frac{I_k - I_a}{I_k} = 1 - \frac{T_a}{T_k} = 1 - \left(\frac{p_a}{p_k}\right)^{\frac{k-1}{k}}$$

or

$$\eta_t = 1 - \frac{1}{\delta_c^{\frac{k-1}{k}}}. \qquad (22)$$

As indicated by eq.(22), the efficiency of the cycle depends on the expansion ratio δ_c and on the adiabatic exponent k of the working fluid. The efficiency in-

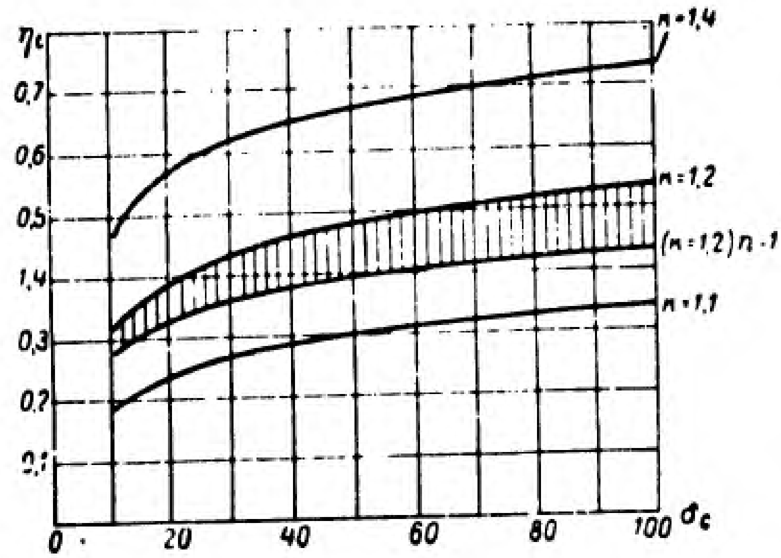

Fig.57 - Effect of the Expansion Ratio in Nozzle δ_c and of the Adiabatic Exponent k on the Efficiency of the Ideal Cycle of a Rocket Engine at p = c

creases with increasing δ_c and k (Fig.57). However, the rate of increase of η_t slows down with increasing δ_c and k. This is also obvious from the expressions for the first derivatives $\frac{d\eta_t}{d\delta_c}$ and $\frac{d\eta_t}{dk}$:

$$\frac{d\eta_t}{d\delta_c} = \frac{k-1}{k} \cdot \frac{1}{\delta_c^{\frac{2k-1}{k}}}; \quad \frac{d\eta_t}{dk} = \frac{1}{k^2} \cdot \frac{\ln \delta_c}{\delta_c^{\frac{k-1}{k}}}.$$

At times it is more convenient to express the work of the cycle in dimensionless form. As the unit of measurement of the work, let us take the work of the cycle at the critical pressure ratio, or the kinetic energy at the nozzle throat.

Then, the relative work $\bar{L}$ will represent the ratio

$$\bar{L} = \frac{L}{L_{cr}} = \frac{w_a^2}{w_{cr}^2} = \lambda_a^2 \tag{23}$$

or

$$\bar{L} = \frac{k+1}{2} \cdot \frac{M_a^2}{1 + \frac{k-1}{2} M_a^2}, \tag{24}$$

where M_a is the Mach number in the exit section f_a of the nozzle;

λ_a is the velocity coefficient in the same section.

Accordingly, the thermal efficiency of the engine will be

$$\eta_t = 1 - \frac{1}{\delta_c^a} = \frac{1}{1 + \frac{2}{(k-1) M_a^2}} = \frac{k-1}{k+1} \lambda_a^2. \tag{25}$$

Since

$$M_a^2 = \frac{2}{k-1} (\delta_c^a - 1),$$

then in the case of a convergent nozzle, with $f_a = f_{cr}$, we have

$$\eta_{t\,cr} = 1 - \frac{T_{cr}}{T_k} = 1 - \frac{2}{k+1} = \frac{k-1}{k+1}. \tag{26}$$

Setting up the expressions for the ratios $\frac{\eta_t}{\eta_{t\,cr}} = \bar{\eta}_t$, we get

$$\bar{\eta}_t = \bar{L}.$$

2. The Thrust of a Rocket Engine and its Components

Figure 58 is a graph of the gas pressure on the internal walls of the chamber. The internal thrust P_i, due to this pressure, consists of three characteristic components:

P_I, the positive force acting on the intake section of the chamber, where the pressure is the same and is equal to p_k;

P_{II}, the negative force acting on the walls of the convergent section of the nozzle;

P_{III}, the positive force acting on the divergent section of the nozzle.

The internal force is the sum of these forces:

$$P_i = P_I + P_{II} + P_{III}.$$

For a flow rate of 1 kg/sec,

$$P_I = p_k f_k,$$

where f_k is the projection of the inner surface of the chamber intake section onto a plane perpendicular to the chamber axis.

The resultant on the second section is defined by the integral

$$P_{II} = \int_{f_k}^{f_{cr}} p\,df.$$

In an arbitrary section, three forces act on an elementary mass of the gas, imparting to it an impulse along the chamber axis (Fig.59):

$$\overrightarrow{fp};\quad (f+\overleftarrow{df)(p+dp)};\quad \overleftarrow{dP_{st}},$$

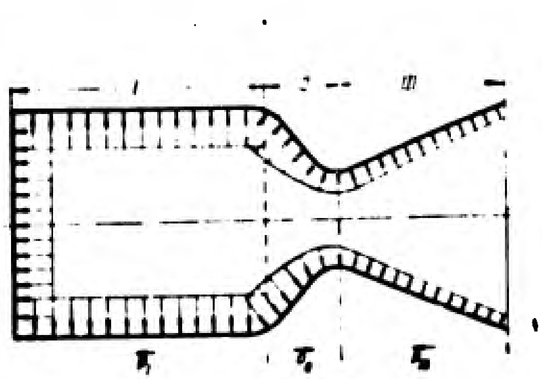

Fig.58 - Pressure Distribution Along the Chamber Walls of the Liquid Rocket Engine

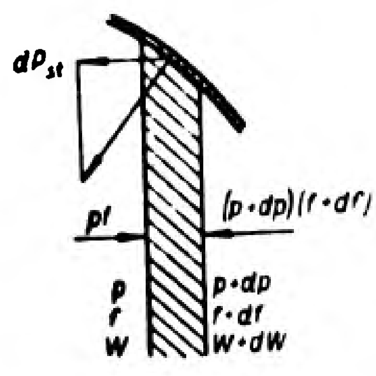

Fig.59 - State of Motion of the Gas in an Arbitrary Section of the Nozzle

The impulse varies the momentum of the mass; relating it to 1 kg of weight, we may write

$$fp-(f+df)(p+dp)-dP_{st} = \frac{1}{g}\,dW,$$

whence

$$dP_{st\,1} = -\frac{dW}{g} - d(fp).$$

The same force, but with opposite sign, acts from the direction of the gas on the nozzle walls:

$$dP = -dP_{st\,1} = \frac{dW}{g} + d(fp).$$

In final form, we have

$$P_{II} = \int_{W_k}^{W_{cr}} \frac{dW}{g} + \int_{f_k p_k}^{f_{cr} p_{cr}} d(fp)$$

or

$$P_{II} = \frac{W_{cr}}{g} + f_{cr} p_{cr} - f_k p_k.$$

The sum of the forces P_I and P_{II} is the thrust $P_{i\cdot cr}$ of a chamber with convergent nozzle:

$$P_{i\cdot cr} = \frac{W_{cr}}{g} + f_{cr} p_{cr}.$$

After transformation, we have

$$P_{i\cdot cr} = \frac{W_{cr}}{g}\left(1 + g\,\frac{f_{cr} p_{cr}}{W_{cr}}\right).$$

However,

$$\frac{f_{cr} p_{cr}}{RT_{cr}} \cdot W_{cr} = 1,$$

therefore

$$P_{i\cdot cr} = \frac{W_{cr}}{g}\left(1 + \frac{gRT_{cr}\,k}{W_{cr}^2\,k}\right).$$

Since

$$\frac{W_{cr}^2}{kgRT_{cr}} = M_{cr}^2 = 1,$$

then

$$P_{i\cdot cr} = \frac{k+1}{k} \cdot \frac{W_{cr}}{g}.$$

Eliminating the quantity W_{cr}, we get

$$P_{i\cdot cr} = \sqrt{\frac{2}{g}\,\frac{k+1}{k}\,RT_k}\,. \tag{27}$$

Consequently, the internal specific thrust of a chamber with convergent nozzle does not depend on the sections of the chamber nor on the pressures in it; it depends exclusively on the temperature of the gas in front of the nozzle, T_k.

For a positive force P_{III}, we get

$$P_{III} = \frac{1}{g}\int_{W_{cr}}^{W_a} dW + \int_{f_{cr}p_{cr}}^{f_a p_a} d(pf) = \frac{W_a}{g} + f_a p_a - \frac{W_{cr}}{g} - f_{cr}p_{cr}.$$

Adding the three forces so obtained, we can calculate the internal thrust:

$$P_i = \frac{W_a}{g} + p_a f_a \tag{28}$$

or

$$P_i = \frac{W_a}{g}\left(1 + \frac{g p_a f_a}{W_a}\right) = \frac{W_a}{g}\left(1 + \frac{1}{kM_a^2}\right). \tag{29}$$

To evaluate the influence of the divergent section of the nozzle on the thrust, we find the ratio $\frac{P_i}{P_{i\ cr}}$:

$$\frac{P_i}{P_{i\cdot cr}} = \frac{k}{k+1}\,\frac{W_a}{W_{cr}}\left(1 + \frac{1}{kM_a^2}\right) = \frac{k}{k+1}\,\lambda_a\left(1 + \frac{1}{kM_a^2}\right)$$

However,

$$M_a^2 = \frac{\frac{2}{k+1}\lambda_a^2}{1 - \frac{k-1}{k+1}\lambda_a^2}\,.$$

Making use of the last two equations, we get

$$\frac{P_i}{P_{i\cdot cr}} = \frac{1+\lambda_a^2}{2\lambda_a}. \tag{30}$$

Figure 60 shows the variation of this ratio as a function of the velocity coefficient in the exit section of the nozzle. The existence of a divergent section has a substantial influence on the increase in internal thrust; at $\delta c = 100$, for example, the thrust increases by 42%. The internal thrust is real if the engine is in a vacuum or, practically, at an altitude of 30 - 40 km. In denser layers of the at-

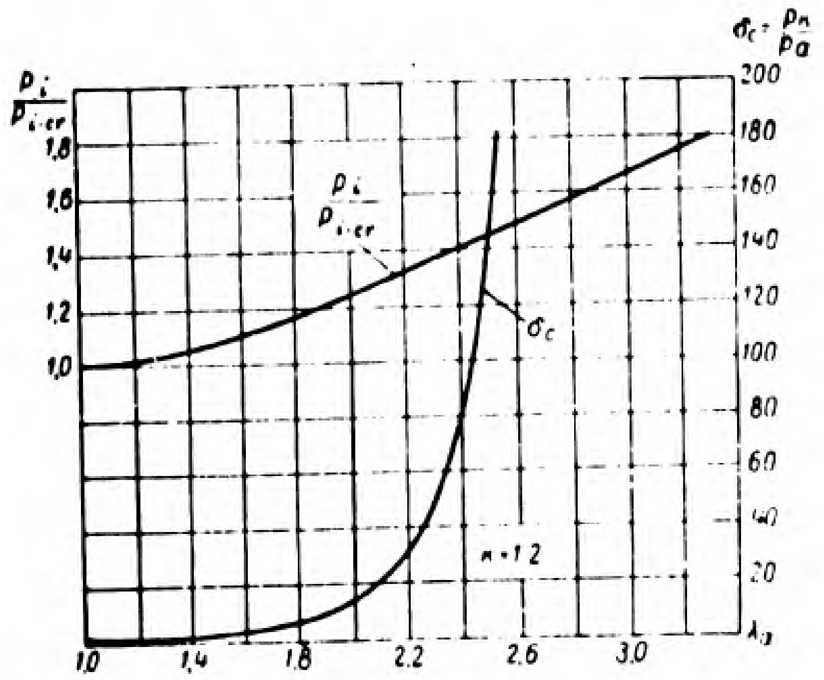

Fig.60 - Effect of Diverging Part of Nozzle on the Increase in Internal Thrust of a Rocket Engine

mosphere, the external thrust must be taken into account, i.e., the axial component of the external atmospheric forces acting on the outer shell of the chamber and nozzle. According to Fig.60, we may write

$$P'_{ex} = -\int_{f_0}^{f_a} p_{ex}\,df = -p_{ex}\int_{f_0}^{f_a} df = -p_{ex} f_a. \tag{31}$$

Adding eqs.(28) and (31), we obtain the true specific engine thrust:

$$P_{sp} = \frac{W_a}{g} + f_a(p_a - p_{ex}). \tag{32}$$

In the case of calculation in which the expansion takes place to atmospheric pressure, and $p_a = p_{ex}$, we have

$$P_{sp} = \frac{W_a}{g}. \tag{33}$$

The condition of underexpansion corresponds to $p_a > p_{ex}$; in overexpansion, we have $p_a < p_{ex}$. The specific thrust in the general case consists of two components - the dynamic component P_W depending only on the exhaust velocity, and the static component P_{st}, determined by the dimensions of the exit section and the pressure difference $p_a - p_{ex}$.

Figure 61 shows two pf-diagrams. The magnitude of the dynamic thrust in the

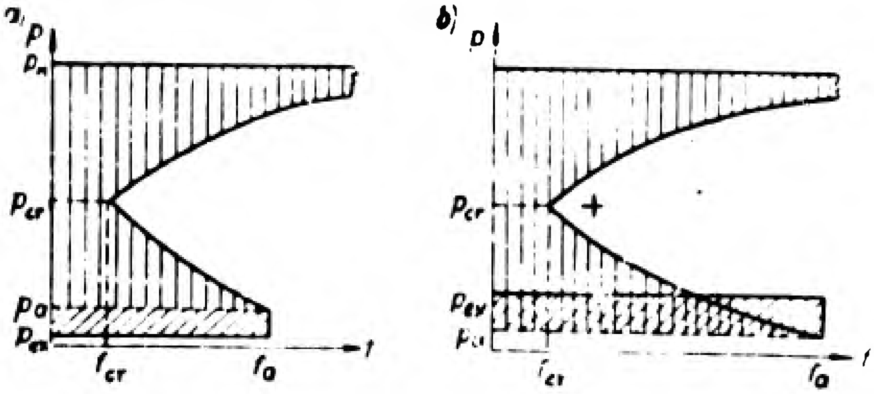

Fig.61 - pf-Diagram for a Rocket Engine at p = c

a - With underexpansion; b - With overexpansion

case of underexpansion is proportional to the area shown by vertical hatching and the magnitude of the static thrust, to the area shown by diagonal hatching.

Let us transform the second summand of the right-hand side of eq.(32):

$$f_a(p_a - p_{ex}) = f_a p_a\left(1 - \frac{p_{ex}}{p_a}\right) = f_a p_a \beta = \frac{f_a p_a W_a}{RT_a \lambda_c''} \cdot \frac{RT_k}{W_a}\beta.$$

However,

$$f_a \frac{p_a}{RT_a} W_a = 1.$$

Then, instead of eq.(32), we write

$$P_{sp} = \frac{W_a}{g} + \frac{RT_k}{\lambda_c'' W_a}\beta = \frac{W_a}{g}\left(1 + \frac{\beta}{kM_a^2}\right), \qquad (34)$$

where β is the non-design ratio, equal to

$$\beta = 1 - \frac{p_{ex}}{p_a} = 1 - \frac{\delta_c}{\delta_{ex}}. \qquad (35)$$

The value of the thrust, like that of the work, may sometimes be more conveniently expressed in relative units. Let us take as the unit of measurement for relative thrust the value of its dynamic component in a convergent nozzle.

Since

$$P_{W_{cr}} = \frac{W_{cr}}{g},$$

then

$$\overline{P}_W = \frac{P_W}{P_{W_{cr}}} = \frac{W_a}{W_{cr}} \text{ and } \overline{P}_{st} = \frac{\beta}{kM_a^2} \cdot \frac{W_a}{W_{cr}}.$$

Expressing the relative thrusts as a function of the Mach number and λ, we get

$$\overline{P}_W = \lambda_a = M_a \sqrt{\frac{k+1}{2\left(1 + \frac{k-1}{2} M_a^2\right)}}; \qquad (36)$$

$$\overline{P}_{st} = \frac{\beta}{kM_a} \sqrt{\frac{k+1}{2\left(1 + \frac{k-1}{2} M_a^2\right)}} = \beta \frac{k+1}{2k\lambda_a}\left(1 - \frac{k-1}{k+1}\lambda_a^2\right). \qquad (37)$$

The variation in $\overline{P}$ with external pressure and the gas expansion in the nozzle is shown in generalized form, with variable β, in Fig.62.

The variation in β over the wide range from 0.6 to -1.2, which is attainable by installing nozzles with various values of δ_c, leads to fluctuations of $\overline{P}$ no greater than 2% of the calculated value. The variation in external pressure, on the other hand, does cause substantial changes in the value of the thrust at small fluctuations of β.

It is easy to prove that the maximum of specific thrust corresponds to an expansion ratio such that the pressure in the cross section of the nozzle p_a equals the atmospheric pressure p_{ex}, i.e., corresponds to the rated operating conditions.

Let us write the general expression for the specific thrust in the following form:

$$P_{sp} = \int_0^f (p - p_{ex})\, df.$$

The value of the internal pressure p depends on f. For the divergent section of the nozzle, the relation between p and f is expressed by eq.(43), where

$$\frac{dp}{df} < 0.$$

Let us introduce the notation

$$(p - p_{ex}) = \varphi(f).$$

Then,

$$P_{sp} = \int_0^{f_a} \varphi(f)\, df.$$

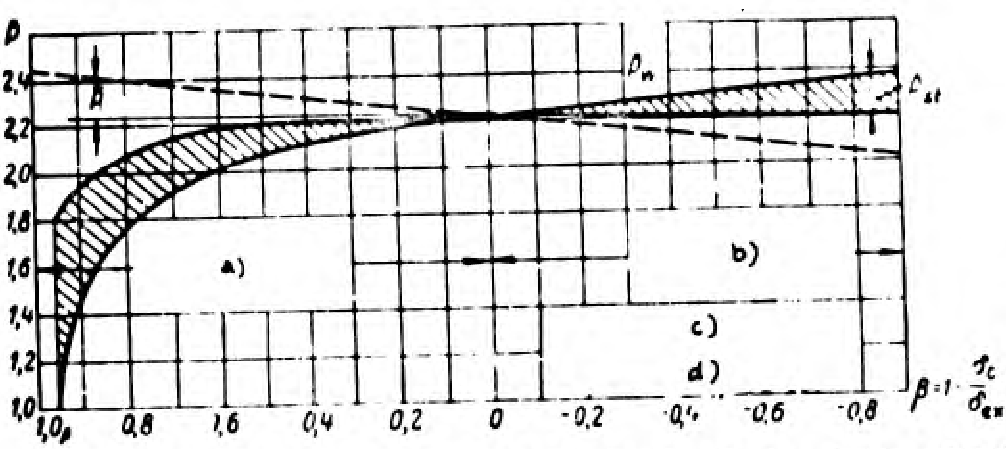

Fig.62 - Variation in Relative Thrust with the Non-Design Ratio of Exhaust

a) Underexpansion; b) Overexpansion; c) δ_{ex} = 40, δ_c is varied; d) δ_c = 40, δ_{ex} is varied, P_w = const

We determine the condition for obtaining maximum specific thrust from the expression

$$\frac{\partial P_{sp}}{\partial f_a} = 0,$$

or

$$\frac{\partial P_{sp}}{\partial f_a} = \frac{d\left(\int_0^{f_a} \varphi(f)\, df\right)}{df_a} = \varphi(f) = 0,$$

which leads to the equation

$$p = p_a = p_{ex}.$$

Since

$$\frac{\partial^2 P_{sp}}{\partial f_a^2} = \frac{d\,[\varphi(f)]}{df_a} = \frac{dp}{df_a} < 0,$$

the condition $p_a = p_{ex}$ corresponds to the maximum of P_{sp}.

In evaluating the economy of a rocket engine, it is logical to compare the available thrust with the ideal thrust, obtainable at full utilization of the energy imparted to the working fluid. At full expansion of the gas to a pressure of $p_a = 0$, the exhaust velocity will be

$$W_{max} = \sqrt{2g\frac{k}{k-1}RT_c} = \sqrt{2gQ_1}.$$

and the thrust will be

$$P_{sp\,max} = \frac{W_{max}}{g}.$$

The ratio

$$\psi_c = \frac{P_{sp}}{P_{sp\,max}} \tag{38}$$

will be termed the force factor or takeoff factor of the rocket engine. For the rated exhaust regime, at $\beta = 0$, we have

$$\psi_c = \frac{W}{W_{max}} = \frac{\lambda_a}{\lambda_\infty} = \lambda_a\sqrt{\frac{k-1}{k+1}} \tag{39}$$

or

$$\psi_c = \sqrt{\eta_t} = \sqrt{1 - \frac{1}{\delta_c^a}}. \tag{40}$$

In the general case, the takeoff factor will be equal to

$$\psi_c = \frac{W}{W_{max}}\left(1 + \frac{\beta}{kM_a^2}\right) = \sqrt{1 - \frac{1}{\delta_c^a}}\left(1 + \frac{\beta}{kM_a^2}\right)$$

or

$$\psi_c = \sqrt{\eta_t}\left(1 + \frac{\beta}{kM_a^2}\right).$$

However, since

$$M_a^2 = \frac{2}{k-1}\left(\delta_c^a - 1\right)$$

and

$$\delta_c^a - 1 = \frac{\eta_t}{1 - \eta_t}.$$

then

$$M_a^2 = \frac{2}{k-1} \cdot \frac{\eta_t}{1-\eta_t}.$$

As a result

$$\psi_c = \sqrt{\eta_t}\left(1 + \frac{k-1}{2k} \cdot \frac{1-\eta_t}{\eta_t}\beta\right). \tag{41}$$

On ejection into a vacuum, $\beta = 1.0$ and

$$\psi_c|_{\beta=1.0} = \sqrt{\eta_t}\left(1 + \frac{k-1}{2k} \cdot \frac{1-\eta_t}{\eta_t}\right). \tag{42}$$

From eq.(41) it is easy to determine the value of η_t at which, in the case of underexpansion, the minimum values of the takeoff factor and P_{sp} are obtained. Thus, at $\beta = 1.0$,

$$\eta_t|_{P_{sp\,min}} = \frac{k-1}{k+1} = \frac{1}{\lambda_\infty^2}.$$

Figure 63 shows the relations $\psi_c = f(\eta_t)$ for $\beta = 0$, $\beta = 1.0$, and $\beta = 0.5\ kM_a^2$. As shown by a comparison of the curves, an increase in the adiabatic exponent k will cause an increase in ψ_c.

The curves in Fig.64 represent ψ_c as a function of the expansion ratio in the nozzle δ_c.

The variation in the lateral dimensions of the nozzle duct f may be represented in the form of a plot versus δ_c, λ, and M.

Let us recall these relations, derived in the courses on gas dynamics. The equation of the rate of flow

$$G_{sec} = 1{,}0 = f\gamma W$$

may be reduced to the following form:

$$f \frac{p_k}{\sqrt{RT_k}} \cdot \sqrt{2g\frac{k}{k-1}} \cdot \sqrt{\left(\frac{1}{\delta_c}\right)^{\frac{2}{k}} - \left(\frac{1}{\delta_c}\right)^{\frac{k+1}{k}}} = 1{,}0.$$

For the critical cross section, at

$$\frac{p_{cr}}{p_{\kappa}}=\left(\frac{2}{k+1}\right)^{\frac{k}{k-1}}.$$

$$f_{cr}\frac{p_{\kappa}}{\sqrt{RT_{\kappa}}}\cdot\sqrt{kg\left(\frac{2}{k+1}\right)^{\frac{k+1}{k-1}}}=1{,}0.$$

Combining these two expressions, we get

$$\frac{f}{f_{cr}}=\bar{f}=\frac{\sqrt{\frac{k-1}{2}}\cdot\sqrt{\left(\frac{2}{k+1}\right)^{\frac{k+1}{k-1}}}}{\sqrt{\left(\frac{1}{\pi_c}\right)^{\frac{2}{k}}-\left(\frac{1}{\pi_c}\right)^{\frac{k+1}{k}}}}, \tag{43}$$

where $\bar{f}$ is the relative cross-sectional area of the nozzle.

Making use of the general equation of rate of flow, we write

$$\bar{f}=\frac{\gamma_{cr}W_{cr}}{\gamma W}=\frac{\gamma_{cr}}{\gamma}\cdot\frac{1}{\lambda}.$$

However,

$$\frac{\gamma}{\gamma_{cr}}=\frac{\left(1-\frac{k-1}{k+1}\lambda^2\right)^{\frac{1}{k-1}}}{\left(1-\frac{k-1}{k+1}\right)^{\frac{1}{k-1}}},$$

or

$$\frac{\gamma_{cr}}{\gamma}=\frac{\left(1-\frac{k-1}{k+1}\right)^{\frac{1}{k-1}}}{\left(1-\frac{k-1}{k+1}\lambda^2\right)^{\frac{1}{k-1}}}=\frac{1}{\left(\frac{k+1}{2}-\frac{k-1}{2}\lambda^2\right)^{\frac{1}{k-1}}}.$$

Consequently, the relation between the relative cross section and the relative velocity will be of the form

$$\bar{f}=\frac{1}{\lambda\left(\frac{k+1}{2}-\frac{k-1}{2}\lambda^2\right)^{\frac{1}{k-1}}}. \tag{44}$$

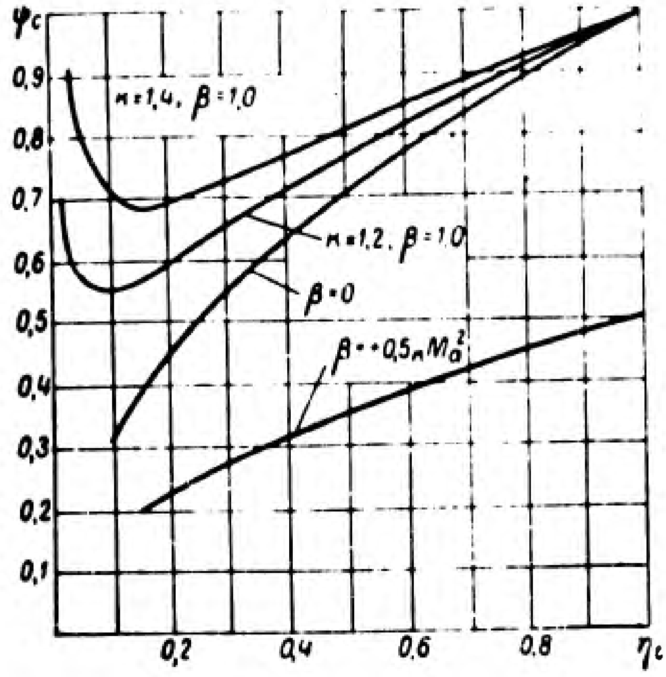

Fig.63 - Relation between Force Factor and Thermal Efficiency

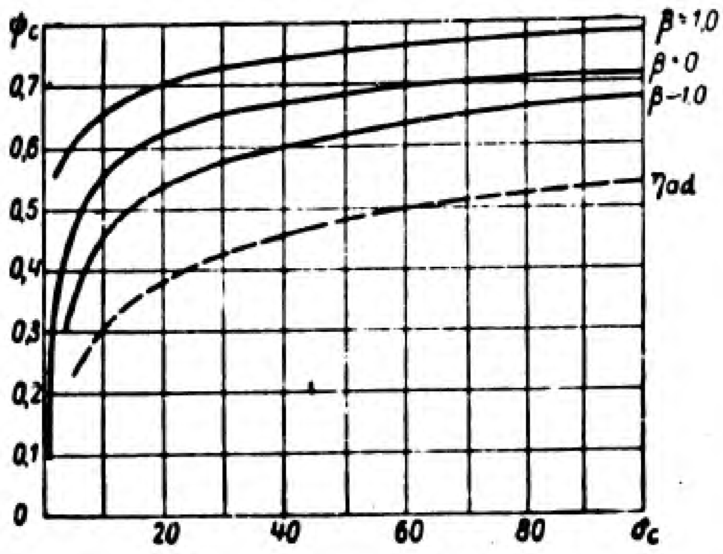

Fig.64 - Relation between the Force Factor and Expansion Ratio in the Nozzle, at Various Non-Design Conditions β ($k = 1.2$)

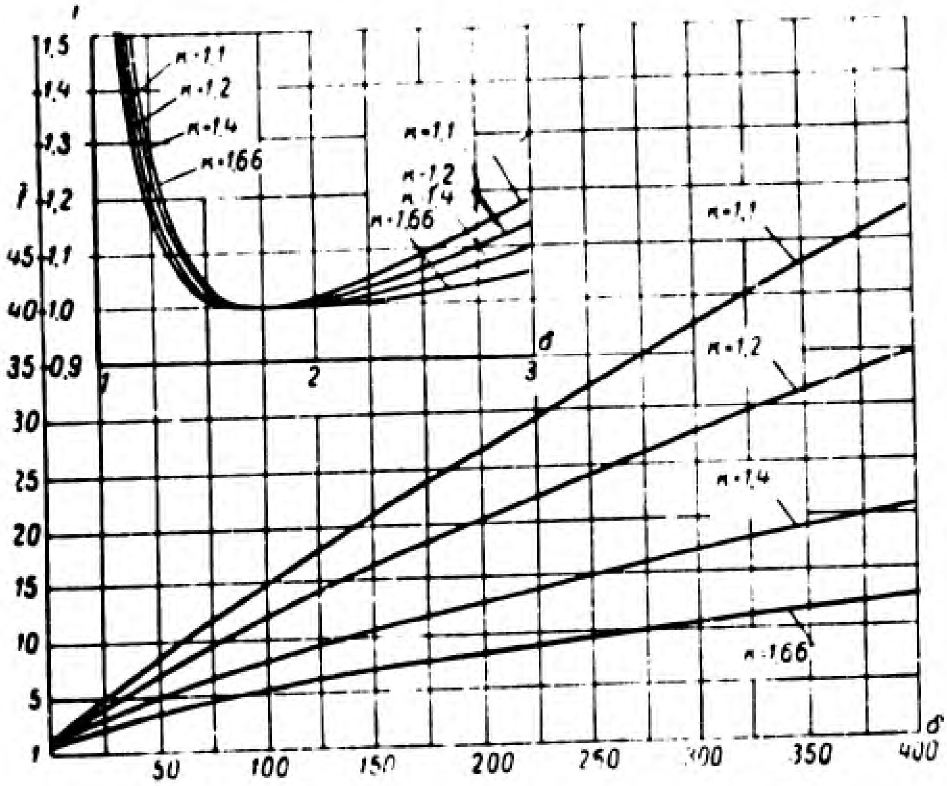

Fig.65 - Relation between Relative Cross Section of the Nozzle and Expansion Ratio

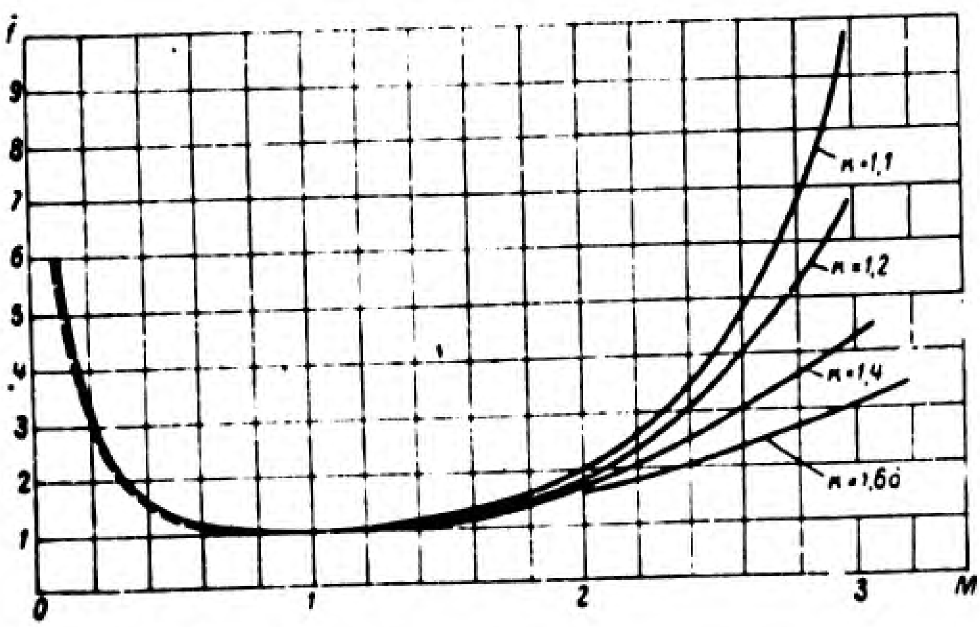

Fig.66 - Relation between Relative Cross Section of the Nozzle and Mach Number

Then it is easy to establish that

$$f = \frac{1}{M}\left[\frac{2}{k+1}\left(1+\frac{k-1}{2}M^2\right)\right]^{\frac{k+1}{2(k-1)}}. \qquad (45)$$

These relations are shown graphically in Figs.65 and 66.

3. Limits of Variation in the Ratio of Non-Design Conditions

Non-design conditions arise in the case of a discrepancy between the available expansion ratio δ_{ex} and the expansion ratio in the nozzle δ_c. At constant nozzle dimensions, this may occur by varying p_{ex} (for instance, in a high-altitude flight) or by varying the propellant consumption, which leads to a change in chamber pressure p_k.

At constant available pressure drop, a change in the expansion ratio in the nozzle δ_c leads to non-design conditions. Let us consider the variation in β at unchanged nozzle, p_c = const, and varying p_{ex}.

A decrease in p_{ex} below its design value causes an underexpansion of the gases in the nozzle. In this case, β is positive and, with increasing underexpansion, increases from $\beta = 0$ to $\beta = 1.0$. The latter value is obtained on ejection into a vacuum, at $p_{ex} = 0$. The non-design conditions become negative at $p_{ex} > p_a$, when overexpansion begins. It is well known that beyond the exit of a supersonic nozzle a system of shock waves becomes established. With increasing overexpansion, the disturbances in the ambient medium, while propagating, may penetrate into the nozzle itself. The beginning of such penetration, coinciding with the appearance of shock waves at the nozzle exit, can be defined as the instant at which normal flow in the nozzle duct becomes disturbed, corresponding to the lower limit of β.

Assuming that, in the ideal case, the transition from the pressure p_a to atmospheric pressure is accomplished by way of a straight shock wave, we find

$$\frac{p_{as}}{p_a} = \frac{2k}{k+1}M_a^2 - \frac{k-1}{k+1}$$

and

$$\beta = \frac{2k}{k+1}\left(1 - M_a^2\right). \tag{46}$$

However, the experimental data obtained with actual nozzles show that the terminal or critical overexpansion is considerably less. In fact, downstream of the nozzle exit, complex phenomena of energy absorption occur. If we knew them precisely, we could determine the instant of disturbance of the normal interaction of forces between the gas and the nozzle walls. These processes depends not only on the energetic parameters of the jet, but also on other auxiliary processes which are governed by the properties of the working fluid and the design features of the nozzle duct. In this respect, it is suggested to make use of empirical relations between the terminal values of β and M_a. Thus, for nozzles similar in their geometric parameters, characterizing the exhaust conditions from the nozzle of a liquid rocket engine, we may establish an empirical relation of the form

$$\frac{p_{cr}}{p_a} = \xi M_a$$

or

$$\beta = 1 - \xi M_a, \tag{47}$$

where ξ is an experimental coefficient.

In this case,

$$P_{sp} = \frac{W}{g}\left(1 + \frac{1 - \xi M_a}{k M_a^2}\right). \tag{48}$$

Equation (47) sets the lower limit for the non-design ratio β.

A further increase in the external pressure is accompanied by penetration of a shock wave into the nozzle. The shock becomes established between the nozzle exit and the nozzle throat. Figure 67 shows the slope of the curve for the pressure exerted on the nozzle wall at a shock wave inside the nozzle.

The experimental data justify the conclusion that, at the existing shapes of rocket-engine nozzles, the pressure in the jet after the arrival of the shock wave varies very little and is practically equal to the ambient pressure. This means that the diffusion effect of the end section of the nozzle is slight. It is also found that the end section of the nozzle, adjacent to the site of the shock wave, does not produce thrust, since the external and internal pressures on the wall are in equilibrium. Consequently, in approximate calculations, the thrust of a nozzle with a compression shock may be determined as the thrust of a normal nozzle with an expansion ratio $\frac{p_c}{p_x}$, where p_x is the pressure before the shock.

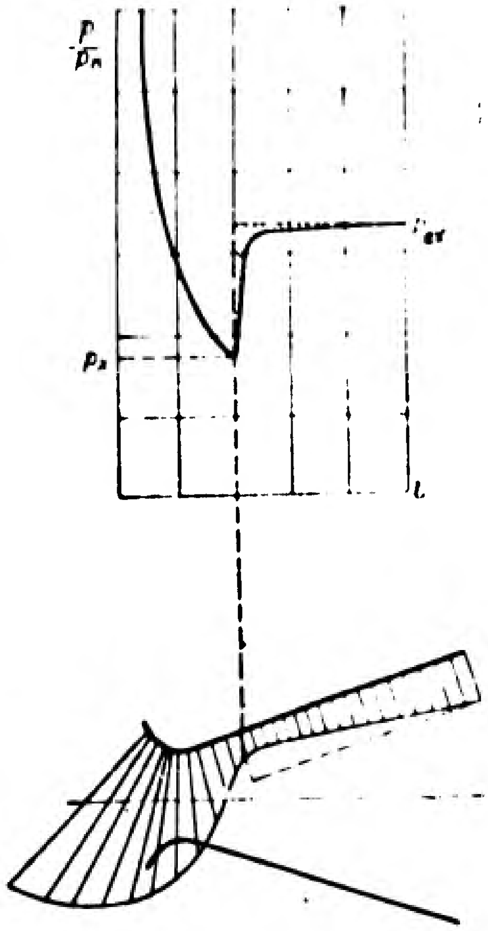

Fig.67 - Pressure Variation Inside the Nozzle in the Presence of a Shock Wave

As before, we may write

$$P_{sp} = P_i - P_{ex} - p_n f_n + \int_0^{W_x} \frac{dW}{g} + \int_{f_n p_n}^{f_x p_x} d(fp) - p_{ex} f_x.$$

After integration, we get

$$P_{sp} = p_n f_n + \frac{W_x}{g} + f_x p_x - p_n f_n - p_{ex} f_x,$$

or

$$P_{sp} = \frac{W_x}{g}\left[1 + \frac{gRT_x}{w_x^2}\left(1 - \frac{p_{ex}}{p_x}\right)\right].$$

If

$$\frac{p_{ex}}{p_x} = \xi M_x,$$

then

$$P_{sp} = \frac{W_x}{g}\left(1 + \frac{1 - \xi M_x}{kM_x^2}\right) \qquad (49)$$

However,

$$W_x = M_x\sqrt{kgRT_x} = M_x \frac{\sqrt{kgRT_n}}{\sqrt{1 + \frac{k-1}{2} M_x^2}}.$$

and, therefore,

$$P_{sp} = \frac{1 + kM_x^2 - \xi M_x}{M_x\sqrt{1 + \frac{k-1}{2}M_x^2}}\sqrt{\frac{RT_k}{kg}}. \tag{50}$$

To determine the parameters of the jet in the x^{th} section, we adopt the additional condition

$$\frac{p_k}{p_{ex}} = \frac{p_k}{p_x}\cdot\frac{p_x}{p_{ex}} = \frac{\left(1 + \frac{k-1}{2}M_x^2\right)^{\frac{k}{k-1}}}{\xi M_x}. \tag{51}$$

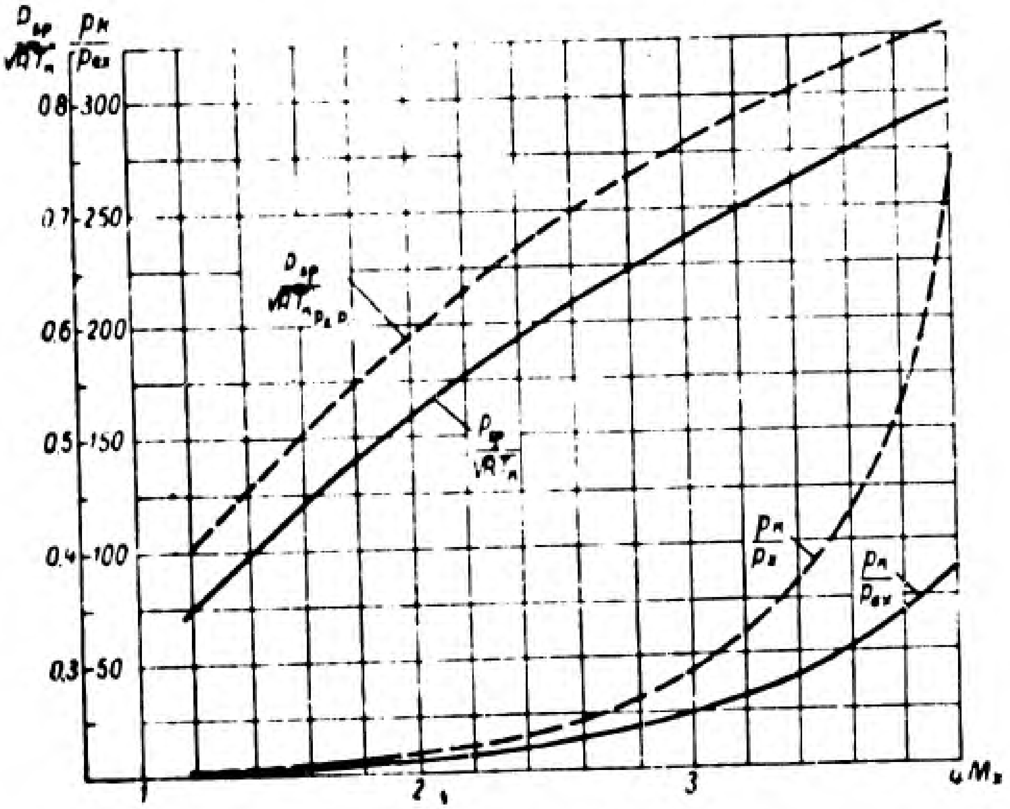

Fig.68 - Variation of Ratios $\frac{P_k}{P_{ex}}$ and $\frac{P_{sp}}{\sqrt{RT_k}}$ with the Mach Number in the x^{th} Section of the Nozzle (k = 1.2)

Simultaneous solution of eqs.(50) and (51) permits determining the site of the compression shock and the value of P_{sp}.

The above definition of P_{sp} should be regarded as an example of the utilization of one of the special empirical relations which define the site of a compression shock inside the nozzle.

The relations (50) and (51) are represented graphically in Fig.6P. The dashed line $\frac{p_k}{p_x}$ denotes the expansion ratio of a gas to the section with the shock. Consequently, the ratio of the ordinates $\frac{p_k}{p_x}$ to $\frac{p_k}{p_{ex}}$ equals the quantity ξM_x, i.e., the degree of pressure rise in the end diffuser section of the nozzle. If, at the expansion ratio $\frac{p_k}{p_x}$ found in the nozzle duct, the nozzle is working at rated conditions, when

$$p_x = p_a = p_{ex}$$

then the specific thrust would be of a value corresponding to the upper curve

$$\left(\frac{P_{sp}}{\sqrt{RT_k}}\right)_{p_x = p_a = p_{ex}}$$

Under non-design conditions, when the shock coincides with the exit section of the nozzle, the specific thrust is less, owing to the increase in external pressure and, consequently, also to the increase in external thrust.

Section 10. The Ideal p = c Rocket Engine with Nonuniform Temperature Distribution over the Chamber Cross Section

In many cases, the temperature nonuniformity in the cross section of the chamber or of the nozzle must be taken into account.

Such nonuniformity may arise as a result of random deviations during mixture formation and heat liberation; in practice it is always present to some degree.

Nonuniformity of temperature distribution may also be artificially produced. This is the case, for instance, when the propellant is fed through the injectors at the chamber intake section, at a predetermined different component ratio, with the object of protecting the walls of the chamber and nozzle from overheating, or else when the working fluid flowing along the chamber walls is gradually heated by the central heat source. Knowing the law of component distribution in the chamber and the laws of heat transfer, one can establish the state of the working fluid at various points of the cross section on entering the nozzle.

Let us consider the influence of the nonuniformity of the thermal state of the gas on the performance parameters of the engine, for several simple versions of the temperature distribution inside the chamber.

Assume that, in the mouth section of the nozzle the composition of the working fluid and its pressure are equal over the entire cross section; similarly, assume that the pressure over the entire exit cross section is also equal. The temperature in the section varies symmetrically with respect to the axis of the chamber. The law of temperature variation along the radius is specified. It is assumed in the calculations that, on efflux, each annular unit jet, having its own initial temperature, is expanded and accelerated independently of the neighboring ones. These simplifications permit us to show, in a simpler form, the influence of the nonuniformity of temperature distribution as the factor with the strongest influence on rocket-engine performance, and, at the same time, to give an idea of the results of using chambers with an elevated temperature of the axial core of the flow.

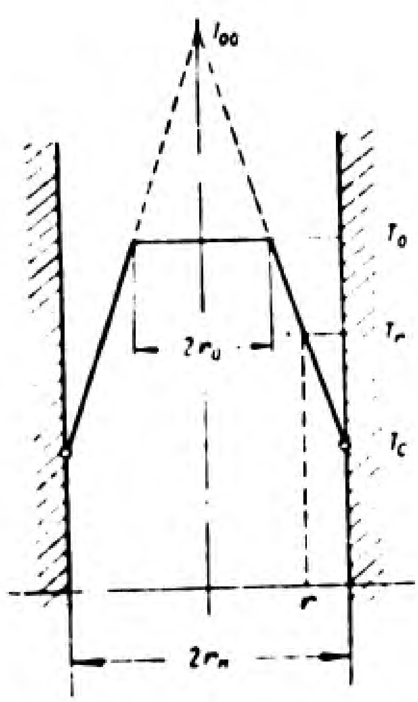

Fig.69 - Version of Temperature Distribution along the Chamber Diameter

Let us consider first the version of conical temperature distribution in the mouth section of the nozzle duct. A graph of the temperature along the chamber is given in Fig.69. Across the central part of the section G_0 kg/sec of gas flows at constant temperature T_0. Since the initial pressure p_k and the expansion ratio δ_c are the same for all unit jets taken separately, it follows that the thrust per unit area of the exit section, which is the same for all the unit jets, will be

$$\frac{P_{sp}}{f_a} = p_a k M_a^2 = \text{const}. \tag{52}$$

If

$$\Delta T = T_0 - T_c \text{ and } \bar{r} = \frac{r}{r_k},$$

then it is easy to find the relation between the temperature and the radius of the chamber in the peripheral portion of the flow, in the following form

$$T_r = T_0 - \Delta T \frac{\bar{r} - \bar{r}_0}{1 - \bar{r}_0}. \tag{53}$$

Determining $\bar{r}$ from eq.(53), we get

$$\bar{r} = \bar{r}_0 + \frac{T_0 - T_r}{\Delta T}(1 - \bar{r}_0). \tag{54}$$

Let us now find the cross section of the chamber

$$f_k = f_{k0} + f_{kc},$$

corresponding to the weight rate of flow

$$G_0 + G_c = 1 \ \text{kg/sec}.$$

Obviously,

$$G_0 = \frac{\pi r_0^2 p_k}{RT_0} W_k = \frac{\pi r_k^2 \bar{r}_0^2}{RT_0} p_k W_k.$$

Assume that the velocity at the nozzle mouth is negligibly small, i.e., that it is W_k = 1.0 m/sec. Then,

$$G_0 = f_k \gamma_{k0} \bar{r}_0^2. \tag{55}$$

In an annular section of the flow, we have

$$dG_c = \frac{p_k}{RT_r} df_k = \frac{2\pi p_k r dr}{RT_r} = 2 f_k \gamma_{k0} \frac{\bar{r} d\bar{r}}{\left(\frac{T_r}{T_0}\right)}.$$

Making use of eq.(54), we eliminate from this expression the quantity

$$\bar{r} d\bar{r} = \frac{(1 - \bar{r}_0)^2}{\left(1 - \frac{T_c}{T_0}\right)^2} \cdot \left(\frac{T_r}{T_0} - \frac{T_0}{T_0}\right) d\frac{T_r}{T_0}.$$

where T_{00} is the fictitious temperature of the gas along the axis of the chamber for the case $\bar{r}_0 = 0$ at the specified radial temperature gradient:

$$\frac{T_{00}}{T_0} = \frac{1 - \bar{r}_0 \frac{T_c}{T_0}}{1 - \bar{r}_0}. \qquad (56)$$

Then,

$$dG_c = \frac{2 f_k \gamma_{k0} (1 - \bar{r}_0)^2}{\left(1 - \frac{T_c}{T_0}\right)^2} \cdot \left[d\left(\frac{T_r}{T_0}\right) - \frac{T_{00}}{T_0} \frac{d\left(\frac{T_r}{T_0}\right)}{\left(\frac{T_r}{T_0}\right)} \right]; \qquad (57)$$

$$G_c = \frac{2 f_k \gamma_{k0} (1 - \bar{r}_0)^2}{\left(1 - \frac{T_c}{T_0}\right)^2} \cdot \left(\frac{T_{00}}{T_0} \ln \frac{T_0}{T_c} + \frac{T_c}{T_0} - 1 \right). \qquad (58)$$

From the condition

$$G_0 + G_c = 1,0 = f_k \gamma_{k0} \left[\bar{r}_0^2 + \frac{2 (1 - \bar{r}_0)^2}{\left(1 - \frac{T_c}{T_0}\right)^2} \left(\frac{T_{00}}{T_0} \ln \frac{T_0}{T_c} + \frac{T_c}{T_0} - 1 \right) \right]$$

we now determine the cross section f_k:

$$f_k = \frac{\left(1 - \frac{T_c}{T_0}\right)^2}{\gamma_{k0} \left[\bar{r}_0^2 \left(1 - \frac{T_c}{T_0}\right)^2 + 2 (1 - \bar{r}_0)^2 \left(\frac{T_{00}}{T_0} \ln \frac{T_0}{T_c} + \frac{T_c}{T_0} - 1 \right) \right]}. \qquad (59)$$

To determine the annular part of the flow in the exit section of the nozzle, we set up the equality:

$$dG_c = W_{ac} df_a.$$

Hence,

$$df_a = \frac{dG_c R T_{ac}}{W_{ac} p_a} = \frac{R T_r \delta^{\frac{1}{k}}}{W_{ac} p_k} dG_c.$$

However,

$$W_{ac} = W_{a0} \sqrt{\frac{T_r}{T_0}} \quad \text{and} \quad \frac{p_k}{R T_0} = \gamma_{k0}.$$

Then,

$$df_a = \frac{\delta^{\frac{1}{k}}}{W_{a0} \gamma_{k0}} \sqrt{\frac{T_r}{T_0}} \, dG_c.$$

Substituting the value of dG_c from eq.(57) in this expression, we get

$$df_a = \frac{2 f_k \delta^{\frac{1}{k}} (1-\bar r_0)^2}{W_{ao}\left(1-\frac{T_c}{T_0}\right)^2}\left[\sqrt{\frac{T_r}{T_0}}\, d\left(\frac{T_r}{T_0}\right) - \frac{T_{ao}}{T_0}\, d\left(\frac{T_r}{T_0}\right)\right]. \tag{60}$$

After integration, we have

$$f_{ac} = B\left(\frac{2}{3}\frac{T_r}{T_0}\sqrt{\frac{T_r}{T_0}} - 2\frac{T_{ao}}{T_0}\sqrt{\frac{T_r}{T_0}}\right)\Bigg|_{1.0}^{\frac{T_c}{T_r}},$$

or

$$f_{ac} = -\frac{4}{3}\,\frac{f_k \delta^{\frac{1}{k}} (1-\bar r_0)^2}{W_{ao}\left(1-\frac{T_c}{T_0}\right)^2}\cdot\left(\sqrt{\frac{T_c}{T_0}}-1\right)\left(\frac{T_c}{T_0}+\sqrt{\frac{T_c}{T_0}}+1-3\frac{T_{ao}}{T_0}\right). \tag{61}$$

Equation (61) determines the total value of the exit section for that part of the gas which has the variable initial temperature from T_c to T_o.

To find the relation $T_a = f(\bar r_a)$, the right-hand side of eq.(60) must be integrated within the limits $\frac{T_r}{T_o}$ and 1.0.

On the left-hand side, we have

$$df = 2\pi r\, dr = 2\pi r_a^2 \bar r\, d\bar r = 2 f_a \bar r\, d\bar r,$$

which gives

$$f = f_a\left(\bar r^2 - \bar r_0^2\right).$$

Consequently,

$$f_a\left(\bar r^2 - \bar r_0^2\right) = \frac{4 f_k \delta_c^{\frac{1}{k}} (1-\bar r_0)^2}{3 W_{ao}\left(1-\frac{T_c}{T_0}\right)^2}\times$$

$$\times\left(\sqrt{\frac{T_r}{T_0}}-1\right)\left(\frac{T_r}{T_0}+\sqrt{\frac{T_r}{T_0}}+1-3\frac{T_{ao}}{T_0}\right). \tag{62}$$

However, since

$$\frac{T_r}{T_0} = \frac{T_a}{T_{ao}},$$

then

$$f_a\left(\bar r^2 - \bar r_0^2\right) = \frac{4 f_k \delta_c^{\frac{1}{k}} (1-\bar r_0)^2}{3 W_{ao}\left(1-\frac{T_c}{T_0}\right)^2}\times$$

$$\left(\sqrt{\frac{T_a}{T_{a0}}}-1\right)\left(\frac{T_a}{T_{a0}}+\sqrt{\frac{T_a}{T_{a0}}}+1-3\frac{T_{00}}{T_0}\right). \tag{63}$$

Let us write the same expression for $\bar{r} = 1.0$ and divide eq.(63) by it. As a result, we obtain the law of temperature variation along the radius in the exit section of the nozzle:

$$\frac{\bar{r}^2-\bar{r}_0^2}{1-\bar{r}_0^2}=\frac{\left(\sqrt{\frac{T_a}{T_{a0}}}-1\right)\left(\frac{T_a}{T_{a0}}+\sqrt{\frac{T_a}{T_{a0}}}+1-3\frac{T_{00}}{T_0}\right)}{\left(\sqrt{\frac{T_{ac}}{T_{a0}}}-1\right)\left(\frac{T_{ac}}{T_{a0}}+\sqrt{\frac{T_{ac}}{T_{a0}}}+1-3\frac{T_{00}}{T_0}\right)}. \tag{64}$$

The total area of the exit section for a weight rate of flow of the gas of 1 kg/sec must have the value

$$f_a=f_{a0}+f_{ac}.$$

From the equality

$$f_{\kappa}\gamma_{\kappa 0}\bar{r}_0^2=f_{a0}\gamma_{a0}W_{a0}$$

we find the section f_{a0}:

$$f_{a0}=\frac{f_{\kappa}\delta_c^{\frac{1}{k}}\bar{r}_0^2}{W_{a0}}. \tag{65}$$

We then determine the specific thrust from eq.(52):

$$P_{sp}=p_a k M_a^2 (f_{a0}+f_{ac}).$$

Making use of eq.(53), we obtain the following expression for the specific thrust:

$$P_{sp}=\frac{4}{3}\left(1-\bar{r}_0^2\right)P_{sp\,0}\frac{\left(\sqrt{\frac{T_c}{T_0}}-1\right)\left(\frac{T_c}{T_0}+\sqrt{\frac{T_c}{T_0}}+1-3\frac{T_{00}}{T_0}\right)}{\bar{r}_0^2\left(1-\frac{T_c}{T_0}\right)^2+2\left(1-\bar{r}_0\right)^2\left(\frac{T_{00}}{T_0}\ln\frac{T_0}{T_c}+\frac{T_c}{T_0}-1\right)}. \tag{66}$$

Since all the unit jets have the expansion ratio δ, it follows that, for the individual jet, the thermal efficiency is the same as for the entire gas flow:

$$\eta_t=1-\frac{1}{\delta_c^{a}}.$$

For the same reason, the force factor of the engine will be

$$\psi_c = \sqrt{1 - \frac{1}{\delta_c''}}.$$

Let us determine the quantity of heat transferred to the gas in the chamber, and the value of the critical energy of the flow:

$$Q_0 = \frac{k}{k-1} R T_0 G_0 = \frac{k}{k-1} R T_0 f_{k0} \bar{r}_0^2.$$

In the annular flow, we have

$$Q_c = \int \frac{k}{k-1} R T_k dG_c = \frac{k}{k-1} 2\pi r_k^2 p_k \int_{\bar{r}_0}^{1.0} \bar{r}\, d\bar{r},$$

or

$$Q_c = \frac{k f_k p_k (1 - \bar{r}_0^2)}{k-1}.$$

After summation, we get

$$Q_1 = Q_0 + Q_c = \frac{k}{k-1} p_k f_k. \tag{67}$$

The quantity of heat transferred to 1 kg of gas equals the quantity of heat transferred in a chamber of the same cross section by a flow of gas at constant temperature T_0 or T_c.

The kinetic energy of the gas in the exit section of the nozzle is

$$E = \eta_t Q_1 = \frac{k}{k-1} p_k f_k \left(1 - \frac{1}{\delta_c''}\right). \tag{68}$$

At the same consumption of heat per kg of gas, the cross section of the nozzle in a variable-temperature chamber is found to be less than in a maximum-temperature chamber. At the same time the impulses and the force factor ψ_c are found to be the same in both chambers. This conclusion is correct for chambers with heating of the gas. In chemical chambers, a temperature drop is accompanied by the generation of chemical losses; when these are taken into account, the values of η_t and ψ_c in the variable-temperature chamber are lower than in the chamber at temperatures T_0 = const.

A simpler version of the temperature distribution is represented by an extreme special case of the preceding (Fig.70). Here $T_{00} = T_0$ and r_0. Bearing this in mind, we obtain the following expressions for determining the specific area at the nozzle mouth, instead of eq.(59):

$$f_{\kappa} = \frac{\left(1 - \frac{T_c}{T_0}\right)^2}{2\gamma_{\kappa 0}\left(\ln \frac{T_0}{T_c} + \frac{T_c}{T_0} - 1\right)}. \tag{69}$$

For the exit section of the nozzle, we get, accordingly,

$$f_a = \frac{4 f_{\kappa} \bar{r}_a^{\frac{1}{k}}}{3 W_a \left(1 - \frac{T_c}{T_0}\right)^2} \cdot \left[2 - \sqrt{\frac{T_c}{T_0}\left(\frac{T_c}{T_0} - 3\right)}\right]. \tag{70}$$

Substituting this value in eq.(52), we determine the specific thrust

$$P_{sp} = \frac{2}{3} P_{sp\,0} \frac{2 - \sqrt{\frac{T_c}{T_0}\left(\frac{T_c}{T_0} - 3\right)}}{\ln \frac{T_0}{T_c} + \frac{T_c}{T_0} - 1} = \frac{2}{3} P_{sp.c} \frac{2 - \sqrt{\frac{T_c}{T_0}\left(\frac{T_c}{T_0} - 3\right)}}{\ln \frac{T_0}{T_c} + \frac{T_c}{T_0} - 1}. \tag{71}$$

Figure 71 shows the variation in the specific thrust ratios $\frac{P_{sp}}{P_{sp\,o}}$ and $\frac{P_{sp}}{P_{sp.c}}$ plotted versus the ratios of the extreme temperatures $\frac{T_c}{T_o}$.

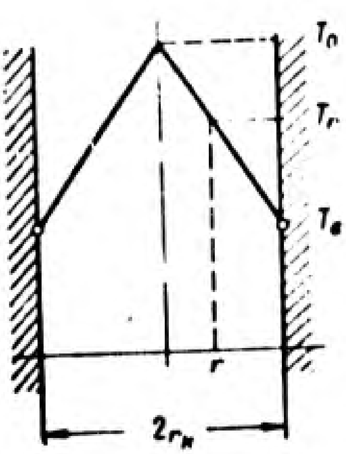

Fig.70 - Version of Linear Temperature Distribution along the Radius of the Chamber

To find the law of temperature variation in the exit section of the nozzle, we now rewrite eq.(64), bearing in mind that $\bar{r}_{ao} = 0$ and $T_{oo} = T_o$. After finding such an expression for the total area of the exit section, we set up the ratio

$$\left(\frac{r_a}{r_{ac}}\right)^2 = \bar{r}_a^2 \frac{2 - \sqrt{\frac{T_a}{T_{a0}}\left(3 - \frac{T_a}{T_{a0}}\right)}}{2 - \sqrt{\frac{T_c}{T_0}\left(3 - \frac{T_c}{T_0}\right)}}. \tag{72}$$

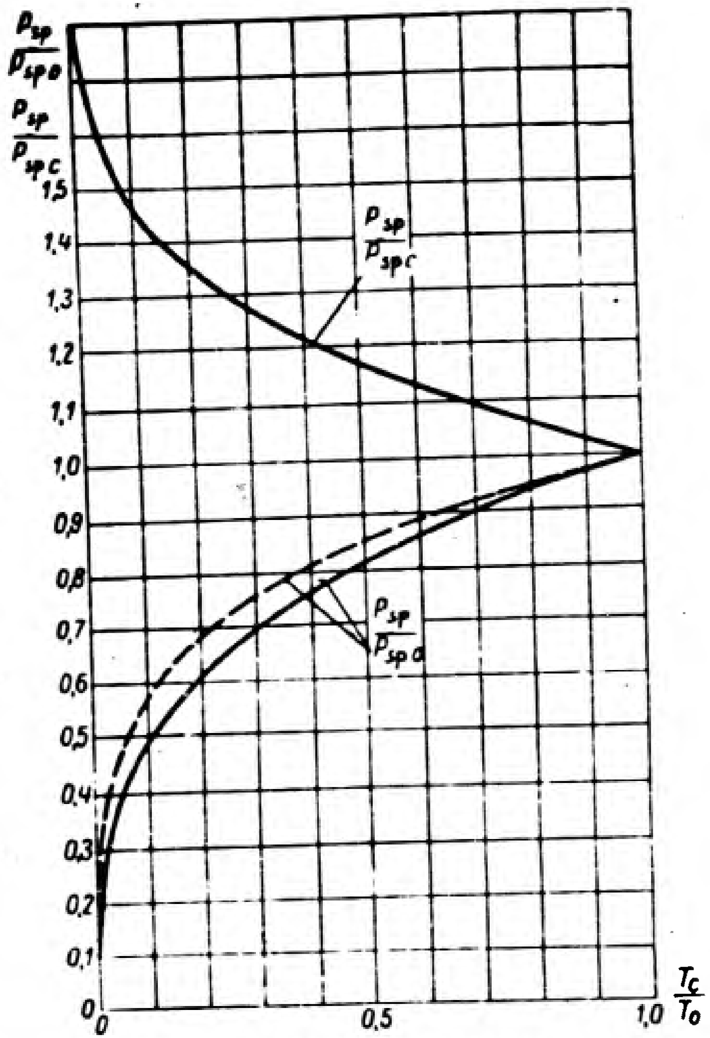

Fig.71 - Variation in Relative Specific Thrust of Chamber with Linear Law of Temperature Variation over Cross Section of the Chamber (Solid Lines) and with Parabolic Law (Broken Lines)

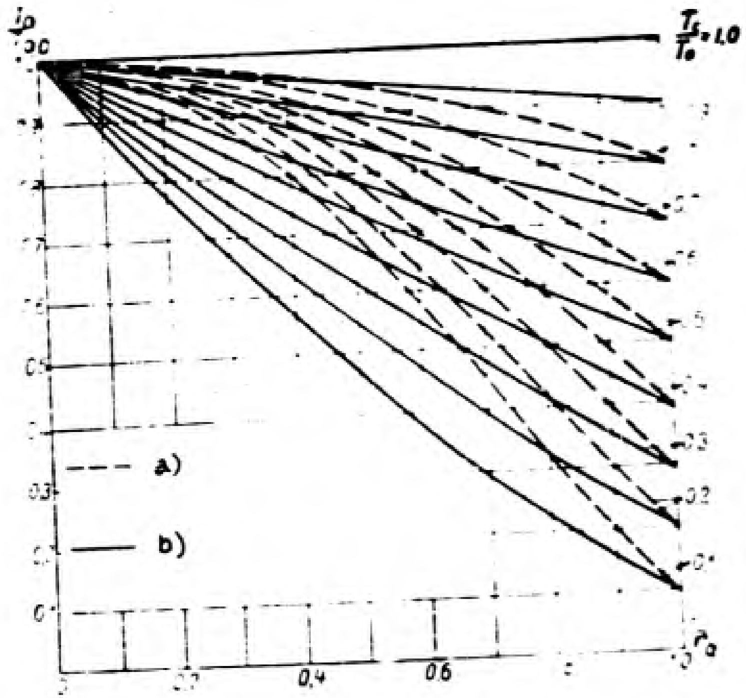

Fig.72 - Variation in Relative Temperature over Nozzle Exit Section

a) --- Parabolic law of temperature distribution; b) —— Linear law of temperature distribution

Figure 72 shows the character of the temperature variation along the radii of the nozzle mouth and exit sections.

From these expressions for a chamber with linear temperature distribution along the radii of the chamber sections, we reach the following conclusions:

1. The thrust per unit area of the exit section is independent of the law of temperature distribution over the cross section of the chamber.

2. With increasing $\frac{T_0}{T_c}$, the specific thrust varies as shown in Fig.71.

3. The temperature gradient along the radius varies on transition from the first cross section of the nozzle to the succeeding cross sections.

The version with parabolic temperature variation along the radius of the chamber is the closest to the actual picture of its distribution. The relation between a radius and the temperature is established at specified extreme temperatures T_0 and T_c (Fig.73). Starting from the equation of the parabola with respect to its vertex, $y^2 = 2px$, and bearing in mind that, in our case,

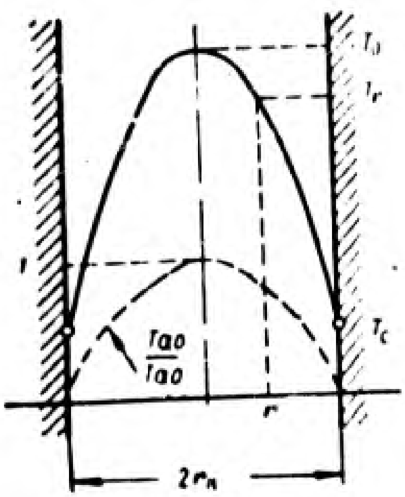

Fig.73 - Version of Parabolic Temperature Distribution over Cross Section of Chamber (Solid Line) and over Exit Section of Nozzle (Broken Line)

$$y = r \text{ and } x = T_0 - T_r,$$

we get the equation

$$\frac{T_r}{T_0} = 1 - \left(1 - \frac{T_c}{T_0}\right)\bar{r}^2. \qquad (73)$$

We now find the value of f_k corresponding to a gas flow rate of 1 kg/sec, by making use of the equation of discontinuity:

$$dG_k = \frac{p_k}{RT_r} W_k \, df_k.$$

Taking, as before, W_k = 1 m/sec, and substituting T_r from eq.(73), we obtain, after transformations and integration,

$$f_{\kappa}=\frac{1-\frac{T_c}{T_0}}{\gamma_{\kappa 0}\ln\frac{T_0}{T_c}}. \tag{74}$$

As in the previous version,

$$df_a=\frac{\delta^{\frac{1}{\kappa}}}{W_a}\,df_{\kappa}.$$

After substitutions and integration we get

$$\frac{f_{ax}}{f_{\kappa}}=\frac{2\delta^{\frac{1}{\kappa}}}{W_0}\cdot\frac{1-\sqrt{\frac{T_{\kappa}}{T_0}}}{1-\frac{T_c}{T_0}}=\frac{2\delta^{\frac{1}{\kappa}}\left(1-\sqrt{\frac{T_a}{T_{a0}}}\right)}{\left(1-\frac{T_c}{T_0}\right)W_0}. \tag{75}$$

We find the complete cross section at the exit for $T_a = T_{ac}$:

$$\frac{f_a}{f_{\kappa}}=\frac{2\delta_c^{\frac{1}{\kappa}}}{W_0}\cdot\frac{1-\sqrt{\frac{T_{ac}}{T_{a0}}}}{1-\frac{T_c}{T_0}}. \tag{76}$$

Dividing eq.(75) by eq.(76), and making use of the radial dimensions of the cross sections, we find the relation between the temperature and the radius in the exit section:

$$\frac{f_{ax}}{f_a}=\left(\frac{r_{ax}}{r_a}\right)^2=\bar{r}_{ax}^2=\frac{1-\sqrt{\frac{T_a}{T_{a0}}}}{1-\sqrt{\frac{T_c}{T_0}}},$$

whence

$$\sqrt{\frac{T_a}{T_{a0}}}=1-\left(1-\sqrt{\frac{T_c}{T_0}}\right)\bar{r}_a^2. \tag{77}$$

The temperature variation along the radius is shown by the broken line in Fig.73, according to eq.(77).

The variation in relative temperature in the end section of the nozzle is shown by the broken line in Fig.72.

To determine the specific thrust, we make use of eq.(52), substituting the value of f_a from eq.(71):

$$P_{sp} = 2P_{sp\,0}\frac{1-\sqrt{\frac{T_c}{T_0}}}{\ln\frac{T_0}{T_c}}. \tag{78}$$

The variation of $\frac{P_{sp}}{P_{spo}}$ for the parabolic version is shown by the broken line in Fig.71.

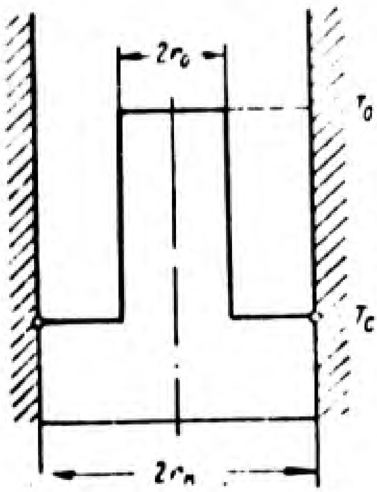

Fig.74 - Schematic Diagram of Stepped Temperature Distribution along the Diameter of the Chamber Section

The quantity of heat transferred to the gas is

$$Q_1=\int dQ=\frac{k}{k-1}p_к\int df_к.$$

Bearing eq.(74) in mind, we get

$$Q_1=\frac{kRT_0}{k-1}\cdot\frac{1-\frac{T_c}{T_0}}{\ln\frac{T_0}{T_c}}.$$

Let us now evaluate, in addition, the features of a chamber with a stepwise temperature distribution along its diameters (Fig.74), remembering that the composition of the gas is the same over the entire cross section of the chamber.

On the basis of eq.(55), we write

$$G_0=f_к\gamma_{к0}\bar{r}_{к0}^2 \text{ and } G_c=f_к(1-\bar{r}_0^2)\gamma_{к.c}.$$

From the equality

$$G_0+G_c=1.0$$

we determine the cross section f_k for a flow rate of 1 kg/sec:

$$f_к=\frac{1}{\gamma_{к0}\left[\bar{r}_0^2+(1-\bar{r}_0^2)\frac{T_0}{T_c}\right]}. \tag{79}$$

The exit sections of the central and peripheral flows are determined, as before, as follows:

$$f_{a0} = f_{\kappa} \frac{\lambda_c^{\frac{1}{\kappa}}}{W_{a0}} \bar{r}_0^2$$

and

$$f_{ac} = f_{\kappa} \frac{\lambda_c^{\frac{1}{\kappa}}}{W_{ac}} \cdot (1 - \bar{r}_0^2).$$

Adding these, we get the following expression for calculating the exit section of a nozzle for a gas flow rate of 1 kg/sec:

$$f_a = \frac{f_{\kappa} \lambda_c^{\frac{1}{\kappa}}}{W_{a0}} \cdot \left[\bar{r}_0^2 + (1 - \bar{r}_0^2) \sqrt{\frac{T_0}{T_c}} \right]. \tag{80}$$

Making use of eq.(52), we now write the following expression for the specific thrust:

$$P_{sp} = P_{sp0} \frac{\bar{r}_0^2 + (1 - \bar{r}_0^2) \sqrt{\frac{T_0}{T_c}}}{\bar{r}_0^2 + (1 - \bar{r}_0^2) \frac{T_0}{T_c}}. \tag{81}$$

Figure 75 shows the relation of the specific thrust at T_0 = const with the degree of temperature rise in the chamber, and the relative dimensions of the central hot flow. Figure 76 shows the variation of the relative specific cross sections of the chamber.

On the basis of Figs.75 and 76 and of eqs.(77) - (79), we arrive at the following conclusions:

1. As in the other versions, the thrust of the chamber per unit area of the exit section does not depend on the initial temperature distribution in the chamber.

2. With increasing size of the hot portion of the flow, the specific thrust increases simultaneously with an increase of the transverse chamber dimensions.

3. With decreasing initial temperature of the cold portion of the flow, the specific thrust decreases with decreasing size of the chamber.

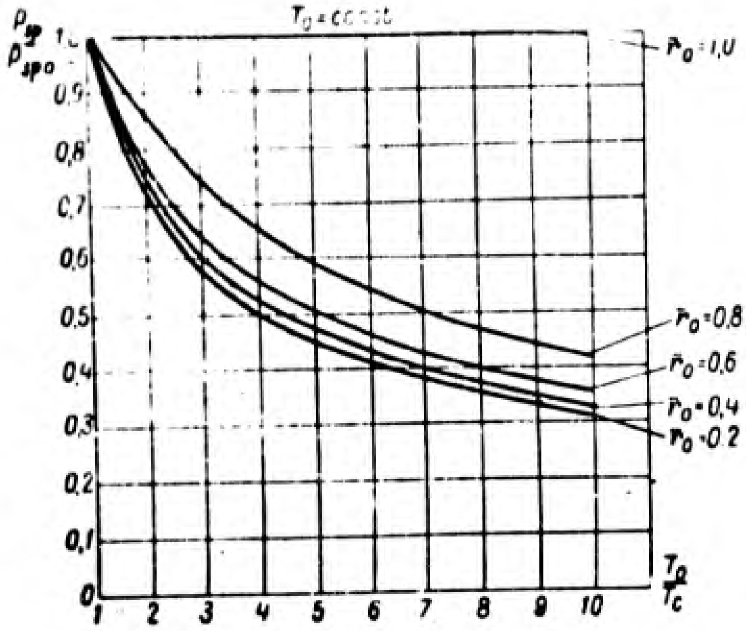

Fig.75 - Relative Specific Thrust of Chamber with Stepwise Temperature Distribution Versus Relative Radius $\bar{r}_0$ and Ratio $\frac{T_0}{T_c}$

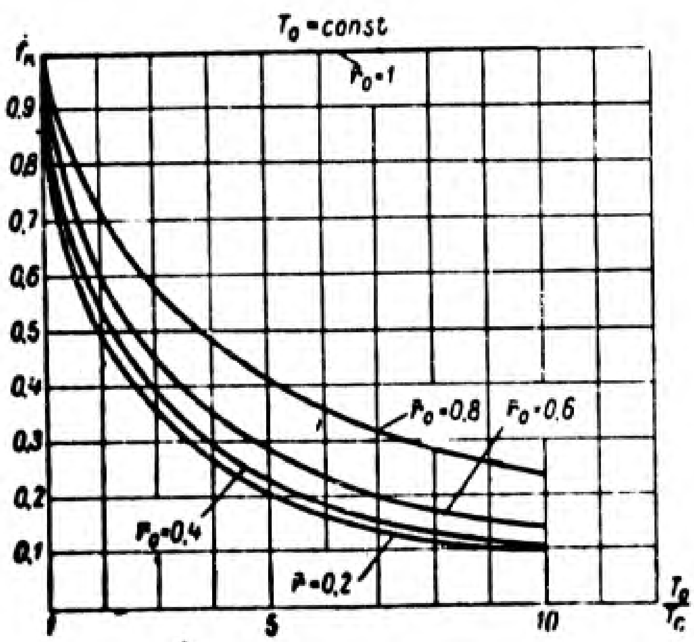

Fig.76 - Relative Specific Cross Section of Chamber with Stepwise Temperature Distribution Versus Relative Radius $\bar{r}_0$ and Ratio $\frac{T_0}{T_c}$

A stepwise temperature distribution can be assumed for engines in which the inner wall of the chamber is protected by a layer of colder gas. If

$$\frac{T_0}{T_c} = 1,5 \text{ and } \bar{r}_0 = 0,9,$$

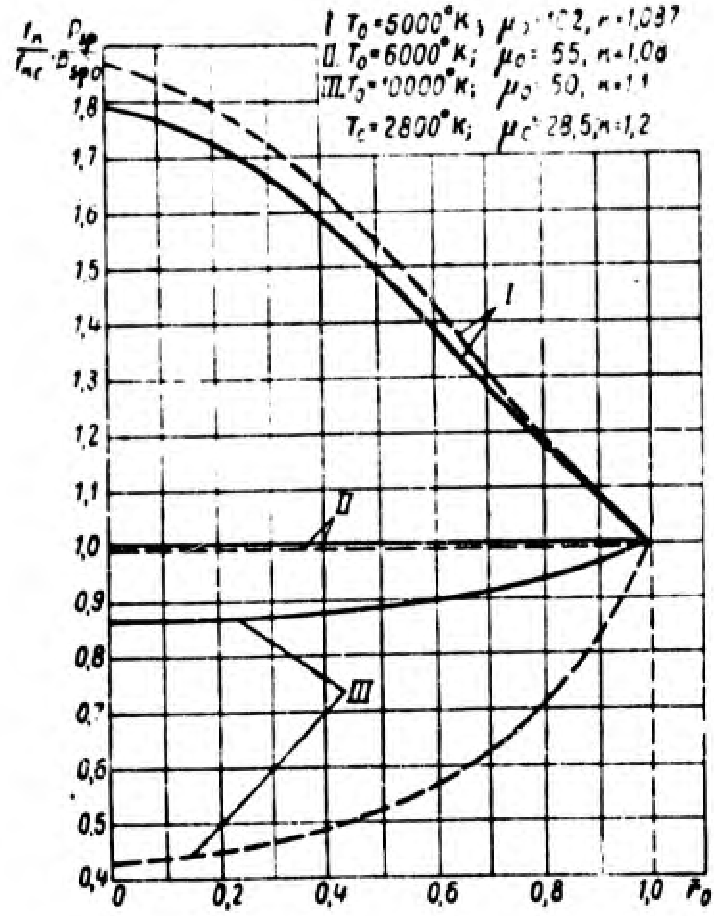

Fig.77 - Variation of Relative Specific Thrust and Relative Area of a Chamber with Stepwise Temperature Distribution in the Case of a Heavy Core

$$\text{———} \ \frac{P'_{sp}}{P_{sp0}}; \ \text{- - -} \ \frac{f_k}{f_{k0}}.$$

which is close to the values in actually existing prototypes, then the losses of specific thrust by comparison with the uniform high-temperature distribution over the section will be about 2.5%, and the losses of thrust will be 8%.

The flows may also have different compositions. Adopting the previous assumptions of independent action of the flows, we obtain the following expressions for f_k'

and the specific thrust

$$f_{\kappa}=\frac{1}{\gamma_{\kappa 0}\left[\bar{r}_0^2+(1-\bar{r}_0^2)\dfrac{R_0T_0}{R_cT_c}\right]}=\frac{848T_0}{p_{\kappa}\mu_0\left[\bar{r}_0^2+(1-\bar{r}_0^2)\dfrac{\mu_cT_0}{\mu_0T_c}\right]};$$

$$\bar{P}_{sp}=\frac{\bar{r}_0^2+(1-\bar{r}_0^2)\cdot\sqrt{\dfrac{\mu_cT_0}{\mu_0T_c}\cdot\dfrac{\left[\dfrac{k}{k-1}\left(1-\dfrac{1}{\delta_c^a}\right)\right]_c}{\left[\dfrac{k}{k-1}\left(1-\dfrac{1}{\delta_c^a}\right)\right]_0}}}{\bar{r}_0^2+(1-\bar{r}_0^2)\dfrac{\mu_cT_0}{\mu_0T_c}},$$

where μ is the molecular weight of the gases.

If one of the gases becomes heavier, the specific dimensions of the chamber and nozzle decrease. The values of R and k affect the variation in the specific thrust. Figure 77 shows the variation in the relative specific thrust $\frac{P_{sp}}{P_{spo}}$ and in the relative area of the chamber $\frac{f_k}{f_{ko}}$ with the dimensionless radius of the heavy core.

Section 11. Effect of Random Fluctuations of Gas Temperature Upstream of the Nozzle on the Specific Thrust of a Rocket Engine

Experience shows that complete temperature uniformity is not obtained in the cross section of a chamber, and that the value of the gas temperature at any arbitrary place of the cross section is not absolutely constant.

Owing to random causes, the local gas temperature fluctuates within certain limits about its mean value. In chemical engines, such fluctuations are due primarily to the process of mixture formation. The random deviations in the phenomena constituting the process of mixture formation are due to the fact that the feed of the components, the fineness of atomization, the collision of the droplets, their evaporation and ignition are not absolutely stationary processes; some of these are essentially discontinuous by nature (for example, the droplet formation).

In a block reactor chamber, the individual channels inevitably differ in dimension, in hydraulic resistance, and in heat-transfer properties, which likewise leads to temperature fluctuations in the cross section of the chamber after the individual flows have merged and mixed.

The temperature fluctuations necessarily exert a certain influence on the specific thrust of the engine; in order to estimate that thrust, accurately experimental data are required on the so-called distribution function $f(T)$, which characterizes these random fluctuations. The probability that the temperature T lies in the range $T - (T + dT)$ is $f(T)\,dT$. The probability that the temperature lies only in the range $T - \Delta T$ to $T + \Delta t$ is

$$\int_{T-\Delta t}^{T+\Delta t} f(T)\,dT.$$

In the case where all values of the varying temperature lie within these limits, we have

$$\int_{T-\Delta t}^{T+\Delta t} f(T)\,dT = 1.0.$$

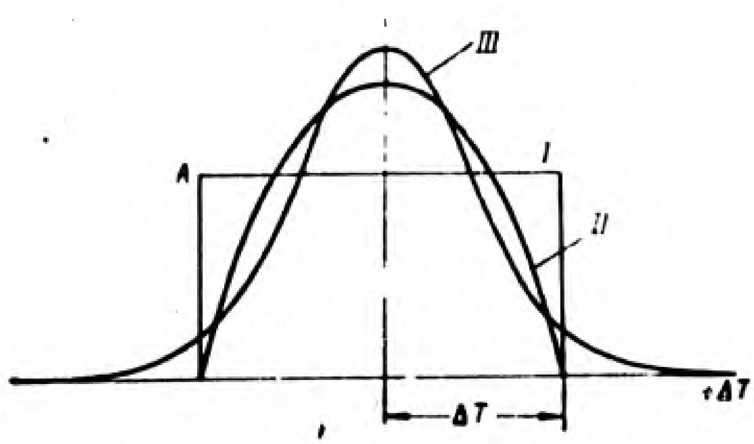

Fig.78 - Versions of the Temperature Distribution Function

If the quantity of interest to us is a function of the temperature, $F(T)$, then its mean value $\bar{F}$ is determined from the expression

$$\bar{F} = \int_{T-\Delta t}^{T+\Delta t} F(T) f(T)\,dT. \tag{82}$$

The form of the distribution function $f(T)$, as already stated, is found from statistical data obtained by experiment.

In our case, there are no experimental data. For this reason, we estimate only the order of the deviations of the specific thrust from the value corresponding to the mean temperature T_0.

In Fig.78 the values of the temperature, which vary between the extreme values $T - \Delta t$ and $T + \Delta t$, are plotted on the abscissa axis. If the probability of any temperature lying within these limits is the same, then the distribution function will be a straight line with constant ordinate $f(T) = a$. In this case,

$$\int_{T-\Delta t}^{T+\Delta t} a\, dT = 2a\,\Delta t = 1{,}0,$$

whence

$$a\,\Delta t = \frac{1}{2}. \tag{83}$$

Of the laws of distribution, the parabolic law shown in Fig.78 by curve II is used frequently, while the exponential law shown by curve III is used most often. The area under the parabola II equals the areas under the straight line I, for the selected temperature range. For convenience of calculation, the exponent is regarded as a curve with unbounded base along the abscissa axis. It is also assumed that $f(0)/f(\Delta t) = e^2$. In this case, the last condition is arbitrarily assigned; in reality it should be based on experimental data.

Let us consider the example of the temperature distribution by the linear law I. Assume that each elementary portion of gas dG, with the initial temperature T at some instant of time, expands in the nozzle without reacting with the adjacent unit jets. To simplify the argument, we assume that the value of dG in the jets with different temperatures is the same.

Then the value of the specific thrust will be determined from the expression

$$P_{sp}\, dG = \sqrt{\frac{2}{g}\frac{k}{k-1}RT\left(1 - \frac{1}{\varepsilon^{m}}\right)}\, dG = B\sqrt{T}\, dG.$$

If the ejection in the unit jet depends on the temperature and if this dependence can be established, then the expression for the thrust of this unit jet is written with allowance for the fluctuation in the flow rate. In our case, the specific thrust is determined from the equation

$$P_{sp} = B\int_{T-\Delta t}^{T+\Delta t} \sqrt{T}\, f(T)\,dT = Ba\int_{T-\Delta t}^{T+\Delta t}\sqrt{T}\,dT,$$

whence

$$P_{sp} = \frac{2}{3}aB\left[(T_0+\Delta t)^{\frac{3}{2}} - (T_0-\Delta t)^{\frac{3}{2}}\right].$$

Let us factorize T_0 and introduce the notation $y = \frac{\Delta t}{T_0}$, where y is the relative amplitude of temperature fluctuation. Then,

$$P_{sp} = \frac{2}{3}aBT_0^{\frac{3}{2}}\left[(1+y)^{\frac{3}{2}} - (1-y)^{\frac{3}{2}}\right].$$

Let us transform the coefficient in front of the brackets as follows:

$$\frac{2}{3}aB\sqrt{T_0}\,T_0 = \frac{2}{3}P_{sp0}a\frac{T_0}{\Delta t} = \frac{2}{3}\frac{a\Delta t}{y}\cdot P_{sp0}.$$

However,

$$a\Delta t = \frac{1}{2}.$$

Consequently,

$$P_{sp} = \frac{P_{sp0}}{3y}\left[(1+y)^{\frac{3}{2}} - (1-y)^{\frac{3}{2}}\right].$$

On expanding the binomials in the brackets into series, we get

$$(1+y)^{\frac{3}{2}} = 1+\frac{3}{2}y+\frac{3}{8}y^2-\frac{y^3}{16}+\ldots$$

$$(1-y)^{\frac{3}{2}} = 1-\frac{3}{2}y+\frac{3}{8}y^2+\frac{y^3}{16}+\ldots$$

Subtracting, we have

$$P_{sp} = \left(1-\frac{y^2}{24}\right)P_{sp0}. \qquad (84)$$

Hence, the relative variation of the specific thrust is determined as follows:

$$\frac{P_{sp\,0}-P_{sp}}{P_{sp\,0}}=\frac{\Delta P_{sp}}{P_{sp\,0}}=\frac{y^2}{24}=\frac{y^2}{0{,}24}\,\%. \qquad (85)$$

Let the extreme temperatures be 10% higher or lower than the mean. Then, $y = 0.1$ and

$$\frac{\Delta P_{sp}}{P_{sp\,0}}=\frac{0{,}01}{0{,}24}=0{,}042\,\%.$$

At $y = 0.5$, which is improbably high for a normally operating engine, we get

$$\frac{\Delta P_{sp}}{P_{sp\,0}}=1{,}04\,\%.$$

Also bearing in mind that the true curves of the distribution function lie between the first version and the following versions shown in Fig.78, it may be considered that the random deviations of the local temperatures from the mean values in the cross section of the chamber ahead of the nozzle mouth have a negligibly slight effect on the specific thrust, but always of a decreasing nature. For versions II and III, the temperatures of the extreme zones, at maximum deviations $F(T)$, are less probable than the temperatures close to the mean T_0. This means that the deviations in the specific thrust are less substantial for versions II and III than for version I.

Let us consider still another case of the effect of the exponential law of distribution, when

$$f(T)=ce^{-a(T-T_0)^2}=ce^{-ax^2},$$

where $x = T - T_0$.

The relation between the coefficients c and a is determined from the equality

$$c\int_{-\infty}^{+\infty}e^{-ax^2}dx=1{,}0.$$

Since

$$\int_{-\infty}^{+\infty}e^{-ax^2}dx=\sqrt{\frac{\pi}{a}}, \qquad (86)$$

then

$$c=\sqrt{\frac{a}{\pi}}.$$

For a specific determination of c and a, experimental data will be necessary.

Not having them, let us assume that

$$\frac{f(0)}{f(\Delta t)} = e^2.$$

Then,

$$e^2 = e^{\alpha \Delta t^2},$$

whence

$$\alpha = \frac{2}{\Delta t^2}$$

and, consequently,

$$c = \sqrt{\frac{\alpha}{\pi}} = \frac{1}{\Delta t}\sqrt{\frac{2}{\pi}}.$$

Thus, the distribution function will be in the form

$$f(x) = \frac{1}{\Delta t}\sqrt{\frac{2}{\pi}}\, e^{-\frac{2}{\Delta t^2}x^2}. \qquad (87)$$

Let us determine the specific thrust:

$$P_{sp} = \int B\sqrt{T_0 + x}\, f(x)\, dx = \frac{B}{\Delta t}\sqrt{\frac{2}{\pi}} \int_{-\infty}^{\infty} \sqrt{T_0 + x}\, e^{-\frac{2}{\Delta t^2}x^2}\, dx.$$

Introducing the notation

$$\frac{\Delta t}{T_0} = y; \quad \frac{x}{T_0} = \frac{T - T_0}{T_0} = \xi'; \quad \frac{x^2}{T_0^2}\cdot\frac{T_0^2}{\Delta t^2} = \frac{(\xi')^2}{y^2}; \quad dx = T_0\, d\xi'.$$

we get

$$P_{sp} = P_{sp\,0}\frac{1}{y}\sqrt{\frac{2}{\pi}} \int_{-\infty}^{\infty} \sqrt{1 + \xi'}\, e^{-\frac{2}{y^2}(\xi')^2}\, d\xi'.$$

In this case, $\xi' < 1.0$. For this reason, on expanding $\sqrt{1+\xi'}$ in a series, we terminate the series after the first three terms

$$\sqrt{1+\xi'} = 1 + \frac{1}{2}\xi' - \frac{1}{8}\xi'^2 + \frac{3}{48}\xi'^3 - \dots.$$

Then, the value of the integral is decomposed into its three components

$$\int \sqrt{1+\xi'}\, e^{-\frac{2}{y^2}(\xi')^2}\, d\xi' =$$

$$= \int e^{-\frac{2}{y^2}(\xi')^2} d\xi' + \frac{1}{2}\int \xi' e^{-\frac{2}{y^2}(\xi')^2} d\xi' - \frac{1}{8}\int (\xi')^2 e^{-\frac{2}{y^2}(\xi')^2} d\xi'.$$

According to eq.(86), the value of the first integral is

$$\int_{-\infty}^{\infty} e^{-\frac{2}{y^2}(\xi')^2} d\xi' = \sqrt{\frac{\pi}{\alpha}} = y\sqrt{\frac{\pi}{2}},$$

while the second is zero. In fact,

$$\frac{1}{2}\int_{-\infty}^{\infty} \xi' e^{-\frac{2}{y^2}(\xi')^2} d\xi' = -\frac{1}{4}\frac{y^2}{2}\int_{-\infty}^{\infty} d\left(e^{-\frac{2}{y^2}(\xi')^2}\right) = 0.$$

Within these limits of integration, any positive differential has a negative differential equal to it. The third and last integral may be written in the following form:

$$\int_{-\infty}^{\infty} (\xi')^2 e^{-\frac{2}{y^2}(\xi')^2} d\xi' = -\frac{\partial}{\partial\alpha}\int_{-\infty}^{\infty} e^{-\alpha(\xi')^2} d\xi',$$

where

$$\alpha = \frac{2}{y^2}.$$

However,

$$\int_{-\infty}^{\infty} e^{-\alpha\xi'^2} d\xi' = \sqrt{\frac{\pi}{\alpha}}.$$

As a result, we obtain

$$\int_{-\infty}^{\infty} (\xi')^2 e^{-\alpha(\xi')^2} d\xi' = -\frac{\partial\sqrt{\frac{\pi}{\alpha}}}{\partial\alpha} = \frac{\sqrt{\pi}}{2\alpha^{\frac{3}{2}}} = \frac{\sqrt{\pi}}{4\sqrt{2}}y^3.$$

Returning to the formula for the specific thrust, we get

$$P_{sp} = P_{sp\,0}\frac{1}{y}\sqrt{\frac{2}{\pi}}\left(y\sqrt{\frac{\pi}{2}} + 0 - \frac{1}{8}\frac{\sqrt{\pi}}{4\sqrt{2}}y^3\right)$$

or

$$P_{sp} = P_{sp0}\left(1 - \frac{y^2}{32}\right). \qquad (88)$$

The relative variation in specific thrust is determined as

$$\frac{\Delta P_{sp}}{P_{sp0}} = \frac{y^2}{82}$$

and is of the same order as the variation in the case of linear distribution.

As should be remembered, the conclusion that the random temperature fluctuations have only a slight effect on the specific thrust is valid only in the case where the temperature affects the specific thrust in accordance with the law $P_{sp} = B\sqrt{T}$, as, for example, in an ideal engine.

On transition to an actual chemical engine, allowance must be made for the relation between the temperature and the component ratio, and the influence of this relation and of the component ratio itself, on the adiabatic exponent k and on the gas constant R. The value of the coefficient B in the expression for P_{sp} is variable. Under these conditions, it is expedient to make use of the experimental relations $P_{sp} = f(x)$ and $T = \varphi(x)$, where x represents the component ratio, i.e., the ratio of the quantity of oxidizer to the quantity of the fuel.

These relations will be different if we consider them at various values of T_0, and therefore the deviation of the specific thrust also depends on T_0.

Cases are possible in which P_{sp} will hardly vary under random temperature fluctuations, but there are also cases in which, at certain values of T_0, the variations will be greater than those obtained above for an ideal engine [cf. also Chapter V, the relations $P_{sp} = f(x)$].

Section 12. Characteristics of an Ideal Rocket Engine at p = c

The term "characteristic of a rocket engine" is applied to the relations between the basic performance parameters of the engine, on the one hand, and some parameter determining its operating condition on the other. The principal performance parameters include: specific thrust, total thrust, specific heat consumption, specific fuel consumption, and specific dimensions.

Characteristics of two forms must be differentiated, those of the series rocket engine and those of the operating conditions.

Series rocket engines are a train of rocket engines operating under design conditions, dissimilar with respect to one of the parameters of these conditions and correlated by some criterion of the operating conditions.

The so-called operating characteristics give the relations for single rocket engines whose operating conditions are determined by the flight program. The main variables in this case are most often the gas efflux per second and the external pressure.

1. Characteristics of Series Rocket Engines

Consider one of the examples of the characteristics of a train of rocket engines under the following conditions: The chamber cross sections ahead of the nozzle are the same for all engines (F_k = const), the gas velocity in the initial cross sections is low and constant (W_k = 1 m/sec), the expansion ratio is one and the same in engines of the entire series or train ($\frac{p_k}{p_a} = \delta_a$ = const).

At certain values of p_{ko} and T_{ko}, let the weight rate of flow be G_o = 1 kg/sec. Then,

$$F_{\kappa} = \frac{RT_{\kappa 0}}{p_{\kappa 0}} \quad \frac{1}{w_{\kappa 0}}.$$

In an arbitrary engine train, the thrust and the specific thrust are determined under rated operating conditions by the formulas

$$P_{\text{уд}} = A\sqrt{T_{\kappa}}; \quad P = \frac{A}{R}\frac{p_{\kappa}}{\sqrt{T_{\kappa}}}F_{\kappa},$$

and the relative thrust, by the formulas

$$\bar{P}_{\text{уд}} = \frac{P_{\text{уд}}}{P_{\text{уд}0}}; \quad \bar{P} = \frac{P}{P_0}.$$

Then,

$$\bar{P} = \frac{p_{\kappa}}{p_{\kappa 0}}\sqrt{\frac{T_{\kappa 0}}{T_{\kappa}}}; \quad \bar{P}_{\text{уд}} = \sqrt{\frac{T_{\kappa}}{T_{\kappa 0}}}$$

or

$$\bar{P} = \frac{\bar{p}_\kappa}{\sqrt{\bar{T}_\kappa}}; \quad \bar{P}_{sp} = \sqrt{\bar{T}_\kappa}. \tag{89}$$

The exit section is

$$F_a = A\frac{G\sqrt{T_\kappa}}{p_\kappa} = \frac{A}{R}\frac{F_\kappa}{\sqrt{T_\kappa}}$$

and, accordingly,

$$\bar{F}_a = \sqrt{\frac{\bar{T}_{\kappa'}}{\bar{T}_\kappa}} = \sqrt{\frac{1}{\bar{T}_\kappa}}. \tag{90}$$

Taking these relations into account, let us consider the following four series of engines: $\bar{P} = 1.0$; γ_k = const; T_k = const; and p_k = const. In the first series, the thrust of all engines is the same, while the state of the gas in the chamber is different. From eqs.(89) we find

$$\bar{p}_\kappa^2 = \bar{T}_\kappa, \tag{91}$$

while from eqs.(89) and (91) we get

$$\bar{P}_{sp} = \bar{p}_\kappa, \tag{92}$$

and from eq.(90),

$$\bar{F}_a = \frac{1}{\bar{p}_\kappa}. \tag{93}$$

The results of the determination of the principal parameters for the engines of all four series are presented in Table 13.

Figure 79 shows the relations between the initial parameters for various versions of the characteristics, and Figs.80 and 81 give the relations between the relative thrust and the specific thrust, on the one hand, and the variables $\bar{p}_k$ and $\bar{T}_k$ on the other.

The thrust of the chamber may be considerably increased by increasing the density of the gas ahead of the nozzle mouth. However, the specific thrust in this case decreases in the order of position of the versions in Table 13.

Assuming that, on transition from one engine to another, the expansion ratio varies, and considering $p_a = p_{ex}$, we get a series of engines differing from the pre-

Table 13

Indices of Rocket Engine Trains with F_k = const and δ = const

Engine Version	Designation of Version in Figs. 86 - 88	Relation to Initial Conditions	Total Thrust, $\bar{P}$	Specific Thrust, $\bar{P}_{sp}$	Exit Section, $\bar{F}_a$	Specific Thrust with Respect to Exit Section, $\frac{\bar{P}}{\bar{F}_a}$
$\bar{P} = 1{,}0$	I	$\bar{T}_\kappa = \bar{p}_\kappa^2$	1,0	$\bar{p}_\kappa$	$\frac{1}{\bar{p}_\kappa}$	$\bar{p}_\kappa$
γ_κ = const	II	$\bar{p}_\kappa = \bar{T}_\kappa$	$\sqrt{\bar{p}_\kappa}$	$\sqrt{\bar{p}_\kappa}$	$\sqrt{\frac{1}{\bar{p}_\kappa}}$	$\bar{p}_\kappa$
T_κ = const	III	$\bar{T}_\kappa = 1{,}0$	$\bar{p}_\kappa$	1,0	1,0	$\bar{p}_\kappa$
p_κ = const	IV	$\bar{p}_\kappa = 1{,}0$	$\sqrt{\frac{1}{\bar{T}_\kappa}}$	$\sqrt{\bar{T}_\kappa}$	$\sqrt{\frac{1}{\bar{T}_\kappa}}$	1

ceding: F_k = const and p_{ex} = const, for which

$$P_{sp} = B\sqrt{T_\kappa}\sqrt{\eta_t};\quad P = B\sqrt{T_\kappa \eta_t}\cdot\frac{p_\kappa F_\kappa}{RT_\kappa}$$

and

$$\bar{P}_{sp} = \sqrt{\bar{T}_\kappa \bar{\eta}_t};\quad \bar{P} = \bar{p}_\kappa\sqrt{\frac{\bar{\eta}_t}{\bar{T}_\kappa}}. \tag{94}$$

Taking, as before, $\bar{P}$ = 1.0 for version I, we get

$$\bar{p}_\kappa^2\left(1-\frac{1}{\delta_0^e \bar{p}_\kappa^e}\right) = \eta_{t0}\bar{T}_\kappa \tag{95}$$

and

$$\bar{P}_{sp} = \bar{p}_\kappa\left(1-\frac{1}{\delta_0^e \bar{p}_\kappa^e}\right)\frac{1}{\eta_{t0}}. \tag{96}$$

The principal relations for the other versions of this series are given in Table 14.

Figures 82, 83, and 84 show the internal parameters, the relative thrust, and the specific thrust as functions of variable $\bar{p}_k$ and $\bar{T}_k$, for four versions of the

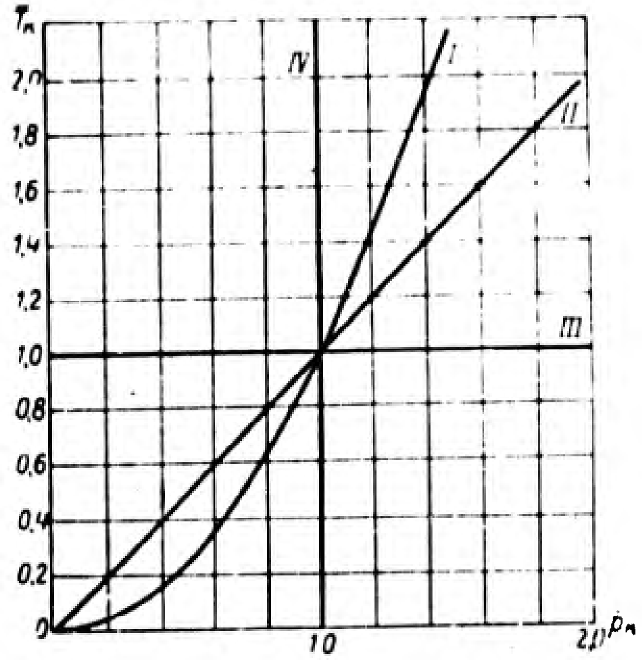

Fig.79 - For Characteristic of Rocket Engine Trains with F_k = const and δ_c = const. Four versions of the correlation between the internal parameters

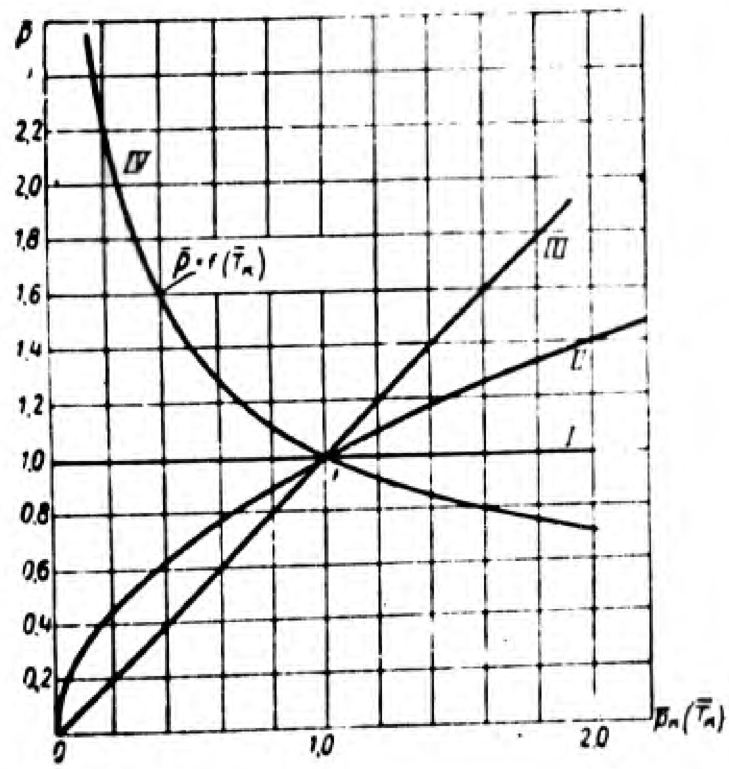

Fig.80 - For Characteristic of Rocket Engine Trains with F_k = const and δ_c = const. Four versions of variation in relative thrust

Table 14

Indices of Rocket Engine Trains with F_k = const and p_{ex} = const

Engine Version	Relation between Initial Conditions	Designation of Versions in Figs.86 - 88	Total Thrust $\bar{P}$	Specific Thrust $\bar{P}_{sp}$
$\bar{P} = 1$	$\bar{p}_к^2\left(1-\frac{1}{\delta_0^a \bar{p}_к^a}\right) = \tau_{ц0}\bar{T}_к$	I	1,0	$\bar{p}_к\left(1-\frac{1}{\delta_0^a \bar{p}_к^a}\right)\frac{1}{\tau_{ц0}}$
$T_к$ = const	$\bar{p}_к = T_к$	II	$\sqrt{\frac{\bar{p}_к\left(1-\frac{1}{\delta_0^a \bar{p}_к^a}\right)}{\tau_{ц0}}}$	$\sqrt{\frac{\bar{p}_к\left(1-\frac{1}{\delta_0^a \bar{p}_к^a}\right)}{\tau_{ц0}}}$
$T_к$ = const	$\bar{T}_к = 1,0$	III	$\bar{p}_к\sqrt{\frac{\left(1-\frac{1}{\delta_0^a \bar{p}_к^a}\right)}{\tau_{ц0}}}$	$\frac{1}{\bar{\tau}_{ц}} = \sqrt{\frac{1-\frac{1}{\delta_0^a \bar{p}_к^a}}{\tau_{ц0}}}$
$p_к$ = const	$\bar{p}_к = 1,0$	IV	$\sqrt{\frac{1}{\bar{T}_к}}$	$\sqrt{\bar{T}_к}$

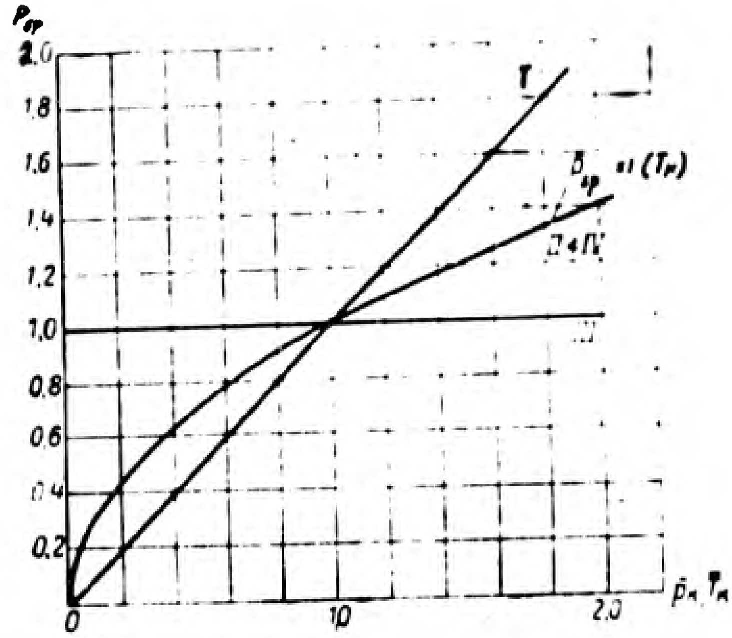

Fig.81 - For Characteristics of Rocket Engine Trains with F_k = const and δ_c = const. Four versions of variation in relative specific thrust

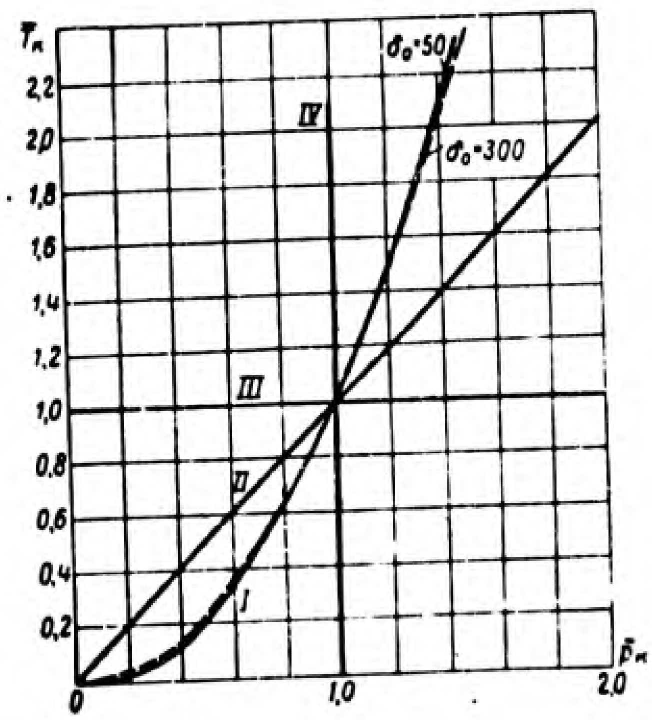

Fig.82 - Relation between Internal Parameters in Different Versions of Rocket-Engine Chamber with F_k = const; Pex = const

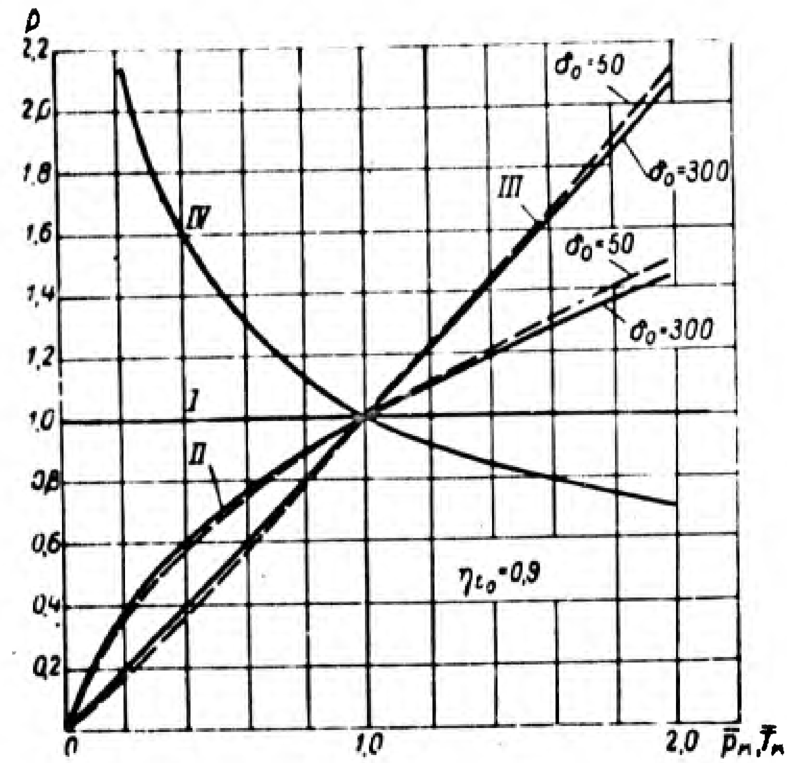

Fig.83 - Relative Thrust Versus $\bar{p}_k$ and $\bar{T}_k$ for Different Versions of a Rocket-Engine Chamber with F_k = const and p_k = const

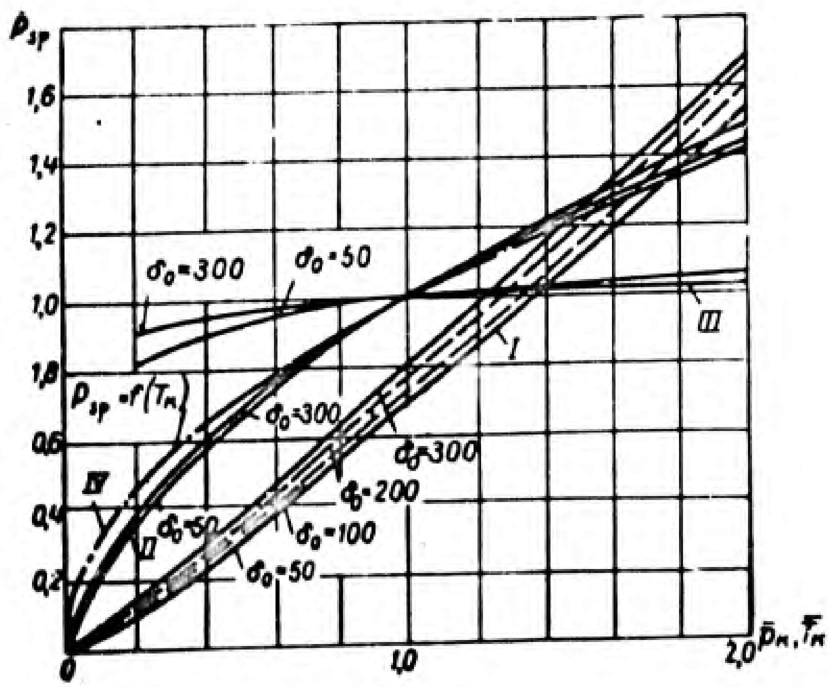

Fig.84 - Relative Specific Thrust Versus $\bar{p}_k$ and $\bar{T}_k$ for Different Versions of a Rocket-Engine Chamber with F_k = const and p_{ex} = const

series.

The other versions of the characteristics of engine trains can be investigated in a similar manner.

2. Operating Characteristics of Rocket Engines

Of the operating characteristics, the most important are the thrust-to-flow rate characteristic (quantitative regulation of the thrust); the thrust-to-mixture composition characteristic (qualitative regulation of the thrust); and the altitude characteristic.

Let us consider three chamber versions:

1) With constant nozzle (Fig. 85a), characterized by F_a = const; F_{cr} = const; and δ_c = const ($p_a \gtrless p_{ex}$);
2) With adjustable nozzle exit section (Fig. 85b), characterized by $F_a \neq$ const; F_{cr} = const; $\delta_c \neq$ const ($p_{ex} = p_a$);
3) With adjustable exit and critical sections of the nozzle (Fig. 85c), corresponding to $F_a \neq$ const; $F_{cr} \neq$ const, δ = const.

Adjustment of the area of the principal nozzle sections, as will be shown below, improves the engine characteristics and changes its thrust.

The thrust of an engine may be changed at constant external pressure by two simple methods, either by varying the propellant feed rate or by varying the propellant component ratio.

Let us consider the flow-rate characteristics of a liquid-propellant rocket engine with various chambers.

For the chambers of the first version, $\bar{F}_a = 1.0$ and $\bar{F}_{cr} = 1.0$. In this case, the main parameter of the discharge characteristics is the propellant flow rate per second, or the pressure in the chamber which is directly proportional to the former. The flow rate of the fuel through the chamber is

$$G = F_{cr}\frac{p_{\kappa}}{\sqrt{RT_{\kappa}}}\sqrt{kg\left(\frac{2}{k+1}\right)^{\frac{k+1}{k-1}}}. \qquad (97)$$

In the ideal chamber, at constant gas composition and neglecting dissociation, the temperature may be taken as constant. This means that, if the quantities G_0, W_0, $p_{\kappa 0}$, and p_{a0} are all at rated operating conditions, then

$$\frac{G}{G_0} = \frac{p_{\kappa}}{p_{\kappa 0}} = \frac{p_a}{p_{a0}}.$$

We shall henceforth use the notation:

$$\frac{f_a}{f_{a0}} = \bar{f}_a; \quad \frac{G}{G_0} = \bar{G}; \quad \frac{p_{\kappa}}{p_{\kappa 0}} = \bar{p}_{\kappa};$$

$$\frac{W}{W_0} = \bar{W}; \quad \frac{T_{\kappa}}{T_{\kappa 0}} = \bar{T}_{\kappa}. \qquad (98)$$

Then,

$$\bar{G} = \bar{p}_{\kappa} = \bar{p}_a = \frac{1}{\bar{f}_a}.$$

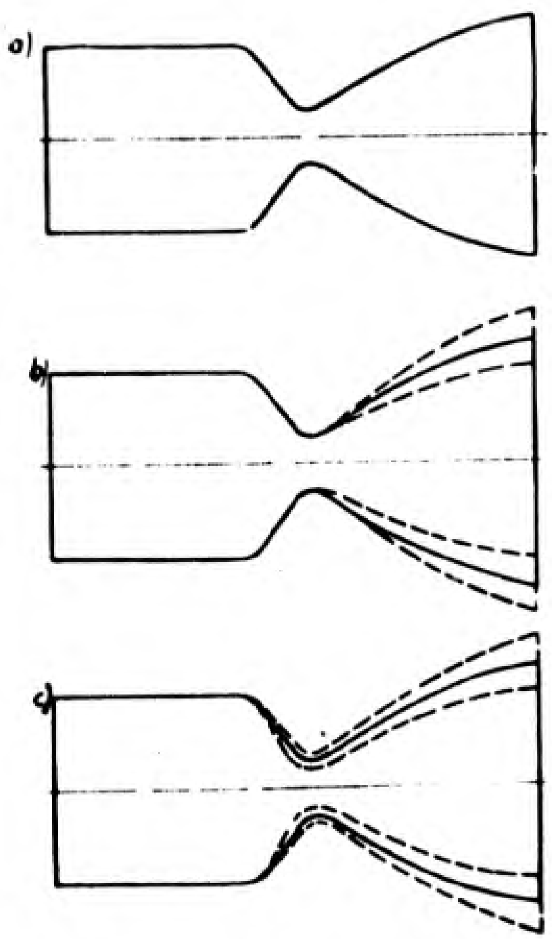

Fig.85 - Versions of Chambers of a Rocket Engine at p = c

Since the temperature in the chamber and the expansion ratio are constant, a change in the gas flow rate has no effect on the exhaust velocity. We determine the thrust by the usual formula

$$P = G\frac{W}{g} + F_a p_a - F_a p_{ex}$$

After introducing the relative quantities (98), we get

$$P = \bar{G}\left(G_0\frac{W_0}{g} + F_a p_{a0}\right) - F_a p_{ex} = \bar{G}P_{i0} - F_a p_{ex} \qquad (99)$$

where P_i is the internal thrust of the engine.

We determine the specific thrust from the expression

$$P_{sp} = \frac{P}{G} = \frac{\bar{G} P_{i0} - F_a p_{ex}}{G_0 \bar{G}} = P_{i.sp0} - \frac{f_a p_{ex}}{\bar{G}}. \qquad (100)$$

Figure 86 shows the flow-rate characteristic of a rocket engine, at p = c with constant nozzle. With varying $\bar{G}$, the engine has only a single set of rated operating conditions. As the flow rate increases from its rated value, conditions of underexpansion set in; a decrease in the flow rate causes overexpansion, which may

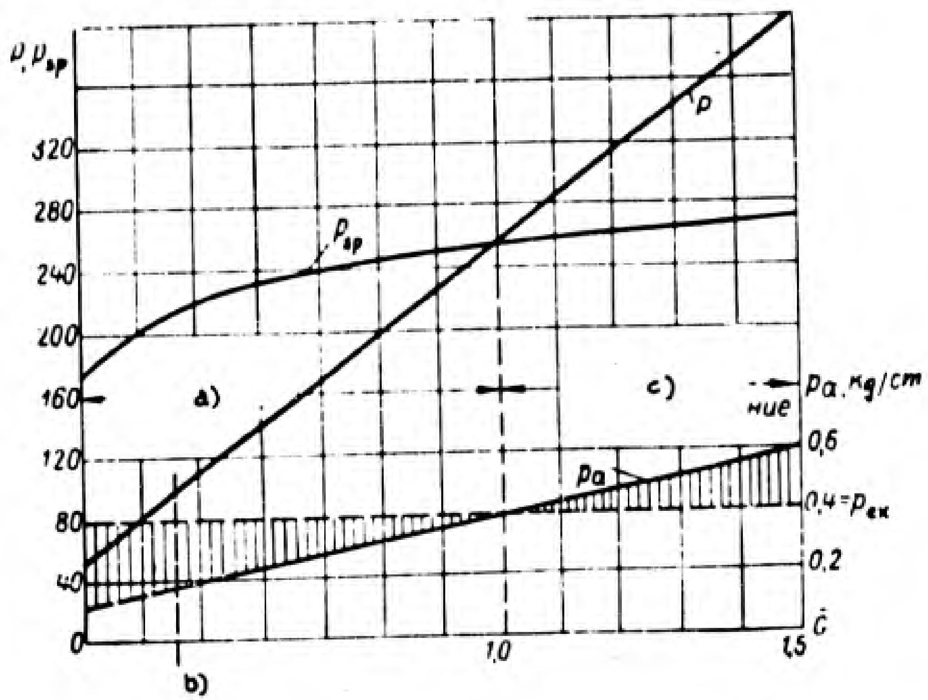

Fig.86 - Flow-rate Characteristic of Rocket Engine with Constant Nozzle (G_0 = 1 kg/sec)

a) Overexpansion; b) Compression shock; c) Underexpansion

lead to the appearance of a compression shock in the nozzle duct. The increase in specific thrust depends on the external pressure; at very low external pressures, P_{sp} is practically independent of the mass rate of flow.

Solving for P_{i0} and considering G_0 = 1 kg/sec, we get

$$P_{i0} = \sqrt{\frac{2}{g}\frac{k}{k-1}RT_k\left(1 - \frac{1}{\delta_c^n}\right)}\left(1 + \frac{k-1}{2k}\cdot\frac{1}{\delta_c^n - 1}\right).$$

It follows from this expression that the rate of thrust increase with increasing G is greater in chambers with a higher temperature T_k and a higher degree of expansion δ_c.

For chambers of the second version, we have $F_a \neq$ const, while $p_a = p_{ex}$ = const. In this case, expansion to external pressure takes place and the expansion ratio δ_c is variable, i.e.,

$$\delta_c = \frac{p_k}{p_{ex}} = \frac{p_k}{p_{k0}}\,\frac{p_{k0}}{p_{ex}} = \delta_{c0}\overline{p}_k.$$

However, $\overline{p}_k = \overline{G}$, so that $\delta_c = \delta_{c0}\overline{G}$.

The static term in the expression for the thrust is absent; therefore

$$P = G\frac{W}{g};\quad P_{sp} = \frac{W}{g}$$

and, accordingly,

$$\overline{P} = \overline{G}\,\overline{W};\quad \overline{P}_{sp} = \overline{W}. \tag{101}$$

The relative velocity, and the relative specific thrust equal to it, are determined from the expression

$$\overline{W} = \overline{P}_{sp} = \frac{\sqrt{1-\frac{1}{\delta_c^a}}}{\sqrt{1-\frac{1}{\delta_{c0}^a}}} = \frac{\sqrt{1-\frac{1}{(\delta_{c0}\overline{G})^a}}}{\sqrt{1-\frac{1}{\delta_{c0}^a}}}, \tag{102}$$

while the total thrust is obtained from the expression

$$\overline{P} = \overline{G}\,\overline{P}_{sp}.$$

Under conditions of decreased flow rate, the second version is more advantageous than the first, since the specific thrust is somewhat higher in that case. Its greater economy is explained by a more complete utilization of the available degree of pressure drop.

The exit section should vary by the law

$$\frac{F_a}{F_{a0}} = \overline{F}_a = \frac{\sqrt{\left(\frac{1}{\delta_{c0}}\right)^{\frac{2}{k}} - \left(\frac{1}{\delta_{c0}}\right)^{\frac{k+1}{k}}}}{\sqrt{\left(\frac{1}{\delta_{c0}\overline{G}}\right)^{\frac{2}{k}} - \left(\frac{1}{\delta_{c0}\overline{G}}\right)^{\frac{k+1}{k}}}}. \tag{103}$$

In a chamber of the third version, which is most complicated in design, the exhaust velocity is constant. By a suitable change in the critical cross section, the pressure may be held constant in the chamber, and by regulating or controlling the exit section, the pressure across the nozzle exit may be held constant. At constant p_k, p_a, and T_k, we have

$$P_{sp} = \frac{W}{g} = \text{const}; \quad P = G\frac{W}{g}$$

and, accordingly,

$$\bar{P}_{sp} = 1{,}0 \text{ and } \bar{P} = \bar{G}.$$

The sections must be varied proportionally to each other and to the flow rate:

$$\bar{F}_{cr} = \bar{F}_a = \bar{G}.$$

The considered flow-rate characteristics are compared in Fig.87. The greatest increase in thrust with increasing flow rate is obtained in a chamber of the first version, i.e., in an engine with constant nozzle dimensions.

The versions of chambers with adjustable or controllable nozzles are convenient since they prevent the possibility of a compression shock in the nozzle duct.

In the region of underloads ($\bar{P} < 1.0$), the chamber with controllable main sections of the nozzle is most economical. In the region of overloads, however ($\bar{P} > 1.0$), the second version gives a greater increase in thrust and greater economy with increasing mass rate of flow.

Consequently, in selecting a version of some given chamber, independently of evaluating its design, one must also know the critical operating conditions of the engine and the approximate region of the operating conditions.

Let us now consider the thrust characteristics related to temperature, mixture composition at constant flow rate through the chamber, and at constant pressure in the chamber.

Let the chamber have constant cross sections.

If G = const, then

$$\frac{p_k}{\sqrt{T_k}} = \frac{p_k'}{\sqrt{T_k'}}$$

and

$$\bar{p}_k' = \sqrt{\bar{T}_k}. \qquad (104)$$

Consequently, at constant mass rate of flow, the pressure will also increase with increasing chamber temperature, but more slowly than that temperature.

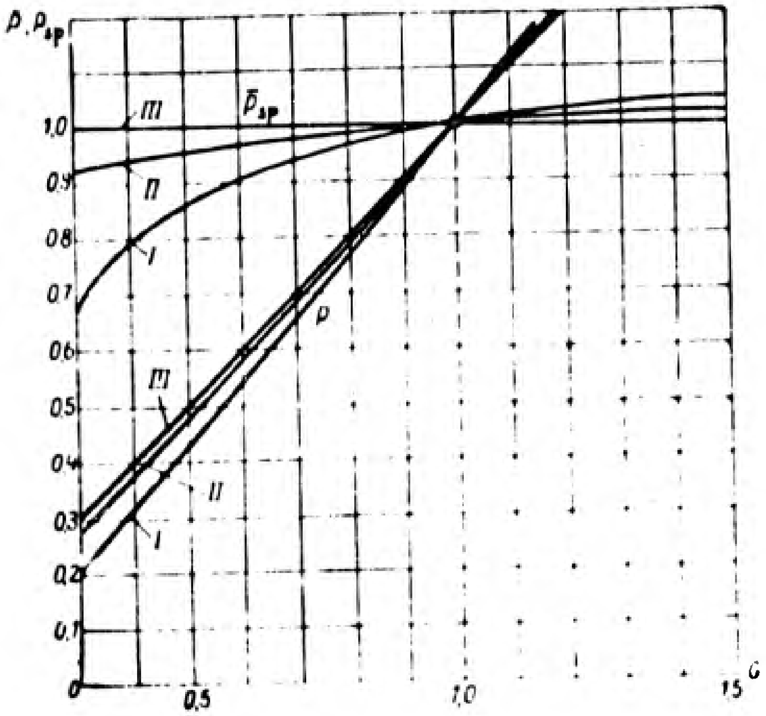

Fig.87 - Three Versions of the Flow-Rate Characteristics of a Rocket Engine at p = c (T_k = const)

I - Uncontrolled nozzle; II - Nozzle with adjusted F_a; III - Nozzle with adjusted F_a and F_{cr}

The expansion ratio in the nozzle is constant, but the velocity and pressure across its exit section increase with increasing temperature.

The specific engine thrust is determined from the expression

$$P_{sp} = \left(\frac{W_a}{g} + f_a p_{ex}\right)\sqrt{\bar{T}_k} - f_a p_{ex}, \qquad (105)$$

where f_a is the specific area of the nozzle exit.

If, however, p_k = const and $\bar{p}_k$ = 1, then

$$\bar{G} = \frac{\bar{p}_к}{\sqrt{\bar{T}_к}} = \frac{1}{\sqrt{\bar{T}_к}}. \qquad (106)$$

As will be seen from eq.(106), the mass rate of flow in this case varies in inverse proportion to the square root of the temperature. In this case, the pressure across the nozzle exit remains constant, so that the exhaust velocity and the specific thrust will vary proportionally to the square root of the temperature, $\bar{W} = \sqrt{\bar{T}_k}$ and $\bar{P}_{sp} = \sqrt{\bar{T}_k}$, while the thrust will not vary, since

$$P = \bar{P}_{sp}\bar{G} = 1{,}0.$$

In the second version of the chamber, the variation of the exit section is such that $p_a = p_{ao} = p_{ex}$. Since the critical cross section remains constant, the relation between the pressure and the temperature is the same as in a simple chamber, i.e., with increasing temperature the pressure also increases. In this case, at constant flow rate,

$$\bar{P} = \bar{P}_{sp} = \bar{W} = \frac{\sqrt{T_к\left(1 - \frac{1}{\delta_c^a}\right)}}{\sqrt{T_{к0}\left(1 - \frac{1}{\delta_{c0}^a}\right)}},$$

However,

$$\delta_c = \frac{p_к}{p_{ex}} \cdot \frac{p_{к0}}{p_{к0}} = \delta_{c0}\bar{p}_к = \delta_{c0}\sqrt{\bar{T}_к};$$

and

$$\bar{P} = \bar{P}_{sp} = \sqrt{\bar{T}_к \frac{1 - \left(\frac{1}{\delta_{c0}\bar{p}_к}\right)^a}{1 - \frac{1}{\delta_{c0}^a}}}.$$

The pressure in a chamber of the third version is held constant by varying the critical cross section, while the pressure across the nozzle exit is kept equal to the external pressure, which is accomplished by adjusting the value of F_a. In this case,

$$\bar{P} = \bar{P}_{sp} = \bar{W} = \sqrt{\bar{T}_к}$$

and

$$\frac{F_a}{F_{cr}} = f(\lambda) = \text{const.}$$

According to eq.(103) and the conditions of the third version, we have

$$\bar{F}_{cr} = \bar{F}_a = \bar{T}_\kappa.$$

Figure 88 shows the characteristics of a rocket engine with respect to the initial gas temperature in the case of G = const.

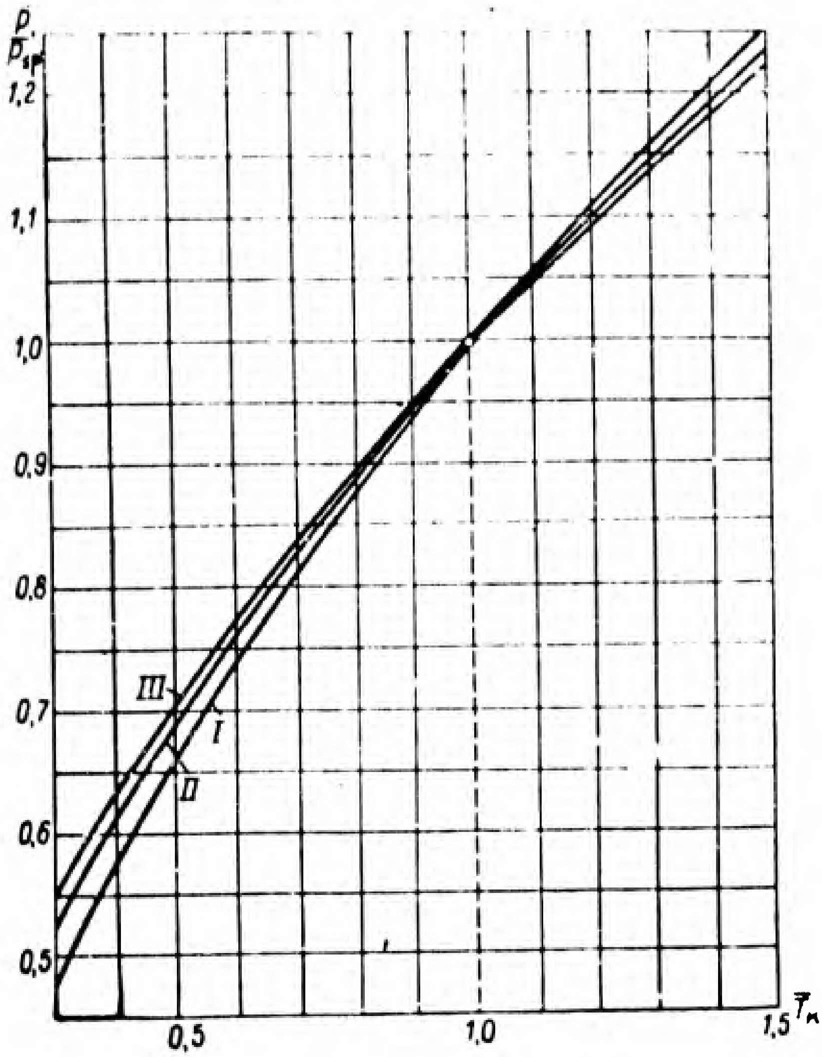

Fig.88 - Thrust Characteristics of a Rocket Engine at p = c Plotted against the Chamber Temperature (G = const)

I - Uncontrolled nozzle; II - Nozzle with adjusted F_a; III - Nozzle with adjusted F_a and F_{cr}

Let us also consider the version of the thrust characteristic of a chamber with mixed control, when, at constant nozzle, the condition

$$p_к^2 T_к = \text{const.}$$

is satisfied.

Such a relation between pressure and temperature corresponds roughly to the same intensity of convective heat transfer to the walls of the chamber. The increase in the mass rate of flow is due, in this case, to increased pressure and decreased temperature.

From eq.(97) and the condition that $p_k^2 T_k$ = const, we get

$$\bar{G} = \bar{p}_к^2 = \frac{1}{\bar{T}_к}. \tag{107}$$

The exhaust velocity at δ = const equals

$$\bar{W} = \sqrt{\bar{T}_к},$$

and the pressure across the nozzle exit is

$$p_a = p_{ak}\bar{p}_к = p_{ak}\sqrt{\frac{1}{\bar{T}_к}}.$$

We obtain the following expression for the total thrust:

$$P = P_{i\cdot 0}\cdot\frac{1}{\sqrt{\bar{T}_к}} - F_a p_{ex} = P_{i\cdot 0}\bar{p}_к - F_a p_{ex} = P_{i\cdot 0}\sqrt{\bar{G}} - F_a p_{ex}, \tag{108}$$

where

$$P_{i\cdot 0} = G_0\frac{W_0}{g} + F_a p_{ak}.$$

The thrust increment is

$$\Delta P = P_{i\cdot 0}\left(\sqrt{\bar{G}} - 1\right) = P_{i\cdot 0}(\bar{p}_к - 1) = P_{i\cdot 0}\left(\frac{1}{\sqrt{\bar{T}_к}} - 1\right).$$

If the specific internal thrust at rated operating conditions is

$$\frac{W_0}{g} + \frac{F_a p_{ak}}{G} = m,$$

then the specific thrust, on the basis of the above, is determined from the expression

$$P_{sp} = \frac{m}{\sqrt{G}} - \frac{F_a p_{ex}}{G_* G} = m\sqrt{T_*} - \frac{F_a p_{ex} T_*}{G}$$

and

$$\Delta P_{sp} = m\left(\frac{1}{p_*} - 1\right) + \frac{F_a p_{ex}}{G_*}\left(1 - \frac{1}{p_*^2}\right).$$

In the allowable range of variation of the mass rate of flow, the increment in specific thrust decreases with increasing initial flow rate.

Figure 89 shows the thrust characteristic of a chamber with mixed regulation, together with the flow-rate characteristic.

The characteristics of actual engines differ from ~~those~~ obtained above by

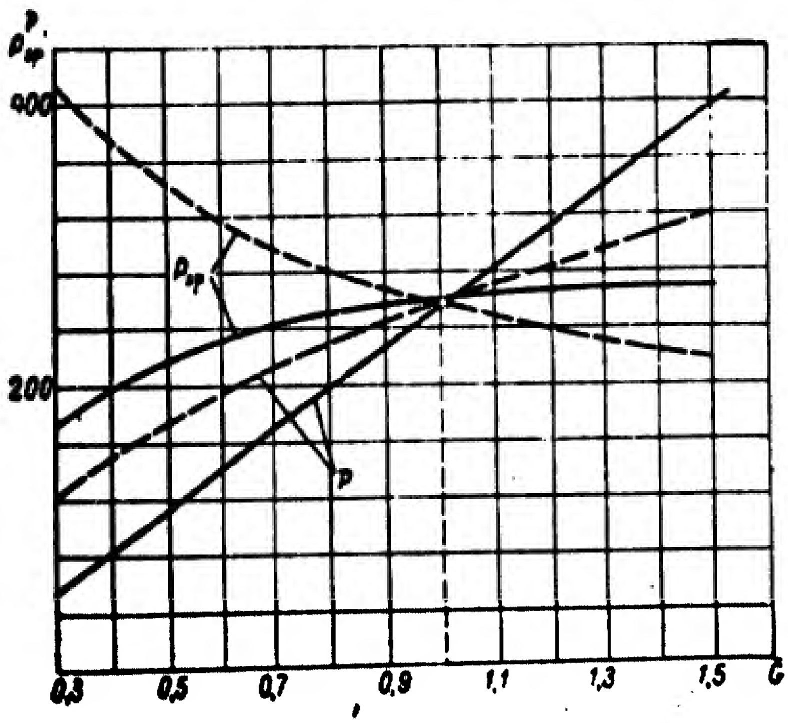

Fig.89 - Thrust Characteristic of Chamber with p^2T = const, Compared with the Usual Flow-Rate Characteristic

——— Flow-rate characteristic;
- - - Characteristic of chamber with p^2T = const

slight corrections in the exhaust velocities, because of losses in the chamber and nozzle. Moreover, the values of p_a and F_a are slightly refined.

The refinements of the former and latter types partially compensate each other.

3. Altitude Characteristics of a Rocket Engine

With increasing altitude above sea level, the atmospheric pressure declines, leading to a decrease in the external engine thrust $F_a p_{ex}$. For example, at an altitude of 20 km, the external thrust per m^2 of nozzle exit section is 540 kg. This quantity, at the specific thrusts of modern rocket engines (50,000 kg/m^2), must be taken into account. At an altitude of 40 km, however, the external thrust becomes equal to 28 kg/m^2, and the correction for it may already be neglected.

The operation of an engine with uncontrolled nozzle is characterized by the following conditions:

$$G=\mathrm{const};\quad p_k=\mathrm{const};\quad T_k=\mathrm{const};\quad \delta_c=\mathrm{const};\quad p \neq \mathrm{const}.$$

At supercritical efflux, the internal thrust remains constant, i.e.,

$$P_{sp} = P_{i.sp} - f_a p_{ex}$$

and

$$P = P_i - F_a p_{ex}.$$

Making use of eq.(34), we write

$$P_{sp} = \frac{W_a}{g}\left(1+\frac{1}{kM_a^2}\right) - \frac{W_a}{gkM_a^2}\,\frac{p_{ex}}{p_{ex.r}}. \qquad (109)$$

The rated operating conditions correspond to a rated altitude with the atmospheric pressure $p_{ex\ r}$. At the rated altitude, the specific thrust equals

$$P_{sp.r} = \frac{W_a}{g}.$$

The change in specific thrust is determined by the difference

$$\Delta P_{sp} = P_{sp} - P_{sp.r} = \frac{W_a\left(1-\frac{p_{ex}}{p_{ex.r}}\right)}{gkM_a^2}. \qquad (110)$$

For very high altitudes,

$$\Delta P_{sp.max} = \frac{W_a}{gkM_a^2} = \frac{1}{M_a}\sqrt{\frac{\frac{RT_k}{kg}}{1+\frac{k-1}{2}M_a^2}}.$$

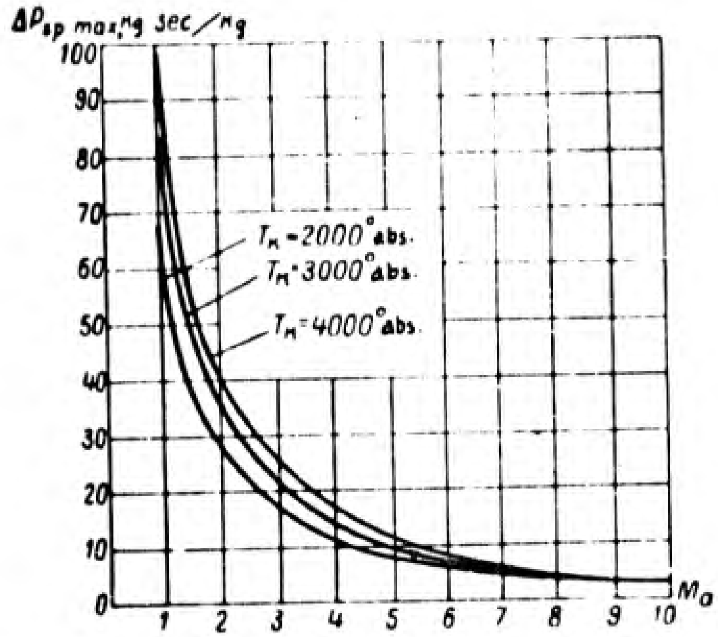

Fig.90 - Effect of the Mach Number at the Exit Section and of the Temperature in the Chamber on the Maximum Variation in Specific Thrust during High-Altitude Flight (Uncontrolled Nozzle)

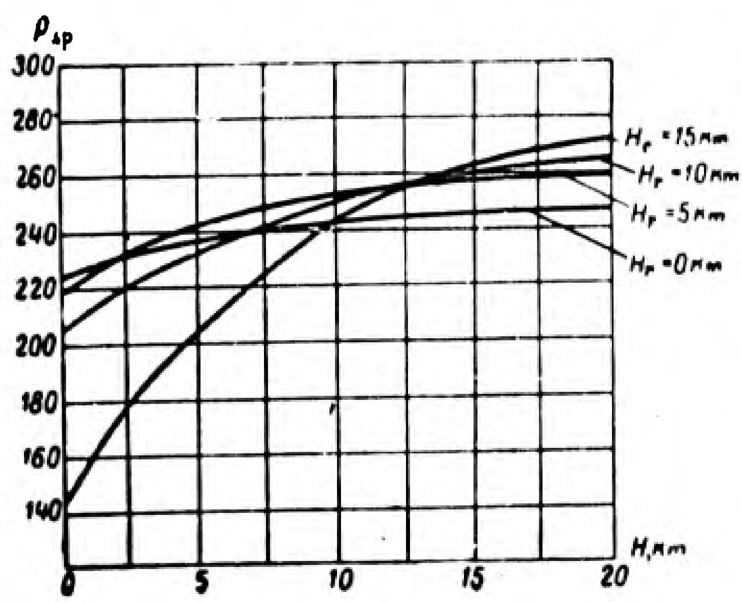

Fig.91 - Altitude Characteristics of a Rocket Engine at p = c (Uncontrolled Nozzle)

It will be seen from the expressions for ΔP_{sp} that the specific thrust varies more intensely in engines with a higher chamber temperature and with a lower expansion ratio (Fig.90).

Bearing in mind the relation between external pressure and altitude (see Appendix I), a direct relation between thrust and altitude may be found from eq.(110).

Figure 91 shows the altitude characteristics of a rocket engine under the con-

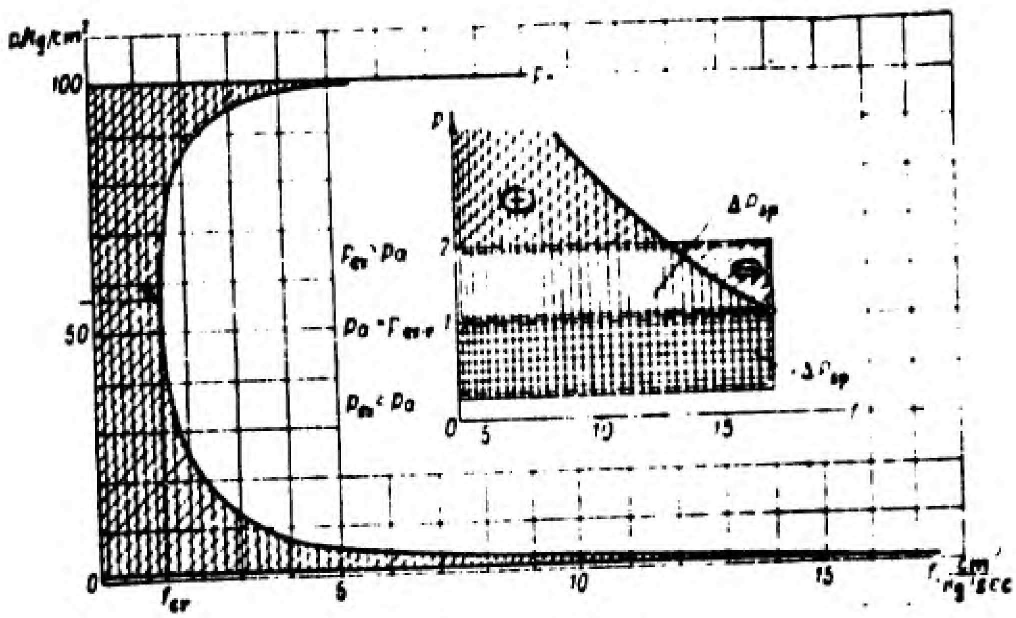

Fig.92 - pf-Diagram for Varying Altitude

ditions H_r = 0, 5, 10, and 15 km. The drawback of a rocket engine with constant nozzle is that, at all altitudes other than the rated altitude, it operates under non-design conditions. Consequently, at all altitudes except the rated altitude, the possibilities of maximum economy are not utilized, and, further than that, if the rated altitude is very high, overexpansion at low altitudes may lead to the appearance of a shock wave in the nozzle duct.

Figure 92 shows pf-diagrams of an engine for various altitudes. To decrease the losses due to non-design operating conditions, the rated altitude should be intermediate between the extreme values. The rated altitude may be selected exactly on the basis of an analysis of the results of a specified flight path of the vehicle, allowing for the influence of changes, not only in the characteristic but also in the weight and drag of the vehicle due to the change-over from one nozzle to another.

If, as the altitude is continuously diminished, the shock wave begins to enter the nozzle and then advances inside it, the rate at which the specific thrust declines will be somewhat lower (Fig.93). Let the pressure $p_{ex\ r}$ correspond to the

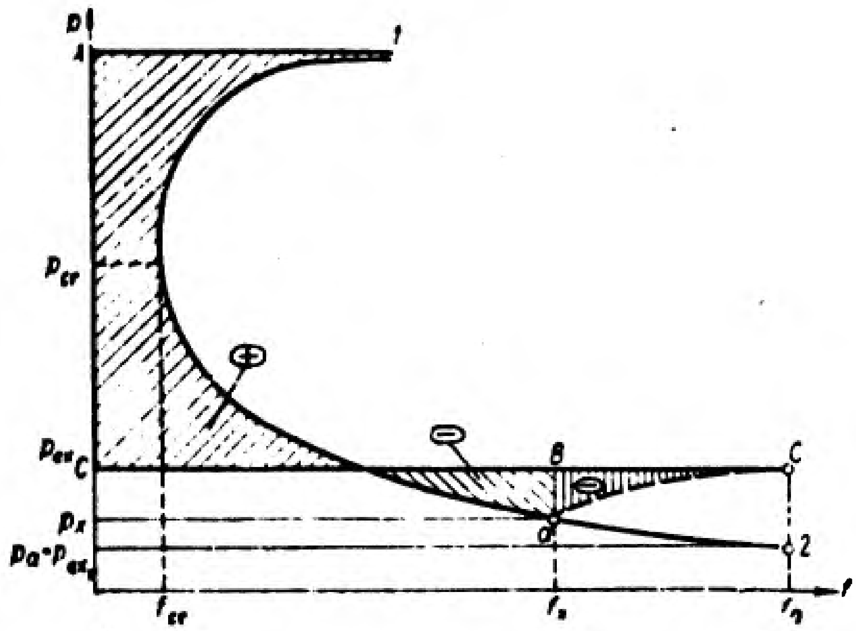

Fig.93 - pf Diagram for the Case of Entrance of a Shock Wave into the Nozzle Duct of a Rocket Engine at p = c

altitude H_r at which $p_{ex\ r} = p_a$. When the external pressure is increased to p_{ex}, the shock wave will be in the nozzle duct in the section f_x.

If, as we did before, the diffuser effect of the exit section of the duct is neglected, then the pressure in the section f_x at once rises to the atmospheric pressure p_{ex}, and the diagram takes the form corresponding to the contour A-I-O-B-p_{ex}. The specific thrust will be less than the rated value for altitude H_r, but will be greater than the thrust at the same altitude in the case of normal over-expansion without formation of shock waves. The gain in thrust corresponds on the pf-diagram to the area O-B-C-2.

In the presence of a diffuser effect of the nozzle exit, the line O-B is replaced by the line O-C, and the thrust is somewhat decreased.

On the whole, it may be stated that a simple nozzle with a high rated altitude may, at low altitudes, have the properties of self-control.

Let us consider the following example. Given:

$$p_\kappa,\ p_{ex\cdot r},\ \delta = \frac{p_\kappa}{p_{ex\cdot r}} \text{ and } M_a.$$

The shock wave begins at the nozzle exit at

$$\frac{p'_{ex}}{p_{ex\cdot r}} = \xi M_a \text{ and } P_{sp} = \frac{W_a}{g}\left(1 + \frac{1-\xi M_a}{kM_a^2}\right).$$

From H_r to H, the specific thrust varies in accordance with the law

$$\bar{P}_{sp} = 1 + \frac{1}{kM_a^2} - \frac{1}{kM_a^2}\frac{p_{ex}}{p_{ex\cdot r}}.$$

With a further decrease in H, the shock enters the nozzle. The Mach number M_x before the shock is determined from eq.(51), i.e.,

$$\frac{p_\kappa}{p_{ex}} = \frac{\left(1 + \frac{k-1}{2}M_x^2\right)^{\frac{k}{k-1}}}{\xi M_x}.$$

The rated specific thrust is determined from the formula

$$P_{sp\cdot r} = \frac{W_a}{g} = \frac{W_a\sqrt{kgRT_a}}{g\sqrt{kgRT_a}} =$$

$$= M_a\sqrt{\frac{kRT_a}{g}} = \frac{M_a}{\sqrt{1+\frac{k-1}{2}M_a^2}}\cdot\sqrt{\frac{kRT_\kappa}{g}}.$$

On the basis of eq.(48), we get

$$\frac{P_{sp\cdot sh}}{P_{sp\cdot r}} = \frac{\sqrt{1+\frac{k-1}{2}M_a^2}}{M_a}\cdot\frac{1+kM_x^2-\xi M_x}{kM_x\sqrt{1+\frac{k-1}{2}M_x^2}}.$$

Figure 94 shows the altitude characteristics for an engine at H_r = 12 km. It is obvious that allowance for the entrance of the shock wave into the nozzle introduces extensive corrections to the altitude characteristic.

By varying the area of the exit section F_a, we may utilize, without disturbing the process in the chamber, the available expansion ratio $\varepsilon_{ex} = \frac{p_k}{p_{ex}}$ in the nozzle. Then, at each altitude, the static component of the specific thrust will be absent, i.e.,

$$P_{sp} = \frac{W_a}{g}$$

and, accordingly,

$$P_{sp} = \frac{W_a}{W_{ap}} = \frac{\sqrt{1-\left(\frac{p_{ex}}{p_k}\right)^a}}{\sqrt{1-\left(\frac{p_{ex \cdot r}}{p_k}\right)^a}}.$$

Figure 94 also shows the characteristic of an engine with altitude thrust con-

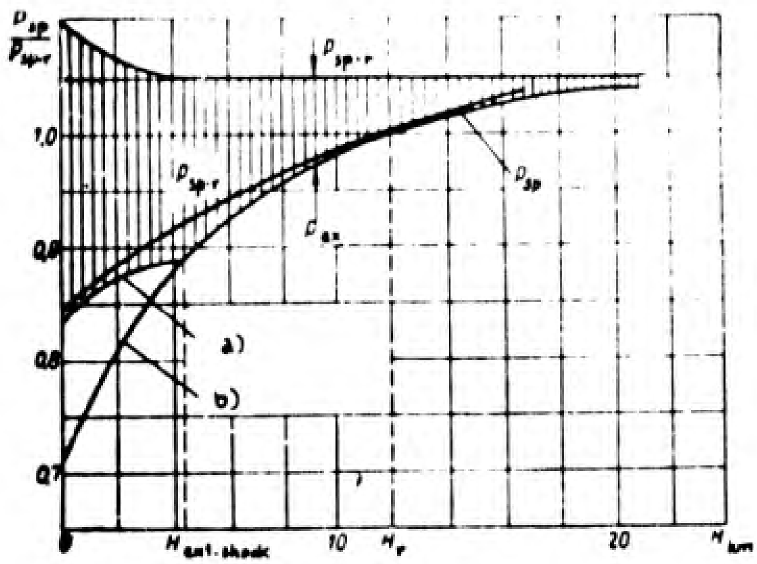

Fig.94 - Altitude Characteristic of Engine with Overexpansion (p_k = 50 kg/cm; T_k = 3000°K; $\varkappa$ = 1.2; R = 30 kg-m/kg deg)

a) On entrance of shock into nozzle; b) Without shock

trol. The gain in thrust by comparison with the gain without control is substantial for great changes in the flight altitude, and therefore attempts to accomplish altitude thrust control are of considerable importance.

The nozzle exit section F_a may be controlled by various methods. Let us consider several basic systems for a stepwise regulation of F_a.

Figure 95 a shows a nozzle system in which the exit section may be increased by adding, to the nozzle face, conical rings which match the nozzle profile in shape and size. Two such additions to the profile (Fig.95 a) will yield three values for the expansion ratio.

In the system shown in Fig.95 b, the original nozzle is designed to provide

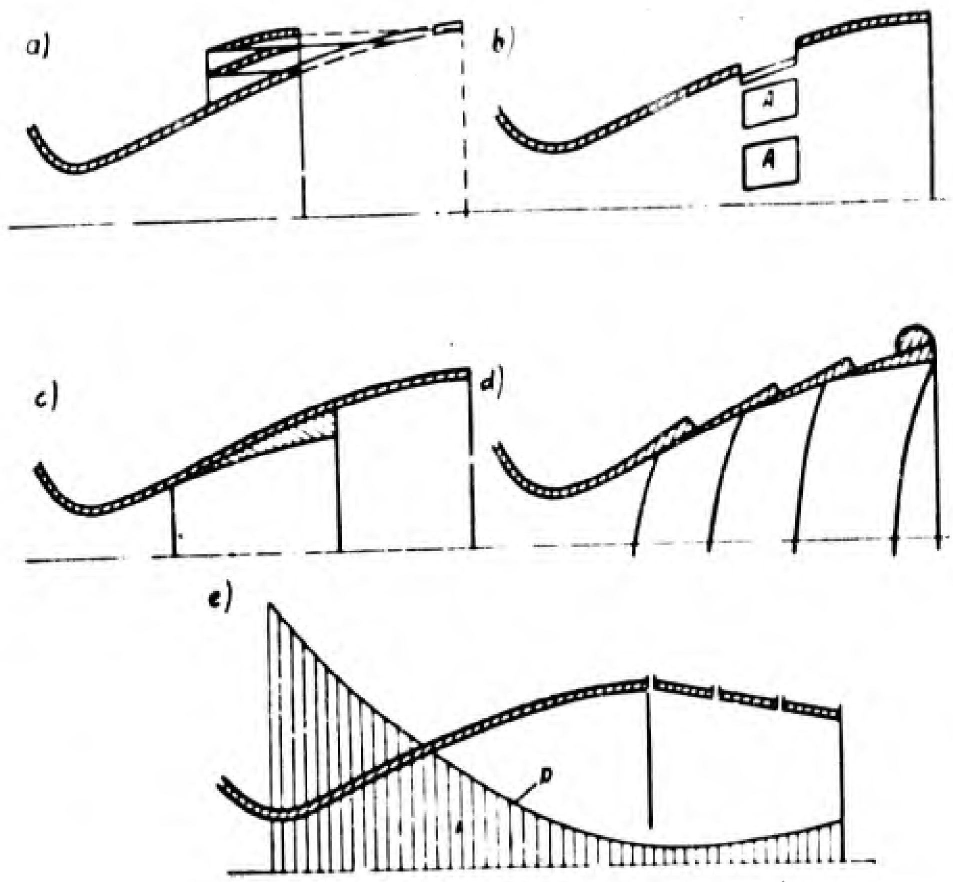

Fig.95 - Schematic Diagrams of Exit Section Control:

a - Altitude control of rocket engine; b - Slot method of controlling expansion in the nozzle; c - Two-stage nozzle with liner; d - Nozzle with elastic shell; e - Nozzle with diffuser control of overexpansion

maximum expansion ratio. The actual expansion ratio is decreased by opening the slots A. At an altitude corresponding to the pressure in the section A, the slots open. The atmospheric air enters the nozzle, and the main flow of gas no longer expands and does not act on the walls of the nozzle zone aft of the slots. It is more difficult to shift the slots along the axis of the nozzle than to displace the rings in the first version, and therefore the slot method is more conveniently used for cases in which only a single change of the expansion ratio is desired.

Figure 95c gives a sketch of a nozzle with a liner. The nozzle liner operates at low altitudes and is jettisoned at high altitudes.

Methods are known for varying the cross sections F_a in elastic nozzles (Fig. 95d). The exit section of the nozzle is formed by a conical strip; twisting this strip around the axis of the chamber shortens the length of the exit section and decreases its cross-sectional dimensions.

Figure 95e shows the system of a nozzle with control diffuser. Such a diffuser, installed in a high-altitude nozzle, is separated into individual parts as the rocket altitude increases or is gradually burned away.

For engine plants on rockets, the versions of controllable nozzles with program burn-away of individual parts are suitable. Thus, if a liner (Fig. 95c), covering the entire nozzle, is burned away or sublimed over the inner surface at a rate that depends on altitude, and if the necessary law of cross-sectional variation is not distorted, the altitude control will be continuous.

The same thing will take place if, in a system with a diffuser, this diffuser is melted away or burned from the end, according to a program responsive to the rate of ascent.

The above methods of altitude control of rocket engines have not yet been used in practice. This is partly explained by the frequently small limits of variation of the operating ceiling of the engine, and also by the inadequate material strength of the nozzle-exit control elements at high gas temperatures and high gas velocity, the complex design variations of the shape and dimensions of the nozzle walls, and sometimes by the increase in engine weight.

The above circumstances do not exclude the possibility of the use of adjustable nozzles for special cases of program flight.

Section 13. The Ideal Constant-Volume Engine with Adiabatic Expansion

1. Characteristics of the Cycle

There are various reasons for believing in the usefulness of a rocket engine with pulsating chamber pressure. Thus, the weight and cost of the engine feed system can be reduced if the propellant is introduced into the chamber when the chamber pressure is low. Moreover, there are working units, for example certain types of water-injection jet engines, into which the gas must be fed periodically. Finally, there might be cases in which it is more convenient to supply the working fluid with energy from its source in pulses.

The working fluid may undergo various changes of state during the pressure pulses. Let us consider the simplest case, where the chamber is of the constant-volume type and the change of state of the gas in the chamber during the flow of gas is adiabatic.

Figure 96 shows a pv-diagram of a constant-volume rocket engine. In the initial state, the working fluid occupies the volume V_k under the pressure of the end of expansion p_{ex}. After heat has been transferred at constant volume V_k, the gas assumes the state corresponding to point 1 (p_{ko}, T_{ko}). The heat transferred is measured by the difference in internal energies $U_1 - U_A$. Consequently,

$$Q_1 = U_1 - U_A = \frac{R}{k-1}(T_{k0} - T_A) = \frac{RT_{k0}}{k-1}\left(1 - \frac{T_A}{T_{k0}}\right).$$

Since

$$\frac{T_A}{T_{k0}} = \frac{p_{ex}}{p_{k0}} = \frac{1}{\delta_0},$$

it follows that

$$Q_1 = \frac{RT_{k0}}{k-1} \cdot \frac{\delta_0 - 1}{\delta_0}. \qquad (112)$$

At high values of δ ($\delta_0 \geq 100$), which is recommended in rocket engines at $V = c$, we may consider

$$Q_1 = \frac{RT_{kn}}{k-1} = C_v T_{kn}. \qquad (113)$$

In the latter case, the individual lines of the pv-diagrams correspond to the processes:

1-2, expansion in the chamber and the nozzle;

2-A, cooling in atmosphere at p_{ex} = const;

A-B, cooling at V_k = const down to absolute zero;

B-1, transfer of heat at V_k = const.

Each issuing gas particle first expands in the chamber from the initial pressure p_k to the current pressure p_x and then, in the nozzle, to atmospheric pressure. When an elementary particle dG is ejected, the pressure p_x in the chamber may be considered constant. This means that each particle flowing through the nozzle performs the mechanical cycle p_x = const. For particles with initial p_x, such a cycle corresponds to the contour p_x - 1' - 2 - p in Fig.96.

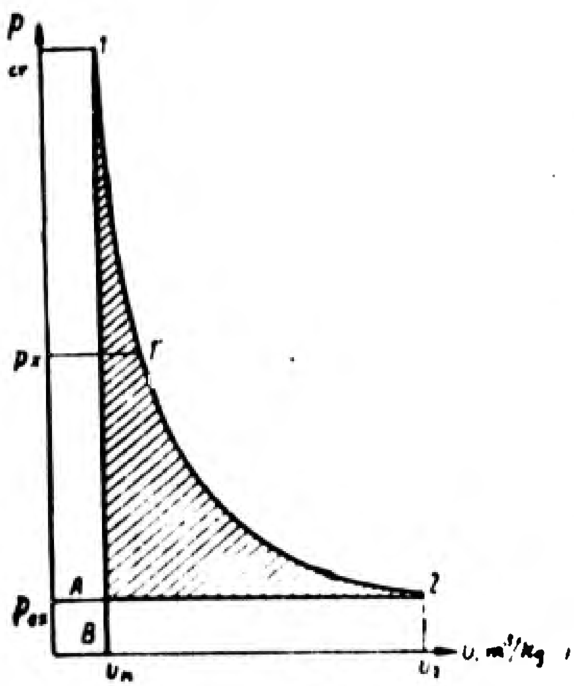

Fig.96 - pv-Diagram of Constant-Volume Engine

Each succeeding particle undergoes less expansion in the nozzle than the preceding particle.

Consequently, as the gas flows out of the chamber, the expansion ratio of the nozzle must decrease, and accordingly there should be an adjustment of the principal cross sections of the nozzle - critical or exit sections (controllable nozzle).

The specific work of expansion of each particle, and also of the entire charge, is measured by the area under the expansion adiabatic 1 - 2. The negative work of the back pressure corresponds to the area under the line A - 2.

The value of the work of the cycle on the diagram may be represented as the difference of the areas p_{ko}-1-2-p_{ex} and p_{ko}-1-A-p_{ex}:

$$L = L_0 - v_k(p_{k0} - p_{ex}) = L_t - RT_{k0}\left(1 - \frac{p_{ex}}{p_{k0}}\right)$$

or

$$L = \frac{k}{k-1} RT_{k0}\left(1 - \frac{1}{\delta_0^a}\right) - RT_{k0}\left(1 - \frac{1}{\delta_0}\right). \tag{114}$$

The same expression may be obtained by summing the work of the elementary particles issuing successively from the chamber:

$$L = \int L_x dG = \int \sqrt{2g \frac{k}{k-1} RT_x \left(1 - \frac{1}{\delta_x^a}\right)}\, dG.$$

The work is related to 1 kg of working fluid at the instant the efflux begins. The work is proportional to the initial temperature and increases with the initial expansion ratio δ_0 and with decreasing adiabatic exponent k.

The thermal efficiency is determined from the ratio

$$\eta_{tv} = \frac{L}{Q_1}.$$

If

$$\eta_{t0} = 1 - \frac{1}{\delta_0^a},$$

then, making use of eqs.(112) and (114), we get

$$\eta_{tv} = k \frac{\delta_0}{\delta_0 - 1} \eta_{t0} - (k-1) = 1 - k\left(1 - \frac{\delta_0}{\delta_0 - 1} \eta_{t0}\right).$$

At $\delta_0 > 100$,

$$\eta_{tv} = 1 - k(1 - \eta_{t0}) = 1 - \frac{k}{\delta_0^a}. \tag{115}$$

It will be clear from this that the thermal efficiency of the cycle V = const is always less than the thermal efficiency of the cycle p = const, if the expansion ratio is the same. The greater the value of k and the smaller that of δ_0, the

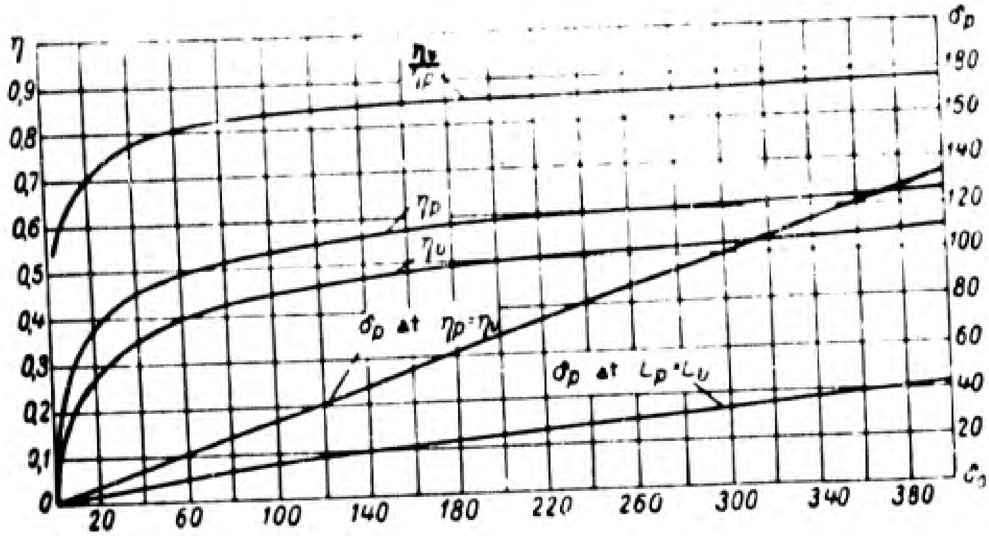

Fig.97 - Comparative Characteristics of Indices of Cycles p = const and V = const for the Case of a Controllable Nozzle

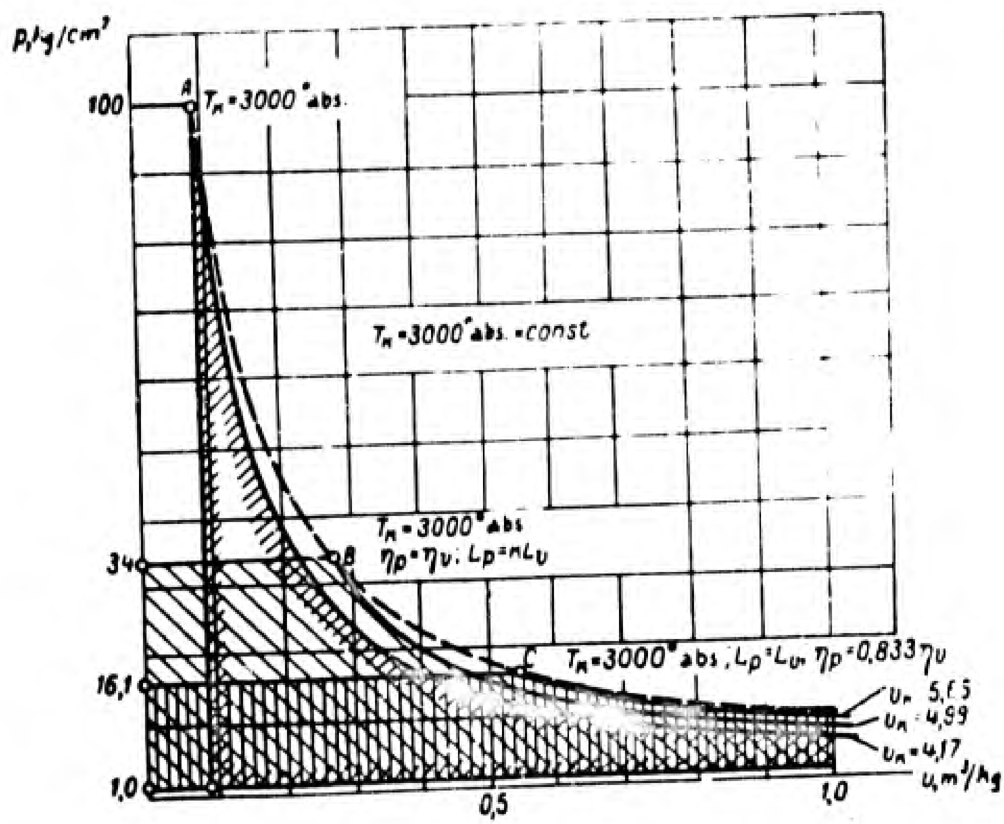

Fig.98 - Comparison of Cycles p = const and V = const at the same Values of Efficiency and Specific Work

greater will be the difference between η_{to} and η_{tv}, which is equal to

$$\eta_{to} - \eta_{tv} = \frac{k-1}{\delta_0^a}.$$

The value of the specific work at high expansion ratios δ_0 may be determined from the formula

$$L = \frac{RT_{k0}}{k-1}\left(1 - \frac{1}{\delta_0^a}\right). \tag{116}$$

Figure 97 shows the thermal efficiency of a rocket engine at p = c and of one at V = c, together with their ratios, as a function of δ_0. To simplify the notation of the individual quantities, only p and v have been retained in the subscripts. The lines $\delta_p = f\delta_v$ have also been plotted on the same diagram. They indicate that, in one case, the specific work is equal in both cycles and, in the other case, that the efficiency is equal. At one and the same economy, the pressure in a rocket engine at p = c is about a third the maximum pressure in the chamber of a rocket engine at V = c. At $L_p = L_v$, the pressure is lower by a factor of 9.5.

The cycles p = const and V = const are compared in Fig.98 for the same efficiency and the same specific work. Let us compare the cycles at the same exhaust-gas temperature. In this case, the line of expansion in the cycle p = const should merge with part of the line of expansion of the cycle V = const. If we assume that the cycles have the same efficiency, the beginning of expansion in the cycle p = const should lie at point b. Comparing the specific work, we find that $L_p = L_v$. Consequently, we may find a pair of cycles p = const and V = const such that, at the same state of the exhaust gases, the same efficiency and specific work are obtained. Here, in a rocket engine at p = c, the maximum temperature is lower by a factor of k, and the pressure is lower by a factor of $k^{\frac{k}{k-1}}$, than in the cycle V = const.

It must be remembered that, in this comparison, the expansion of the gases in a rocket engine at V = c takes place in the nozzle duct at variable expansion ratio, and each portion of gas expands only to the external pressure.

2. Internal Thrust of a Rocket Engine at V = c

Consider the case of determining the engine thrust when the external pressure equals zero and the nozzle dimensions are fixed. Let us also assume that the end of the efflux is specified by the expansion ratio in the chamber, δ_k:

$$\delta_{\kappa} = \frac{p_{\kappa 0}}{p_{\kappa}},$$

where p_{ko} and p_k are the chamber pressures at the beginning and end of the exhaust.

According to eq.(34), the specific thrust of an elementary portion of gas, at an arbitrary time during the efflux, is

$$P_x = \frac{W_{ax}}{g} + \frac{RT_x}{\delta_c^a W_a} \beta.$$

However,

$$W_a = \sqrt{2g \frac{k}{k-1} RT_x \left(1 - \frac{1}{\delta_c^a}\right)} = \sqrt{2g \frac{k}{k-1} RT_{\kappa 0} \left(1 - \frac{1}{\delta_c^a}\right)} \times$$
$$\times \sqrt{\frac{1}{\delta_x^a}}$$

and, since $\beta = 1.0$,

$$P_{st} = \frac{RT_x}{\delta_c^a W_a} = \frac{RT_{\kappa 0}}{\delta_c^a \delta_x^a} \cdot \frac{\sqrt{\delta_x^a}}{W_0} = \frac{RT_{\kappa 0}}{\delta_c^a W_0} \cdot \sqrt{\frac{1}{\delta_x^a}}.$$

As a result,

$$P_x = \left(\frac{W_0}{g} + \frac{RT_{\kappa 0}}{\delta_c^a W_0}\right) \frac{1}{\sqrt{\delta_x^a}} = P_{sp0} \sqrt{\frac{1}{\delta_x^a}}, \tag{117}$$

where P_{spo} is the specific thrust of the first portion discharged from the chamber.

Obviously,

$$P_{sp} = \int_0^{G_a = 1.0} P_x dG$$

or

$$P_{sp} = \int P_{sp0} \sqrt{\frac{1}{\delta_x^a}} dG.$$

However,

$$G = \frac{V}{v_x} = \frac{V}{v_0}\left(\frac{p_x}{p_{\kappa 0}}\right)^{\frac{1}{k}} = \frac{G_0}{\delta_x^{\frac{1}{k}}} = \frac{1}{\delta_x^{\frac{1}{k}}},$$

where V is the volume of a unit chamber, corresponding to a weight rate of flow of 1 kg/sec.

We find the following expression for dG:

$$dG = -\frac{1}{k}\frac{d\delta_x}{\delta_x^{\frac{k+1}{k}}}.$$

Now

$$P_{sp} = P_{sp\,0}\frac{1}{k}\int_1^{\delta_\kappa}\frac{d\delta_x}{\delta_x^{\frac{3k+1}{2k}}}.$$

After integration, we have

$$P_{sp} = -\frac{2k}{k+1}\cdot\frac{P_{sp\,0}}{k}\,\delta_x^{-\frac{k+1}{2k}}\Bigg|_{1,0}^{\delta_\kappa}$$

and, finally,

$$P_{sp} = \frac{2}{k+1}P_{sp\,0}\left(1 - \frac{1}{\delta_\kappa^{\frac{k+1}{2k}}}\right). \tag{118}$$

Equation (118) permits determining the internal specific thrust of a rocket engine at V = c or the specific thrust under the condition δ_c = const and $p_{ex} = 0$.

Figure 99 shows the lines of expansion of the first and last portions of gas issuing from the chamber of a rocket engine at V = c. The expansion ratio in both cases is the same, i.e.,

$$\frac{p_{\kappa 0}}{p_{a0}} = \frac{p_\kappa}{p_{a\kappa}} = \delta_c.$$

On complete efflux, in this case, $\delta_\kappa = \infty$, and

$$P_{sp\cdot i} = \frac{2}{k+1}P_{sp\,0} = \frac{2}{k+1}\frac{W_0}{g}\left(1 + \frac{1}{kM_{a0}^2}\right). \tag{119}$$

Let us find the necessary ideal maximum thrust $P_{sp\ max}$, which must be compared with the true value to obtain the force factor.

Assume $\delta_c = \infty$ and $\delta_k = \infty$. This means that the weight flow of gas completely enters a medium with zero pressure through a nozzle with an infinite expansion ratio.

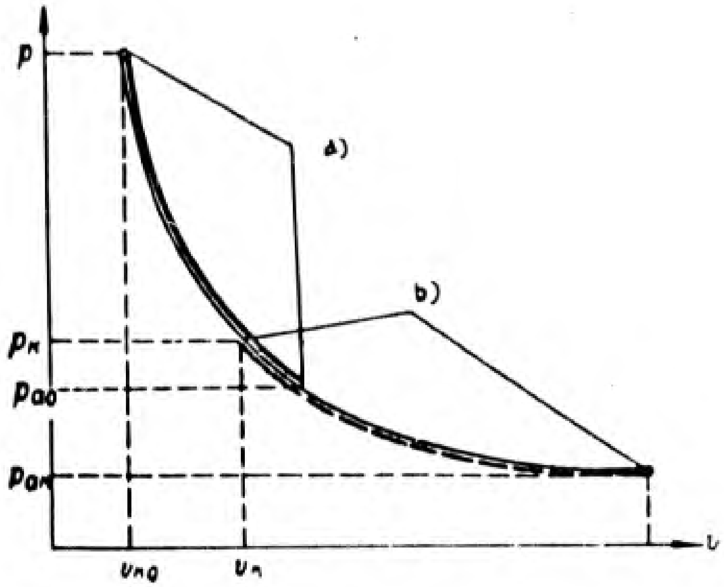

Fig.99 - Lines of Expansion of First and Last Portions of Gas
(δ_c = const, p_{ex} = 0)

a) Expansion of first portion of gas; b) Expansion of last portion of gas

Then, the maximum specific thrust may be calculated by means of the formula

$$P_{sp\ max} = \frac{2}{k+1} P_{sp\ 0\ max}. \tag{120}$$

Here,

$$P_{sp\ 0\ max} = \frac{W_{0\ max}}{g} = \sqrt{\frac{2k}{k-1} \cdot \frac{RT_{K0}}{g}}.$$

Consequently,

$$P_{sp\ max} = \frac{2}{k+1} \sqrt{\frac{2k}{k-1} \cdot \frac{RT_{K0}}{g}}. \tag{121}$$

We now set up an expression for the force factor of the engine with efflux into a vacuum:

$$\psi_c = \sqrt{1 - \frac{1}{\delta_c^n} \cdot \left(1 + \frac{1}{kM_{a0}^2}\right)\left(1 - \frac{1}{\delta_K^{\frac{k+1}{2k}}}\right)}. \tag{122}$$

To increase the force factor, both δ_c and δ_κ must be increased.

In the special case of a convergent nozzle ($M_a = 1.0$) and of complete exhaust ($\delta_k = \infty$), the force factor becomes equal to

$$\psi_c \Big|_{\delta_\kappa = \infty}^{M_a = 1} = \frac{k+1}{k}\sqrt{\frac{k-1}{k+1}} = \sqrt{1 - \frac{1}{k^2}}.$$

3. Thrust of a Rocket Engine at V = c in the Case of a Controllable Nozzle

Let p_{ko} and p_{ex} be given. Moreover, the extent of deviation from the rated exhaust conditions is always equal to $\beta = 0$. This is accomplished by varying the nozzle exit section f_a.

Then, the specific thrust, at an arbitrary instant of exhaust, will be

$$P_x = \frac{W_{ax}}{g} = \frac{1}{g}\sqrt{2g\frac{k}{k-1}RT_{\kappa 0}\frac{1}{\delta_{\kappa x}^{a}}\left[1 - \left(\frac{p_{ex}}{p_x}\right)^a\right]},$$

where

$$\frac{p_{ex}}{p_x} = \frac{p_{ex}}{p_{\kappa 0}}\cdot\frac{p_{\kappa 0}}{p_x} = \frac{\delta_{\kappa x}}{\delta_{\kappa 0}}.$$

The specific thrust at a weight rate of flow of $G_o = 1$ kg/sec is

$$P_{sp} = \int P_x dG.$$

At any instant of time, the quantity of gas in the chamber will be

$$G_x = \frac{V}{v_x} = \frac{V}{v_0}\cdot\left(\frac{p_\kappa}{p_{\kappa 0}}\right)^{\frac{1}{k}} = G_0\left(\frac{p_{ex}}{p_{\kappa 0}}\right)^{\frac{1}{k}}\left(\frac{p_\kappa}{p_{ex}}\right)^{\frac{1}{k}}.$$

Hence,

$$dG = G_0\frac{1}{\delta_{\kappa 0}^{\frac{1}{k}}}d\left(\frac{p_\kappa}{p_{ex}}\right)^{\frac{1}{k}}.$$

We now introduce the notation

$$\left(\frac{p_\kappa}{p_{ex}}\right)^{\frac{1}{k}} = y.$$

Then,

$$dG = G_0 \frac{dy}{\delta_{\kappa 0}^{\frac{1}{k}}}$$

and, since $\delta_{\kappa o} = \delta_{ex\ o}$, we have

$$\sqrt{\frac{1}{\delta_\kappa^a} - \frac{1}{\delta_{ex0}^a}} = \sqrt{\frac{1}{\delta_{\kappa 0}^{\frac{1}{k}}}} \sqrt{y^a - 1}.$$

At $G_0 = 1.0$,

$$P_{sp} = \frac{1}{g} \sqrt{2g \frac{k}{k-1} RT_{\kappa 0}}\ \delta_{ex0}^{\frac{1-k+1}{2k}} \int_{y=\left(\frac{p_{\kappa 0}}{p_{ex}}\right)^{\frac{1}{k}}}^{1.0} \sqrt{y^{k-1} - 1}\, dy. \quad (123)$$

The integration is performed for k = 1.25, 1.286, 1.333, and 1.4. For example, for k = 1.25,

$$P_{sp} = 0{,}141 \sqrt{T_{\kappa 0} \frac{1}{\delta_{ex0}^{1.8}}} \left(\delta_{ex0}^{0.2} - 1\right)^{1.5} \left(35\delta_{ex0}^{0.6} + 30\delta_{ex0}^{0.4} + 24\delta_{ex0}^{0.2} + 16\right). \quad (124)$$

Comparing this value with the maximum thrust as determined by eq.(121), we get the force factor:

$$\psi_c = 0{,}0283 \sqrt{\frac{1}{\delta_{ex0}^{1.8}}} \left(\delta_{ex0}^{0.2} - 1\right)^{1.5} \left(35\delta_{ex0}^{0.6} + 30\delta_{ex0}^{0.4} + 24\delta_{ex0}^{0.2} + 16\right).$$

Figure 100 shows the change in thrust related to a flow rate of G = 1 kg/sec, as a function of the expansion ratio of the first portion of gas. Usually $\delta_{ex\ o}$ is large, and most of the gas is ejected at supersonic speed. Let us calculate the time of efflux of that portion of the gas that issues at $M_a \geq 1.0$.

Until the onset of subcritical flow, the quantity issuing from the chamber will be

$$\Delta G = G_0 - G_{x\,cr} = G_0\left(1 - \frac{\gamma_{x\,cr}}{\gamma_{\kappa 0}}\right) = G_0\left[1 - \left(\frac{p_{x\,cr}}{p_{\kappa 0}}\right)^{\frac{1}{k}}\right] =$$

$$= G_0\left[1 - \left(\frac{p_{x\,cr}}{p_{ex}}\right)^{\frac{1}{k}} \left(\frac{p_{ex}}{p_{\kappa 0}}\right)^{\frac{1}{k}}\right].$$

However,

$$\frac{p_{x\,cr}}{p_{ex}} = \delta_{cr} = \left(\frac{k+1}{2}\right)^{\frac{1}{k-1}}$$

and

$$\Delta G = G_0\left[1 - \frac{1}{\delta_{k0}^{\frac{1}{k}}}\left(\frac{k+1}{2}\right)^{\frac{1}{k-1}}\right]. \tag{125}$$

For example, at $\delta_{K0} = 100$, $\frac{\Delta G}{G_0} = 0.939$. If, however, $\delta_{K0} = 400$, then $\frac{\Delta G}{G_0} =$ $= 0.979$.

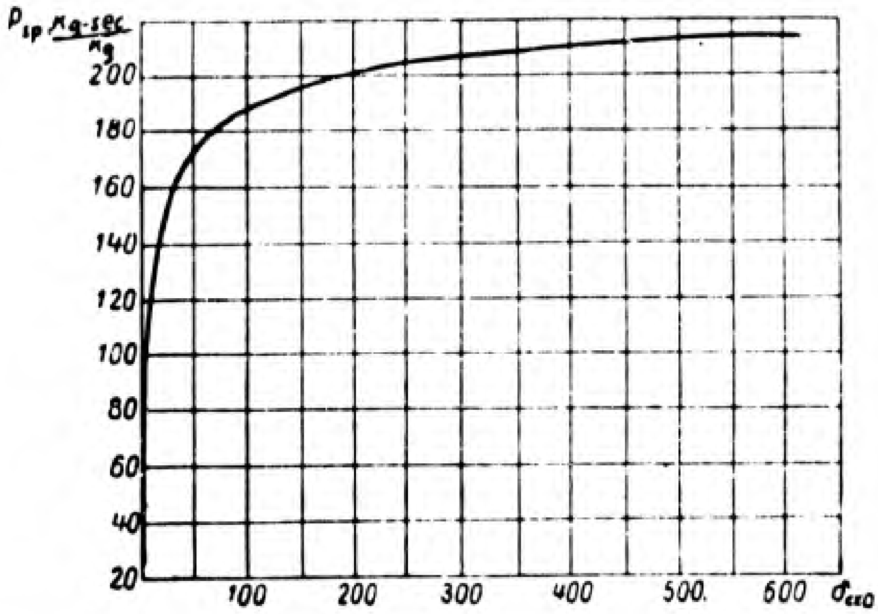

Fig.100 - Variation in Specific Thrust of an Engine at V = const with Controllable Nozzle, as a Function of the Initial Expansion Ratio $\delta_{ex\,o}$

To determine the efflux time, we make use of the relation

$$dG = G_{sec}\,d\tau,$$

However,

$$G_{sec} = F_{cr}\frac{p_x}{\sqrt{RT_x}}\sqrt{kg\left(\frac{2}{k+1}\right)^{\frac{k+1}{k-1}}} = A\frac{1}{\delta_k}\sqrt{\delta_k^{a}}.$$

where δ_k is the expansion ratio in the chamber, up to an arbitrary instant of time.

Since

$$G = \frac{V}{v_{k0}}\left(\frac{p_k}{p_{k0}}\right)^{\frac{1}{k}} = G_0 \frac{1}{\delta_k^{\frac{1}{k}}},$$

then

$$dG_k = -\frac{G_0}{k}\cdot\frac{d\delta_k}{\delta_k^{\frac{k+1}{k}}},$$

where dG_k is the gas loss in the chamber,

$$dG = -dG_k.$$

Omitting intermediate calculations, we write the expression for determining the efflux time at supersonic speed, as follows:

$$\tau = \frac{2G_0}{A\,(k-1)}\left(\sqrt{\frac{2}{k+1}\,\delta_{k0}^{a}} - 1\right), \tag{126}$$

where

$$A = F_{cr}\,\frac{p_{k0}}{\sqrt{RT_{k0}}}\sqrt{kg\left(\frac{2}{k+1}\right)^{\frac{k+1}{k-1}}}. \tag{127}$$

4. Thrust of a Rocket Engine at V = c with Fixed Nozzle

The rocket engine at V = c with a fixed nozzle is simple in layout. The exhaust of the last portions of gas should be accompanied by extreme overexpansion, by entry of a shock wave into the nozzle, and by expansion at subcritical pressure drops.

We shall use the following notation in determining the specific engine thrust:

$\delta_{ex\ o} = \frac{p_{ko}}{p_{ex}}$ is the disposable expansion ratio at the initial instant of exhaust;

$\delta_k = \frac{p_{ko}}{p_k}$ is the expansion ratio of the gas in the chamber;

$\delta_c = \frac{p_x}{p_a}$ is the constant expansion ratio in the nozzle.

Assume that these expansion ratios are so combined that the flow in the nozzle duct is not disturbed by shock stall.

According to eq.(34), the current specific thrust is determined by the formula

$$P_x = \frac{W_x}{g}\left(1 + \frac{\beta}{kM_a^2}\right).$$

So long as the nozzle has not changed over to conditions of extreme overexpansion, the Mach number across the exit section is the same for all portions of gas, since

$$M_a^2 = \frac{2}{k-1}\left(\delta_c^a - 1\right).$$

Let us take, as the main variable, the expansion ratio in the chamber $\delta_{kx} = \frac{p_{ko}}{p_x}$. Then, the degree of non-design conditions will be

$$\beta = 1 - \frac{\delta_c}{\delta_{ex}} = 1 - \delta_c \frac{p_{k0}}{p_x} \cdot \frac{p_{ex}}{p_{k0}} = 1 - \frac{\delta_c}{\delta_{ex0}} \delta_{kx}.$$

Moreover,

$$\frac{W_x}{W_0} = \sqrt{\frac{T_x}{T_{k0}}} = \sqrt{\frac{1}{\delta_{kx}^a}},$$

where W_0 is the exhaust velocity at the initial instant.

Then,

$$P_x = \frac{W_0}{g}\left[\left(1 + \frac{1}{kM_a^2}\right)\frac{1}{\delta_{kx}^{\frac{k-1}{2k}}} - \frac{1}{kM_a^2} \cdot \frac{\delta_c}{\delta_{ex0}} \delta_{kx}^{\frac{k+1}{2k}}\right]$$

or

$$P_x = \frac{W_0}{g}\left(1 + \frac{1}{kM_a^2}\right)\left(\frac{1}{\delta_{kx}^{\frac{k-1}{2k}}} - \frac{1}{1 + kM_a^2} \cdot \frac{\delta_c}{\delta_{ex0}} \delta_{kx}^{\frac{k+1}{2k}}\right).$$

The specific thrust is determined from the formula

$$P_{sp} = \int_0^1 P_x dG = -\frac{1}{k}\int_1^{\delta_k} P_x \frac{d\delta_{kx}}{\delta_{kx}^{\frac{k+1}{k}}},$$

or

$$P_{sp} = -\frac{W_0}{kg}\left(1 + \frac{1}{kM_a^2}\right)\left(\int_1^{\delta_k} \delta_{kx}^{-\frac{3k+1}{2k}} d\delta_{kx} - \frac{1}{1 + kM_a^2} \cdot \frac{\delta_c}{\delta_{ex0}} \int_{1,0}^{\delta_k} \delta_{kx}^{-\frac{k+1}{2k}} d\delta_{kx}\right).$$

After integration, bearing in mind that

$$\frac{W_0}{g}\left(1 + \frac{1}{kM_a^2}\right) = P_{sp.c.0},$$

we get

$$P_{sp} = \frac{2}{k+1} P_{sp\,i.o} \left[1 - \frac{1}{\delta_{\kappa}^{\frac{k+1}{2k}}} - \frac{1}{1+kM_a^2} \cdot \frac{\delta_c}{\delta_{ex\,0}} \cdot \frac{k+1}{k-1} \left(\delta_{\kappa}^{\frac{k-1}{2k}} - 1 \right) \right]. \tag{128}$$

Here, P_{sp} may be represented as a function of δ_c and δ_K. In this case,

$$P_{sp} = \frac{2}{k+1} \sqrt{\frac{2}{g} \cdot \frac{k}{k-1} RT_{\kappa 0}} \sqrt{1 - \frac{1}{\delta_c^a} \cdot \frac{\delta_c^a - \frac{k+1}{2k}}{\delta_c^a - 1}} \times$$

$$\times \left[1 - \frac{1}{\delta_{\kappa}^{\frac{k+1}{2k}}} - \frac{1}{\frac{2k}{k+1}\delta_c^a - 1} \cdot \frac{\delta_c}{\delta_{ex\,0}} \left(\delta_{\kappa}^{\frac{k-1}{2k}} - 1 \right) \right]. \tag{129}$$

We now obtain the following expression for the force factor:

$$\psi_c = \frac{P_{sp}}{P_{sp\cdot max}} = \frac{1 - \frac{k+1}{2k\delta_c^a}}{\sqrt{1 - \frac{1}{\delta_c^a}}} \left[1 - \frac{1}{\delta_{\kappa}^{\frac{k+1}{2k}}} - \frac{1}{\frac{2k\delta_c^a}{k+1} - 1} \cdot \frac{\delta_c}{\delta_{ex\,0}} \left(\delta_{\kappa}^{\frac{k-1}{2k}} - 1 \right) \right]. \tag{130}$$

In eqs.(129) and (130), the specific thrust and the force factor depend on δ_c, $\delta_{ex\ o}$, and δ_K.

In eqs.(129) and (130), the variable part, depending on δ_K, equals

$$-\frac{1}{\delta_{\kappa}^{\frac{k+1}{2k}}} - \frac{\delta_c}{\delta_{ex\,0}} \cdot \frac{1}{\frac{2k}{k+1}\delta_c^a - 1} \cdot \delta_{\kappa}^{\frac{k-1}{2k}}.$$

The maximum of this quantity is reached at the following expansion ratio in the chamber:

$$\delta_{\kappa} = \frac{\delta_{ex\,0}}{\delta_c} \left(\frac{2k}{k-1} \delta_c^a - \frac{k+1}{k-1} \right). \tag{131}$$

Determining the optimum value of δ_K from eq.(131), it is necessary to check whether it is physically possible to obtain this value of δ_K at normal flow inside the nozzle.

Figure (101) shows the variation of P_{sp} as a function of δ_K for the special case $\delta_{ex\ 0} = 400$ and $\delta_c = 50$. The value of P_{sp} reaches a maximum at $\delta_K = 96.22$.

Let us determine the extreme value of δ_k corresponding to the entry of a shock wave into the exit section of the nozzle, assuming that the shock reaches the nozzle at

$$\frac{p_{ex}}{p_{a\xi}} = \xi M_a.$$

However,

$$\frac{p_{ex}}{p_{a\xi}} = \frac{p_{ex}}{p_{k0}} \frac{p_{k0}}{p_{k\xi}} \frac{p_{k\xi}}{p_{a\xi}} = \frac{\delta_c}{\delta_{ex0}} \delta_{k\xi}.$$

Consequently,

$$\delta_{k\xi} = \frac{\delta_{ex0}}{\delta_c} \xi M_a = \frac{\delta_{ex0}}{\delta_c} \xi \sqrt{\frac{2k}{k-1}\left(\delta_c^{a} - 1\right)}. \qquad (132)$$

Substituting this value of $\delta_{k\xi}$ in eqs.(128) and (130), we obtain expressions

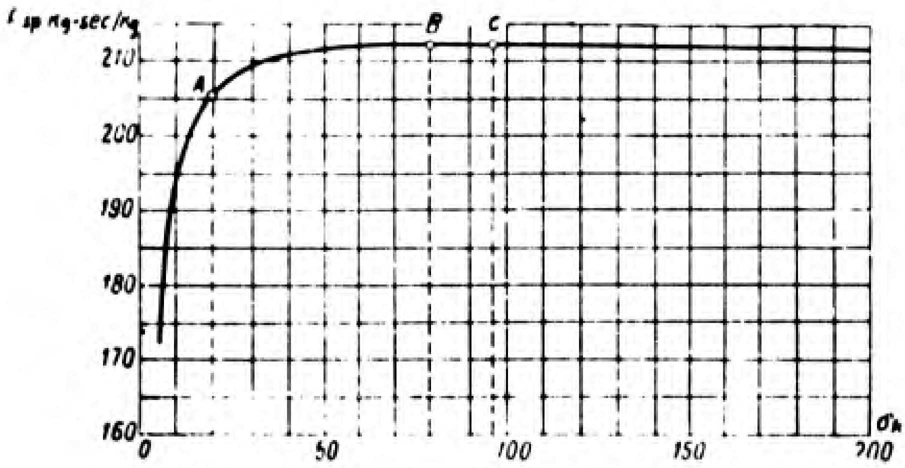

Fig.101 - Influence of Expansion Ratio in Chamber on the Specific Thrust, at $\delta_{ex\ o} = 400$ and $\delta_c = 50$

Point A - Instant of entry of shock wave, according to eq.(47);
Point B - Instant of entry of shock wave, according to eq.(46);
Point C - $P_{sp\ max}$

for the specific thrust and force factor at the instant of entry of the shock into the nozzle.

For the case shown in Fig.101, $\delta_{k\xi} = 19.5$. On comparing eqs.(131) and (132), we reach the conclusion that for specified values of δ_{ex} and δ_c, the shock wave at the exit section of the nozzle always corresponds to an expansion ratio in the chamber lower than the theoretical optimum.

This conclusion is true only for the simple relation adopted, $\frac{p_{ex}}{p_a} = \xi M_a$ at low values of ξ. Other relations between p_{ex} and p_a on entry of the shock wave into the nozzle might lead to a different relation between $\delta_{k\xi}$ and δ_k - the optimum.

In eqs.(129) and (130), P_{sp} and ψ_o depend on the values of $\delta_{ex\ o}$ and δ_c. Assigning one of these, the second may be found as the optimum.

It is simpler to specify δ_c and find $\delta_{ex\ o}$.

Let us assume that, in eq.(132),

$$\delta_{k\xi} = B\delta_{ex\,0}.$$

Then the variable in eq.(129) that depends on $\delta_{ex\ o}$ will be

$$y = -\frac{1}{B^{\frac{k+1}{k}}\,\delta_{ex\,0}^{\frac{k+1}{2k}}} - \frac{\delta_c}{\delta_{ex\,0}}\,\delta_{ex\,0}^{\frac{k-1}{2k}}\,\frac{B^{\frac{k-1}{2k}}}{\frac{2k}{k+1}\delta_c^a - 1} + \frac{\delta_c}{\delta_{ex\,0}}\,\frac{1}{\frac{2k}{k+1}\delta_c^a - 1}.$$

Determining the maximum of this quantity under the condition

$$\frac{dy}{d\delta_{ex\,0}} = 0,$$

by the ordinary method, we find that it occurs at

$$\delta_{ex\,0} = \left(\frac{2k}{k+1}\cdot\frac{D}{1+c}\right)^{\frac{2k}{k-1}}. \tag{133}$$

Here,

$$c = \frac{\xi\sqrt{\frac{2}{k-1}\left(\delta_c^a - 1\right)}}{\frac{2k}{k+1}\delta_c^a - 1}$$

and

$$D = \frac{\sqrt{\delta_c^a}\left[\xi\sqrt{\frac{2}{k-1}\left(\delta_c^a - 1\right)}\right]^{\frac{k+1}{2k}}}{\frac{2k}{k+1}\delta_c^a - 1}.$$

Figure 102 shows the specific thrust of the engine as a function of the expansion ratio in the nozzle and chamber. The broken line corresponds to the time of entry of the shock wave into the nozzle. Figure 103 is an example of the variation of Ψ_c with $\delta_{ex\ o}$, under the condition that the optimum value of δ_c is found for each

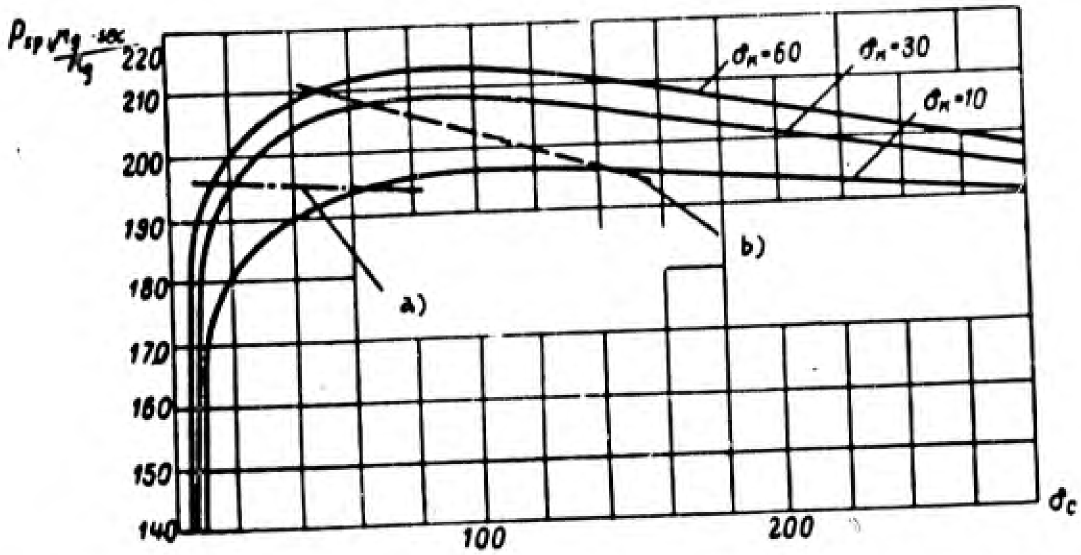

Fig.102 - Variation in Specific Thrust of a Rocket Engine at V = const with the Expansion Ratio in the Chamber and Nozzle ($\delta_{ex\ o}$ = 300)

a) Boundary of appearance of shock wave at nozzle exit; b) Theoretical boundary of appearance of shock wave at nozzle exit

specified $\delta_{ex\ o}$ and that the efflux ceases at the instant of entry of the shock wave into the nozzle.

Let us determine, in conclusion, the time of efflux from the chamber up to the instant of entry of the shock wave into the nozzle exit, when δ_c is determined by eq.(132).

The exhaust will be exclusively supersonic, and for this reason, as in the case of a controllable nozzle (p.172),

$$d\tau = \frac{G_0}{Ak}\,\delta_{k.x}^{\frac{k+1}{2k}}\,d\delta_{k.x}.$$

Hence,

$$\tau = \frac{G_0}{A}\cdot\frac{2}{k+1}\,\delta_{kx}^{\frac{k-1}{2k}}\Big|_{\delta_k}^{1.0} = \frac{2G_0}{A(k-1)}\left(\delta_k^{\frac{k-1}{2k}} - 1\right)$$

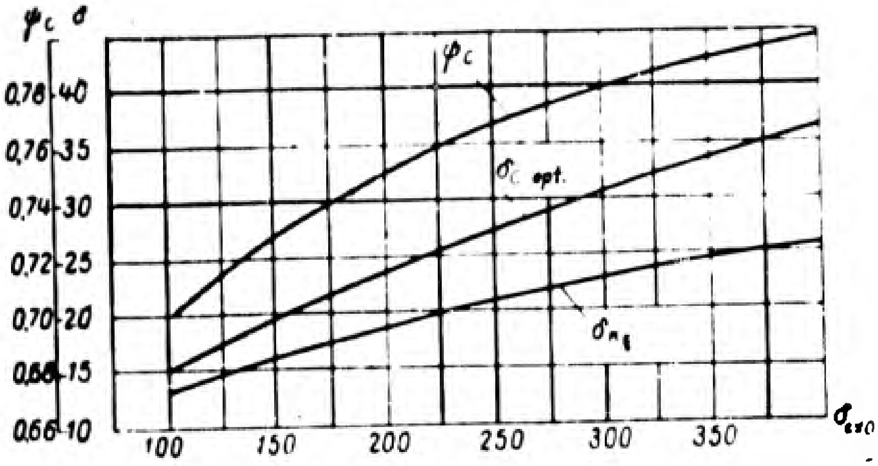

Fig.103 - Effect of Initial Gas Expansion $\delta_{ex\ o}$ on the Force Factor ψ_c at Optimum Expansion Ratio in the Chamber and Efflux until the Instant of Entry of the Shock Wave into the Nozzle

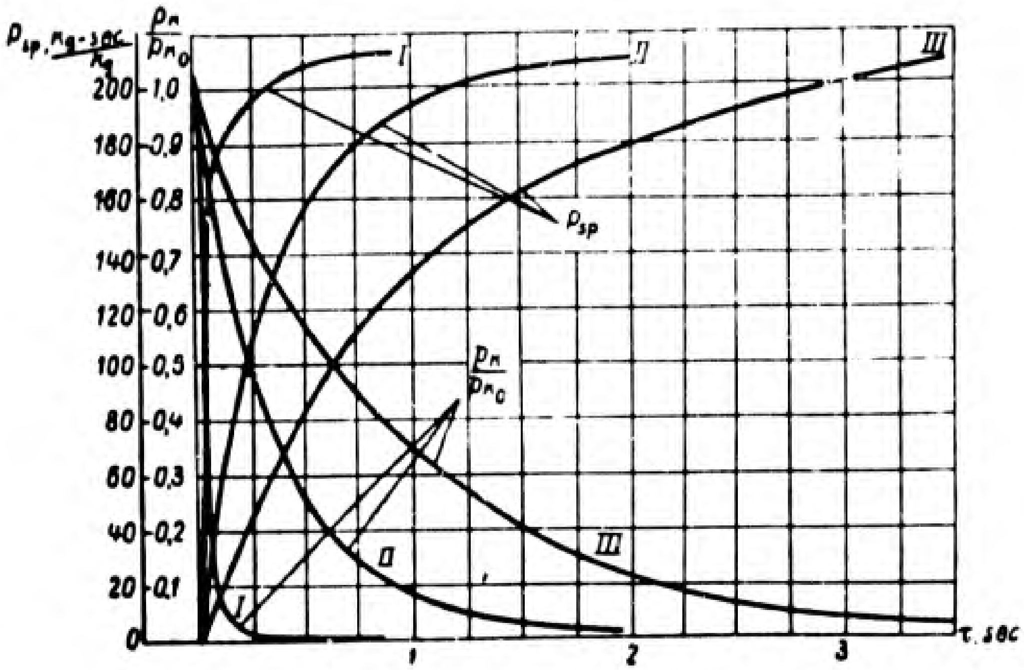

Fig.104 - Variation of Relative Chamber Pressure and of Specific Thrust during Efflux from the Chamber of a Rocket Engine at V = c (T_{ko} = 3000°K; P_{ko} = 100 atm; $\delta_{ex\ o}$ = 400; δ_c = 40)

I - $f_{cr\ max} = 38.9 \times 10^{-4}$ m^2; II - $f_{cr\ max} = 20 \times 10^{-4}$ m^2; III - $f_{cr\ max} = 1.49 \times 10^{-4}$ m^2

or, for $\delta_k \xi$,

$$\tau = \frac{2G_0}{A(k-1)}\left[\left(\frac{\delta_{k0}}{\delta_c}\xi M_a\right)^{\frac{k-1}{2k}} - 1\right], \qquad (134)$$

where

$$A = F_{cr}\frac{p_{k0}}{\sqrt{RT_{k0}}}\sqrt{kg\left(\frac{2}{k+1}\right)^{\frac{k+1}{k-1}}}.$$

Figure 104 shows the variation in relative chamber pressure $\frac{p_k}{p_{ko}} = \frac{1}{\delta_k}$ and in impulse $P_{sp\,x}$ during the exhaust.

The greatest influence on the duration of the exhaust is exerted by the values of the critical section and the initial temperature.

5. Cycle of a Rocket Engine at V = c with Fixed Nozzle

In cases where the chamber of a rocket engine at V = c is used as a gas generator for a turbine, the specific work of the exhaust must be determined instead of the specific thrust.

Given a chamber with incomplete expansion, for which, at the end of the process of expansion, $\delta_k = \frac{p_{ko}}{p_k}$. If the exit section of the nozzle is so regulated that the pressure at the end of expansion is always equal to the external pressure, then the operating diagram will have the form shown in Fig.105. The hatched area corresponds to the work during the cycle, related to 1 kg of gas in state I. All the expansion adiabatics of the exhausted portions of gas end at point II and originate at the points I and A. The line II-c, the adiabatic c-a, and the line a-I are plotting lines for the area determining the work of the cycle.

Let us determine the specific work and thermal efficiency for the chamber of a rocket engine at V = c, having a constant-dimension nozzle, which is closer to the practical design.

The specific work, at an arbitrary instant of exhaust, is

$$L_x = \frac{W_x^2}{2g} = \frac{k}{k-1} RT_x \left(1 - \frac{1}{\delta_c^a}\right)$$

$$= \frac{k}{k-1} RT_{\kappa 0} \left(1 - \frac{1}{\delta_c^a}\right) \frac{1}{\delta_{\kappa x}^a} = \frac{L_0}{\delta_{\kappa x}^a}.$$

The work of an elementary particle dG is

$$dL = L_x dG.$$

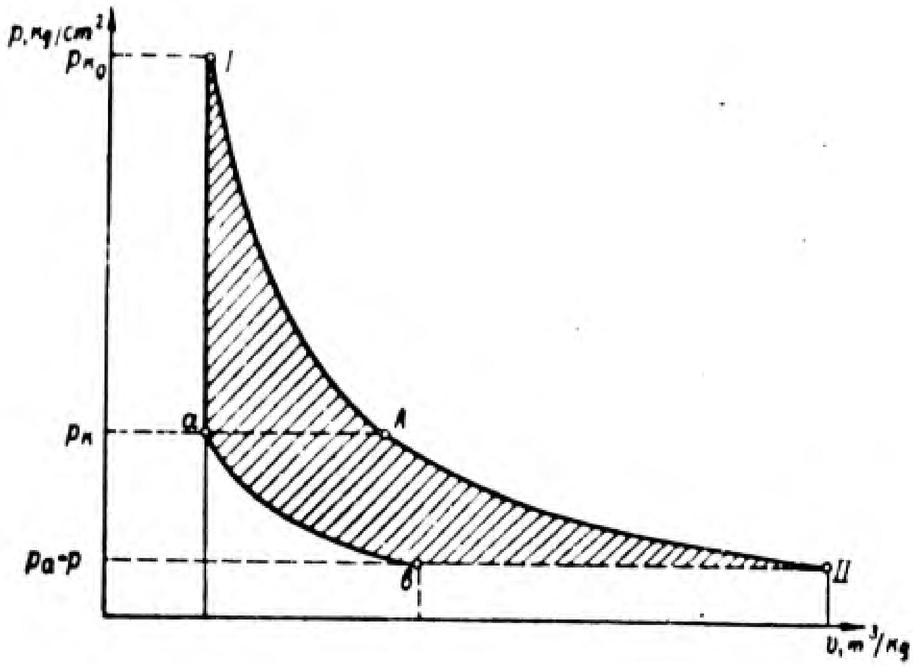

Fig.105 - Determining the Work of the Engine V = const at Incomplete Expansion of the Gases in the Chamber (Controllable Nozzle)

The absolute magnitude of the exhausted portion of gas is

$$dG = -\frac{1}{k} \cdot \frac{d\delta_{\kappa x}}{\delta_{\kappa x}^{\frac{k+1}{k}}}.$$

Consequently,

$$dL = -\frac{L_0}{k} \frac{d\delta_{\kappa x}}{\delta_{\kappa x}^2} = -\frac{L_0}{k} d\left(\frac{1}{\delta_{\kappa x}}\right)$$

and

$$L = \frac{L_0}{k}\left(1 - \frac{1}{\delta_\kappa}\right) = \frac{L_0}{k}\left(1 - \frac{p_\kappa}{p_{\kappa 0}}\right). \qquad (135)$$

Figure 106 shows the pv-diagram of a rocket engine at V = c, from which we may determine the work during the cycle of the engine at incomplete expansion in the chamber and constant nozzle duct.

The work, according to eq.(135), may be represented as consisting of two parts:

$$L_T = \frac{L_0}{k} - \frac{L_0}{k}\,\frac{p_к}{p_{к0}}.$$

The first part

$$\frac{L_0}{k} = \frac{1}{k-1} RT_{к0}\left(1 - \frac{1}{\delta_c^{a}}\right)$$

corresponds on the diagram to the area under the segment 1-2 of the adiabatic.

To obtain the second part from the point A, denoting the end of expansion in

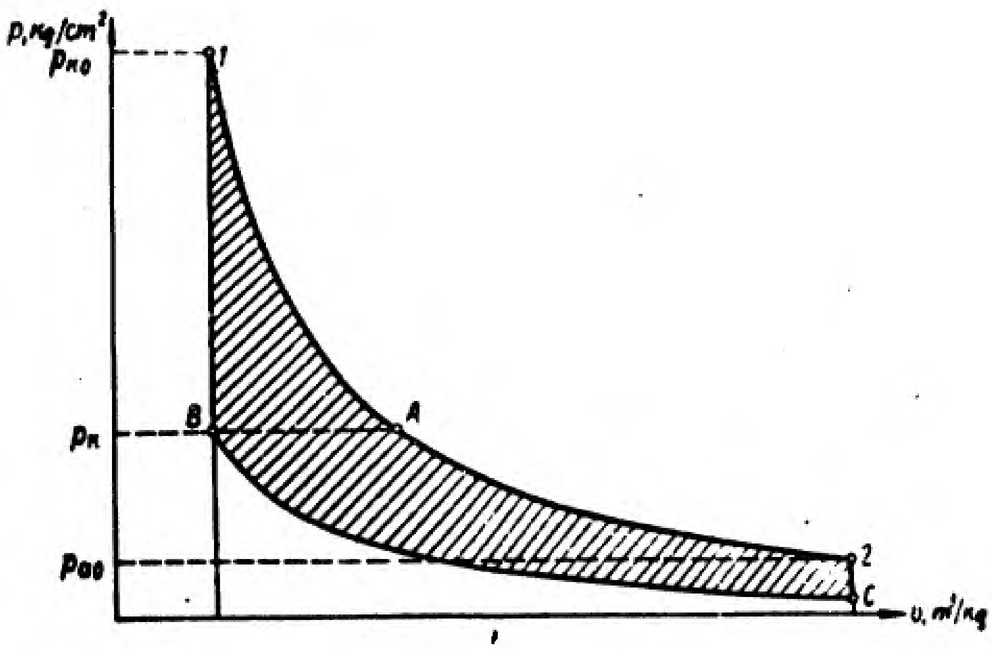

Fig.106 - Determination of Work of a Rocket Engine at V = const, with Incomplete Expansion of Gas in the Chamber (Fixed Nozzle)

the chamber, we draw a horizontal to intersection with the vertical 1 at point B, through which we lay the adiabatic B-C. The area under the adiabatic B-C represents the value of the second part.

Consequently, the hatched area of the diagram 1-2-C-B is proportional to the engine work during the cycle.

The value of the heat expended must be determined as the difference of the internal energies in the states 1 and A of the working fluid. In state 1, at a temperature T_{ko}, 1 kg of the gas possesses an internal energy of $\frac{RT_{ko}}{k-1}$. At the time A in the chamber there is an amount

$$G_{\kappa}=\frac{1}{\delta_{\kappa}^{\frac{1}{k}}}$$

of gas at a temperature of

$$T_{\kappa}=\frac{T_{\kappa 0}}{\delta_{\kappa}^{a}},$$

Consequently,

$$Q_{1}=\frac{1}{k-1}RT_{\kappa 0}-\frac{1}{\delta_{\kappa}^{\frac{1}{k}}}\cdot\frac{RT_{\kappa 0}}{(k-1)\,\delta_{\kappa}^{a}}=\frac{RT_{\kappa 0}}{k-1}\left(1-\frac{1}{\delta_{\kappa}}\right). \tag{136}$$

Making use of eqs.(135) and (136), we find the thermal efficiency

$$\eta_{t}=\frac{L}{Q_{1}}=1-\frac{1}{\delta_{c}^{a}}. \tag{137}$$

The thermal efficiency is the same as that in a rocket engine at p = c in the case of the same nozzle, but is higher than the thermal efficiency for an engine with a controllable nozzle at complete exhaust, which is explained by the greater expansion of all portions of gas except the first.

The specific work related to 1 kg of gas at the initial time of efflux is determined from eq.(135). However, at incomplete exhaust, the available work must be related to 1 kg of ejected gas. By the end of exhaust, the quantity of gas remaining in the chamber will be

$$G_{\kappa}=\frac{1}{\delta_{\kappa}^{\frac{1}{k}}}.$$

We again specify

$$\Delta G=1-G_{\kappa}=1-\frac{1}{\delta_{\kappa}^{\frac{1}{k}}},$$

after which

$$L_{sp} = \frac{L}{\Delta G} = \frac{L_n}{k} \cdot \frac{\delta_k - 1}{\delta_k^a \left(\delta_k^{\frac{1}{k}} - 1 \right)}. \tag{138}$$

If the initial temperature does not depend on the amount of working fluid supplied (case of heating) then it must be preset. In the case of a chemical fuel, the temperature T_{k0} is a function of δ_k.

After feeding the propellant to the chamber, $\frac{1}{\delta_k^{\frac{1}{k}}}$ kg of residual gases are mixed, at a temperature $T_k = \frac{T_{k0}}{\delta_k^a}$, with $1 - \frac{1}{\delta_k^{\frac{1}{k}}}$ of propellant having a heat value of $\frac{RT_0}{k - 1}$, where T_0 is the temperature of the working fluid after heat liberation, in the absence of residual gases.

The heat balance of the process of heat liberation and gas mixing has the form

$$\left(1 - \frac{1}{\delta_k^{\frac{1}{k}}} \right) \cdot \frac{RT_0}{k - 1} + \frac{1}{\delta_k^{\frac{1}{k}}} \cdot \frac{RT_{k0}}{(k - 1)\, \delta_k^a} = \frac{RT_{k0}}{k - 1}.$$

Hence, we determine the gas temperature for the initial instant of efflux

$$\frac{T_{k0}}{T_0} = \frac{\delta_k^a \left(\delta_k^{\frac{1}{k}} - 1 \right)}{\delta_k - 1}. \tag{139}$$

In the practical case, the heat is not liberated instantaneously, and the calculations of work and thrust are complicated. Usually, based on practical data, a time law of heat liberation is used, after which the velocity of the exhausted particles can be calculated even during the time of heat liberation.

6. The Pulsejet Rocket Engine with Open Throat

Heat liberation at constant volume may be obtained by periodic closing of the nozzle throat. A device for periodic variation of the throat section seriously complicates the engine.

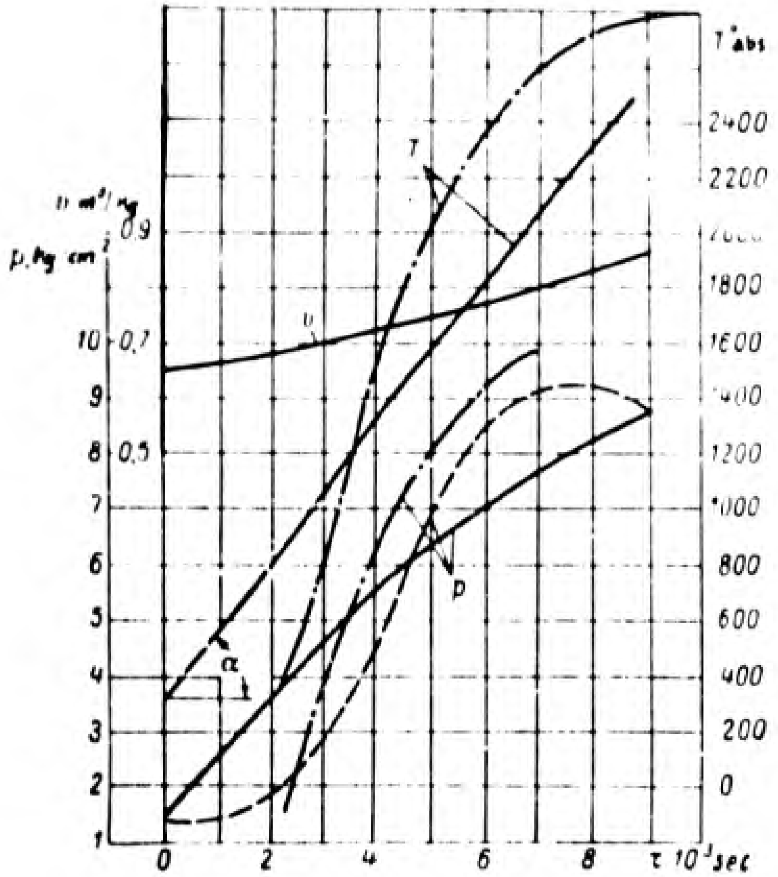

Fig.107 - Variation of Gas Parameters in Chamber with Time, for Various Laws of Heat Liberation (According to A.V.Kozyukov)

——— With linear law of heat liberation;
— · — With parabolic law of heat liberation;
— — — With sinusoidal law of heat liberation

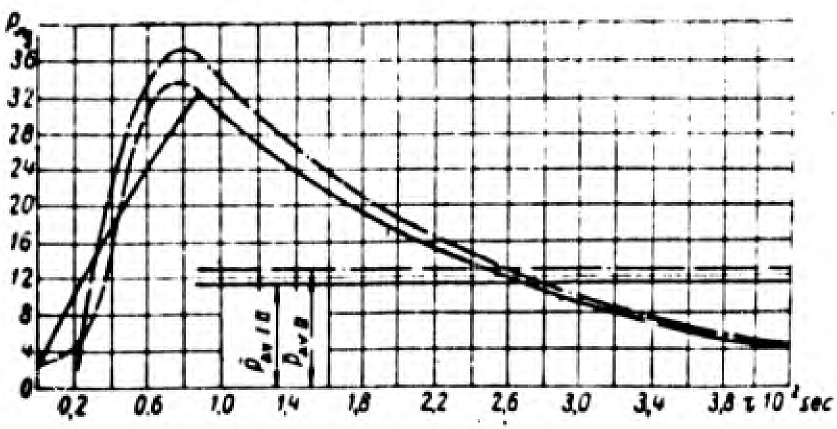

Fig.108 - Variation of Thrust with Time, for Various Laws of Heat Liberation in the Chamber (According to A.V.Kozyukov)

I ——— With rectangular law of heat liberation;
II — — — With sinusoidal law of heat liberation;
III — · — With parabolic law of heat liberation

Since the liberation of heat in chemical engines is accomplished in about 0.001 - 0.01 sec, one may assume that the creation of an economical pulsating rocket engine with open throat is entirely possible. In such an engine, exhaust also takes place during heat liberation.

The law of heat liberation, i.e., the relation between the quantity of heat liberated and the time, must be selected from experimental data. Various authors at various times have used the following laws of heat liberation in a chemical engine:

The linear law is

$$\frac{dQ}{d\tau} = \text{const.} \tag{140}$$

The parabolic law is

$$\frac{dQ}{d\tau} = \frac{2}{\tau_b}\left(1 - \frac{\tau}{\tau_b}\right), \tag{141}$$

where τ_b is the burning time of the propellant, established experimentally. In this form, the law was used by I.I.Bibe in studying the combustion of fuel in a compressorless Diesel engine ["Dizelestroyeniye", Nos.5 and 6 (1939)].

The sinusoidal law is

$$\frac{dQ}{d\tau} = \frac{Q}{\tau_r}\left[1 + \sin\left(4\frac{\tau}{\tau_b} - 1\right)\frac{\pi}{2}\right], \tag{142}$$

where τ_r is the heat value of the fuel at constant volume.

In the form (142), the law was used by Ye.S.Shchetinkov to study the combustion of fuel in a compressorless pulsejet engine. The exponential law

$$\frac{dQ}{d\tau} = \frac{2}{\tau_1}\left(\frac{\tau}{\tau_1}\right)^2 e^{-\frac{2}{3}\left(\frac{\tau}{\tau_1}\right)^3} Q, \tag{143}$$

derived from the fundamental relation of the chamber pressure and the reaction time of combustion, which was obtained at the Institute of Petroleum, can be expressed by

$$\frac{dp}{d\tau} = \frac{2}{\tau_1}\left(\frac{\tau}{\tau_1}\right)^2 e^{-\frac{2}{3}\left(\frac{\tau}{\tau_1}\right)^3} p'_{k\,max}, \tag{144}$$

where $p'_{k\,max}$ is the maximum pressure at the end of combustion;

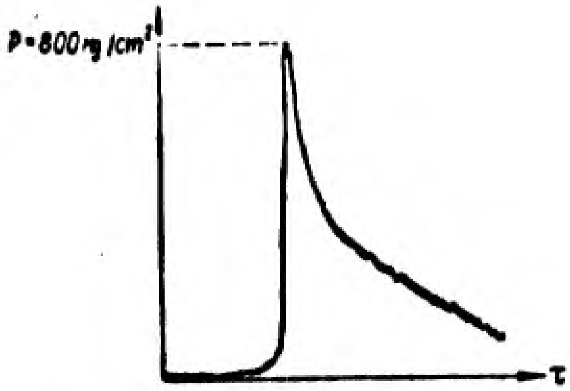

Fig.109 - Example of Indicator Card for a Model of a Rocket-Engine Chamber with V = c at High Initial Pressure

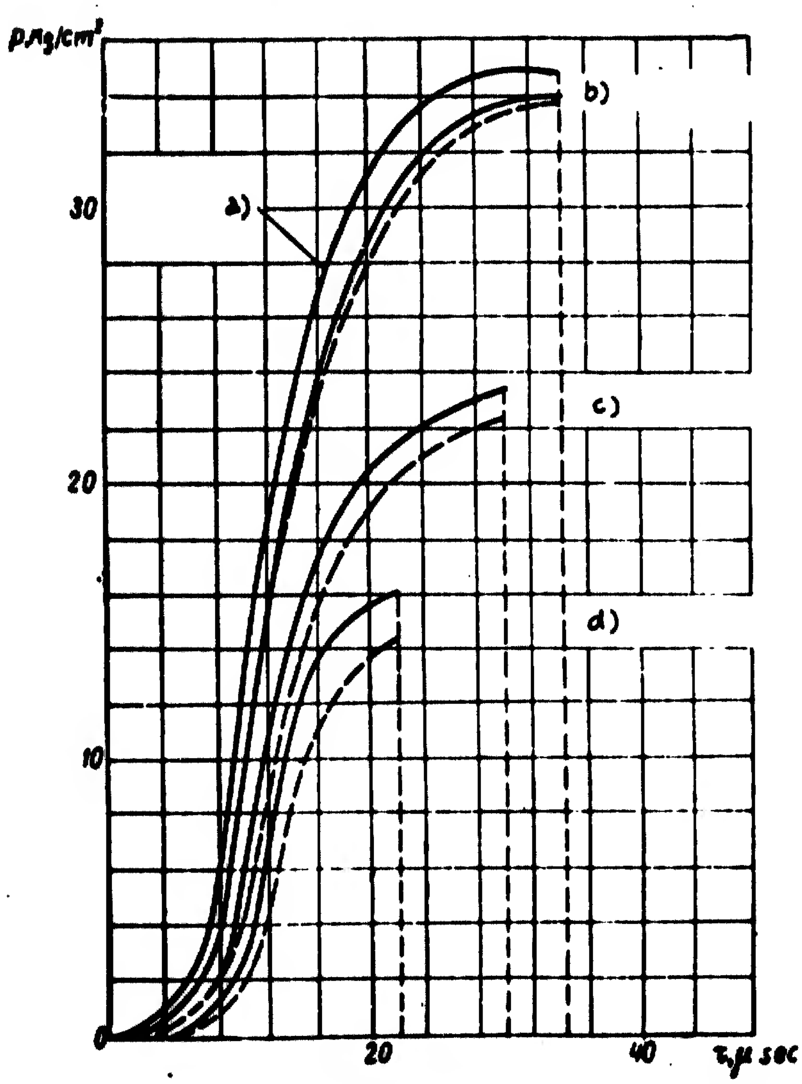

Fig.110 - Experimental and Theoretical Relations p = f (τ) for a Closed Chamber and a Chamber with a Nozzle

a) Closed chamber; b) Nozzle d_{cr} = 6 mm; c) Nozzle d_{cr} = 10 mm; d) Nozzle d_{cr} = 15 mm

τ_1 is the burning time to reach $(\frac{dp}{d\tau})_{max}$.

Figures 107 and 108 show the relations of the time rate of change of the gas parameters in the chamber with the thrust, for different laws of heat liberation.

Figure 109 is an example of the indicator card of a model of a rocket engine chamber with V = c at high initial pressure

$$(p_{\kappa\, max} \approx 800\, atm.abs).$$

For the sinusoidal law, B.A.Adamovich has established the following relation between pressure and time:

$$\frac{p_\kappa}{p'_{\kappa\, max}} = 0{,}5\left[\sin\left(\frac{2\tau - \tau_b}{2\tau_b}\pi\right) + 1\right] + \left(1 + \frac{\tau}{a}\right)^{-\frac{2k}{k+1}} - 1. \tag{145}$$

For the exponential law he also found

$$\frac{p_\kappa}{p'_{\kappa\, max}} = \left(1 + \frac{\tau}{a}\right)^{-\frac{2k}{k-1}} - e^{-\frac{2}{3}\left(\frac{\tau}{\tau_1}\right)^3}. \tag{146}$$

In eqs.(145) and (146), we have

$$a = \left(\frac{2}{k+1}\right)^{-\frac{3-k}{2(\kappa-1)}} \cdot \frac{V}{\mu F_{cr}\sqrt{kgRT_{\kappa\, max}}}. \tag{147}$$

Figure 110 shows that the experiment confirms the validity of eq.(146). The drawback of this equation, which is the necessity of finding the values of τ_1 and $p_{k\ max}$ experimentally, is partly compensated by the simple shape of the rocket-engine chamber and by the ease with which the experiments can be run in a closed bomb. If the propellant components are well known, then $p_{k\ max}$ may also be found with sufficient accuracy by calculation.

CHAPTER IV

THEORY OF IDEAL ROCKET ENGINE WITH COMPLEX CYCLES

Section 14. Thermodynamic Cycle of a Rocket Engine with Polytropic Chamber

In the last Chapter we assumed that the gas velocity in the chamber was negligibly small, i.e., that its cross-sectional dimensions were great. In practice, such an assumption is true whenever the ratio of the diameter of the chamber to the diameter of the nozzle throat is $\frac{D_k}{D_{cr}} > 4$.

With decreasing transverse chamber dimensions and increasing flow rate per second, the heat liberation in the chamber begins to be accompanied by expansion and a marked increase in gas velocity, even before the gas reaches the nozzle. We shall apply the term velocity chambers to chambers in which heat transfer is accompanied by gas expansion.

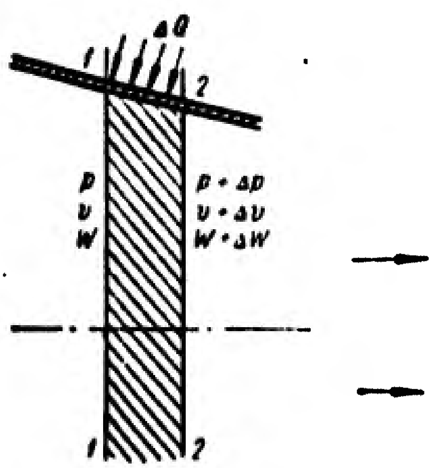

Fig.111 - Schematic Diagram of Motion of Elementary Gas Volume in a Velocity Chamber

In engines with velocity chambers, the differences between the processes in the chamber and the nozzle are slight. On transfer of heat to the gas in the nozzle duct, this difference disappears entirely.

Setting up an energy balance for the mass of gas between sections 1-1 and 2-2 of the chamber which are infinitely close together (Fig.111), we may write

$$dQ = dU + (p + dp)(v + dv) - pv + d\frac{W^2}{2g}$$

or, after canceling,

$$d\frac{W^2}{2g} = dQ - C_p dT.$$

Let us consider the energetic transformations in an engine with a velocity chamber, assuming the change of state of the gas to be polytropic, and disregarding, for the time being, the question of the necessary change in cross sections.

Let the process in the chamber proceed in such a manner that, in each section, a certain constant portion of the heat transferred is converted into kinetic energy, i.e.,

$$d\frac{W^2}{2g} = \alpha_1 dQ,$$

where α_1 is a constant less than unity.

Then,

$$\alpha_1 dQ = dQ - C_p dT$$

and

$$C_p dT = (1 - \alpha_1)\, dQ. \tag{148}$$

On the other hand, making use of the second form of the first law of thermodynamics, we get

$$dQ = C_p dT - v dp. \tag{149}$$

Dividing eq.(149) by eq.(148), we obtain

$$\frac{1}{1-\alpha_1} = 1 - \frac{v dp}{C_p dT} = 1 - \frac{R}{C_p}\frac{v dp}{p\, dv + v\, dp} = 1 - \frac{k-1}{k}\frac{1}{\frac{p dv}{v dp} + 1}.$$

After minor transformations, we derive the equation of expansion in the chamber, in the coordinates p - v:

$$-\frac{dp}{p} = \frac{\alpha_1 k}{k - 1 + \alpha_1}\frac{dv}{v}.$$

Denoting the polytropic exponent of expansion by the letter n, i.e., taking

$$n = \frac{\alpha_1 k}{k - 1 + \alpha_1}, \tag{150}$$

we get

$$pv^{k\frac{a_1 k}{1+a_1}} = pv^n = \text{const.}$$

Let us determine the quantity of heat liberated in the chamber. At a polytropic change of state, we have

$$Q_n = C_n T_\kappa = C_v \frac{n-k}{n-1} T_\kappa.$$

Substituting in this equation the value of the index n from eq.(150), we find

$$Q_n = \frac{kR}{(k-1)(1-a_1)} T_\kappa, \qquad (151)$$

where T_k is the true temperature of the gas at the end of the chamber ahead of the nozzle.

Let us determine the kinetic energy of the gas upstream of the nozzle from the equation

$$L_n = \frac{W_\kappa^2}{2g} = a_1 Q_n = \frac{ka_1}{(k-1)(1-a_1)} RT_\kappa. \qquad (152)$$

Figure 112 shows the cycles of the engine under the condition that the state of the gas at the end of the chamber, ahead of the nozzle, shall be the same.

The specific work of the gas is

$$L = L_n + L_{ad \cdot c}.$$

Substituting L_n and $L_{ad\ c}$ by their values from eqs.(152) and (21), we get

$$L = \frac{k}{k-1} RT_\kappa \left(\frac{1}{(1-a_1)} - \frac{1}{\delta_c^a} \right). \qquad (153)$$

The thermal efficiency is determined in the conventional manner

$$\eta_t = \frac{L}{Q}$$

and, finally,

$$\eta_t = 1 - \frac{1-a_1}{\delta_c^a}. \qquad (154)$$

Thus, the cycles of engines with a velocity chamber are more advantageous than the normal cycle p = const, if the state of the gas ahead of the nozzle is the same.

We must direct attention to the fact that, in a velocity chamber, the pressure increases with approach to the mouth.

In the ideal cycle under consideration, the pressure is infinitely high. If we

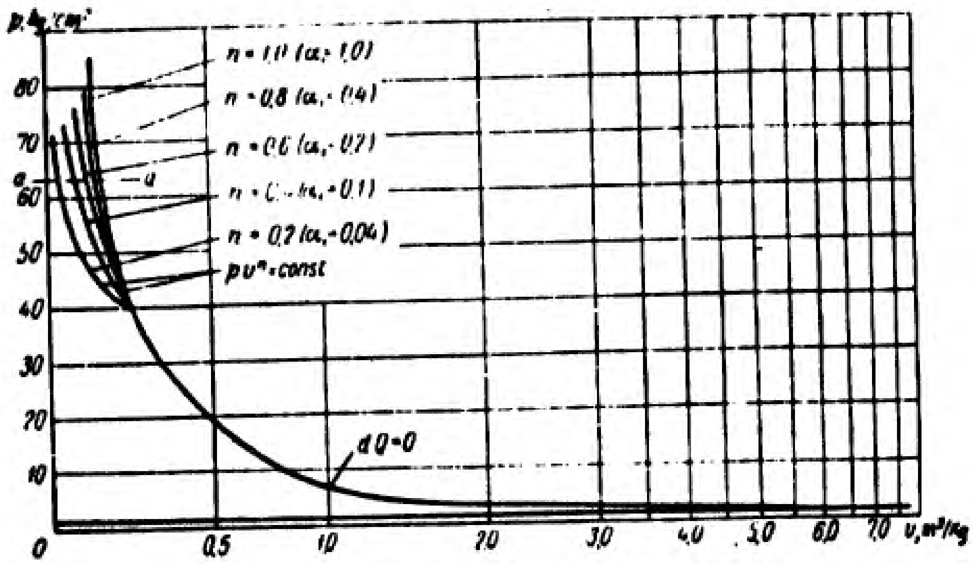

Fig.112 - pv-Diagrams of Cycles of an Engine with Velocity Chamber, at the same State of Gas ahead of the Nozzle (k = 1.2)

confine the maximum pressure by some limit (Fig.112, line a-a), then the chamber becomes a compound chamber which will be more advantageous than a constant-pressure chamber with a pressure equal to that ahead of the nozzle in the compound chamber. However, this chamber will be less advantageous than a chamber at p_k = const, if p_k is the maximum pressure in the compound chamber. The pv-diagrams of the compound chamber and the chamber of p = const for the same maximum pressure, temperature, and expansion ratio are shown in Fig.113.

To compare the cycles, it is necessary to preset the pressure or the temperature T_k at the beginning of expansion in the chamber. At constant pressure p_{k1}, let the temperature rise to T_{k1}, so that

$$T_{k1} = \beta_1 T_k,$$

where $\beta_1 < 1.0$.

Then the expansion ratio in the chamber will be determined from the formula

$$\frac{p_k}{p_{k1}} = \left(\frac{T_k}{T_{k1}}\right)^{\frac{n}{n-1}} = \left(\frac{1}{\beta_1}\right)^{\frac{\alpha_1 k}{(k-1)(\alpha_1-1)}} = \beta_1^{\frac{\alpha_1 k}{(k-1)(1-\alpha_1)}}.$$

The heat expended is communicated partly at constant pressure and partly during the time of polytropic expansion. At constant pressure, the temperature rises to $T_{k1} = \beta_1 T_k$; consequently,

$$Q_p = \frac{k}{k-1}\beta_1 R T_k.$$

Bearing in mind that according to eq.(151), in polytropic expansion, the heat

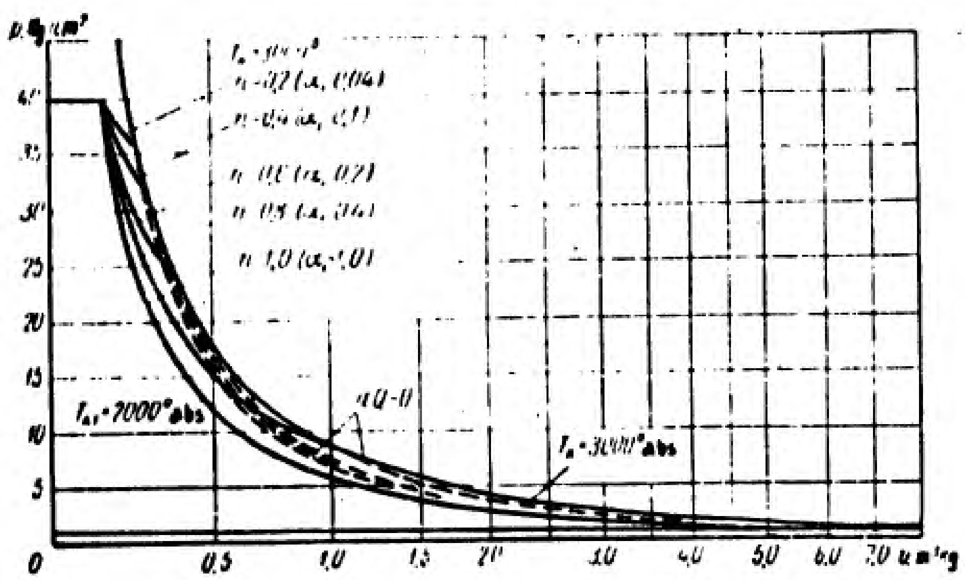

Fig.113 - pv-Diagrams of Cycles for an Engine with Polytropic Velocity Chamber, at the same Maximum Pressure and Temperature (k = 1.2)

transfer begins as soon as the temperature of the gas reaches $\beta_1 T_k$, the consumption of heat is determined from the formula

$$Q_n = \frac{k(1-\beta_1)}{(k-1)(1-\alpha_1)} R T_k.$$

The total heat consumption is equal to the sum of Q_p and Q_n:

$$Q = \frac{k}{k-1} R T_k\left(\beta_1 + \frac{1-\beta_1}{1-\alpha_1}\right) = \frac{1-\beta_1\alpha_1}{1-\alpha_1}\cdot\frac{k}{k-1} R T_k. \qquad (155)$$

It is easy to see that this quantity of heat is greater than what must be supplied to the constant-pressure chamber in order to obtain the same temperature.

The specific work may likewise be represented as consisting of two parts. The work of expansion in the chamber is converted into kinetic energy of the gas. This work is equal to

$$L=\frac{n}{n-1}RT_{\kappa 1}\left(1-\frac{T_{\kappa}}{T_{\kappa 1}}\right)=\frac{nR}{n-1}\beta_1 T_{\kappa}\left(1-\frac{1}{\beta_1}\right)$$

or

$$L_n=\frac{a_1 k(1-\beta_1)}{(k-1)(1-a_1)}RT_{\kappa}.$$

In the nozzle duct, the work done is

$$L_{ad\cdot c}=\frac{k}{k-1}RT_{\kappa}\left(1-\frac{1}{\delta_c^a}\right)=\frac{k}{k-1}RT_{\kappa}\left(1-\frac{1}{\delta^a}\cdot\frac{1}{\beta_1^{\frac{a_1}{1-a_1}}}\right),$$

where $\delta_{ex}=\frac{p_k}{p_{ex}}$.

Adding L_n and $L_{ad\ c}$, we obtain the value of the specific work

$$L=\frac{k}{k-1}RT_{\kappa}\left(\frac{1-a_1\beta_1}{1-a_1}-\frac{1}{\delta_{ex}^a}\cdot\frac{1}{\beta_1^{\frac{a_1}{1-a_1}}}\right). \tag{156}$$

Dividing eq.(156) by eq.(155), we find the efficiency of the cycle

$$\eta_t=\frac{L}{Q}=1-\frac{1}{\delta_{ex}^a}\cdot\frac{1-a_1}{(1-\beta_1 a_1)\beta_1^{\frac{a_1}{1-a_1}}}. \tag{157}$$

Figure 114 shows the change in the value of the specific work L, the thermal efficiency η_t, and the velocity ratio in the chamber upstream of the nozzle, W_c to the exit velocity W_a at $\delta_{ex}=40$; $k=1.2$; and $\beta_1=0.666$.

As a_1 increases, the specific work and rate of acceleration of the gas in the chamber increase, while the efficiency decreases. At a certain magnitude of a_1, the value of L reaches a maximum. The equation $\frac{dL}{da_1}=0$, derived on the basis of eq.(156), makes it possible to determine the value of a_1 necessary to obtain L_{max}. This equation has the form

$$a_1 = \frac{\lg\left[\frac{\ln \beta_1}{\delta^{a}_{ex}(\beta_1 - 1)}\right]}{\lg\left[\frac{\ln \beta_1}{\delta^{a}_{ex}(\beta_1 - 1)}\right] + \lg \beta_1}. \qquad (158)$$

The maximum L_{max} occurs at $a_1 \approx 0.507$ (Fig.114). The work increases 12% by comparison with the adiabatic version of the engine p = const and the thrust is

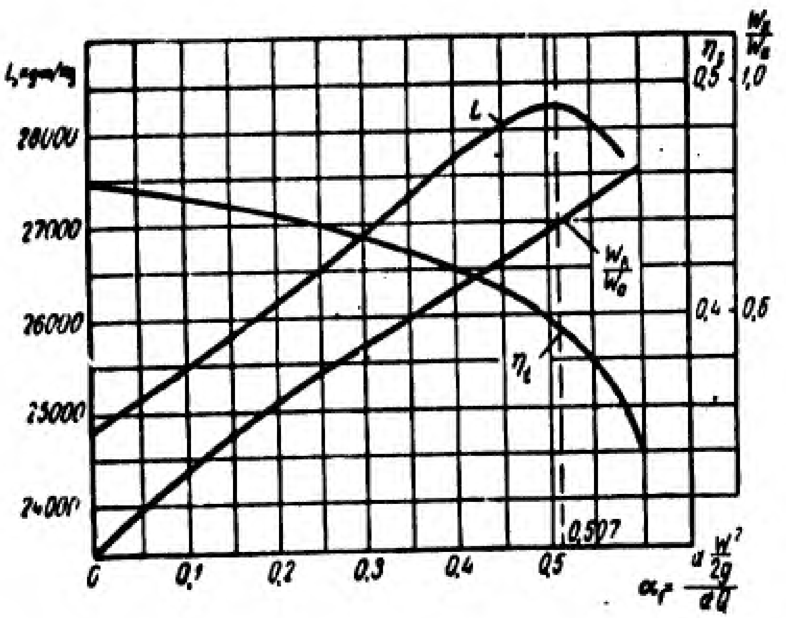

Fig.114 - Example of Variation of Specific Work and Thermal Efficiency of an Engine with a Polytropic Velocity Chamber, as a Function of the Coefficient of Heat Distribution in the Chamber, a_1 ($\delta_{ex\ o} = 40$; $\varkappa = 1.2$; $T_{k1} = 0.666\ T_{k\ max}$)

augmented by 6%, while the thermal efficiency decreases by 14%. Consequently, in a velocity chamber, the specific work may be somewhat greater than in a constant-pressure chamber.

Naturally, the profile of the chamber, viewed along the flow, is strictly determinate for each case of polytropic expansion.

Section 15. The Rocket Engine with Athodyd

Velocity chambers, in which the heat is not liberated at constant pressure, are used for various reasons. Thus, at the same heat consumption and the same available expansion, such a velocity chamber is smaller in volume and lighter in weight than the conventional chamber.

In some cases, a gradual feed of the propellant along the length of the chamber is unavoidable. For example, a chamber with its entire inner surface utilized for heat transfer is a heat-consuming duct. Such a system of propellant feed protects the walls of the chamber from overheating.

To obtain good mixture formation, as well as complete and stable combustion of the propellant under the operating conditions of the engine, a flat forward section can be used; fuel injectors are arranged not only over this section, so as to ensure introduction of all the propellant into a single section of the chamber, but also over the chamber walls and on feeder elements inside the chamber.

On increase of the consumption stress $g = \frac{G}{F_k}$, in a conventional chamber with a flat forward section, the gas velocity increases, and the process of transformation of the main portion of the liquid propellant into combustion products begins to cover an ever greater part of the chamber volume. This fact may lead to the appearance of heat-consuming chambers with the usual disposition of injectors over the flat forward section.

The rate of heat liberation per unit chamber surface may be determined by the ratio of the amount of heat liberated to the surface available for propellant feed. In a cylindrical chamber with a flat forward section, occupied by fuel injectors, the heat liberation per unit volume of combustion space q_f equals

$$q_f = \frac{Q_1}{F_\kappa} = \frac{k}{k-1} \frac{RT_\kappa}{f_\kappa}. \tag{159}$$

If the ratio of the chamber cross sections to the throat cross section of the nozzle is c_k, then

$$q_f = \frac{k}{k-1} \cdot \frac{RT_\kappa}{c_\kappa f_{\kappa p}}.$$

However,

$$f_{cr}=\frac{1}{W_{cr}\gamma_{cr}}=\frac{1}{a_k\gamma_k}\left(\frac{k+1}{2}\right)^{\frac{1}{k-1}}\sqrt{\frac{k+1}{2}}=\frac{1}{a_k\gamma_k}\sqrt{\left(\frac{k+1}{2}\right)^{\frac{k+1}{k-1}}},$$

where a_k is the velocity of sound in the chamber.

Consequently, the heat liberation per unit volume in the chamber will be

$$q_f=\frac{k}{k-1}\sqrt{\left(\frac{2}{k+1}\right)^{\frac{k+1}{k-1}}}\cdot\frac{a_k p_k}{c_k}=$$

$$=\frac{k}{k-1}\sqrt{kgR\left(\frac{2}{k+1}\right)^{\frac{k+1}{k-1}}}\;\frac{p_k\sqrt{T_k}}{c_k}. \qquad (160)$$

Thus the heat liberation per unit volume is directly proportional to the pressure and the velocity of sound in the chamber, and inversely proportional to the ratio of the cross sections $\frac{f_k}{f_{cr}}=c_k$. In addition, q_f depends on the value of k and decreases with increasing k. In modern liquid rocket engine chambers, we have

$$q_f=(6-14)\cdot 10^5\ \text{kcal}/\text{m}^3\text{sec}.$$

When q_f is twice these values, or even greater, the chemical cylindrical chamber begins to be converted into a velocity chamber.

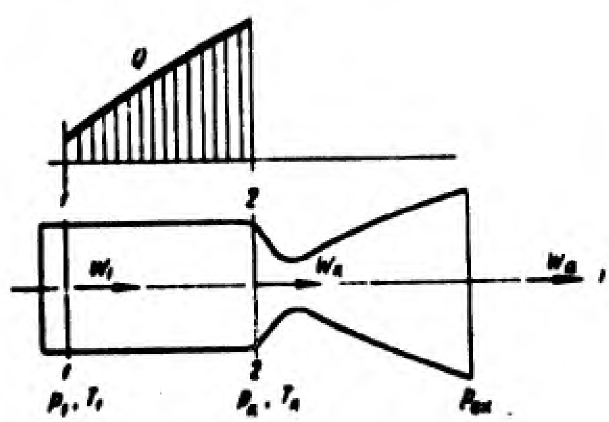

Fig.115 - Cylindrical Chamber with Gradual Transfer of Part of the Heat

In certain versions of gas-nuclear engines, the heat will gradually be transferred to the working fluid. This is also unavoidable in engines with a reactor, in which the heat is supplied to a gas from the heated surfaces. It is possible that, in order to absorb the heat of thermonuclear reactions, the working fluid will have to be supplied over the entire surface of the chamber walls to protect the latter from the high temperature.

Let us first consider the version of a thermal chamber in which a constant quantity of gas flows through all the sections.

The heat is liberated in the section 1-2 (Fig.115).

Up to the section 1-1, the heat is liberated in the same manner as in the conventional chamber at p = const. The heat consumed up to this section is equal to Q_1; the gas parameters in this section are characterized by the quantities p_1, v_1, T_1, and W_1. The gas is accelerated in section 1-2 to subsonic velocity if the duct is cylindrical, and to any desired velocity if the duct is of variable cross section.

To evaluate the process in the athodyd, for each instant of residence of the gas in the chamber, the quantities Q, W, p, v, T, f must be defined. The relation between the latter is established on the basis of the general laws of thermodynamics and gas dynamics. Let us write these down.

Equation of state:

$$pv = RT.$$

Equation of constant rate of flow:

$$fW\gamma = \frac{fWp}{RT} = \text{const}.$$

Equation of variation of momentum:

$$fdp = -\frac{dW}{g}.$$

Equation of conservation of energy:

$$dQ = \frac{k}{k-1} RdT + \frac{W}{g} dW.$$

We shall make use of these equations in the dimensionless form.

In the initial section of the athodyd, the values of p_1, v_1, T_1, W_1 and f_1 are known. Let

$$\bar{f} = \frac{f}{f_1};\quad \bar{p} = \frac{p}{p_1};\quad \bar{T} = \frac{T}{T_1};\quad \bar{W} = \frac{W}{W_1};\quad \bar{v} = \frac{v}{v_1};$$

$$d\bar{Q} = \frac{dQ}{\frac{k}{k-1} RT_1}.$$

Then, the third equation takes the form

$$f_1 p_1 \bar{f} d\bar{p} = -W_1 \frac{d\bar{W}}{g},$$

or

$$\bar{f} d\bar{p} = -\frac{W_1}{f_1 p_1}\frac{d\bar{W}}{g} = -\frac{W_1 W_1}{RT_1 g} d\bar{W} = -kM_1^2 d\bar{W}.$$

Suitable transformations of the equation of energy will yield

$$d\bar{Q} = d\bar{T} + (k-1) M_1^2 \bar{W} d\bar{W}.$$

The final system of equations takes the following form:

$$\begin{gathered} \bar{p}\bar{v} = \bar{T}; \\ \bar{f}\bar{W}\bar{p} = \bar{T}; \\ \bar{f} d\bar{p} = -kM_1^2 d\bar{W}; \\ d\bar{Q} = d\bar{T} + (k-1) M_1^2 \bar{W} d\bar{W} \end{gathered} \qquad (161)$$

or

$$\bar{Q} = \bar{T} - 1 + \frac{k-1}{2} M_1^2 (\bar{W}^2 - 1) = \bar{T} - \bar{T}_1^* + \frac{k-1}{2} M_1^2 \bar{W}^2.$$

If one of the six variables, for instance Q, is taken as the independent variable, then in order to obtain the relations between the remaining variables and the independent variable, one more relation must be added to the four equations given above.

In special cases the equations are simplified.

Let us consider the possible basic versions, taking one of the dependent variables ($\bar{p}$, $\bar{v}$, $\bar{T}$, $\bar{W}$, $\bar{f}$) as constant.

1. The Cylindrical Chamber

By hypothesis, $\bar{f} = 1.0$. Consequently, the actual system of equations is

$$\left.\begin{aligned} &\bar{p}\bar{v} = \bar{T} \\ &\bar{W}\bar{p} = \bar{T} \\ &d\bar{p} = -kM_1^2 d\bar{W} \\ &Q = \bar{T} - \bar{T}_1^* + \frac{k-1}{2} M_1^2 \bar{W}^2 \end{aligned}\right| \bar{f} = 1{,}0. \qquad (162)$$

From the third equation, we determine the relation between the pressure and the gas velocity:

$$\bar{p} = 1 - kM_1^2(\overline{W} - 1). \quad (163)$$

From the first and second equations, we derive the following equality:

$$\bar{v} = \overline{W}. \quad (164)$$

Comparing these expressions, we obtain the equation of change of state, which, when plotted in p - v coordinates, is represented by a straight line:

$$\bar{p} = 1 - kM_1^2(\bar{v} - 1). \quad (165)$$

If, making use of the equation $\overline{W}\,\bar{p} = \overline{T}$, we first eliminate $\bar{p}$ from eq.(163) and then $\overline{W}$, we shall obtain an expression correlating the temperature with the gas pressure and velocity:

$$\overline{T} = (1 + kM_1^2)\overline{W} - kM_1^2\overline{W}^2; \quad (166)$$

$$\overline{T} = \frac{(1 + kM_1^2)\bar{p}}{kM_1^2} - \frac{\bar{p}^2}{kM_1^2}. \quad (167)$$

By eliminating the energy $\overline{T}$ from this expression by the aid of eq.(166), we establish the relation between the gas velocity and the quantity of heat transferred:

$$\overline{Q} = (1 + kM_1^2)\overline{W} - \frac{k+1}{2}M_1^2\overline{W}^2 - \overline{T}_1^*, \quad (168)$$

where

$$\overline{T}_1^* = 1 + \frac{k-1}{2}M_1^2.$$

Equations (163), (164), (165), (166), (167), and (168) fully characterize the process taking place in a cylindrical thermal chamber. The final velocity in such a chamber may reach a maximum value equal to the speed of sound in this section. Let us determine the relation between the gas velocity and the Mach number in an arbitrary cross section of the duct. Obviously,

$$\overline{W}^2 = \frac{W^2}{W_1^2} = \frac{W^2 T_1 T}{T W_1^2 T_1} = \frac{M^2}{M_1^2}\overline{T}. \quad (169)$$

For the throat section, where $M = 1$, we get,

$$\overline{W}^2_{cr} = \frac{\overline{T}_{cr}}{M_1^2}. \qquad (170)$$

Eliminating $\overline{T}_{cr}$ by the aid of eq.(166), we derive the following expression for the maximum velocity obtainable in the thermal chamber:

$$\overline{W}_{cr} = \frac{1 + kM_1^2}{(1 + k)\,M_1^2}. \qquad (171)$$

The initial data necessary to solve the question of the thrust and the economy of an engine with a thermal chamber may be of various kinds. It is possible to specify parameters in the first and second sections, if temperature restrictions are compulsory. Let us consider one of the versions of the problem and its solution.

Given the total expansion $\delta_{ex\ o}$ and the gas parameters in the initial part of the athodyd, i.e., p_1, T_1, W_1. In addition, we must establish, for the final section, either the pressure and temperature or the Mach number. If there are no temperature restrictions, the value of the heat Q to be transferred should be specified.

Given the pressure p_k. Then, eq.(163) will yield the terminal velocity W_k and the specific volume v_k. Comparing the resultant velocity with the critical velocity determined by eq.(171), we can demonstrate that $\overline{W}_k \leq \overline{W}_{cr}$. Now we find the temperature $\overline{T}_k$, and then, from eq.(168), the heat transferred to the section 1-2.

The total heat consumption is

$$Q_1 = Q_k + Q_1$$

or

$$\overline{Q}_1 = \overline{Q}'_k + 1.$$

The work done is

$$L = \frac{W_k^2}{2g} + L_{ad} = \frac{W_k^2}{2g} + \frac{k}{k-1}RT_k\left(1 - \frac{1}{\delta_c^{a}}\right) = \frac{W_c^2}{2g}.$$

Dividing both sides of this equation by $\frac{k}{k-1}RT_1$, after minor transformations, we get

$$\frac{L}{\frac{k}{k-1}RT_1} = \overline{L} = \frac{k-1}{2}M_1^2\overline{W}_\kappa^2 + \overline{T}_\kappa\left(1-\frac{1}{\delta_c^a}\right). \qquad (172)$$

We determine the thermal efficiency by the usual formula

$$\eta_t = \frac{L}{Q_1} = \frac{\overline{L}}{\overline{Q}_1}.$$

The specific thrust is

$$P_{sp} = \frac{W_a}{g} = \frac{\sqrt{W_\kappa^2 \cdot 2g\frac{k}{k-1}RT_\kappa\left(1-\frac{1}{\delta_c^a}\right)}}{g}.$$

Since, at $\delta_c = \infty$, we have

$$P_{sp \cdot max} = \frac{\sqrt{2gL_{max}}}{g} = \frac{\sqrt{2gQ_1}}{g}$$

and

$$P_{sp} = \frac{\sqrt{2gL}}{g},$$

the force factor for rated operating conditions is

$$\psi_c = \sqrt{\eta_t}.$$

If the chamber has no throat, then the velocity ahead of the geometric nozzle is determined by eq.(171). In this case, all the parameters are functions of the initial Mach number M_1. Thus, substituting the value of $\overline{W}_{cr}$ in eq.(168), we get

$$\overline{Q}_{cr} = \frac{(1+kM_1^2)^2}{2(1+k)M_1^2} - \left(1+\frac{k-1}{2}M_1^2\right).$$

Comparing eqs.(163) and (171), we now derive the following equation for the critical pressure:

$$\overline{p}_{cr} = \frac{1+kM_1^2}{k+1}; \qquad (173)$$

We determine the temperature from eq.(170) by substituting $\overline{W}_{cr}$ with its value from eq.(171):

$$\overline{T}_{cr} = \frac{(1+kM_1^2)^2}{(1+k)^2M_1^2}.$$

Figure 116 shows the relation between the critical temperature T_{cr} and the velocity W_1 in the initial cross section of the chamber, for the case where $T_1 =$ = 100, 300, and 600°K and k = 1.2.

Let us consider an example. Given the values: T_1 = 300°K, W_1 = 30 m/sec,

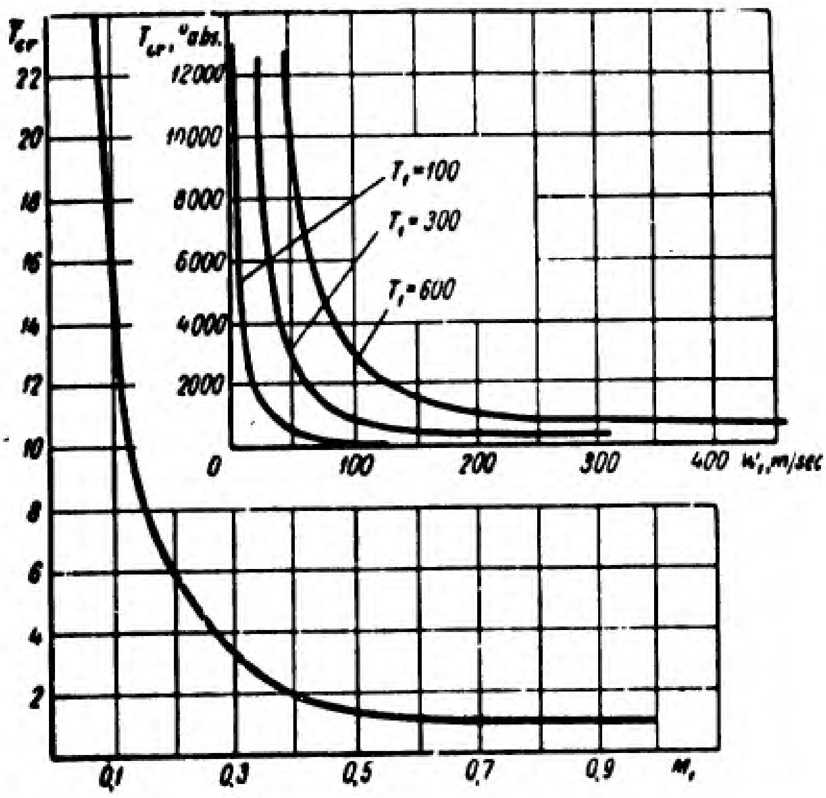

Fig.116 - Relation between the Relative Critical Temperature $\overline{T}_{cr}$ and the Mach Number M_1 for a Cylindrical Polytropic Chamber

p_1 = 80 kg/cm^2, k = 1.2, R = 30, and the stagnation temperature at the end of the chamber, $T_c^* = 3800$°K.

For the specified conditions, M_1 = 0.0922; the quantity of heat transferred up to the boost phase is

$$Q_1 = \frac{k}{k-1} RT_1^* = \frac{1,2}{1,2-1} \cdot 30 \cdot 300 = 54\,000 \ Kg{\cdot}m/Kg;$$

In the athodyd,

$$Q_k = \frac{k}{k-1} R\,(\overline{T}_k^* - \overline{T}_1^*) = \frac{1,2}{1,2-1} \cdot 30\,(3800-300) = 630\,000 \ Kg{\cdot}m/Kg.$$

The gas velocity at the end of the chamber may be determined from eq.(168):

$$\overline{W}^2 - \frac{2(1+kM_1^2)}{(k+1)M_1^2}\overline{W} + \frac{2(\overline{Q}+\overline{T}_1^*)}{(k+1)M_1^2} = 0;$$

$$\overline{W} = \frac{1+1{,}2\cdot 0{,}0922^2}{(1{,}2+1)\cdot 0{,}0922^2} \pm \sqrt{\left(\frac{1+1{,}2\cdot 0{,}0922^2}{(1{,}2+1)\cdot 0{,}0922^2}\right)^2 - \frac{2\left(\frac{630\,000}{54\,000}+1\right)}{(1{,}2+1)\cdot 0{,}0922^2}}.$$

The solution of this last equation gives two values of the velocity:

$$\overline{W}' = 14{,}3 \text{ and } \overline{W}'' \quad 94{,}1.$$

For the chamber, if the sign of the supply of heat did not change, we should take $\overline{W} = \overline{W} = 14.3$. Then,

$$W_\kappa = \overline{W}W_1 = 14{,}3\cdot 30 = 429{,}0 \ m/sec.$$

We determine the temperature at the end of the chamber from eq.(166):

$$\overline{T}_\kappa = (1+kM_1^2)\,\overline{W} - kM_1^2\overline{W}^2 = 12{,}385;$$

$$T_\kappa = \overline{T}_\kappa T_1 = 12{,}385\cdot 300 \approx 3720^\circ \text{ abs}.$$

The temperature at the end of the chamber is then calculated on the basis of eq.(163):

$$\overline{p} = 1 - kM_1^2(\overline{W} - 1) = 0{,}8642; \ p_\kappa = \overline{p}p_1 = 69 \ kg/cm^2.$$

The Mach number M_K at the end of the chamber is

$$M_\kappa = \frac{W_\kappa}{\sqrt{kgRT_\kappa}} = 0{,}375.$$

In this example, we obtained a chamber with a throat; to reach the velocity of sound in the chamber, a geometric nozzle is installed with the following cross-sectional ratio:

$$\frac{f_\kappa}{f_{cr}} = \frac{\left(1+\frac{k-1}{2}M_\kappa^2\right)^{\frac{k+1}{2(k-1)}}}{M_\kappa\left(\frac{k+1}{2}\right)^{\frac{k+1}{2(k-1)}}} = 1{,}7.$$

To obtain a chamber without a throat, we must change the gas parameters in the section 1-1. In this case, $T_k^* = T_{cr}^*$, and

$$T_{cr} = T_{cr}^* \cdot \frac{2}{k+1} = 3800 \cdot \frac{2}{1,2+1} = 3450^\circ \text{ abs}.$$

From the graph (Fig.116), we determine the velocity that must be reached in the section 1-1 to obtain a temperature of $T_{cr} = 3450^\circ K$ at the end of the chamber:

$$W_1 = 41,5 \text{ m/sec}.$$

Figures 117, 118, and 119 give the p-v, p-f, and T-S diagrams of the cycles of a polytropic chamber. For comparison, the graph of the cycle of a chamber at p = const has been plotted in the same diagram.

In Fig.117, the expansion adiabatics of the cycles are so close together that they are covered by the thickness of a single line.

In eqs.(162), (163), (164), (166), and (168), determining the gas parameters at the end of the chamber and the quantity of heat consumed, the Mach number may be introduced instead of the variable $\bar{W}$.

Then, dividing both sides of the second equation in the system (162) by $\sqrt{\bar{T}}$, we get

$$\frac{M}{M_1} \bar{p} \sqrt{\bar{T}},$$

whence

$$\bar{T} = \bar{p}^2 \frac{M^2}{M_1^2} = \bar{p}^2 M^2. \qquad (174)$$

From eq.(163) it is easy to find

$$\bar{p} = \frac{1 + kM_1^2}{1 + kM^2}. \qquad (175)$$

Combining eqs.(174) and (175) we get, instead of eq.(166),

$$\bar{T} = \left(\frac{M}{M_1}\right)^2 \left(\frac{1 + kM_1^2}{1 + kM^2}\right)^2. \qquad (176)$$

We find the specific volume from the equation of state:

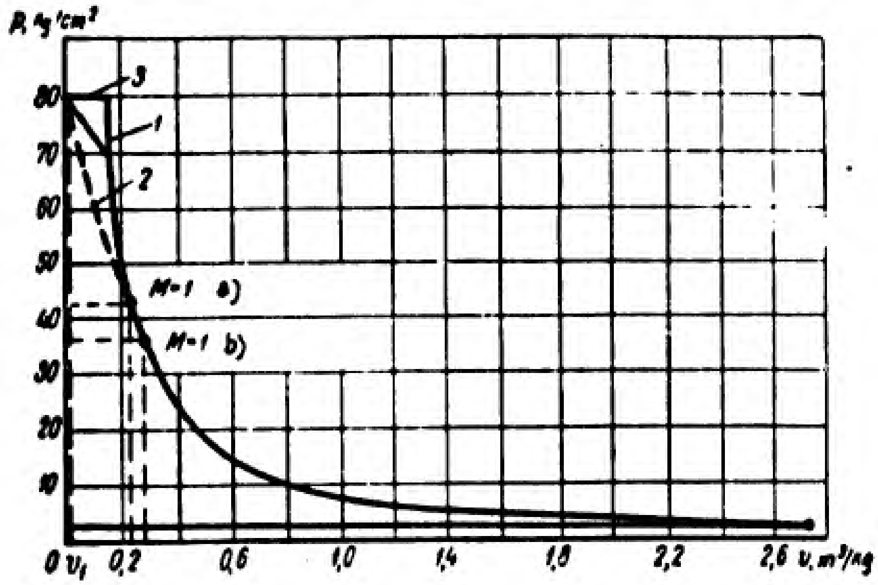

Fig.117 - p-v Diagram of Cycles of an Engine with Cylindrical Velocity Chamber at $T_k^* = 3800°K$

1 - $M_k = 0.375$; 2 - $M_k = 1.0$; 3 - p_k = const

a) M = 1 (First case); b) M = 1 (second case)

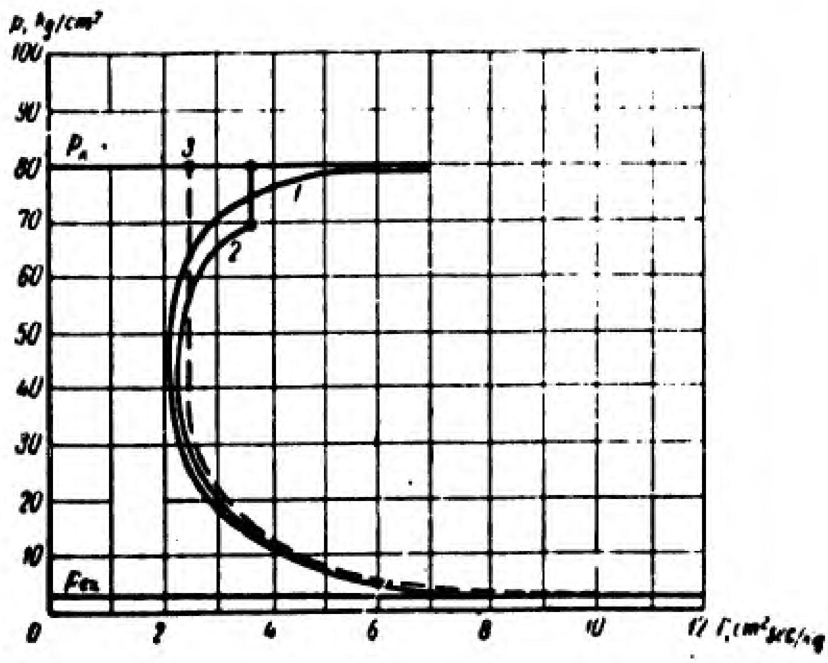

Fig.118 - p-f Diagram of Cycles of an Engine with Cylindrical Velocity Chamber

1 - p = const; 2 - $M_k = 0.375$; 3 - $M_k = 1$

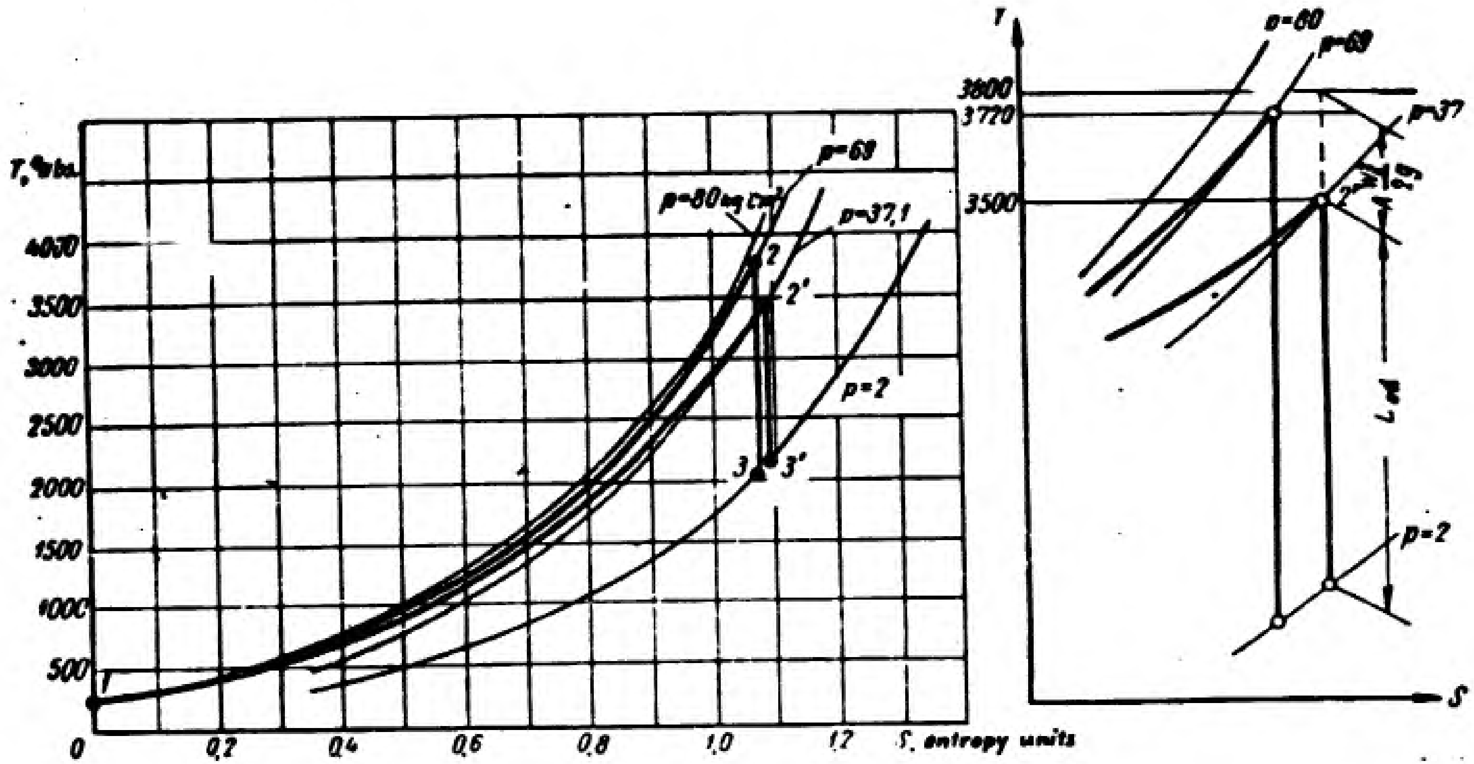

Fig.119 - T-S Diagram of Cycles of an Engine with Cylindrical Velocity Chamber

Curves 1-2-3 correspond to $M_k = 0.375$; Curves 1'-2'-3' correspond to $M_k = 1.0$

$$\bar{v}=\bar{W}=\frac{\bar{T}}{\bar{p}}=\frac{M}{M_1}\frac{(1+kM_1^2)}{(1+kM^2)}. \tag{177}$$

Finally, substituting the value of $\bar{W}$ from eq.(177) in eq.(168), will yield

$$\bar{Q}=\bar{T}^*-\bar{T}_1^*=\frac{(1+kM_1^2)^2}{2(1+k)M_1^2}-\left(1+\frac{k-1}{2}M_1^2\right). \tag{178}$$

Equations (174), (175), (176), (177), and (178) may also be used to determine the parameters of the cycle of a thermal chamber of constant cross section.

2. Isothermal Heat Chamber

Bearing in mind that $\bar{T}=1.0$, in the isothermal chamber, let us set up the system of fundamental equations:

$$\left.\begin{array}{l}\bar{p}\bar{v}=1{,}0\\ \bar{f}\bar{W}\bar{p}=1{,}0\\ \bar{f}d\bar{p}=-kM_1^2d\bar{W}\\ \bar{Q}_{e}=\frac{k-1}{2}M_1^2(\bar{W}^2-1)\end{array}\right|\ \bar{T}=1{,}0. \tag{179}$$

Eliminating $\bar{f}$ from the second and third equations of the system (179), we get

$$-\frac{d\bar{p}}{\bar{p}}=kM_1^2\bar{W}d\bar{W}.$$

Integrating, we find

$$\ln\bar{p}=\frac{kM_1^2}{2}(1-\bar{W}^2). \tag{180}$$

The specific volume is determined from the equation $\bar{p}\bar{v}=1$, and the specific cross section from the equation

$$\bar{f}=\frac{1}{\bar{W}\bar{p}}=\frac{e^{\frac{kM_1^2}{2}(\bar{W}^2-1)}}{\bar{W}}. \tag{181}$$

The minimum cross section of the athodyd at T = const is found from the conditions

$$\frac{\partial \bar{f}}{\partial \bar{W}} = 0; \quad \bar{f}_{\min} = M_1 \sqrt{k}\, e^{\frac{1-kM_1^2}{2}}.$$

The velocity in this section is

$$\bar{W} = \frac{1}{M_1}\sqrt{\frac{1}{k}}.$$

and $M = \sqrt{\frac{1}{k}}$.

The quantity of heat transferred to the minimum cross section is

$$\bar{Q} = \frac{k-1}{2}\left(\frac{1}{k} - M_1^2\right).$$

The heat transfer may be limited by the value of the stagnation temperature T^*, which is

$$T^* = T\left(1 + \frac{k-1}{2}M^2\right).$$

Bearing in mind that $M^2 = M_1^2\bar{W}^2$, we get

$$\frac{T^*}{T_1} = \bar{T}^* = 1 + \frac{k-1}{2}M_1^2\bar{W}^2. \qquad (182)$$

The pressure, volume, and velocity of the gas in the isothermal chamber may be correlated directly with the independent variable $\bar{Q}$. Thus, from the fourth equation of the system (179) it follows that

$$\bar{W} = \sqrt{1 + \frac{2\bar{Q}}{(k-1)M_1^2}}.$$

From eqs.(180) and (179), we obtain the relation between $\bar{p}$ and $\bar{Q}$:

$$\bar{p} = e^{-\frac{k}{k-1}\bar{Q}}$$

and

$$\bar{f} = \frac{1}{\bar{W}\bar{p}} \cdot \frac{e^{\frac{k}{k-1}\bar{Q}}}{\sqrt{1 + \frac{2\bar{Q}}{(k-1)M_1^2}}}.$$

Let us consider an example. Given the gas parameters in the initial cross section of the chamber: $T_1 = 1850°K$; $W_1 = 30$ m/sec; $p_1 = 100$ kg/cm^2; $k = 1.2$; $R = 30$ kg-m/kg deg.

The gas expands isothermally to $M = 1$; its further expansion to the pressure $p_a = 0.5$ kg/cm^2 takes place in the geometric nozzle.

Let us plot the variation of the gas parameters $\bar{p}$, $\bar{T}$, $\bar{v}$, $\bar{W}$, $\bar{f}$ under isothermal and adiabatic expansion and determine the fundamental parameters of the cycle η_t, P_{sp}, and ψ_c.

Heat transferred before reaching the isothermal duct:

$$Q_1 = \frac{k}{k-1} RT_1 = 334\,000 \text{ Kg·m/Kg}.$$

Stagnation temperature at the end of the isothermal duct ($M = 1$):

$$T^* = T\left(1 + \frac{k-1}{2}\right) = 1850 \cdot \frac{1{,}2+1}{2} = 2033° \text{ abs}.$$

Heat transferred in the isothermal duct:

$$Q = \frac{k}{k-1} R\left(T^* - T_1^*\right) = \frac{1{,}2}{1{,}2-1}\, 30\,(2033 - 1850) = 32\,900 \text{ Kg·m/Kg}.$$

Then,

$$\bar{Q} = \frac{Q}{Q_1} = 0{,}0984.$$

Relative velocity at the end of the isothermal duct:

$$\bar{W}_2 = \sqrt{\frac{2\bar{Q}}{(k-1)M_1^2} + 1} = 26{,}9; \quad W_2 = 30 \cdot 26{,}9 = 806 \text{ m/sec}.$$

Pressure $\bar{p}$ and the area $\bar{f}$ at the end of the isothermal duct:

$$\bar{p}_2 = e^{\frac{kM_1^2}{2}(1-\bar{W})} = 0{,}55;$$

$$p_2 = \bar{p}_2 p_1 = 100 \cdot 0{,}55 = 55 \text{ Kg/cm}^2.$$

The exhaust velocity at the end of the adiabatic expansion is calculated by the formula

$$W_a = \sqrt{W_2^2 + 2g\frac{k}{k-1}RT_2\left[1-\left(\frac{p_a}{p_2}\right)^{\frac{k-1}{k}}\right]} = 2040 \ m/sec.$$

Specific thrust:

$$P_{sp} = \frac{W_a}{g} = 208 \ Kg\text{-}sec/Kg.$$

Work of the cycle:

$$L = \frac{W_a^2}{2g} = 212\,000 \ Kg\text{-}m/Kg.$$

Thermal efficiency:

$$\eta_{it} = \frac{L}{Q_{tot.}} = \frac{212\,000}{334\,000 + 32\,900} = 0{,}577.$$

Force factor:

$$\psi_c = \sqrt{\eta_{it}} = 0{,}76.$$

Figure 120 shows the dimensionless gas parameters $\bar{p}$, $\bar{W}$, $\bar{T}^*$ as a function of $\bar{f}$.

Figure 121, in T-S coordinates, shows the cycles of the following chambers: isobaric, p = const (curves 1-2-3); polytropic, f = const (curves 1'-2'-3'); and polytropic T = const (curves 1"-3") without an adiabatic nozzle, at the same maximum stagnation temperature $T_k^* = 3800°$ abs and the same available pressure drop $\delta_{ex} = 550$.

3. Isobaric Heat Chamber

If heat transfer to the gas, flowing through the duct at a velocity W_1, involves no change in pressure, this implies that the velocity of the gas in the duct is likewise constant.

The system of fundamental equations (161) now assumes the following form:

$$\left.\begin{array}{l}\bar{v}=\bar{T}\\ \bar{f}=\bar{T}\\ \bar{W}=1{,}0\\ \bar{Q}=\bar{T}-1\end{array}\right|\ \bar{p}=1{,}0. \qquad (183)$$

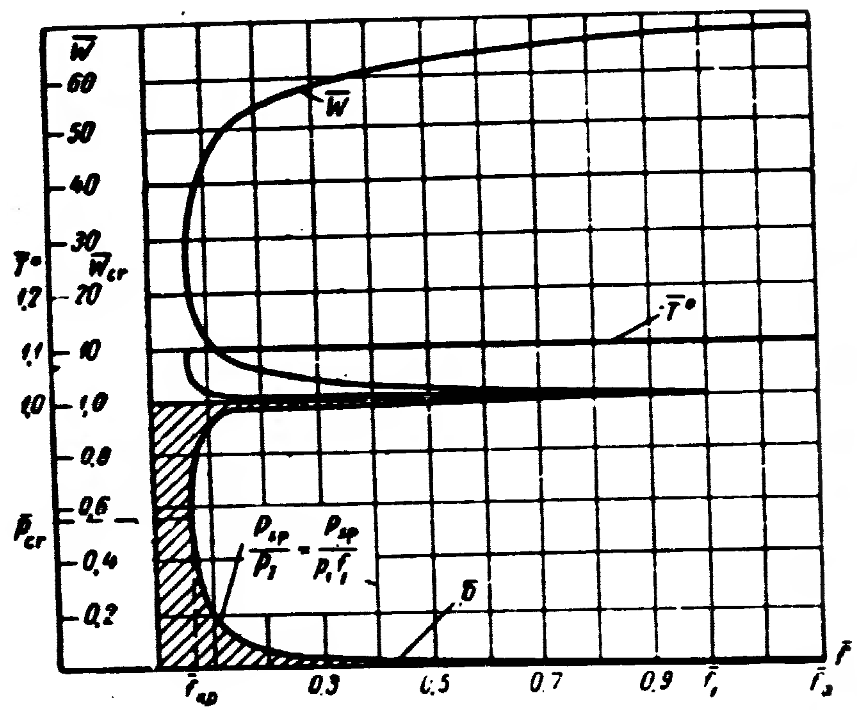

Fig.120 - Variation of Fundamental Gas Parameters with the Relative Cross Section, for the Case of Isothermal Expansion of the Gases in the Chamber to M = 1 and Subsequent Expansion of the Gases in the Geometric Nozzle to p_a = 0.5 kg/cm^2

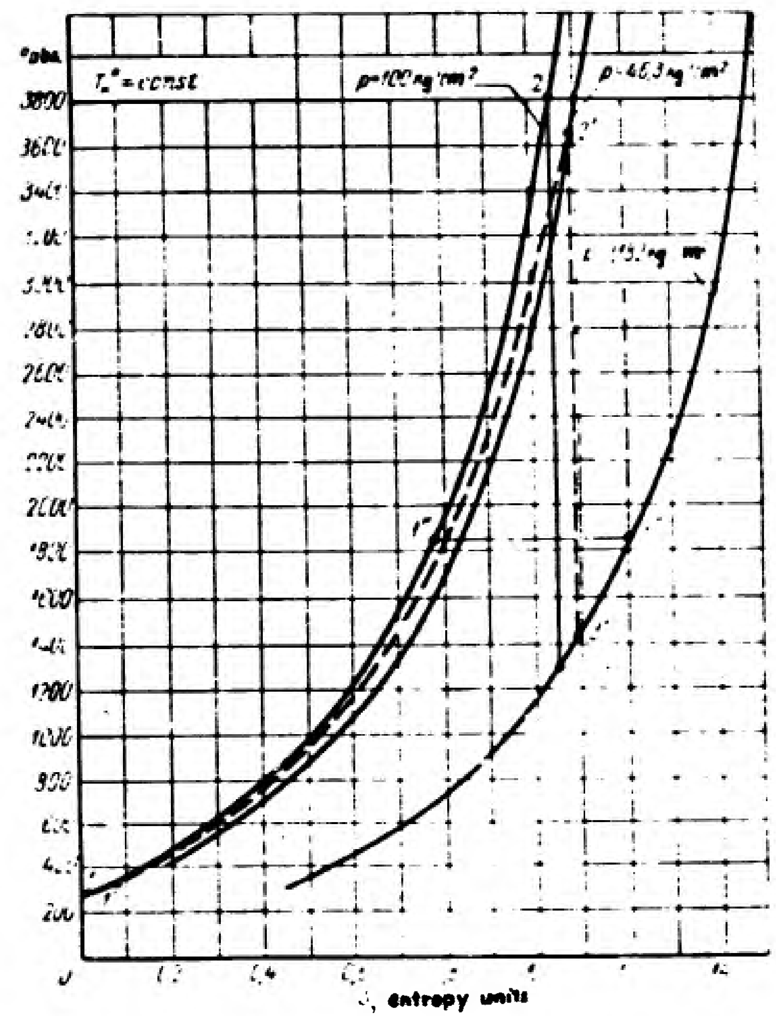

Fig.121 - T-S Diagram of Cycles at the same Stagnation Temperature $T_k^* = 3800°K$ and the same Available Pressure Drop $\delta_{ex\ o}$ = 550

Curves 1-2-3 correspond to p = const;
curves 1"-3" correspond to T = const;
curves 1'-2'-3' correspond to f = const

Consequently, during heat transfer in such a chamber, its cross section will vary, together with its specific volume and the gas temperature, in accordance with the law

$$\bar{v} = \bar{T} = \bar{f} = 1 + \bar{Q}. \qquad (184)$$

4. <u>Isochoric Heat Chamber</u>

Since $\bar{v}$ = 1.0 in this case, we obtain, instead of the system (161), the following

$$\left.\begin{aligned} &\bar{p} = \bar{T} \\ &\bar{f}\,\bar{W} = 1 \\ &\bar{f}d\bar{p} = -kM_1^2 d\bar{W} \\ &\bar{Q} = \bar{T} - 1 + \frac{k-1}{2} M_1^2(\bar{W}^2 - 1) \end{aligned}\right| \bar{v} = 1{,}0. \qquad (185)$$

Since

$$\bar{f} = \frac{1}{\bar{W}},$$

it follows that

$$\bar{f}d\bar{p} = \frac{d\bar{p}}{\bar{W}} = -kM_1^2 d\bar{W},$$

whence

$$\bar{p} = 1 - \frac{kM_1^2}{2}(\bar{W}^2 - 1) = \bar{T}. \qquad (186)$$

Substituting this value of $\bar{T}$ in the equation of energy, we obtain the following relation between the velocity and the transferred heat:

$$\bar{Q} = -\frac{kM_1^2}{2}(\bar{W}^2 - 1) + \frac{k-1}{2} M_1^2(\bar{W}^2 - 1)$$

and

$$\bar{Q} = \frac{M_1^2}{2}(1 - \bar{W}^2),$$

or

$$\bar{W} = \sqrt{1 - \frac{2\bar{Q}}{M_1^2}}.$$

On transfer of heat, the gas velocity in the chamber declines. Eliminating $\bar{W}$ from eq.(186), we establish the following relation between the pressure, temperature, and transferred heat:

$$\overline{T}=\overline{p}=1+k\overline{Q}. \qquad (187)$$

The cross section of the duct increases on transfer of heat:

$$\overline{f}=\frac{1}{\overline{W}}=\frac{1}{\sqrt{1-\frac{2}{M_1^2}\overline{Q}}}.$$

At an infinitely great cross-sectional area of the duct ($\overline{f}_k = \infty$),

$$\overline{Q}|_\infty=\frac{M_1^2}{2} \text{ and } \overline{p}|_\infty=\overline{T}|_\infty=\frac{2+kM_1^2}{2}.$$

In the four chamber versions examined, the fundamental equations and the auxiliary conditions permit a simple analytic solution of the problem of the variation of the gas parameters in the athodyd. There are many other additional conditions ($\overline{T} = \overline{W}$, $\overline{f} = \overline{W}$, $\overline{p}\,\overline{T} = 1.0$, $\overline{f}\,\overline{p} = 1.0$, etc.), which likewise lead to simple solutions, but the practical importance of such versions is negligible.

5. Variation of Cross Sections and Profile in a Series of Polytropic Chambers

Above, we have considered special examples of thermal chambers. In our subsequent discussion, we shall present general conclusions for polytropic chambers, where the general equations (161) will be supplemented by an additional equation of polytropy, permitting us to establish all the necessary relations between the parameters of the working fluid.

In dimensionless form, the equation of polytropy has the form:

$$\overline{p}\,\overline{v}^n=1{,}0 \quad \text{or} \quad \overline{T}=\overline{p}^{\frac{n-1}{n}}.$$

We shall conceive the independent variable as the relative quantity of heat transferred:

$$\overline{Q}_k=\frac{Q_k}{\frac{k}{k-1}RT_1}.$$

Let us establish the corresponding relation of the quantities $\bar{p}$, $\bar{T}$, $\bar{W}$, and $\bar{f}$.

In the sense of the polytropic process, we have

$$\frac{W_1^2}{2g}\left(\bar{W}^2-1\right)=\alpha_1 Q_\kappa=\alpha_1 \bar{Q}_\kappa \frac{k}{k-1} RT_1,$$

where α_1 is the fraction of the transferred heat that is converted into kinetic energy of the gas.

Hence,

$$\frac{2\alpha_1}{k-1}\bar{Q}_\kappa = M_1^2\left(\bar{W}^2-1\right).$$

It follows from eq.(150) that

$$\alpha_1 = \frac{k-1}{k-n}\,n.$$

Substituting the value of α_1 in the preceding equation, we obtain the gas velocity $\bar{W}$ for an arbitrary instant of heat liberation:

$$\bar{W} = \sqrt{1+\frac{2n}{k-n}\cdot\frac{\bar{Q}_\kappa}{M_1^2}}. \qquad (188)$$

We determine the temperature from the expression

$$\bar{T}=1+\bar{Q}_\kappa(1-\alpha_1)=1+\frac{k(1-n)}{k-n}\bar{Q}_\kappa. \qquad (189)$$

Consequently,

$$\bar{p}\,\bar{v}=1+\frac{k(1-n)}{k-n}\bar{Q}_\kappa. \qquad (190)$$

The relation between pressure and heat transferred is established by the equation of polytropy, having the form

$$\bar{p}=\left[1+\frac{k(1-n)}{k-n}\bar{Q}_\kappa\right]^{\frac{n}{n-1}}. \qquad (191)$$

We determine the value of the specific cross section $\bar{f}$ from the equation of the rate of flow:

$$\bar{f}=\frac{\bar{T}}{\bar{W}\bar{p}}=\frac{1}{\bar{W}\bar{T}^{\frac{1}{n-1}}}=\frac{1}{\bar{W}\bar{p}^{\frac{1}{n}}}. \qquad (192)$$

Making use, in addition, of eqs.(188) and (189), we obtain

$$\bar{f} = \frac{1}{\left(1 + \frac{k(n-1)}{n-k}\bar{Q}_{\kappa}\right)^{\frac{1}{n-1}} \sqrt{1 - \frac{2n}{n-k}\frac{\bar{Q}_{\kappa}}{M_1^2}}} . \tag{193}$$

Let us also find the relation between the gas velocity and the chamber cross section.

For this purpose, using eq.(188), we eliminate the quantity $\bar{Q}_k$ from eq.(193). We may also use the equation of momentum and rate of flow:

$$\bar{f} = \frac{1}{\bar{W}\bar{p}^{\frac{1}{n}}};\quad \bar{f}d\bar{p} = -kM_1^2 d\bar{W}.$$

Eliminating $\bar{f}$, we get

$$\frac{1}{\bar{W}\bar{p}^{\frac{1}{n}}} = -kM_1^2\frac{d\bar{W}}{d\bar{p}}$$

and

$$\bar{W}^2 = 1 - \frac{2n}{k(n-1)M_1^2}\left(\bar{p}^{\frac{n-1}{n}} - 1\right) = 1 - \frac{2n}{k(n-1)M_1^2}(\bar{T} - 1), \tag{194}$$

whence

$$\bar{T} = 1 - \frac{k(n-1)}{2n} M_1^2 (\bar{W}^2 - 1)$$

and

$$\bar{f} = \frac{1}{\bar{W}\bar{T}^{\frac{1}{n-1}}} = \frac{1}{\bar{W}\left[1 - \frac{k(n-1)}{2n}M_1^2(\bar{W}^2 - 1)\right]^{\frac{1}{n-1}}} \tag{195}$$

Figure 122 shows the variation of the specific chamber cross section for seven values of the polytropic exponent n = 0, 0.05, 0.2, 0.4, 0.6, 0.8 and 1.0. Using eq.(193) to determine $\frac{d\bar{f}}{d\bar{Q}_k} = 0$, we find that the minimum cross section corresponds to the value

$$\bar{Q}_{\kappa}\Big|_{\bar{f}_{min}} = \frac{(n-k)(kM_1^2 - n)}{nk(n+1)}. \tag{196}$$

Let us determine M^2 in an arbitrary cross section of the chamber, by the aid of eq.(169):

$$M^2 = M_1^2 \frac{\overline{W}^2}{\overline{T}}.$$

Bearing eqs.(188) and (189) in mind, we obtain

$$M^2 = M_1^2 \frac{1 + \frac{2n}{k-n} \frac{\overline{Q}_\kappa}{M_1^2}}{1 + \frac{k(1-n)}{k-n} \overline{Q}_\kappa}. \tag{197}$$

The exhaust will continue at subsonic velocity until the instant $M^2 = 1.0$ is

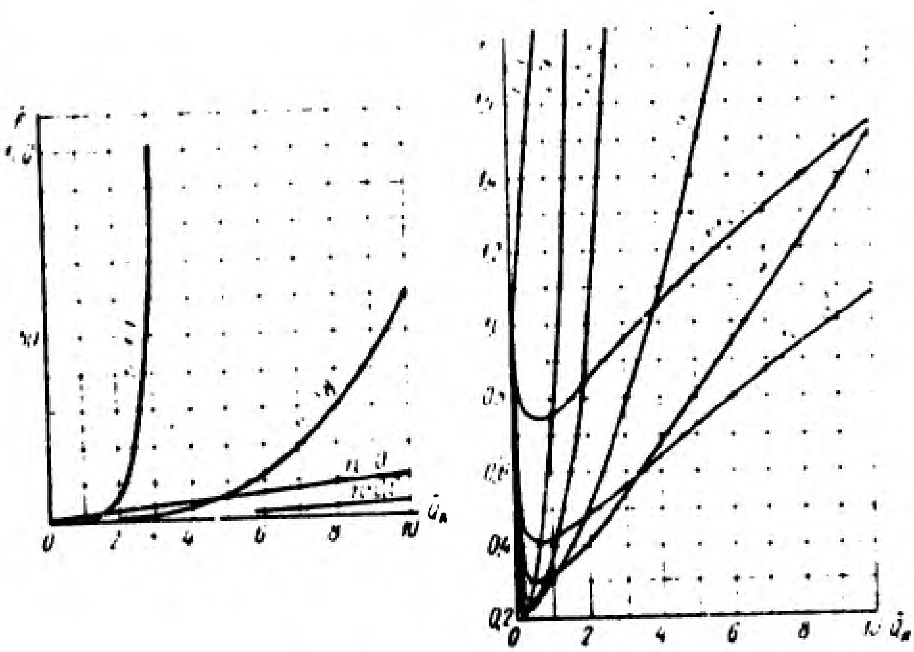

Fig.122 - Variation of the Cross Sections in a Polytropic Chamber for Seven Values of the Polytropic Exponent

reached. Up to this time, the heat transferred to the gas will be $\overline{Q}_{M=1.0}$, which we determine from eq.(197), substituting $M^2 = 1.0$ there:

$$\overline{Q}_\kappa \bigg|_{M=1.0} = \frac{(k-n)(1-M_1^2)}{2n-k+kn}.$$

With further transfer of heat, the exhaust takes place at supersonic velocities. Up to the minimum cross section, the heat $\overline{Q}_{f\,min}$ is transferred, and can be determined by eq.(196). To obtain $M^2_{f\,min}$, we substitute in eq.(197) the value of $\overline{Q}'$

from eq.(196):

$$M^2\Big|_{\bar{f}_{min}} = \frac{n}{k}. \tag{198}$$

Combining eqs.(196) and (188), we obtain the velocity of flow across the minimum cross section:

$$\overline{W}^2\Big|_{\bar{f}_{min}} = \frac{2n + (n-1)kM_1^2}{k(n+1)M_1^2}. \tag{199}$$

Substituting for the quantity $\overline{Q}$ in eqs.(187) and (193) its value from eq.(196), we get

$$\overline{T}\Big|_{\bar{f}_{min}} = \frac{2n + (n-1)kM_1^2}{n(n+1)}; \tag{200}$$

$$\bar{f}_{min} = \frac{\sqrt{\frac{kM_1^2}{n}}}{\left[\frac{2n + (n-1)kM_1^2}{n(n+1)}\right]^{\frac{n+1}{2(n-1)}}}. \tag{201}$$

To determine the thrust under design conditions, we must know the expansion ratio in the adiabatic nozzle:

$$\delta_c = \frac{\delta_{ex}}{\delta_k} = \delta_{ex}\bar{p}_k,$$

where δ_{ex} is the available expansion ratio, equal to $\delta_{ex} = \frac{p_k}{p_{ex}}$.

We determine the spocific thrust, allowing for the parameters obtained at the end of the athodyd.

$$P_{sp} = \frac{W_a}{g} = \frac{\sqrt{W_k^2 + 2gL_{ad}}}{g} = \frac{W_1}{g}\sqrt{\overline{W}_k^2 + \frac{2\overline{T}_k}{(k-1)M_1^2}\left[1 - \frac{1}{(\delta_{ex}\bar{p}_k)^m}\right]}. \tag{202}$$

During expansion, at $\delta_c = \infty$, the maximum specific thrust will be

$$P_{sp.max} = \frac{W_1}{g}\sqrt{\overline{W}_k^2 + \frac{2\overline{T}_k}{(k-1)M_1^2}} \tag{203}$$

while the force factor is

$$\psi_k = \frac{P_{sp}}{P_{sp\,max}} = \sqrt{1 - \frac{1}{\left(\bar{w}_k^2 + \frac{2}{k-1}\frac{\bar{T}_k}{M_1^2}\right)(\bar{v}_{cr}\bar{p}_k)^{n}}} \tag{204}$$

The quantities $\bar{w}_k$, $\bar{T}_k$, and $\bar{p}_k$ determined by eqs.(188), (189), and (191), may be expressed as a function of Q_k, so that we may obtain $P_{sp} = f(\bar{Q}_k)$.

In this case,

$$P_{sp\,max} = \frac{P_{sp\cdot max}}{P_{sp\,1}} = \sqrt{\frac{1}{\bar{T}_1^* - 1}(\bar{T}_1^* + \bar{Q}_k)}, \tag{205}$$

or

$$\bar{P}_{sp\,max} = \sqrt{1 + \frac{\bar{Q}}{\bar{T}^* - 1}},$$

where $\bar{T}^*$ is the relative stagnation temperature in the first cross section of the chamber;

$\bar{Q} = \bar{Q}_k + 1$ is the total quantity of heat transferred in the chamber.

We find the following expression for the specific thrust:

$$\bar{P}_{sp} = \sqrt{\frac{1}{\bar{T}^* - 1}\left\{\bar{T}_1^* + \bar{Q}_k\left[1 - \frac{1}{\bar{v}_{cr}^{u}\left(1 + \frac{k(1-n)}{k-n}\bar{Q}_k\right)^{\frac{n}{n-1}\cdot\frac{k-1}{k}}}\right]\right\}}. \tag{206}$$

In the case of an isothermal chamber, T = 1.0, and, according to eq.(188),

$$\bar{W}'\Big|_{\bar{T}=1.0} = \sqrt{1 + \frac{2}{k-1}\frac{\bar{Q}_k}{M_1^2}}.$$

We determine the pressure from eq.(191), for which we must solve the indeterminate equation, since we get directly from eq.(191)

$$\bar{p} = 1^{\infty}.$$

After taking the logarithms of both sides, we obtain

$$\ln \bar{p} = \frac{n}{n-1}\ln\left[1 + \frac{k(1-n)}{k-n}\bar{Q}_k\right] = \frac{\ln\left[1 + \frac{k(1-n)}{k-n}\bar{Q}_k\right]}{\frac{n-1}{n}}\Bigg|_{n=1} = \frac{0}{0}.$$

We then derive the relation of the derivatives of the numerator and denominator:

$$-\frac{k\bar{Q}_{\kappa}[(n-k)+1-n]n^{2}}{\left[1-\frac{k(1-n)}{k-n}\bar{Q}_{\kappa}\right](k-n)^{2}(n-n+1)}\Bigg|_{n=1} = -\frac{k(1-k)\bar{Q}_{\kappa}}{(k-1)^{2}} = \frac{k}{k-1}\bar{Q}_{\kappa}.$$

Since

$$\ln\bar{p} = -\frac{k}{k-1}\bar{Q}_{\kappa},$$

it follows that

$$\bar{p}\Big|_{\bar{T}=1,0} = e^{-\frac{k}{k-1}\bar{Q}_{\kappa}}. \qquad (207)$$

According to the second equation in the system (179) and eq.(207),

$$\bar{f}\Big|_{\bar{T}=1,0} = \frac{e^{\frac{k}{k-1}\bar{Q}_{\kappa}}}{\sqrt{1+\frac{2}{k-1}\frac{\bar{Q}_{\kappa}}{M_1^2}}}. \qquad (208)$$

From the condition $\frac{d\bar{f}}{d\bar{Q}} = 0$, we get

$$\bar{Q}_{cr}\Big|_{\bar{T}=1} = \frac{k-1}{k}\cdot\frac{1-kM_1^2}{2},$$

so that

$$\bar{W}_{cr}\Big|_{\bar{T}=1,0} = \frac{1}{M_1\sqrt{k}} \text{ and } \bar{f}_{cr}\Big|_{\bar{T}=1,0} = e^{\frac{1-kM_1^2}{2}}M_1\sqrt{k}.$$

This conclusion may also be obtained from eq.(201).

This example has been discussed before (p.208) without relating it to general conclusions on polytropic chambers.

Figure 123 shows the parameters $\bar{W}_k$, $\bar{p}$, $\bar{T}$, $\bar{f}$, as well as P_{sp}, as a function of the relative quantity of supplied heat $\bar{Q}$.

The law of heat liberation along the axis of the chamber depends on the profile of the chamber, whose selection is governed by various factors, specifically by simplicity of shape, small transverse dimensions, convenience of location for heat sources, adequate number of such locations, minimum gas-dynamic losses, etc.

We shall consider below examples in which only simple profile shapes are specified.

Let the chamber duct have a throat and consist of two simple cones (Fig.124).

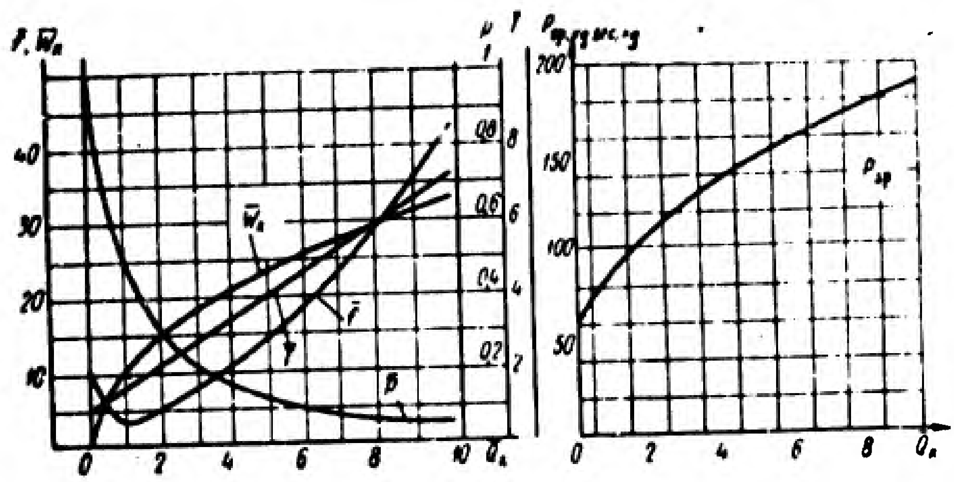

Fig.123 - Variation of $\overline{W}_k$, $\overline{f}$, $\overline{T}$, $\overline{p}$, and P_{sp} as a Function of the Relative Quantity of Supplied Heat $\overline{Q}_k$, for a Polytropic Chamber

The values of $\overline{f}_{min}$, $\overline{f}_k$, M_1^2, $\overline{Q}_k$ are known, so that also $\overline{d}_{min}$ and $\overline{d}_k$ are known.

Considering first the divergent part of the process, we select in addition the divergence half-angle β over the length l.

The equation of the profile generatrix, plotted in the coordinates $\overline{x} - \overline{d}_x$, has the form

$$\overline{d}_x = 1 + (\overline{d}_k - 1)\,\overline{x},$$

where

$$\overline{x} = \frac{x}{l},$$

However,

$$\overline{d}_x = \sqrt{\overline{f}_x} = F(\overline{Q}).$$

For example, for an isothermal chamber, the desired relation has the form:

$$\sqrt{\frac{e^{\frac{k}{k-1}\overline{Q}_k}}{\sqrt{1 + \frac{2}{k-1}\frac{\overline{Q}_k}{M_1^2}}}} = 1 + (\overline{d}_k - 1)\,\overline{x}.$$

The procedure is similar for the region up to the throat.

Figure 125 shows an example of a hyperboloid chamber.

The equation of the generatrix has the following form:

$$\frac{d_x^2}{d_{min}^2} - \frac{x^2}{a^2} = 1,0.$$

We determine the constant a from the conditions $x = l_2$ at $d_x = d_k$.

Then,

$$\frac{d_k^2}{d_{min}^2} - \frac{l_2^2}{a^2} = 1,0,$$

whence

$$a^2 = \frac{l_2^2}{\frac{d_k^2}{d_{min}^2} - 1}.$$

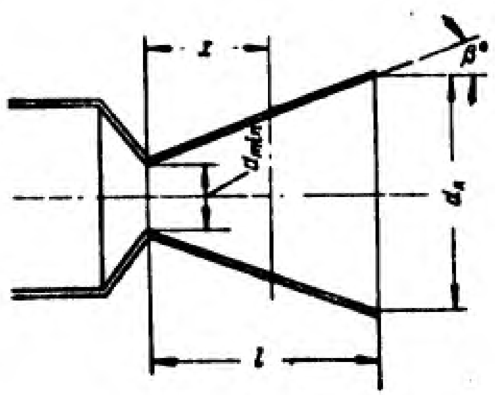

Fig.124 - Example of Chamber Duct Consisting of Two Cones

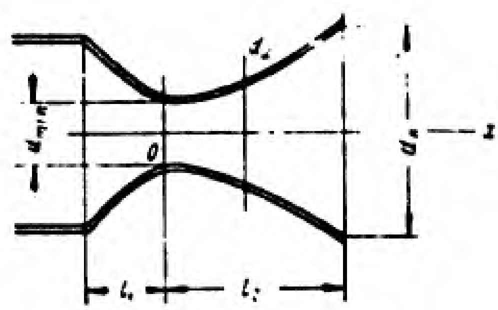

Fig.125 - Example of Chamber Duct Consisting of Two Hyperboloids

Let us introduce the quantity $\bar{f}_x$ into the equation

$$\frac{\bar{f}_x}{\bar{f}_{min}} - \left(\frac{\bar{f}_k}{\bar{f}_{min}} - 1\right)\bar{x}^2 = 1,0,$$

where

$$\bar{x} = \frac{x}{l}.$$

For example, for an isothermal chamber we have

$$\frac{e^{\frac{k}{k-1}\bar{Q}_x}}{\sqrt{1 + \frac{2}{k-1}\frac{\bar{Q}_x}{M_1^2}}} =$$

$$= \left(\frac{e^{\frac{k}{k-1}\bar{Q}_x}}{\sqrt{1+\frac{2}{k-1}\frac{\bar{Q}_x}{M_1^2}}} - \sqrt{kM_1^2}\, e^{\frac{1-kM_1^2}{2}} \right)\bar{x}^2 + \sqrt{kM_1^2}\, e^{\frac{1-kM_1^2}{2}}.$$

or

$$\frac{e^{\frac{k}{k-1}\bar{Q}_x}}{\sqrt{1+\frac{2}{k-1}\cdot\frac{\bar{Q}_x}{M_1^2}}} = A\bar{x}^2 + B.$$

Section 16. Examples of Thermal Chambers with Various Auxiliary Conditions

The profile of the athodyd of a chamber may be specified by the designer. In this case, the thermal calculation must find the relation between the gas parameters and the coordinate length of the chamber.

In some cases the relation between the heat liberation and the coordinate length of the chamber is specified. Let us consider, from an example, the solution of the problem of determining the gas parameters as a function of the main variable x, constituting the axial coordinate of an arbitrary cross section of the duct.

1. Isothermal Chamber with dQ = bdx

Given an isothermal chamber with the simple law of heat liberation

$$dQ = b\,dx,$$

where x is measured from the first cross section in which the gas parameters are completely known.

Let us introduce, instead of the coordinate x, the dimensionless quantity $\bar{x}$ proportional to it, determined from the equality

$$\frac{dQ}{\frac{k}{k-1}RT_1} = d\bar{Q} = \frac{dx}{\frac{k}{b(k-1)}RT_1} = d\bar{x}.$$

Consequently,

$$x = \frac{k}{b(k-1)RT_1}x.$$

The initial equations for the chamber are

$$\bar{p}\,\bar{v}=1{,}0;$$
$$\bar{p}\,\bar{f}\,\bar{W}=1{,}0;$$
$$\bar{f}\,d\bar{p}=-kM_1^2\,d\bar{W};$$
$$\bar{Q}=\frac{k-1}{2}M_1^2(\bar{W}^2-1);$$
$$d\bar{Q}=d\bar{x}.$$

If in the equations found previously for the chamber $\bar{T}$ = 1.0, we substitute the quantity $\bar{Q}$ by the quantity $\bar{x}$, we will find all the relations desired. Thus, the

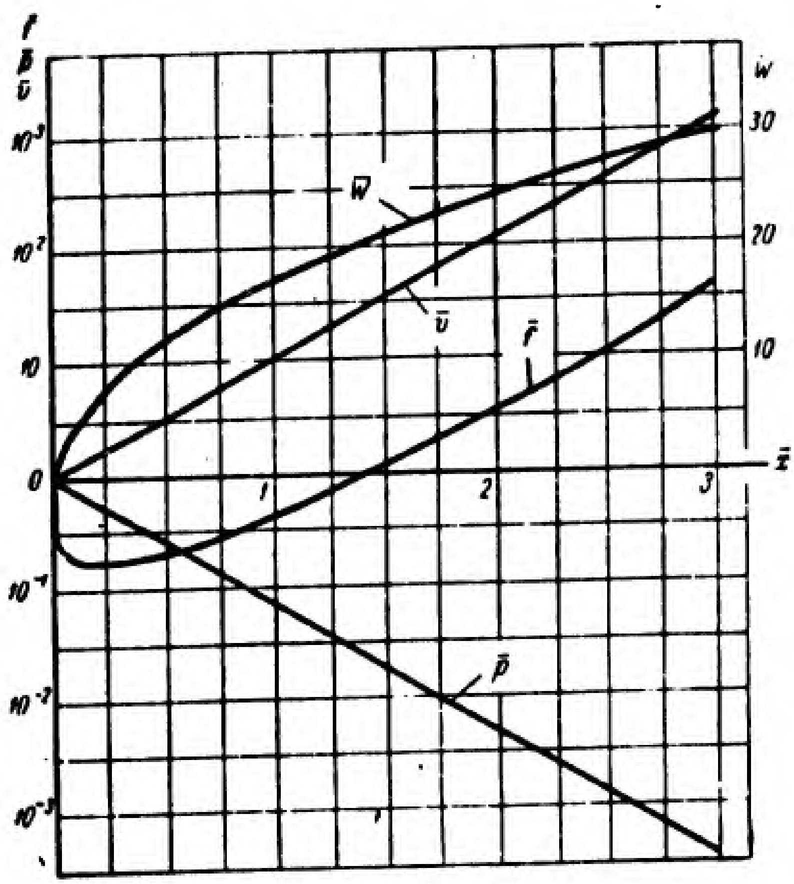

Fig.126 - Variation of Principal Parameters along the Length of the Isothermal Chamber $\bar{T}$ = 1.0 (k = 1.67, M_1 = 0.1)

profile of the walls, according to eq.(208), is determined from the equation:

$$\bar{f}=\frac{e^{\frac{k}{k-1}\bar{x}}}{\sqrt{1+\frac{2}{k-1}\cdot\frac{\bar{x}}{M_1^2}}}=\bar{d}^2;$$

or

$$\bar{d}^4 = \frac{e^{\frac{2k}{k-1}}}{1 - \frac{2}{k-1}\frac{\bar{x}}{M_1^2}}. \qquad (209)$$

Figure 126 shows the variation of the principal parameters along the length of the isothermal chamber $\bar{T}$ = 1.0 (k = 1.67, M_1^2 = 0.01).

2. Cylindrical Chamber with Sinusoidal Heat Transfer

In some cases of the heating of a gas in reactors, the law of heat liberation is close to that shown in Fig.127, where

$$dQ = Q\,dz = Q_0 \sin \pi \frac{z}{l}\,dz = \frac{Q_0 l}{\pi} \sin(\pi \bar{z})\,d(\pi \bar{z}).$$

Here, l is the total length of the duct;

Q_0 is the heat liberated per unit length of the duct, at the midpoint of its length.

If, in the initial state, the enthalpy of the gas was $\frac{k}{k-1}RT_1$, then

$$d\bar{Q} = \frac{dQ}{\frac{k}{k-1}RT_1} = \frac{Q_0 l}{\pi \frac{k}{k-1}RT_1} \sin(\pi \bar{z})\,d(\pi \bar{z}).$$

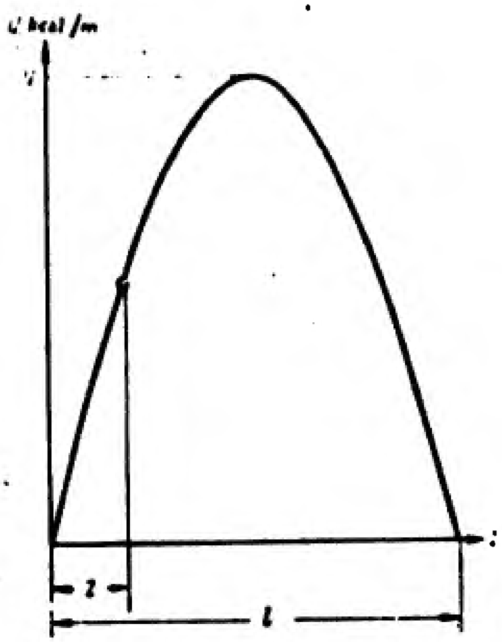

Fig.127 - Sinusoidal Variation of Heat Liberation Per Unit Length of Chamber

Putting

$$\frac{Q_0}{\frac{k}{k-1}RT_1} = \bar{Q}_0 \text{ and } \pi \bar{z} = y,$$

then

$$d\bar{Q} = \frac{l}{\pi}\bar{Q}_0 \sin y\,dy$$

and up to an arbitrary cross section the liberated heat will be

$$\bar{Q} = \frac{l}{\pi}\bar{Q}_0 \int_0^y \sin y\,dy$$

$$= \frac{l}{\pi}\bar{Q}_0 (1 - \cos y). \qquad (210)$$

To the end of the duct, at $y = \pi$, a total quantity of heat of

$$\overline{Q}_{\pi} = 2\frac{l}{\pi}\overline{Q}_{0}.$$

will be liberated.

The fundamental equations in this case are the same as presented earlier in considering the chamber $\overline{f} = 1.0$ [equations of system (162)]:

$$\begin{gathered}\overline{p}\,\overline{v} = \overline{T};\\ \overline{p}\,\overline{W} = \overline{T};\\ d\overline{p} = -kM_1^2 d\overline{W};\\ \frac{l}{\pi}\overline{Q}_0(1-\cos y) = \overline{T} - \overline{T}_1^* + \frac{k-1}{2}M_1^2\overline{W}^2.\end{gathered}$$

After transformations, we get

$$\begin{gathered}\overline{p} = 1 - kM_1^2(\overline{W}-1);\\ \overline{v} = \overline{W};\\ \overline{p} = 1 - kM_1^2(\overline{v}-1);\\ \frac{l}{\pi}\overline{Q}_0(1-\cos y) = (1+kM_1^2)\,\overline{W} - \frac{k+1}{2}M_1^2\overline{W}^2 - \overline{T}_1^*.\end{gathered}$$

From the last equation, we determine the velocity and then $\overline{p}$ and $\overline{v}$.

The exhaust velocity from the athodyd is determined on the basis of the quadratic equation:

$$2\frac{l}{\pi}\overline{Q}_0 = (1+kM_1^2)\,\overline{W} - \frac{k+1}{2}M_1^2\overline{W}^2 - \overline{T}_1. \tag{211}$$

This velocity should be less than maximum [eq.(171)]:

$$\overline{W}_{cr} = \frac{1+kM_1^2}{(1+k)M_1^2}.$$

We find the coordinate of the length y_{cr} from the equation

$$\frac{l}{\pi}\overline{Q}_0(1-\cos y_{cr}) = \frac{(1+kM_1^2)^2}{2(k+1)M_1^2} - \overline{T}_1,$$

which is obtained from eq.(211) after substituting the value of $\overline{W}_{cr}$:

$$y_{cr} = \pi \bar{z}_{cr} = \arccos\left[1 + \frac{\pi}{lQ_0}\bar{T}_1' - \frac{\pi}{lQ_0}\cdot\frac{(1-kM_1^2)^2}{2(1-k)M_1^2}\right]. \qquad (212)$$

3. __Parabolic Chamber with Single Wall and Identical Strength in the Longitudinal Section__

Consider a parabolic chamber in whose walls the longitudinal tensile stresses are about equal.

Roughly, the tensile stress in the longitudinal section is

$$\sigma_1 = \frac{Dp\,dx}{2\delta\,dS_l}, \qquad (213)$$

where D is the local diameter of the duct;

δ is the thickness of the wall;

dS_l is the length of the provile arc.

Since

$$dS_l = \sqrt{1 + \left(\frac{dr}{dx}\right)^2}\,dx,$$

then

$$\sigma_1 = \frac{Dp}{2\delta\sqrt{1 + \left(\frac{dr}{dx}\right)^2}}. \qquad (214)$$

Taking δ as equal along the length of the chamber, we get

$$\frac{Dp}{\sqrt{1 + \frac{1}{4}\left(\frac{dD}{dx}\right)^2}} = \frac{D_1p_1}{\sqrt{1 + \frac{1}{4}\left(\frac{dD}{dx}\right)_1^2}} = \frac{D_1p_1}{m},$$

whence

$$Dp = \frac{1}{m}\sqrt{1 + \frac{1}{4}\frac{D_1^2}{x_1^2}\left(\frac{dD}{dx}\right)^2}.$$

But for a parabolic profile

$$D = \sqrt{f\,1\,x},$$

Consequently,

$$\left(\frac{dD}{dx}\right)^2 = \left(\frac{d\sqrt{x}}{dx}\right)^2 = \left(\frac{1}{2}x^{-\frac{1}{2}}\right)^2 = \frac{1}{4x}.$$

Then,

$$\bar{p}\sqrt{\bar{x}} = \frac{1}{m}\sqrt{1+\frac{1}{16}\frac{D_1^2}{x_1^2}\frac{1}{\bar{x}}}$$

and

$$\bar{p} = \frac{1}{m}\sqrt{\frac{1}{\bar{x}}\left[1+\left(\frac{D_1}{4x_1}\right)^2\frac{1}{\bar{x}}\right]}. \tag{215}$$

Thus from the auxiliary condition results a definite and direct relation between the gas pressure and the coordinate of the duct length. The remaining relations are obtained from the fundamental equations.

From the equations

$$\bar{J}d\bar{p} = -kM_1^2 d\bar{W} = \bar{x}d\bar{p}$$

and from eq.(215), we obtain the relation $\bar{W} = f(\bar{x})$.

To simplify the conclusions, let us vary the conditions of the example. Assume that the length of a single wall decreases as we approach the exit section, in direct proportion to the first derivative $\frac{ds_l}{dx}$, which decreases with increasing x.

This means that

$$\delta = \delta_1\frac{\frac{dS_l}{dx}}{\left(\frac{dS_l}{dx}\right)_1}.$$

Then,

$$\sigma = \frac{Dp\left(\frac{dS_l}{dx}\right)_1}{2\delta_1\left(\frac{dS_l}{dx}\right)^2} = \frac{D_1p_1}{2\delta_1\left(\frac{dS_l}{dx}\right)_1},$$

whence

$$\bar{D}\bar{p} = \frac{\left(\frac{dS_l}{dx}\right)^2}{\left(\frac{dS_l}{dx}\right)_1^2} = \frac{1+\frac{1}{16}\frac{D_1^2}{x_1^2}\frac{1}{\bar{x}}}{1+\frac{1}{16}\frac{D_1^2}{x_1^2}}.$$

Let

$$\frac{1}{16}\frac{D_1^2}{x_1^2} \quad A$$

and, in addition, $\bar{D}^2 = \bar{x}$. Then,

$$\bar{p} = \frac{1}{1+A}\,\frac{1}{\bar{D}}\left(1+\frac{A}{\bar{D}^2}\right) = \frac{1}{1+A}\,\frac{1}{\sqrt{\bar{x}}}\left(1+\frac{A}{\bar{x}}\right) \tag{216}$$

after which the equation of momentum takes the form

$$\bar{f}\,d\bar{p} = \bar{D}^2 d\bar{p} = -kM_1^2 d\bar{W}.$$

From eq.(216), we get

$$d\bar{p} = -\frac{1}{1+A}\left(\frac{1}{\bar{D}^2}+\frac{3A}{\bar{D}^4}\right)d\bar{D}.$$

After substituting this value of $d\bar{p}$ in the preceding expression and integrating, we get

$$\bar{W} = 1+\frac{1}{(1+A)kM_1^2}\left(\frac{\bar{D}^2-3A}{\bar{D}}+3A-1\right) =$$

$$= 1+\frac{1}{(1+A)kM_1^2}\left(\frac{\bar{x}-3A}{\sqrt{\bar{x}}}+3A-1\right). \tag{217}$$

From the equation of the rate of flow, we determine the current temperature:

$$\bar{T} = \bar{f}\,\bar{W}\bar{p} = \bar{x}\,\bar{W}\bar{p}.$$

Making use of eqs.(216) and (217), we get

$$\bar{T} = \left[1+\frac{1}{(1+A)kM_1^2}\left(\frac{\bar{x}-3A}{\sqrt{\bar{x}}}+3A-1\right)\right]\frac{\bar{x}+A}{(1+A)\sqrt{\bar{x}}}. \tag{218}$$

The law of liberation of heat $\bar{Q}$ with respect to the coordinate $\bar{x}$ is found from the equation of energy:

$$\bar{Q} = \bar{T}-\bar{T}_1^* + \frac{k-1}{2}M_1^2\bar{W}^2.$$

Substituting $\bar{T}$ and $\bar{W}$ by their expressions from eqs.(217) and (218), we obtain

$$\bar{Q} = \left[1+\frac{1}{(1+A)kM_1^2}\left(\frac{\bar{D}^2-3A}{\bar{D}}+3A-1\right)\right]\left[\frac{\bar{D}^2+A}{(1+A)\bar{D}}\right.$$

$$+\frac{k-1}{k}\frac{1}{2k(1-A)}\left(\frac{\bar{D}^2-3A}{\bar{D}}+3A-1\right)\cdot\frac{k-1}{2}M_1^2\Big|$$

$$-\left(1+\frac{k-1}{2}M_1^2\right). \qquad (219)$$

The thickness of the wall with increasing $\bar{x}$ or increasing diameter $\bar{D}$ decreases according to the equation

$$\bar{\delta}^2=\frac{1+\frac{A}{\bar{x}}}{1+A}=\frac{1+\frac{A}{\bar{D}^2}}{1+A}. \qquad (220)$$

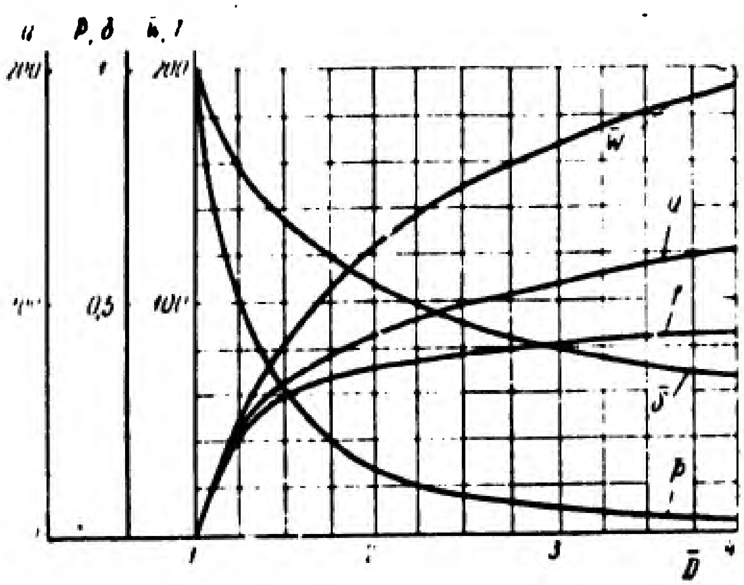

Fig.128 - Relation between Principal Parameters and Relative Diameter of the Parabolic Chamber ($k = 1.67$, $M_1 = 0.1$)

Figure 128 shows the mode of variation of $\bar{p}$, $\bar{W}$, $\bar{Q}$, $\bar{\delta}$, and $\bar{T}$ along the axis of the chamber.

4. Thermal Chamber with Constant Convective Product

Let us consider a chamber with constant intensity of convective heat transfer to the chamber wall along its length.

The factor responsible for heat transfer by convection at low flow velocities is the so-called "convective" product $pl\sqrt{\frac{\mu}{T}}$, where μ is the molecular weight of the gas and I is its enthalpy.

Figure 129 shows the convective product as a function of the temperature of the working fluid, formed from the original material - hydrogen (H_2). The coordinates of the hatched rectangle correspond to a modern gasoil-oxygen engine at a chamber pressure of 50 - 100 atm. For an ideal gas, the convective product is

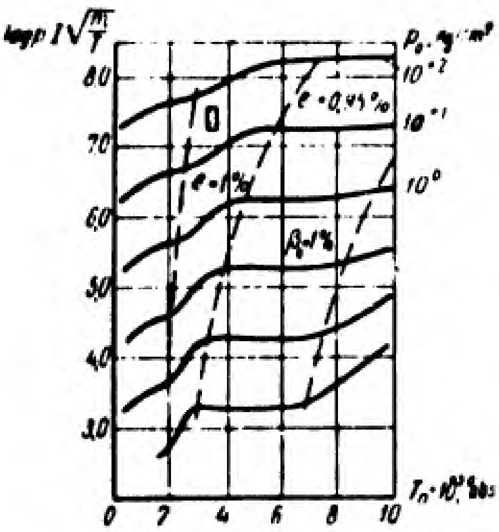

Fig.129 - Convective Product for Hydrogen, as a Function of Temperature and Pressure (the Convective Product for Modern Liquid-Fuel Rocket Engines of Greatest Heat Liberation Rates is Denoted by the Hatched Rectangle)

$$pI\sqrt{\frac{\mu}{T}} = \text{const}\, p\sqrt{T},$$

while the condition of its constancy may be written in the form of

$$\bar{p}^2\bar{T} = 1{,}0. \qquad (221)$$

Besides this condition, the equations of energy, momentum, and state remain valid.

Comparing the equations $\bar{p}\,\bar{v} = \bar{T}$ and eq.(221), we obtain the equation of change of state in p-v coordinates

$$\bar{p}\,\bar{v} = \bar{T} = \frac{1}{\bar{p}^2},$$

whence

$$\bar{p}^3\bar{v} = 1{,}0. \qquad (222)$$

According to the equation of momentum,

$$\bar{f}\,d\bar{p} = -kM_1^2\,d\bar{W}. \qquad (223)$$

Let us eliminate f from eq.(223) by the aid of the equation of the flow rate, which in our case takes the form

$$\bar{f} = \frac{\bar{v}}{\bar{W}} = \frac{1}{\bar{p}^3\bar{W}}. \qquad (224)$$

Combining eqs.(223) and (224), we obtain the relation between the pressure and the gas velocity in the chamber:

$$\frac{1}{\bar{p}^3\bar{W}}\,d\bar{p} = -kM_1^2\,d\bar{W}.$$

or

$$\frac{d\bar{p}}{\bar{p}^2} = -kM_1^2\,\bar{W}\,d\bar{W}.$$

After integration, we find

$$\frac{1}{\bar{p}} = \bar{T} = kM_1^2\,\bar{W}^2 + 1 - kM_1^2. \tag{225}$$

The course of the process will determine the quantity of transferred heat Q. According to the equation of energy,

$$\frac{Q}{C_p T_1} = \bar{Q} = \bar{T} + \frac{k-1}{2} M_1^2 \bar{W}^2 - \bar{T}_1^*,$$

whence

$$\bar{T} = \bar{Q} + \bar{T}_1^* - \frac{k-1}{2} M_1^2 \bar{W}^2. \tag{226}$$

Comparing eqs.(225) and (226), we get a direct relation between the velocity of flow $\bar{W}$ and the heat transferred $\bar{Q}$:

$$\bar{Q} + \bar{T}_1^* - \frac{k-1}{2} M_1^2 \bar{W}^2 = kM_1^2 \bar{W}^2 + 1 - kM_1^2.$$

However,

$$\bar{T}_1^* = 1 + \frac{k-1}{2} M_1^2.$$

Consequently,

$$\bar{Q} = \frac{3k-1}{2} M_1^2 (\bar{W}^2 - 1), \tag{227}$$

whence

$$\bar{W}^2 = 1 + \frac{2}{(3k-1)M_1^2}\bar{Q}. \tag{228}$$

Substituting in eq.(226) the value of $\bar{W}^2$ determined from eq.(228), we get

$$\frac{1}{\bar{p}} = \bar{T} = 1 + \frac{2k}{3k-1}\bar{Q}. \tag{229}$$

In accordance with eq.(224), the cross section of the chamber will vary by the law

$$\bar{f}^2 = \frac{\left(1 + \frac{2k}{3k-1}\bar{Q}\right)^4}{1 + \frac{2}{3k-1}\cdot\frac{\bar{Q}}{M_1^2}}. \tag{230}$$

Consequently, the quantities $\bar{p}$, $\bar{v}$, $\bar{T}$, $\bar{W}$, and $\bar{f}$ may be represented in the form of rather simple functions of $\bar{Q}$.

A chamber of this type may have a throat. From the condition $\frac{d\bar{f}}{d\bar{Q}} = 0$, we determine the quantity of heat delivered to the chamber up to its throat. After simple calculations we find that the maximum constriction of the chamber duct is obtained whenever

$$\bar{Q}=\bar{Q}_{cr}=\frac{3k-1}{4k}\left(1-3kM_1^2\right). \tag{231}$$

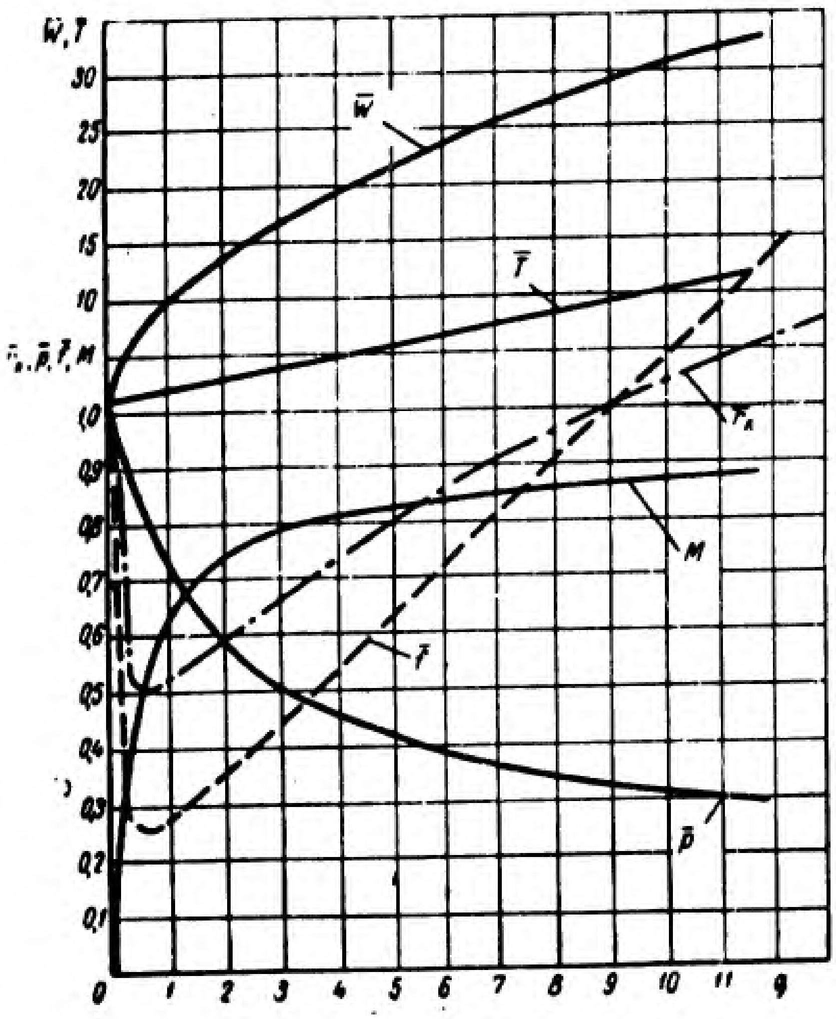

Fig.130 - Principal Gas Parameters and Relative Radius $\bar{r}_k$ as Functions of $\bar{Q}$ in a Chamber at p^2T = const

Substituting this value of $\bar{Q}$ in eq.(229), we determine the temperature in the critical cross section:

$$\bar{T}_{cr}=1.5\left(1-kM_1^2\right). \tag{232}$$

At small values of M_1, we may consider that

$$\bar{T}_{cr} = 1,5.$$

The velocity in the throat does not reach the velocity of sound in this same section. Actually,

$$M^2 = M^2_{cr} = \left(\frac{\bar{W}^2}{\bar{T}}\right)_{cr} M_1^2.$$

From eq.(228), at $\bar{Q} = \bar{Q}_{cr}$, we get

$$\bar{W}^2_{cr} = \frac{1 + kM_1^2}{2kM_1^2}.$$

Making use of eq.(232) yield

$$M^2_{cr} = \frac{1}{3k}. \tag{233}$$

Figure 130 shows the variation of the principal parameters $\bar{p}$, $\bar{T}$, $\bar{W}$, $\bar{f}$, and M with $\bar{Q}$ in a chamber at p^2T = const for the case when, in the initial cross section

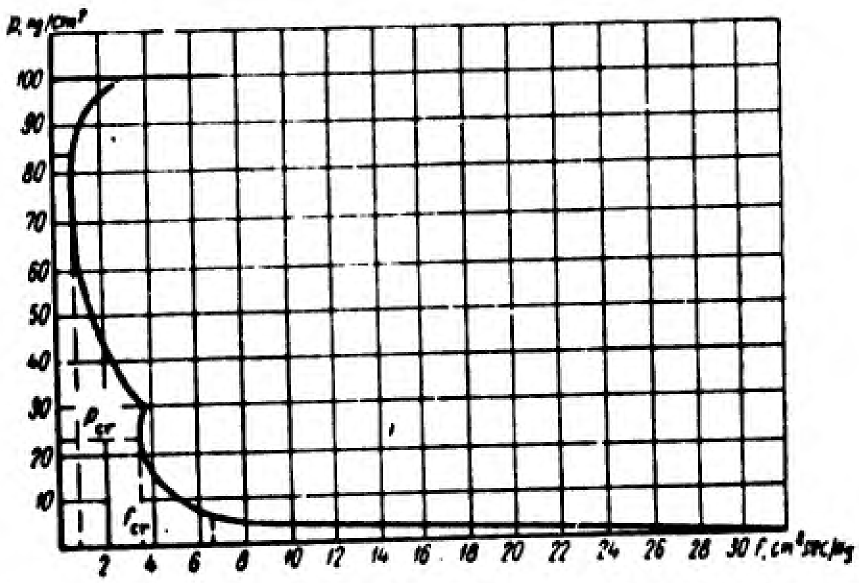

Fig.131 - p-f Diagram of Processes in a Chamber at p^2T = const

(T_1 = 300°K; p_1 = 100 kg/cm², W_1 = 30 m/sec; T_1^* = 3800°K and p_{ex} = 0.1 kg/cm²)

of the chamber, we specify T_1 = 300°K, W_1 = 30 m/sec, p_1 = 100 atm, and a maximum stagnation temperature of T_k^* = 3800°K.

As $\bar{Q}$ increases without limit, the Mach number approaches $\frac{1}{\sqrt{k}}$.

As shown above, the thermal chamber at p^2T = const has a throat.

The specific cross section of the throat is

$$\bar{f}_{thr.} = \frac{3}{2} M_1 \left(1 - kM_1^2\right) \sqrt{3k}.$$

Figure 131 shows the p-f diagram of a chamber at p^2T = const. The chamber has two throats: the first is the throat of the thermal chamber and the second, that of the geometric nozzle. In the latter, the Mach number is 1.

5. Athodyd with Uniform Heat Liberation along the Axis, dQ = bdx

At uniform heat liberation along the axis of the passage, we have

$$d\bar{Q} = c d\bar{x}.$$

The fundamental equations in this case will be

$$\begin{aligned} \bar{p}\bar{v} &= \bar{T}; \\ \bar{p}\bar{f}\bar{W}' &= \bar{T}; \\ \bar{f}d\bar{p} &= -kM_1^2 d\bar{W}'; \\ c(\bar{x}-1) &= \bar{T} - \bar{T}_1^* + \frac{k-1}{2} M_1^2 \bar{W}'^2. \end{aligned} \tag{234}$$

An additional condition is given by the equation of the profile of the duct wall, which permits establishing the relation $\bar{f} = \varphi(\bar{x})$. Different equations of energy will correspond to different profiles. Thus, for a parabolic chamber we have

$$\bar{f} = \bar{x} \text{ and } c(\bar{f} - 1) = \bar{T} - \bar{T}_1^* + \frac{k-1}{2} M_1^2 \bar{W}'^2.$$

In the hyperboloidal chamber, represented in Fig.125, we have

$$\bar{D}^2 = 1 + \left(\frac{x}{a}\right)^2 = 1 + \bar{x}^2 = \bar{f} \text{ and } \bar{x} = \sqrt{\bar{f} - 1}.$$

Then,

$$c\left(\sqrt{\bar{f}-1} - 1\right) = \bar{T} - \bar{T}_1^* + \frac{k-1}{2} M_1^2 \bar{W}'^2.$$

For a conical chamber (Fig.124):

$$\bar{D} = 1 + (\bar{D}_{\kappa} - 1)\bar{x}$$

and

$$\bar{f} = \bar{D}^2 = [1 + (\bar{D}_{\kappa} - 1)\bar{x}]^2.$$

Hence

$$\bar{x} = \frac{\sqrt{\bar{f}} - 1}{\bar{D}_{\kappa} - 1},$$

so that the equation of energy now assumes the form of

$$\bar{Q} = c\left(\frac{\sqrt{\bar{f}} - 1}{\bar{D}_{\kappa} - 1} - 1\right) = \bar{T} - \bar{T}_1^{*} + \frac{k-1}{2} M_1^2 \bar{W}^2.$$

It is a complicated problem to solve the systems of equations found for the profiles in question.

6. Divergent Duct with Uniform Heat Liberation over the Cross Section

Here the system of fundamental equations coincides with the system for a parabolic duct, at uniform heat liberation along the axis. This is explained by the fact that $\bar{f} = \bar{x}$ for a parabolic duct.

In fact,

$$Q = b(f - f_1) \text{ and } \bar{Q} = \frac{b f_1}{\frac{k}{k-1} R T_1} (\bar{f} - 1) = c(\bar{f} - 1).$$

We present the system of equations:

$$\bar{p}\bar{v} = \bar{T};$$

$$\bar{p}\bar{f}\bar{W} = \bar{T};$$

$$\bar{f} d\bar{p} = -kM_1^2 d\bar{W};$$

$$c(\bar{f} - 1) = \bar{T} - \bar{T}_1^{*} + \frac{k-1}{2} M_1^2 \bar{W}^2. \qquad (235)$$

Let us eliminate $\bar{T}$ from the last of these equations, making use of the flow-rate equation

$$c\bar{f} - c = \bar{f}\bar{W}\bar{p} - \bar{T}_1^{*} + \frac{k-1}{2} M_1^2 \bar{W}^2.$$

or

$$\mathcal{J}(c-\overline{W}\overline{p})=c-\overline{T}_1^*+\frac{k-1}{2}M_1^2\overline{W}^2.$$

However, according to the third equation in the system (235),

$$\mathcal{J}=-kM_1^2\frac{d\overline{W}}{d\overline{p}}.$$

Consequently,

$$(\overline{W}\overline{p}-c)\frac{d\overline{W}}{d\overline{p}}=\frac{c-\overline{T}_1^*}{kM_1^2}+\frac{k-1}{2k}\overline{W}^2.$$

We now introduce the notation

$$\frac{c-\overline{T}_1^*}{kM_1^2}=\beta;\ \frac{k-1}{2k}=\alpha.$$

Then,

$$(\overline{W}\overline{p}-c)\frac{d\overline{W}}{d\overline{p}}=\beta+\alpha\overline{W}^2.$$

Dividing both sides of the last equation by $(\beta+\alpha\overline{W}^2)$, we get

$$\frac{\overline{W}\,\overline{p}-c}{\alpha\overline{W}^2+\beta}\cdot\frac{d\overline{W}}{d\overline{p}}-1=0. \qquad (236)$$

Let us assume that

$$\frac{d\overline{W}}{\alpha\overline{W}^2+\beta}=dU.$$

Then,

$$U=\int\frac{d\overline{W}}{\alpha\overline{W}^2+\beta}=\frac{1}{\sqrt{\alpha\beta}}\operatorname{arc\,tg}\sqrt{\frac{\alpha}{\beta}}\,\overline{W}$$

and

$$\overline{W}=\sqrt{\frac{\beta}{\alpha}}\operatorname{tg}\left(\sqrt{\alpha\beta}\,U\right). \qquad (237)$$

Taking account of eq.(237), we get instead of eq.(236),

$$\left[\overline{p}\sqrt{\frac{\beta}{\alpha}}\operatorname{tg}\left(\sqrt{\alpha\beta}\,U\right)-c\right]\frac{dU}{d\overline{p}}=1,0,$$

or

$$\frac{d\overline{p}}{dU}-\overline{p}\sqrt{\frac{\beta}{\alpha}}\operatorname{tg}\left(\sqrt{\alpha\beta}\,U\right)+c=0. \qquad (238)$$

The resultant exact linear differential equation will be solved in two stages.

At first we will solve the homogeneous equation

$$\frac{d\bar{p}}{dU}-\bar{p}\sqrt{\frac{\beta}{\alpha}}\operatorname{tg}\left(\sqrt{\alpha\beta}\,U\right)=0,$$

or

$$\frac{d\bar{p}}{\bar{p}}=\sqrt{\frac{\beta}{\alpha}}\operatorname{tg}\left(\sqrt{\alpha\beta}\,U\right)dU=\frac{1}{\alpha}\operatorname{tg}\left(\sqrt{\alpha\beta}\,U\right)d\left(\sqrt{\alpha\beta}\,U\right).$$

After integration, we get

$$\ln\bar{p}=-\frac{1}{\alpha}\ln\cos\left(\sqrt{\alpha\beta}\,U\right)+c,$$

or

$$\ln\bar{p}=\ln c\left[\cos\left(\sqrt{\alpha\beta}\,U\right)\right]^{-\frac{1}{\alpha}},$$

or

$$\bar{p}=E\left[\cos\left(\sqrt{\alpha\beta}\,U\right)\right]^{-} \tag{239}$$

Here,

$$E=F(U),$$

where E must be such that the exact equation (238) shall be satisfied.

Then,

$$\bar{p}=F(U)\cos^{-\frac{1}{\alpha}}\left(\sqrt{\alpha\beta}\,U\right). \tag{240}$$

Let us derive the expression for the first derivative $\frac{d\bar{p}}{dU}$:

$$\frac{d\bar{p}}{dU}=\cos^{-\frac{1}{\alpha}}\left(\sqrt{\alpha\beta}\,U\right)\frac{dF(U)}{dU}+F(U)\frac{1}{\alpha}\cos^{-\frac{1}{\alpha}}\left(\sqrt{\alpha\beta}\,U\right)\times\frac{\sin\left(\sqrt{\alpha\beta}\,U\right)}{\cos\left(\sqrt{\alpha\beta}\,U\right)}\sqrt{\alpha\beta}=\cos^{-\frac{1}{\alpha}}\left(\sqrt{\alpha\beta}\,U\right)\frac{dF(U)}{dU}+\bar{p}\sqrt{\frac{\beta}{\alpha}}\operatorname{tg}\left(\sqrt{\alpha\beta}\,U\right).$$

Substituting for $\frac{d\bar{p}}{dU}$ its value from eq.(238), we find the form of the function F (U):

$$dF(U)=-\frac{c}{\sqrt{\alpha\beta}}\cos^{\frac{1}{\alpha}}\left(\sqrt{\alpha\beta}\,U\right)d\left(\sqrt{\alpha\beta}\,U\right).$$

For integration, it is necessary to establish the value of the exponent $\frac{1}{\alpha}$. The integration is performed for integral values of $\frac{1}{\alpha}$.

Table 15 shows the adiabatic exponents k at which a simple determination of the function F (U) is possible.

Table 15

Adiabatic Exponents k at which a Simple Determination of the Function F (U) is Possible

k	1,667	1,4	1,333	1,2	1,1
$\frac{1}{a}=\frac{2k}{k-1}$	5	7	8	12	22

Considering the gas to be monatomic, we take for the integration k = 1.667 and $\frac{1}{a}$ = 5. Then,

$$F(U)=-\frac{c}{\sqrt{\alpha\beta}}\int\cos^5\left(\sqrt{\alpha\beta}\,U\right)d\left(\sqrt{\alpha\beta}\,U\right).$$

After integration, we get

$$-F(U)=\frac{c}{\sqrt{\alpha\beta}}\left[\sin\left(\sqrt{\alpha\beta}\,U\right)-\frac{2}{3}\sin^3\left(\sqrt{\alpha\beta}\,U\right)+\right.$$
$$\left.+\frac{1}{5}\sin^5\left(\sqrt{\alpha\beta}\,U\right)+N\right],$$

where N is an integration constant.

Let us substitute the expression found for F (U) in eq.(240):

$$\bar{p}=\cos^{-\frac{1}{a}}\left(\sqrt{\alpha\beta}\,U\right)\frac{c}{\sqrt{\alpha\beta}}\left[\sin\left(\sqrt{\alpha\beta}\,U\right)-\frac{2}{3}\sin^3\left(\sqrt{\alpha\beta}\,U\right)+\right.$$
$$\left.+\frac{1}{5}\sin^5\left(\sqrt{\alpha\beta}\,U\right)+N\right].$$

If we now eliminate U, then, making use of eq.(237), we find the relation between the gas pressure and the gas velocity in explicit form.

According to eq.(237), we have

$$\mathrm{tg}\left(\sqrt{\alpha\beta}\,U\right)=\sqrt{\frac{\alpha}{\beta}}\,\overline{W}.$$

Consequently,

$$\cos\left(\sqrt{\alpha\beta}\,U\right) = \frac{1}{\sqrt{1+\frac{\alpha}{\beta}\overline{W}^2}} = \sqrt{\frac{\beta}{\beta+\alpha\overline{W}^2}};$$

$$\sin\left(\sqrt{\alpha\beta}\,U\right) = \frac{\sqrt{\frac{\alpha}{\beta}}\,\overline{W}}{\sqrt{1+\frac{\alpha}{\beta}\overline{W}^2}} = \sqrt{\frac{\alpha}{\beta+\alpha\overline{W}^2}}.$$

Then,

$$-\bar{p} = \frac{c}{\sqrt{\alpha\beta}}\left(\frac{\beta+\alpha\overline{W}^2}{\beta}\right)^{2.5}\left[\overline{W}\left(\frac{\alpha}{\beta+\alpha\overline{W}^2}\right)^{0.5} - \frac{2}{3}\overline{W}^3\left(\frac{\alpha}{\beta+\alpha\overline{W}^2}\right)^{1.5} + \right.$$

$$\left. + \frac{\overline{W}^5}{5}\left(\frac{\alpha}{\beta+\alpha\overline{W}^2}\right)^{2.5} + N\right],$$

or

$$-\bar{p} = \frac{c}{\beta}\left(\frac{\beta+\alpha\overline{W}^2}{\beta}\right)^2\left[\overline{W} - \frac{2}{3}\overline{W}^3\left(\frac{\alpha}{\beta+\alpha\overline{W}^2}\right) + \frac{\overline{W}^5}{5}\left(\frac{\alpha}{\beta+\alpha\overline{W}^2}\right)^2 + \right.$$

$$\left. + N\sqrt{\frac{\beta+\alpha\overline{W}^2}{\alpha}}\right] = \frac{c\overline{W}}{\beta}\left(\frac{\beta+\alpha\overline{W}^2}{\beta}\right)^2\left[1 - \frac{2}{3}\overline{W}^2\left(\frac{\alpha}{\beta+\alpha\overline{W}^2}\right) + \right.$$

$$\left. + \frac{\overline{W}^4}{5}\left(\frac{\alpha}{\beta+\alpha\overline{W}^2}\right)^2 + N\sqrt{\frac{\beta+\alpha\overline{W}^2}{\alpha\overline{W}^2}}\right]. \qquad (241)$$

The value of the constant N is then determined from the initial conditions, when relative velocity the at $\bar{p} = \bar{p}_1 = 1.0$ will be $\overline{W}_1 = 1.0$. For this case, we find the following expression from eq.(241):

$$-1.0 = \frac{c}{\beta}\left(\frac{\beta+\alpha}{\beta}\right)^2\left[1 - \frac{2}{3}\frac{\alpha}{\beta+\alpha} + \frac{1}{5}\left(\frac{\alpha}{\beta+\alpha}\right)^2 + N\sqrt{\frac{\beta+\alpha}{\alpha}}\right],$$

whence

$$N = -\sqrt{\frac{\alpha}{\beta+\alpha}}\left[1 - \frac{2}{3}\cdot\frac{\alpha}{\beta+\alpha} + \left(\frac{1}{\beta+\alpha}\right)^2\left(\frac{\beta^3}{c\alpha^2} + \frac{1}{5}\right)\right].$$

Since the solution was obtained for k = 1.667 and α = 0.2, it follows that

$$N = -\sqrt{\frac{1}{5\beta+1}}\left[1 - \frac{2}{3(5\beta+1)} + \left(\frac{1}{5\beta+1}\right)^2\left(\frac{25\beta^3}{c} + 0.2\right)\right]. \qquad (242)$$

Having found the relation (241) $\bar{p} = f(\overline{W})$, we can pass to the relations between the gas parameters and the cross section of the athodyd $\bar{f}$.

Let us substitute the quantity $\bar{T}$ in the equation of energy by its expression from the equation of constant rate of flow. Then,

$$c(\bar{f}-1)=\bar{f}\,\bar{W}\bar{p}-\bar{T}_1^*+\frac{k-1}{2}M_1^2\bar{W}^2,$$

whence

$$f(c-\bar{W}\bar{p})=c-\bar{T}_1^*+\frac{k-1}{2}M_1^2\bar{W}^2=kM_1^2\left(\frac{c-\bar{T}_1^*}{kM_1^2}+\frac{k-1}{2k}\bar{W}^2\right)=$$
$$=kM_1^2(\beta+\alpha\bar{W}^2).$$

Hence,

$$\bar{f}=kM_1^2\frac{\beta+\alpha\bar{W}^2}{c-\bar{W}\bar{p}}.$$

Let us eliminate from this equation the second summand $\bar{W}\,\bar{p}$ of the denominator, making use of eq.(241),

$$\bar{f}=\frac{kM_1^2(\beta+\alpha\bar{W}^2)}{A}=\frac{kM_1^2}{c}\cdot\frac{\beta+\alpha\bar{W}^2}{B}, \tag{243}$$

where

$$A=c+\frac{c\bar{W}}{\beta}\left(\frac{\beta+\alpha\bar{W}^2}{\beta}\right)^2\left[\bar{W}-\frac{2}{3}\bar{W}^3\left(\frac{\alpha}{\beta+\alpha\bar{W}^2}\right)+\frac{\bar{W}^5}{5}\left(\frac{\alpha}{\beta+\alpha\bar{W}^2}\right)^2+\right.$$
$$\left.+N\sqrt{\frac{\beta+\alpha\bar{W}^2}{\alpha}}\right];$$
$$B=1+\frac{\bar{W}^2}{\beta}\left(\frac{\beta+\alpha\bar{W}^2}{\beta}\right)^2\left[1-\frac{2}{3}\bar{W}^2\left(\frac{\alpha}{\beta+\alpha\bar{W}^2}\right)+\frac{\bar{W}^4}{5}\left(\frac{\alpha}{\beta+\alpha\bar{W}^2}\right)^2+\right.$$
$$\left.+N\sqrt{\frac{\beta+\alpha\bar{W}^2}{\alpha\bar{W}^2}}\right].$$

Let us next determine the temperature:

$$\bar{T}=\bar{f}\,\bar{W}\bar{p}=kM_1^2\frac{\beta+\alpha\bar{W}^2}{c-\bar{W}\bar{p}}\bar{W}\bar{p}=kM_1^2\frac{\beta+\alpha\bar{W}^2}{\frac{c}{\bar{W}\bar{p}}-1}.$$

Using for $\bar{W}\,\bar{p}$ its expression from eq.(241), we get

$$\bar{T}=\frac{kM_1^2(\beta+\alpha\bar{W}^2)}{A}, \tag{244}$$

where

$$A=1+\frac{\beta}{\bar{W}^2}\left(\frac{\beta}{\beta+\alpha\bar{W}^2}\right)^2\times\left[1-\frac{2}{3}\bar{W}^2\left(\frac{\alpha}{\beta+\alpha\bar{W}^2}\right)+\frac{\bar{W}^4}{5}\left(\frac{\alpha}{\beta+\alpha\bar{W}^2}\right)^2+\right.$$
$$\left.+N\sqrt{\frac{\beta+\alpha\bar{W}^2}{\alpha\bar{W}^2}}\right].$$

The specific volume of the gas is

$$\bar{v} = \frac{\bar{T}}{\bar{p}} = \overline{W}'\bar{f}. \tag{245}$$

Equations (241), (243), (244), and (245) solve the question as to the variation of the gas parameters in the athodyd of arbitrary profile, with the above law of heat liberation $dQ = bdf$. Only the velocity $\overline{W}$ is directly correlated with $\bar{f}$ in eq.(243). The parameters $\bar{p}$, $\bar{v}$, and $\bar{T}$ are given in the computational formulas (241), (244), and (245) as a function of the velocity $\overline{W}$. The quantity of heat supplied is determined from the equation

$$\bar{Q} = \bar{c}(\bar{f} - 1).$$

If the gas parameters must be expressed as functions of the quantity of heat liberated, then we can write

$$\bar{f} = 1 + \frac{\bar{Q}}{\bar{c}}.$$

on the left-hand side of eq.(243).

The resultant formulas are also valid for a duct in which the heat liberation is proportional to the length of the chamber, if a linear relation exists between the cross section $\bar{f}$ and the length. This has been found for a parabolic chamber in which $\bar{f} = \bar{x}$.

7. Athodyd with Uniform Heat Liberation over the Wall Surface

Let us denote the inner surface of the duct by the symbol Φ. Then,

$$dQ = bd\Phi.$$

The solution of the problem of the variation of the gas parameters with Φ or Q is more complex than in the preceding case. If the profile of the chamber is such that

$$d\Phi = cdf,$$

then $\bar{\Phi} = \bar{f}$, and the system of fundamental equations indicated in the preceding example is also valid for this case. The relation between the surface area of the duct walls and its cross section is linear in all conical ducts. Consequently, for thermal conical ducts with uniform heat liberation over the inner surface, eqs. (241), (243), (244), and (245) are valid. The simpler the relations between Φ and f, the simpler will it be to solve the fundamental system of equations, to which the equation of the chamber profile wall is added.

If y is the current radius in a cross section of the duct, then

$$d\Phi = 2\pi y \sqrt{1+\left(\frac{dy}{dx}\right)^2}\, dx \text{ and } df = d(\pi y^2) = 2\pi y dy.$$

Hence,

$$\frac{d\Phi}{df} = \frac{\sqrt{1+\left(\frac{dy}{dx}\right)^2}}{\frac{dy}{dx}} = \sqrt{\left(\frac{dx}{dy}\right)^2+1}. \tag{246}$$

In the solution, we make use of the equations

$$\bar{p}\,\bar{v} = \bar{T};$$
$$\bar{p}\,\bar{f}\,\bar{W} = \bar{T};$$
$$\bar{f}\,d\bar{p} = -kM_1^2 d\bar{W};$$
$$\bar{Q} = \frac{bf_1}{\frac{k}{k-1}RT_1}\int\sqrt{\left(\frac{dx}{dy}\right)^2+1}\,d\bar{f} = c\int\sqrt{\left(\frac{dx}{dy}\right)^2+1}\,d\bar{f} = \bar{T} -$$
$$-\bar{T}_1^* + \frac{k-1}{2}M_1^2\bar{W}^2,$$

where $f = \varphi(x, y)$ or, if the shape of the longitudinal section of the chamber is specified, $y = F(x)$.

As an example, let us derive the equation of energy for a parabolic profile of a duct for which

$$y^2 = \frac{y_1^2}{x_1}x \text{ and } \frac{dy}{dx} = \frac{y_1}{2x_1}\sqrt{\frac{1}{\bar{x}}} = \frac{y_1}{2x_1}\sqrt{\frac{1}{\bar{f}}}.$$

Since, in a parabolic duct, $\bar{x} = \bar{f}$, then

$$\sqrt{\left(\frac{dx}{dy}\right)^2+1} = \sqrt{\frac{4x_1^2}{y_1^2}\bar{f}+1}$$

and

$$\bar{Q} = c\int_{1.0}^{\bar{f}} \sqrt{\frac{4x_1^2}{y_1^2}\bar{f} + 1}\, d\bar{f} = c\,\frac{y_1^2}{6x_1^2}\left(1 + \frac{4x_1^2}{y_1^2}\bar{f}\right)^{1.5} + N.$$

The constant N is determined from the condition $\bar{Q} = 0$ at $\bar{f} = 1.0$:

$$N = -\frac{c}{6x_1^2 y_1}\left(y_1^2 + 4x_1^2\right)^{1.5}.$$

Consequently, the equation of energy for a parabolic duct with uniform heat liberation over the wall surface takes the form

$$c\,\frac{y_1^2}{6x_1^2}\left(1 + \frac{4x_1^2}{y_1^2}f\right)^{1.5} + N = T - T_1 + \frac{k-1}{2}M_1^2 W^2.$$

Section 17. Velocity Chamber with Gradual Supply of Heat and Propellant

A chamber in which the supply of heat and working fluid is distributed by some

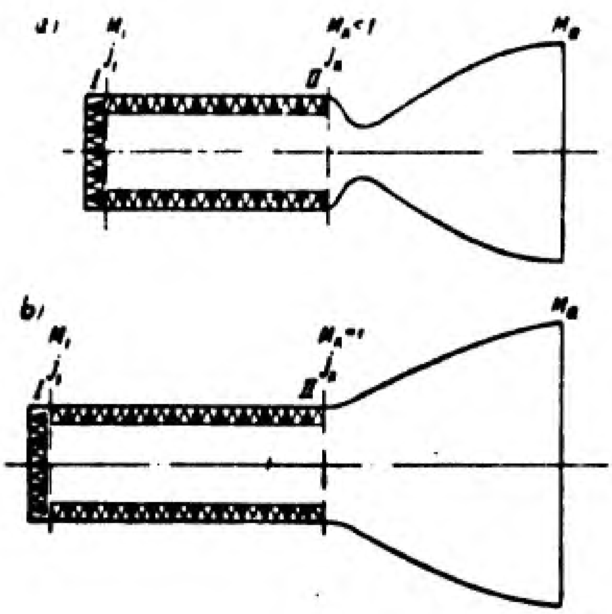

Fig.132 - Schematic Diagram of Chamber with Heat-Consuming Duct

a - Case of $M_k < 1$; b - Case of $M_k = 1$

law over the length of the chamber will be termed heat-consuming. By comparison, this chamber has one more variable than the thermal chamber, namely the rate of flow per second, which is different in each cross section.

The additional relation between the parameters may take various forms. In chemical engines, the relation $Q = f(G)$ may be taken as linear. In gas-nuclear engines it may be more complex.

Figure 132 is a schematic diagram of a chamber with a heat-consuming duct. This duct is located between sections I-I and II-II. Up to this point, a total of G_1 kg of propellant has been supplied to the chamber, and heat liberation has occurred at p = const. In the section I-I, the gas parameters p_1, T_1, W_1 and thus also M_1 are all known. In the end section of the chamber, II-II, the propellant feed and the heat transfer are completed. Here the weight rate of flow is G_k and the gas parameters p_k, T_k, W_k, and $M_k \leq 1.0$.

For the ideal case, instantaneous reaction of the fed components is assumed. This means that the laws of heat supply and of supply of working fluid are the same, i.e.,

$$Q = H_u G,$$

where H_u is the heat value of the propellant in the chemical engine.

Let us write the fundamental equations for the heat-consuming chamber. As before, the equation of state has the following form:

$$\bar{p}\bar{v} = \bar{T}.$$

From the equation of the weight rate of flow,

$$G = WF\frac{p}{RT},$$

it follows that

$$\frac{G}{G_1} = \frac{W}{W_1}\,\frac{F}{F_1}\,\frac{p}{p_1}\,\frac{T_1}{T}.$$

We now introduce the notation $\frac{G}{G_1} = j$. Then, in the generalized form, the equation is written as follows:

$$j = \frac{\bar{W}\bar{F}\bar{p}}{\bar{T}}. \tag{247}$$

The working fluid enters the chamber in the same state in each cross section.

In the ideal case, the elementary portion of gas dG, arriving in the chamber, acquires the velocity W and the temperature T in the entrance section. Then, the equation of energy takes the form

$$dQ = H_u dG = \frac{k}{k-1} Rd(GT) + d\left(\frac{W^2}{2g} G\right).$$

In the final form, it reads

$$H_u(G - G_1) = \frac{k}{k-1} R(GT - G_1T_1) + \frac{W^2}{2g} G - \frac{W_1^2}{2g} G_1;$$

$$H_u(j-1)G_1 = \frac{k}{k-1} RG_1T_1(j\overline{T} - 1) + \frac{W_1^2 G_1}{2g}(\overline{W}^2 j - 1).$$

Setting

$$\frac{H_u}{\frac{k}{k-1} RT_1} = q,$$

we obtain finally

$$\overline{Q} = q(j-1) = j\left(\overline{T} + \frac{k-1}{2} M_1^2 \overline{W}^2\right) - \left(1 + \frac{k-1}{2} M_1^2\right). \tag{248}$$

At variable rate of flow, the equation of momentum has the form

$$Fdp = -\frac{d(WG)}{g},$$

or

$$F_1 p_1 \overline{F} d\overline{p} = -W_1 G_1 \frac{d(\overline{W} j)}{g}.$$

Since

$$G_1 = \frac{W_1 F_1 p_1}{RT_1},$$

it follows that

$$\overline{F} d\overline{p} = -kM_1^2 d(\overline{W} j),$$

or, finally,

$$\int_{1,0}^{p} \overline{F} d\overline{p} = -kM_1^2 (\overline{W} j - 1). \tag{249}$$

Consequently, the fundamental equations of the heat-consuming chamber will be

$$\overline{p}\,\overline{v} = \overline{T};$$

$$\bar{p}\bar{F}\bar{W}=j\bar{T};$$

$$\bar{F}d\bar{p}=-kM_1^2d\left(\bar{W}j\right); \tag{250}$$

$$\bar{Q}=q\,(j-1)=j\left(\bar{T}+\frac{k-1}{2}M_1^2\bar{W}^2\right)-\bar{T}_1^*.$$

Let us consider the case of a cylindrical chamber at $\bar{F}$ = const.

The equation of state and the first equation of the system (250) are still in force. Instead of the second equation of the system (250), we get

$$j=\frac{\bar{W}\bar{p}}{\bar{T}} \tag{251}$$

and, instead of the third equation,

$$\bar{p}=1-kM_1^2(\bar{W}j-1). \tag{252}$$

These four eqs.(250) permit us to express four of the five parameters, $\bar{p}$, $\bar{v}$, $\bar{T}$, $\bar{W}$, j in the form of functions of the fifth parameter. Assigning j, from the equation of energy balance [eq.(248)], the velocity $\bar{W}$ can be determined if we eliminate the quantity $\bar{T}$ from it. According to eq.(251), the temperature will be

$$\bar{T}=\frac{\bar{W}\bar{p}}{j},$$

or, after substituting $\bar{p}$ from eq.(252),

$$\bar{T}=\left(1+kM_1^2\right)\frac{\bar{W}}{j}-kM_1^2\bar{W}^2. \tag{253}$$

Substituting this temperature value in eq.(248), we obtain the following quadratic equation to determine the velocity:

$$jM_1^2\frac{k+1}{2}\bar{W}^2-\left(1+kM_1^2\right)\bar{W}+\left[\bar{T}_1^*+q\,(j-1)\right]=0.$$

We then determine $\bar{p}$ and $\bar{T}$ from eqs.(252) and (253).

It is also convenient to make use of the relations between the gas parameters and the Mach number. Bearing eq.(251) in mind, we may write

$$\bar{W}j = \bar{W}\frac{\bar{W}\bar{p}}{\bar{T}} = \frac{\bar{W}^2\bar{p}}{\bar{T}} = \frac{M^2}{M_1^2}\bar{p}.$$

Substituting this value of $\bar{W}j$ in eq.(252), we obtain, as for the athodyd,

$$\bar{p} = \frac{1 + kM_1^2}{1 + kM^2}. \tag{254}$$

We determine the temperature from the equation of rate of flow [eq.(251)]:

$$\bar{T} = \frac{\bar{W}\bar{p}}{j}.$$

Multiplying the right-hand side of this last equation by $\frac{\bar{W}\bar{p}}{j\bar{T}} = 1$, we get

$$\bar{T} = \frac{M^2}{M_1^2}\cdot\frac{\bar{p}^2}{j},$$

or

$$\bar{T} = \frac{1}{j}\left(\frac{M^2}{M_1^2}\right)\left(\frac{1 + kM_1^2}{1 + kM^2}\right)^2. \tag{255}$$

We determine the specific volume and the velocity from the expressions

$$\bar{v} = \frac{1}{j}\cdot\frac{M^2}{M_1^2}\cdot\frac{1 + kM_1^2}{1 + kM^2};$$

$$\bar{W} = j\bar{v} = \frac{1}{j}\cdot\frac{M^2}{M_1^2}\cdot\frac{1 + kM_1^2}{1 + kM^2}. \tag{256}$$

We then find the Mach number, at a specified value of j, from the equation of energy [eq.(248)] which, after replacing $\bar{T}$ and $\bar{W}$ by their expressions from eqs.(255) and (256), takes the form

$$\left[\frac{k-1}{2}\cdot\frac{(1 + kM_1^2)^2}{M_1^2} - jk^2\bar{Q}_1\right]M^4 + \left[\frac{(1 + kM_1^2)^2}{M_1^2} - 2jk\bar{Q}_1\right]M^2 - j\bar{Q}_1 = 0, \tag{257}$$

where $\bar{Q}_1$ is the total relative quantity of heat transferred to the first and second parts of the chamber, i.e.,

$$\bar{Q}_1 = \bar{Q}_1 + \bar{Q}_k = \bar{T}_1^* + q(j-1).$$

Setting $M_k = 1$ and $q = 1$ in eq.(257), we find the relation $M_1 = f(j)$ shown in Fig.133.

Example. Find the distribution of $\bar{p}$, $\bar{T}$, $\bar{v}$, and $\bar{f}$ along the length of the chamber for the case

$$W_1 = 30\ m/sec; \qquad T_1 = 300°\ abs.; \quad k = 1{,}2;$$
$$R = 30\ kg{\cdot}m/kg{\cdot}deg; \quad j_k = 10; \qquad M_a = 2{,}0; \quad q = 1.$$

In the initial cross section, 0.1 of the total propellant feed is supplied.

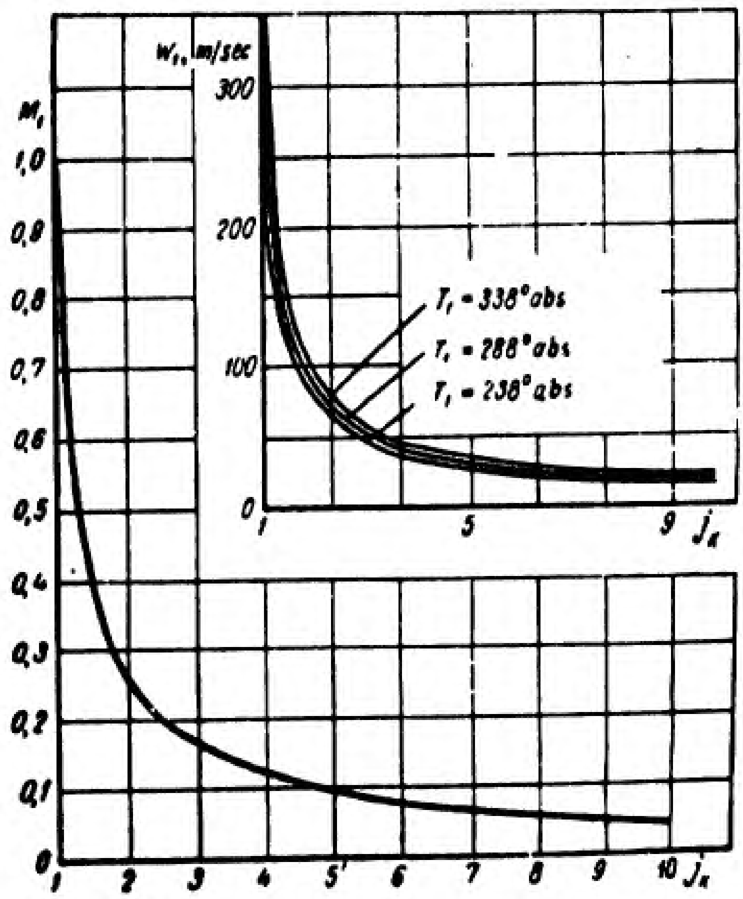

Fig.133 - Relation of the Mach Number M_1 and of W_1 to the Relative Rate of Flow, for the Case $M_k = 1$ and $q = 1$

On the basis of eq.(256), we determine the relation $M = f(j)$. Then, substituting the resultant values of M in eqs.(254), (255), and (256), we find the distribution of $\bar{p}$, $\bar{T}$, and $\bar{v}$ along the length of the combustion chamber.

Table 16 is a summary of the results.

Table 16

Results of Calculation of Gas Parameters as a Function of j

j	1	2	3	4	5	6	7	8	9	10
M	0,02915	0,05847	0,08814	0,1183	0,1493	0,1813	0,2146	0,2496	0,2867	0,3267
$\bar{p}$	1	0,9969	0,9917	0,9845	0,9749	0,9630	0,9466	0,9314	0,9111	0,8873
$\bar{T}$	1	0,9996	0,9992	0,9976	0,9973	0,9968	0,9953	0,9938	0,9915	0,9894
$\bar{\rho}$	1	1,0027	1,0075	1,0134	1,023	1,035	1,049	1,067	1,088	1,115

Table 17

Results of Calculation of Gas Parameters in a Geometric Nozzle

M	0,4	0,6	0,8	1,0	1,2	1,4	1,6	1,8	2,0
$\bar{p}$	0,8598	0,7648	0,6518	0,5338	0,4219	0,3231	0,2408	0,1755	0,1256
$\bar{T}$	0,9842	0,9652	0,9398	0,9091	0,8741	0,8361	0,7962	0,7553	0,7143
$\bar{\rho}$	1,1447	1,2619	1,4419	1,7029	2,0719	2,5876	3,3052	4,3021	5,6870
λ	0,8449	0,6268	0,5444	0,5235	0,5408	0,5919	0,6782	0,8056	0,9852

Table 17 gives the results of a calculation of gas parameters in a geometric nozzle.

Figure 134 shows the gas parameters $\bar{p}$, $\bar{T}$, $\bar{v}$, $\bar{W}$ as a function of j.

Figure 135 shows the processes taking place in the athodyd and nozzle, plotted in the I-S coordinate system.

Let us consider two more special examples.

Let the duct be isothermal, i.e., let $\bar{T} = \bar{T}_1 = 1.0$

Then, the fundamental equations will be

$$\begin{gathered}\bar{p}\bar{v}=1{,}0;\\ \bar{p}\bar{F}\bar{W}=j;\\ \bar{F}d\bar{p}=-kM_1^2 d(\bar{W}j);\\ q(j-1)=j\left(1+\frac{k-1}{2}M_1^2\bar{W}^2\right)-\bar{T}_1^*.\end{gathered} \tag{258}$$

In the last equation, we obtain a direct relation between the gas velocity and the independent variable j:

$$\bar{W}=\sqrt{\frac{2}{(k-1)M_1^2}}\sqrt{q-1-\frac{q-\bar{T}_1^*}{j}}. \tag{259}$$

Eliminating $\bar{F}$ from the second and third equations of the system (258), we may write

$$\frac{d\bar{p}}{\bar{p}}=-kM_1^2\frac{\bar{W}}{j}d(\bar{W}j).$$

However,

$$d(\bar{W}j)=d\left[j\sqrt{\frac{2}{(k-1)M_1^2}}\sqrt{q-1-\frac{q-\bar{T}_1^*}{j}}\right]=$$

$$=\sqrt{\frac{2}{(k-1)M_1^2}}\left[\frac{2j(q-1)-(q-\bar{T}_1^*)}{2j\sqrt{q-1-\frac{q-\bar{T}_1^*}{j}}}\right]dj.$$

Then,

$$\frac{d\bar{p}}{\bar{p}}=-\frac{2k}{k-1}\,\frac{2j(q-1)-(q-\bar{T}_1^*)}{2j^2}\,dj,$$

whence

$$-\ln\bar{p}=\frac{2k(q-1)}{k-1}\ln j-\frac{k(q-\bar{T}_1^*)}{k-1}\left(1-\frac{1}{j}\right). \tag{260}$$

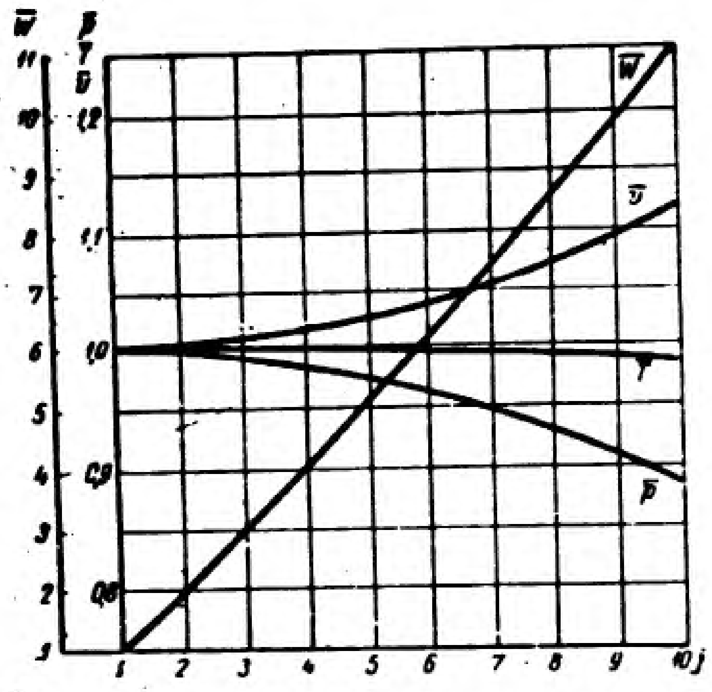

Fig.134 - Variation of Gas Parameters in a Heat-Consuming Chamber at $\bar{F} = 1$, as a Function of the Relative Rate of Flow j

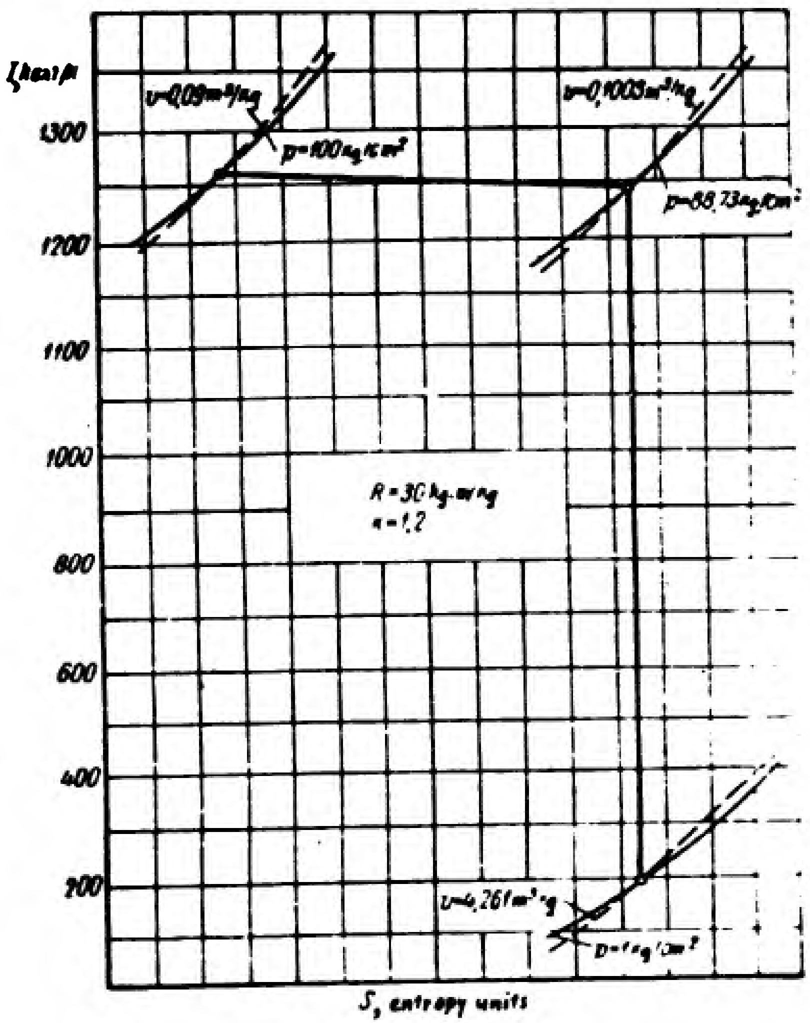

Fig.135 - I-S Diagram of Process in a Heat-Consuming Chamber at $\bar{F} = 1$ and in the Nozzle

We determine the cross-sectional variation of the duct as a function of j, from the equation of constant rate of flow, by taking the logarithms of both sides:

$$\ln \bar{F} = \ln j - \ln \overline{W} - \ln \bar{p},$$

or

$$\ln \bar{F} = \frac{k(2q-1)-1}{k-1} \ln j - 0{,}5 \ln\left(q - 1 - \frac{q - \bar{T}_1^*}{j}\right) - \frac{k\left(q-\bar{T}_1^*\right)}{k-1}\left(1 - \frac{1}{j}\right) - 0{,}5 \ln \frac{2}{(k-1) M_1^2}. \qquad (261)$$

For an isobaric heat-consuming chamber, the fundamental equations are now substantially simplified

$$\begin{aligned} \bar{v} &= \bar{T}; \\ \bar{F}\,\overline{W} &= j\bar{T}; \\ d(\overline{W}j) &= 0; \\ q(j-1) &= j\left(\bar{T} + \frac{k-1}{2} M_1^2 \overline{W}^2\right) - \bar{T}_1^*. \end{aligned} \qquad (262)$$

From the third equation of the system (262), we get

$$\frac{dj}{j} = -\frac{d\overline{W}}{\overline{W}}$$

and

$$\overline{W} = \frac{1}{j}. \qquad (263)$$

The gas velocity decreases with increasing propellant feed.

Substituting the value of $\overline{W}$ from eq.(263) in the equation of energy, we find the relation between the temperature and the amount of propellant supplied:

$$q(j-1) = j\left(\bar{T} + \frac{k-1}{2} M_1^2 \frac{1}{j^2}\right) - \bar{T}_1^*.$$

Hence,

$$\bar{T} = q - \frac{1}{j}\left(q - \bar{T}_1^*\right) - \frac{k-1}{2} M_1^2 \frac{1}{j^2}. \qquad (264)$$

Finally,

$$\bar{F} = \frac{\bar{T}}{\overline{W}} = j^2 \bar{T} = qj^2 - j\left(q - \bar{T}_1^*\right) - \frac{k-1}{2} M_1^2. \qquad (265)$$

These equations indicate that, in a thermal isobaric duct, the temperature and the cross section increase with increasing j, while the velocity decreases.

The characteristics of a spherical heat-consuming chamber are considerably more complex.

It follows from the geometric properties of this chamber that

$$d\bar{\Phi} = d\bar{x}.$$

In our case,

$$d\bar{\Phi} = dx = dj.$$

The relation between the cross section F and the coordinates x or j is established on the basis of the equation of the surface of a sphere:

$$F = \pi y^2.$$

The equation of the spherical surface, in rectangular coordinates xy (Fig.136), if R is the radius of the surface, reads as follows:

$$y^2 = 2Rx - x^2,$$

Therefore,

$$\bar{F} = \frac{F}{F_1} = \frac{y^2}{y_1^2} = \frac{2Rx - x^2}{y_1^2}.$$

Passing to relative coordinates, we get

$$\bar{F} = \frac{x_1^2}{y_1^2}\left(2\bar{R}\bar{x} - \bar{x}^2\right) = \frac{2\bar{R}\bar{x} - \bar{x}^2}{m},$$

whence

$$\bar{x} = \bar{\Phi} = j = \bar{R} \pm \sqrt{\bar{R}^2 - m\bar{F}}. \quad (266)$$

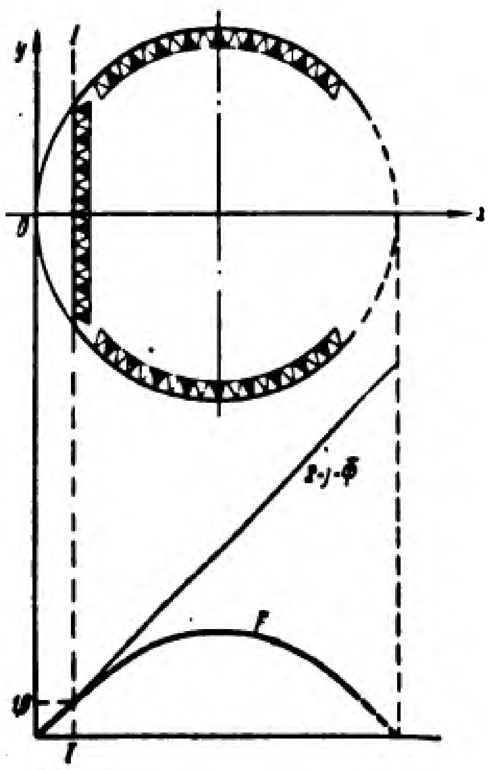

Fig.136 - Schematic Diagram of Heat-Consuming Spherical Chamber

The plus sign corresponds to the second half of the sphere and the minus sign to the first half.

Bearing eq.(266) in mind, the system of fundamental equations of the spherical chamber (first half of the sphere) is of the form

$$\bar{p}\bar{v} = \bar{T};$$
$$\bar{p}\bar{F}\bar{W} = \bar{T}\left(\bar{R} - \sqrt{\bar{R}^2 - m\bar{F}}\right);$$
$$\bar{F}d\bar{p} = -kM_1^2 d\left[\bar{W}\left(\bar{R} - \sqrt{\bar{R}^2 - m\bar{F}}\right)\right];$$
$$q\left(\bar{R} - 1 - \sqrt{\bar{R}^2 - m\bar{F}}\right) = \left(\bar{R} - \sqrt{\bar{R}^2 - m\bar{F}}\right) \times$$
$$\times \left(\bar{T} + \frac{k-1}{2} M_1^2 \bar{W}^2\right) - \bar{T}_1^*. \qquad (267)$$

Simultaneous solution of these equations does not lead to a direct relation between the parameters $\bar{p}$, $\bar{T}$, and $\bar{W}$ and the coordinate $\bar{x} = j$.

In this case, it is necessary to use a computer or to solve the problem by numerous approximations, performed for each cross section of the chamber.

Section 18. Effect of Regeneration on the Parameters of a Rocket Engine at p = c

We know from the theory of heat engines that the transition from a simple cycle to a regenerative cycle increases the economy of an engine.

During the process of regeneration, heat passes from some portions of the working fluid to other portions which are in a different phase of the cycle.

The working fluid may receive heat in the regenerative elements during compression or after compression, and may give up heat to the regenerator during expansion or after expansion. The higher the initial temperature difference between the individual portions of the working fluid participating in the heat exchange, the more readily is a high economy of the cycle obtained.

In a liquid-fuel rocket engine, the temperature of the working fluid during expansion and at the end of expansion is appreciably higher than in atmospheric or air-dependent engines, i.e., in conventional heat engines which use atmospheric air as their working fluid; on the other hand, the temperature of the working fluid which is supplied with the heat is lower in a rocket engine. Moreover, in the initial section, the working fluid of the rocket engine is a liquid, on whose evaporation the temperature remains almost the same. Both these facts make the thermodynamic conditions for regeneration more favorable in the thermal cycle of the rocket engine than in the cycles of atmospheric engines, where the regenerative heat exchange is usually preceded by compression and, consequently, by a temperature rise in that part of the gas which is to be supplied with heat in the regenerator.

The appearance of regeneration in a rocket engine under ordinary operating conditions is favored by still another circumstance. As a rule, the wall of the rocket-engine chamber is cooled by the propellant, which then enters the chamber. Consequently, the heat transferred to the cooling jacket is again returned to the chamber, which process represents a typical case of regeneration of heat losses.

1. Regenerative Cooling

Let us consider first the question of the effect of heat regeneration in the cooling jacket on the parameters of a rocket engine at p = c. We shall make the following assumptions:

1) The gas part of the cycle is performed by an ideal gas;
2) There are no heat losses in the chamber except for the cooling losses;
3) In the initial state, the working fluid is a liquid of zero enthalpy;
4) The relative quantity of heat transferred to the chamber walls is the same for external cooling and regenerative cooling.

Let us compare the indices of the cycles obtained in the following three versions:

1) Ideal cycle without cooling;
2) Cycle with chamber cooling by external cooling agent (external cooling);
3) Cycle with regenerative cooling.

We shall consider that the "chamber" consists of a forward section near which the heat is transferred at constant pressure, and a nozzle in which the gas expands. The dimensions of the throat and exit sections are such that, in all cases, the pressure in the forward section and the expansion ratio of the gases in the nozzle are the same.

The formulas for determining gas temperature, efficiency, and thrust in an adiabatic engine are given in the second column in Table 18.

Cooling in the forward section leads to a decrease in the gas temperature at

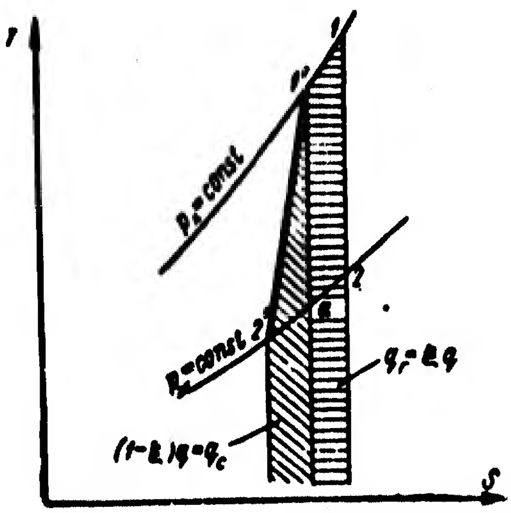

Fig.137 - T-S Diagram of Cycle with External Cooling

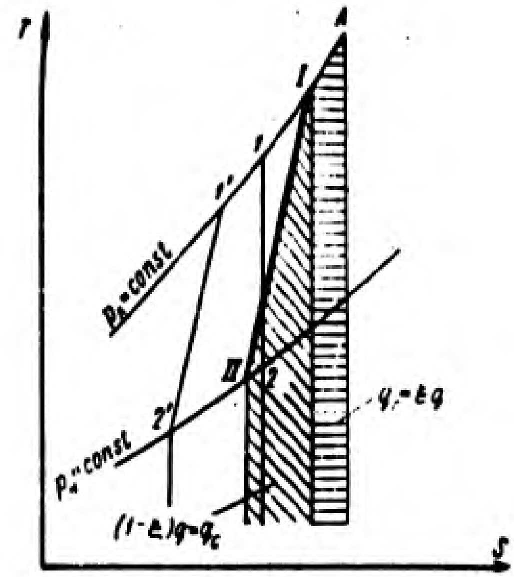

Fig.138 - T-S Diagram of Cycle with Regenerative Cooling (the Magnitude of the Heat Exchange is Indicated in Fractions of I_1)

the beginning of expansion. We shall consider that the expansion with cooling proceeds polytropically; the polytropic exponent n is constant.

Figure 137 is a T-S diagram of the process of expansion in a chamber with external cooling. In the ideal case, the adiabatic 1-2 is the line of expansion. In the presence of cooling, the heat Q_h passes into the walls of the chamber, and the heat Q_c into the walls of the nozzle.

We shall assume below that, of the total heat losses Q_{co}, the quantity passing into the walls of the chamber is

$$Q_r = \xi Q \,, \tag{268}$$

where ξ is the heat-loss separation factor.

We shall evaluate the total heat loss in the walls in the fractions Q_{co} of the

Table 18

Comparison of Performance Characteristics of Cooled and Regenerative Engines

Quantity to be Determined	Adiabatic Chamber	Heat-Conducting Forward Section and Nozzle	
		External Cooling	Regenerative Cooling
Engine efficiency	$\eta_{ad} = 1 - \frac{1}{\delta^{a}}$	$\eta_{ce} = \frac{n}{n-1}\cdot\frac{k-1}{k}\times\left(1-\frac{1}{\delta^{a_n}}\right)\left(1-\xi q\right)$	$\eta_R = \frac{\eta_{ce}}{1-q} = \frac{a}{a_n}\left[1-\frac{1}{\delta^{a_n}}\right]\frac{1-\xi q}{1-q}$
Relative efficiency	1,0	$\eta_0 = \eta_{pol}(1-\xi q) = \frac{n}{n-1}\cdot\frac{k-1}{k}\times\left(1-\xi q\right)\frac{1-\frac{1}{\delta^{a_n}}}{1-\frac{1}{\delta^{a}}}$	$\eta_0 = \frac{a\,(1-\xi q)}{a_n\;1-q}\cdot\frac{1-\frac{1}{\delta^{a_n}}}{1-\frac{1}{\delta^{a}}}$
Specific work	$L_{ad} = \frac{W_{ad}^2}{2g}$	$L_{ce} = \frac{W_{ad}^2}{2g}\eta_0$	$L_R = \frac{W_{ad}^2}{2g}\eta_{pol}\frac{1-\xi q}{1-q} = \frac{W_{ad}^2}{2g}\eta_0$
Initial temperature	T_1	$T_1' = (1-\xi q)T_1$	$T_1 = T_1\frac{1-\xi q}{1-q} = \frac{T_1'}{1-q}$
Final temperature	$T_2 = \frac{T_1}{\delta^{a}}$	$T_2' = (1-\xi q)\frac{T_1}{\delta^{a_n}}$	$T_{11} = \frac{T_2'}{1-q} = \frac{1-\xi q}{1-q}\cdot\frac{T_1}{\delta^{a_n}}$
Specific thrust	$P_{sp} = \frac{W_{ad}}{g}$	$P_{ce} = \frac{W_{ad}}{g}\sqrt{\eta_{pol}(1-\xi q)}$	$P_R = P_{ce}\sqrt{\frac{1}{1-q}} = \frac{W_{ad}}{g}\sqrt{\eta_{pol}\frac{1-\xi q}{1-q}}$

(Cont'd)

Table 18 (Cont'd)

Adiabatic Forward Section and Heat-Conducting Nozzle		Heat-Conducting Forward Section and Adiabatic Nozzle	
External Cooling	Regenerative Cooling	External Cooling	Regenerative Cooling
$\eta_{co} = \frac{n}{n-1}\cdot\frac{k-1}{k}\times\left(1-\frac{1}{\delta^{a_n}}\right)$	$\eta_R = \frac{\eta_{ox}}{1-q}$	$\eta_{co} = (1-q)\times\left(1-\frac{1}{\delta^a}\right)$	$\eta_R = \eta_{ad} = 1-\frac{1}{\delta^a}$
$\eta_o = \frac{n}{n-1}\cdot\frac{k-1}{k}\times(1-q)\frac{1-\frac{1}{\delta^{a_n}}}{1-\frac{1}{\delta^a}}$	$\eta_o = \frac{n}{n-1}\cdot\frac{k-1}{k}\times\frac{\left(1-\frac{1}{\delta^{a_n}}\right)}{\left(1-\frac{1}{\delta^a}\right)}\cdot\frac{1}{(1-q)}$	$\eta_o = 1-q$	$\eta_o = 1{,}0$
$L_{co} = \frac{W_{ad}^2}{2g}\eta_o$	$L_R = \frac{W_{ad}^2}{2g}\eta_o = \frac{L_{co}}{1-q}$	$L_{co} = L_{ad}(1-q)$	$L_R = L_{ad}$
$T_1' = T_1$	$T_1 = \frac{T_1}{1-q}$	$T_1' = T_1(1-q)$	$T_1 = T_1$
$T_2' = \frac{T_1}{\delta^{a_n}} = T_2\delta^{a-a_n}$	$T_{II} = \frac{T_2'}{1-q} = \frac{T_2}{1-q}\delta^{a-a_n}$	$T_2' = T_2(1-q)$	$T_{II} = T_2$
$P_{co} = \frac{W_{ad}}{g}\sqrt{\eta_{pol}\,1-q}$	$P_R = P_{co}\sqrt{\frac{1}{1-q}} = \frac{W_{ad}}{g}\sqrt{\eta_{pol}}$	$P_{co} = \frac{W_{ad}}{g}\sqrt{1-q}$	$P_R = P_{ad}$

initial enthalpy of the gas. If Q_{co} is the absolute value of the losses, then

$$Q_{co}=q_{co}I_1=q_{co}C_pT_1. \tag{269}$$

At equal heat loss, the work in the cycle with cooling is less than the available work L_{ad}. The ratio of the work in a chamber with cooling, i.e., of the polytropic work $L_n = L_{co}$ to the available adiabatic work will be termed the relative efficiency η_o:

$$\eta_o=\frac{L_{co}}{L_{ad}}=\frac{L_{co}}{L'_{ad}}\frac{L'_{ad}}{L_{ad}}.$$

The ratio of polytropic work to adiabatic work L'_{ad} at equal initial temperatures of expansion will be termed the polytropic efficiency η_{pol}. Consequently,

$$\eta_{pol}=\frac{L_{co}}{L'_{ad}}=\frac{\frac{n}{n-1}\left(1-\frac{1}{\delta^{a_n}}\right)}{\frac{k}{k-1}\left(1-\frac{1}{\delta^{a}}\right)}=\frac{a\left(1-\frac{1}{\delta^{a_n}}\right)}{a_n\left(1-\frac{1}{\delta^{a}}\right)}, \tag{270}$$

where

$$a=\frac{k-1}{k} \text{ and } a_n=\frac{n-1}{n}.$$

However, the efficiency of the cycle with cooling is

$$\eta_{co}=\eta_{ad}\eta_o=\eta_{ad}\frac{L_{co}}{L'_{ad}}\cdot\frac{L'_{ad}}{L_{ad}}$$

and

$$\frac{L'_{ad}}{L_{ad}}=\frac{C_pT'_1}{C_pT_1}=\frac{I_1-\xi q_{co}I_1}{I_1}=1-\xi q_{co}.$$

Consequently,

$$\eta_{co}=\eta_{ad}\eta_o=\eta_{ad}\eta_{pol}(1-\xi q_{co})=$$
$$=\frac{a}{a_n}\left(1-\frac{1}{\delta^{a_n}}\right)(1-\xi q_{co}).$$

The third column in Table 18 gives formulas by which the indices of the externally cooled chamber are determined.

Figure 138 compares the lines of expansion for several chambers, including the regenerative chamber. The beginning of expansion in the adiabatic chamber corresponds to the point 1. The regeneration of the heat by the cooling jacket of the nozzle would add the quantity Q_c to the enthalpy I_1. On the diagram, we have $Q_c = I_1 - I_1$ which corresponds to the area under the polytropic curve 1-II or under the segment 1-I of the line p_K = const. Before arrival in the chamber, the working fluid also receives the heat Q_h in the jacket of the chamber. Consequently, the total enthalpy of the working fluid on its entry into the chamber is $I_A = I_1 + Q_c + Q_h$.

On passage through the chamber, the gas gives up the heat Q_h to the walls, and its state upstream of the nozzle corresponds to the point I. After expansion, the gas changes to the state II.

Since the area under the segments 1-I and I-II are the same and the point II lies to the left of the point 2, corresponding to the end of expansion in the adiabatic chamber, then the temperature of the exhaust gases in the regenerative chamber is lower than that in the adiabatic chamber, although the initial temperature in it is higher.

The values of the losses are now determined with respect to I_A:

$$q_{co} = \frac{Q_{co}}{C_p T_A}; \quad q_h = \xi q_{co}; \quad q_c = (1-\xi)\, q_{co}.$$

We determine the temperature ratio in the adiabatic and regenerative chambers:

$$\frac{T_1}{T_A} = 1 - \xi q_{co} \text{ and } \frac{T_1}{T_A} = 1 - q_{co}.$$

Consequently,

$$\frac{T_1}{T_1} = \frac{1-\xi q_{co}}{1-q_{co}}.$$

With external cooling,

$$\frac{T_1}{T_1'} = \frac{1}{1-\xi q_{co}}.$$

Comparing the latter equation with the preceding one, we obtain the ratio of the initial temperatures in the regenerative and simple cycles of the chamber with cooling:

$$\frac{T_1}{T_1'} = \frac{1}{1 - q_{co}}.$$

The efficiency of the regenerative chamber with respect to the initial enthalpy I_A is determined as η_{co}. Actually, however, not I_A but I_1 cal are consumed to obtain the work L_{co}, i.e., less by a factor of $(1 - q_{co})$. For this reason,

$$\eta_R = \frac{\eta_{co}}{1 - q_{co}}.$$

The specific work is directly proportional to the ratio of the efficiencies, so that

$$\frac{L_R}{L_{co}} = \frac{\eta_R}{\eta_{co}} = \frac{1}{1 - q_{co}}$$

and

$$L_R = \frac{W_{ad}^2}{2g} \eta_{pol} \cdot \frac{1 - \xi q_{co}}{1 - q_{co}}.$$

We obtain the following formula for the specific thrust:

$$\frac{P_{R_{sp}}}{P_{co.sp}} = \sqrt{\frac{1}{1 - q_{co}}}$$

and

$$P_{R_{sp}} = \frac{W_{ad}}{g} \sqrt{\eta_{pol}} \sqrt{\frac{1 - \xi q_{co}}{1 - q_{co}}}.$$

The regeneration of heat in the cooling jackets of the chamber and nozzle gives different results. Thus, for the cooled chamber and adiabatic nozzle, we have $\xi = 1.0$ and $n = k$. Under these conditions, $\eta_R = \eta_{ad}$. The heat transferred to the walls of the chamber is compensated by its return to the chamber together with the working fluid.

Consequently, the regeneration of the heat given up to the walls of the chamber is useful work and increases the efficiency of the cycle, the specific work, and the specific thrust of the cooled chamber to a level corresponding to the ideal case.

Taking $\zeta = 0$, we next calculate the version of an adiabatic forward section and a cooled nozzle. In this case,

$$\eta_R = \frac{a}{a_n}\left(1 - \frac{1}{\delta^{a_n}}\right)\frac{1}{1 - q_{co}}.$$

The regeneration of the heat passing into the nozzle walls leads to a cycle more economical than the adiabatic cycle. This is indicated primarily by the temperature drop of the gases in the exit section of the nozzle. The formulas to determine the quantities characterizing the chamber operation are given in Table 18, for the general case and for the special versions of an adiabatic chamber and an adiabatic nozzle.

Owing to the small quantity of heat passing into the nozzle walls, the increase in thrust is slight. On transition from the cooled chamber to the regenerative chamber, the change in efficiency and thrust is more substantial. In this case,

$$\frac{\eta_R}{\eta_{co}} = \frac{1}{1 - q_{co}} \text{ and } \frac{P_{R\,sp}}{P_{co.\,sp}} = \sqrt{\frac{1}{1 - q_{co}}}.$$

This means that, with such a heat exchange at $q_c = 0.02$, the efficiency of the chamber increases by 2% after the change-over to regenerative cooling by 2%, and the thrust increases by 1%. These quantities are entirely comparable with those obtained (for example) when allowing for friction losses or for a nonparallel efflux of the gases from the nozzle.

The value of the regenerative heat exchange increases with decreasing size of the chamber and with increasing ratio of its length to its diameter, when relatively more heat is transferred into the cooling jacket.

At $q_c = 0.1$, the value of $\frac{\eta_R}{\eta_{co}}$ is already 1.11, and the thrust is increased by 5.5%.

Figure 139 shows the mode of variation of the other indices of the cycle with varying q_c; in particular, the diagram gives the polytropic exponent of the expansion line, which depends on q_c and on the expansion ratio δ_c.

If, on cooling of the nozzle alone, we have $q_c = 0.1$, then the efficiency of the chamber is 4.6% greater than η_{ad}, and the thrust is 2.4% greater than the thrust of the adiabatic chamber.

To calculate the thrust and efficiency, empirical relations simpler than those

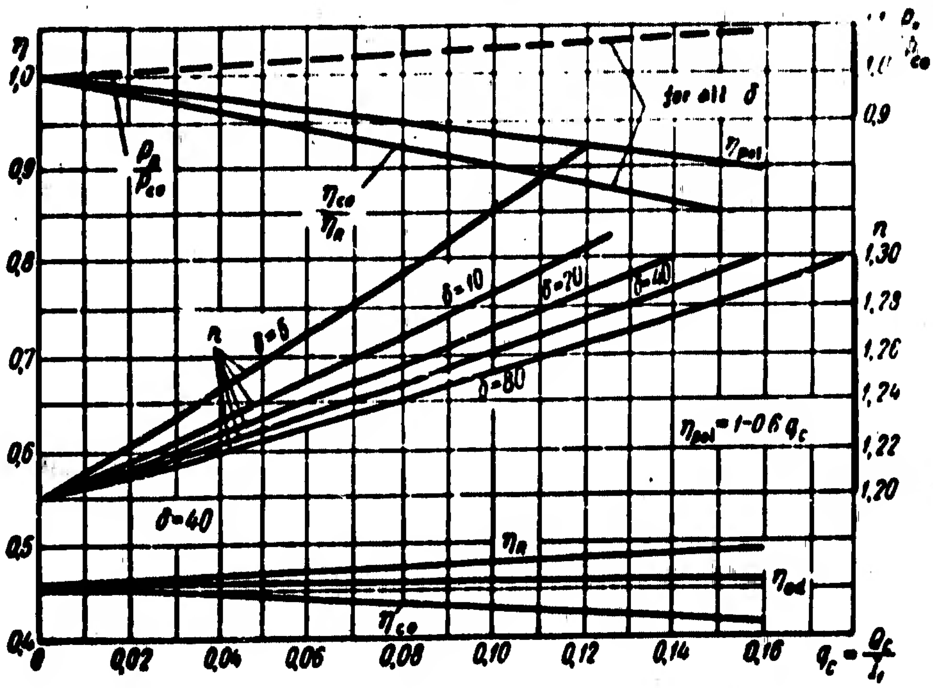

Fig.139 - Effect of Heat Regeneration in the Cooling Jacket of the Nozzle on the Engine Performance

given in Table 18 may be used. Thus, at $\delta_c = 5 - 80$, and a value of k not very different from 1.2, the following relations are valid:

$$\eta_{pol} = 1 - 0,6q_c; \tag{271}$$

$$\frac{P_R}{P_{ad}} = \sqrt{\frac{1-0,6q_c}{1-q_c}}; \tag{272}$$

$$n = \frac{k(1-0,6q_c)}{1-q_c(b+0,6)}, \tag{273}$$

where

$$b = \frac{k-1}{\eta_{ad}}.$$

The heat balance of an engine with regenerative cooling is shown in Fig.140.

The work ΔL, in addition to $\frac{w_{a1}^2}{2g}$, is obtained on utilizing Q_c, which leads to a certain increase in the initial expansion temperature and to a decrease in the final expansion temperature, by comparison with the ideal case. An increase in the expansion ratio reduces the advantages of regeneration.

On the whole, at the quantities of heat removed from the cooling jackets of modern liquid rocket engine, the advantages of regeneration are very slight. Nevertheless, in designing an engine or conducting an experimental study of its heat balance, when individual losses of 1 - 3% of the available heat are often determined, it is necessary to take account of the regenerative exchanges.

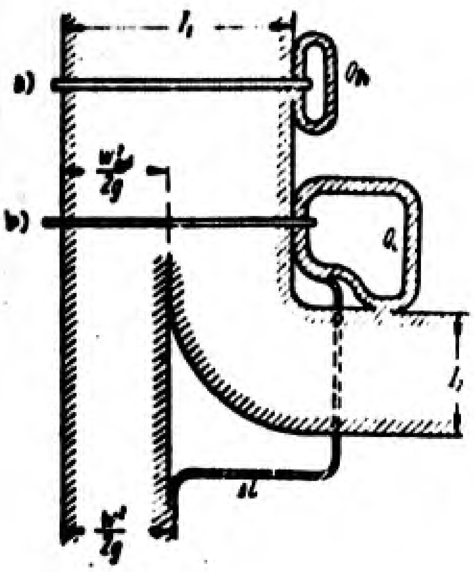

Fig.140 - Heat Balance of Rocket Engine with Regenerative Cooling

a) Forward section; b) Nozzle

In designing the regenerative cycle, an attempt must be made to diminish the heat losses on transfer to the chamber jacket, and to increase the heat exchange through the nozzle walls. From the thermodynamic point of view, it is preferable to facilitate heat transfer to the walls of the exit section of the nozzle, since in this case the heat is removed from the less valuable portions of the expanded gas.

There are two serious obstacles to the utilization of regeneration in liquid rocket engines. First, the cooling power of the propellant used is low, and second, the methods of increasing the quantity of heat tapped from the surfaces of the regenerator lead to increased friction losses in its passages, and to a corresponding loss of thrust.

We shall now evaluate the cooling power of the propellant β_{co} on the basis of the ratio of the maximum allowable quantity of heat that can be removed by the propellant in the cooling jacket to the heat value of the fuel.

On the whole, regenerative cooling of liquid rocket engine chambers is accompanied by favorable side processes in the engine system, resulting in increased economy.

It may be noted that the increase in economy is promoted by phenomena which favor the increase in heat exchange with the nozzle walls: greater nozzle-wall surface area as compared to nozzle volume, longer residence time of the gas in the nozzle, and increase in the coefficient of heat consumption on the outer and inner wall surfaces.

At the intense cooling in modern liquid rocket engines, regenerative cooling produces no appreciable changes in engine economy and gas temperature ahead of the nozzle.

2. External Regeneration

Regeneration of the heat of the gas after its expansion in the nozzle will be termed "external regeneration".

The regenerator is located beyond the nozzle, and adjoins it as shown in Fig.141.

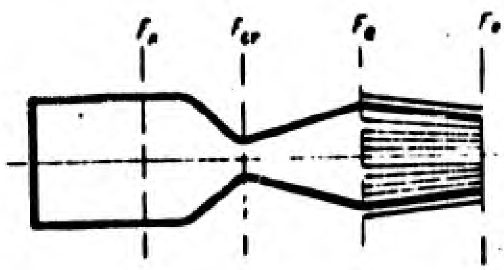

Fig.141 - Schematic Diagram of Position of Regenerator in External Regeneration

Figure 142 is a T-S diagram of the cycle of a liquid rocket engine with external regeneration. After expansion 1-2, the gas enters the regenerator in the state corresponding to point 2. The heat available for regeneration is measured by the enthalpy I_2. The extent of heat exchange depends on the size of the heat-transfer surfaces of the regenerator. For an ideal engine, the heat of regeneration is $Q_R = I_3$. We shall term the ratio

$$q_R = \frac{Q_R}{I_2} = \frac{I_3}{I_2}$$

the regeneration ratio in the cycle.

At the same initial state of the gas in the conventional and regenerative cycles, the specific work will be the same. The thermodynamic efficiency will be different, since the consumption of heat in the regenerative cycle will be measured by the quantity $I_1 - I_3$ instead of by I_1. Consequently,

$$\eta_R = \eta_{ad}\frac{I_1}{I_1 - I_3} = \eta_{ad}\frac{T_1}{T_1 - T_3} = \frac{\delta_c^a}{\delta_c^a - q_R}\eta_{ad}.$$

Finally,

$$\eta_R = \frac{\delta_c^a - 1}{\delta_c^a - q_R}. \qquad (274)$$

The value of the specific thrust remains as before, just like the specific fuel consumption. The quantity of heat consumed per unit thrust decreases in inverse

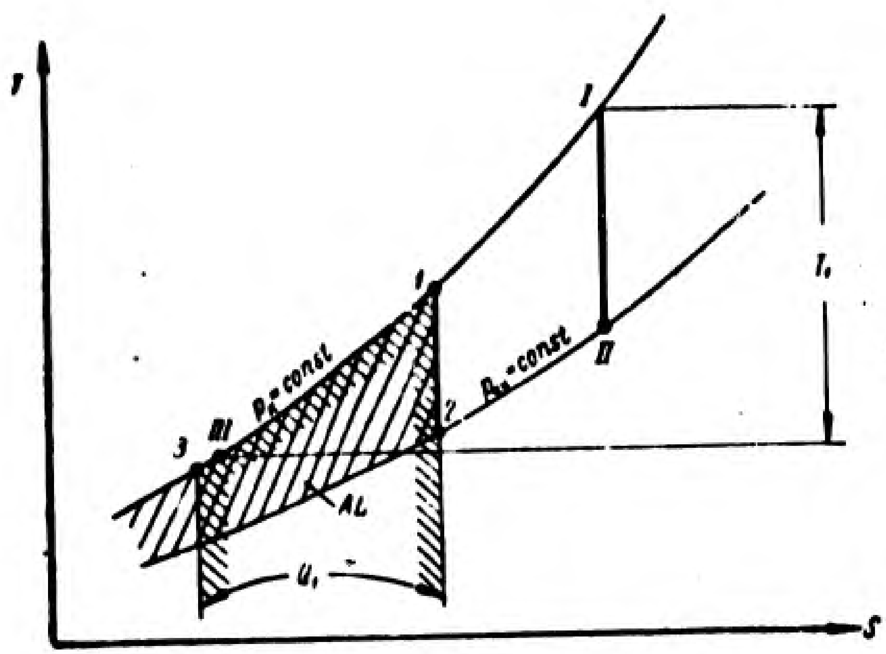

Fig.142 - T-S Diagram of Regenerative Cycle of a Rocket Engine

proportion to the efficiency. The extreme value of q_R is unity in the case of $I_3 = I_2$.

If the quantity of heat supplied to the working fluid is always the same, and is determined, for example, by its heat value, then regeneration will change not only the efficiency but also the specific thrust.

Figure 142 represents the normal adiabatic cycle by a diagram with the expansion line 1-2. The heat value is numerically equal to $I_1 = C_pT_1$. The addition of the regenerator leads to an "acceleration" of the cycle: The initial temperature of expansion begins to rise, and the useful work and thrust increase.

The parameters of a cycle are established when the heat liberation in the chamber and the subsequent expansion lead to a temperature of the exhaust gases such that the prescribed regeneration ratio q_R is obtained. In Fig.142 the expansion I-II corresponds to the regenerative cycle.

Here,

$$I_1 - I_{III} = I_1 - q_R I_{II} = I_1$$

and

$$T_1 - q_R T_{II} = T_1\left(1 - \frac{q_R}{\delta_c^e}\right) = T_1,$$

Hence,

$$\frac{T_1}{T_1} = \frac{\delta_c^e}{\delta_c^e - q_R}.$$

The maximum temperature increases as we pass to the regenerative cycle; this temperature rise will be greater, the lower the efficiency of the initial adiabatic cycle. Since the value of δ_c in the cycles being compared is the same, the work and efficiency increase proportionally to the rise in temperature:

$$\frac{\eta_R}{\eta_{ad}} = \frac{L_R}{L_{ad}} = \frac{T_1}{T_1} = \frac{\delta_c^e}{\delta_c^e - q_R}. \qquad (275)$$

For the thrust:

$$\frac{P_R}{P_{ad}} = \sqrt{\frac{L_R}{L_{ad}}} = \sqrt{\frac{T_1}{T_1}} = \sqrt{\frac{\delta_c^e}{\delta_c^e - q_R}}. \qquad (276)$$

Figure 143 shows the change in η_R and in the ratio $\frac{\eta_R}{\eta_{ad}}$ at various values of δ_c and q_R. The efficiency ratio also represents the ratio of the maximum temperatures in the compared cycles. The resultant temperature rise is greater, the greater will be the value of q_R and the smaller the value of δ_c.

If T_1 is assigned as the maximum permissible temperature, then T_1 may be determined and, from this value, the required heat value of the propellant. Thus, at $T_1 = 3200°K$ in the regenerative cycle, we get $T_1 = 2430°K$ if $\delta_c = 80$ and $q_R = 0.5$.

Consequently, in the regenerative cycle, the ordinary value of specific thrust can be obtained by using a propellant with a considerably lower heat value.

Since the cooling agent in the jacket of the chamber must be the propellant

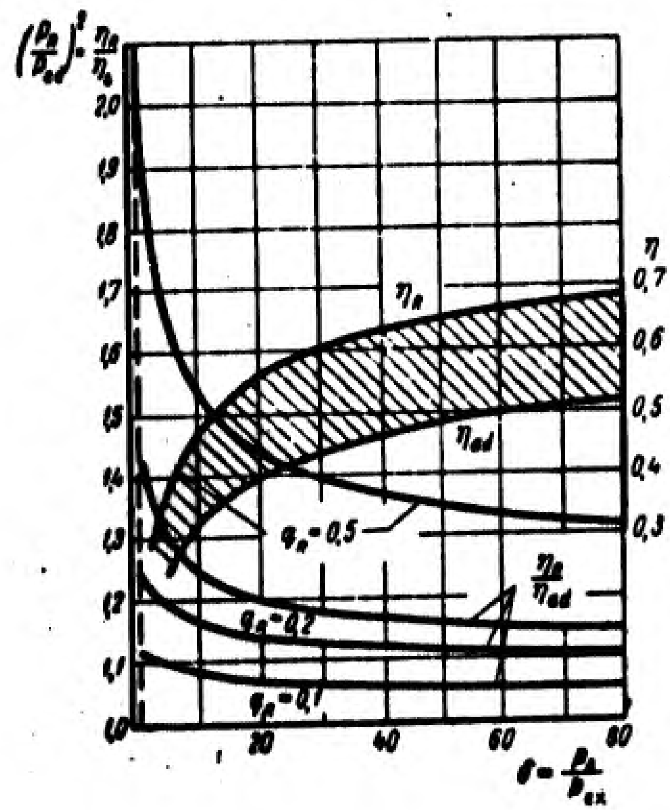

Fig.143 - Effect of Expansion Ratio δ_c on the Efficiency of the Regenerative Cycle of a Liquid Rocket Engine, at Various Values of q_R

itself, this means that the increase in P_{sp} depends on the cooling power of the propellant, or on its cold capacity.

By definition, already given, the cold capacity of a propellant is

$$\beta_{co} = \frac{Q_{co}}{H_u}.$$

For the individual propellant components, we have

$$\beta_{co.o} = \frac{Q_{co.o}}{H_u} \text{ and } \beta_{co.h} = \frac{Q}{H_u}$$

and for the propellant as a whole,

$$\beta = \beta_{.o} + \beta_{.f} = \frac{Q_{.o} + Q_{co.f}}{H_u}.$$

Denoting the weight ratio of the propellant components by the symbol $x = \frac{G_o}{G_f}$, where G_o and G_f denote the weight rate of flow of the fuel and oxidizer respectively, we obtain

$$\beta_{co} = \frac{x}{(1+x)H_u} Q_{co.o} + \frac{1}{(1+x)H_u} Q_{co.f}. \tag{277}$$

The values of $Q_{co.o}$ and $Q_{co.f}$ are determined for the physical data of the components under operating conditions. Thus, for 96% HNO_3, at p = 20 - 40 atm and heating to 180 - 240°C, if the temperature before heating is 20°C, we get $Q_{co.o}$ = = 80 - 110 kcal/kg. Table 19 gives the values of the maximum cooling power for three types of propellant.

Table 19

Values of Maximum Cooling Power for Three Forms of Propellant

Propellant	$x = \frac{G_o}{G_f}$	$\beta_{co\,max}$, %	Remarks
Oxygen and 70% ethyl alcohol	1,217	7,5	without using oxygen
Nitric acid and kerosene	5,38	7,5	without evaporation
Nitric acid and 96% ethyl alcohol	2,34	12 15	" " with evaporation

Let us assume the chamber and nozzle to be adiabatic. Assume further that the heat is removed from the gas aft of the exit section of the nozzle in an external regenerator. This corresponds to the most favorable case of regeneration. Table 20 shows the changes in maximum temperature, economy, and thrust augmentation for these three types of propellant under the conditions of external regeneration. If the cooling power of the propellant is fully utilized in the chamber and nozzle duct, the gain in thrust and economy are about half as great.

Table 20

Change in Maximum Temperature, Economy, and Thrust Gain for Three Types of Propellant under Conditions of External Regeneration

Quantity	Oxygen and 70% Ethanol	Nitric Acid and Kerosene, with Evaporation	Nitric and 96% Ethanol without Evaporation and with Evaporation
$\frac{T_1}{T_1} = \frac{\eta_R}{\eta_{ad}}$	1,075	1,11	1,12—1,15
$\frac{P_R - P_{ad}}{P_{ad}}$, %	3,8	3.5	6,0—7,3

The inadequate cooling power of the propellant may be compensated by using an inert medium for cooling purposes. It should be borne in mind, however, that the gain in economy and thrust is lessened by the additional complication of the plant, by the increase in its weight and, what is highly important, by the increased resistance to the gas flow in the nozzle.

Without considering here the methods of calculating heat transfer and gas resistance in the regenerator, we shall present the results of a determination of thrust and economy, allowing for friction.

Figure 144 shows the heat characteristic of the flow section of a chamber with regenerative cooling, consisting of a nozzle with developed cooling surfaces and an external regenerator. The relative distances $\bar{l}$ traveled by the gas, from its entrance into the nozzle to its emergence from the exit section of the external regenerator, are plotted on the abscissa. The value of $\bar{l}$ is measured along the generatrix of the chamber and nozzle walls. On the ordinate the following quantities are plotted:

q_W, kcal/m^2 hr: specific heat flux from the gas to the coolant;

τ_W, kg/m^2: frictional stress;

q_τ, kcal/m^2 hr: thermal equivalent of the specific work of friction;

$q_W - q_\tau$ kcal/m^2 hr: specific quantity of heat related to unit surface of the duct walls, lost by the gas on expansion in the flow section;

$\frac{Q_{co}}{I_0} = q_{co}$, %: relative quantity of heat passing into the cooling medium of the regenerative duct.

Figure 144 indicated that the heat load due to friction is a quantity of the same order as the heat-transfer load; in the exit section of the nozzle and in the external regenerator the former is greater than the heat-exchange load. In the section where flow is supersonic, the work of friction is so great that utilization of the external regeneration becomes doubtful. Table 21 gives a comparison of the adiabatic original chamber with the regenerative chamber. For the original chamber,

Table 21

Example of Changes in Engine Parameters with Use of Regeneration

Version	q_{co}, %	q_τ, %	W, m/sec	P_{sp}	$\frac{P_{sp}}{P_{sp1}}$	$\frac{\eta_{ad}}{\eta_R}$
Without regeneration, original chamber; r_{cr} = 40 mm	0,00	0,0	1975	201,2	1,0	1,0
Nozzle regeneration, r_{cr} = 4 mm	20,52	10,7	2245	229,0	1,147	0,605
Nozzle and external regeneration; r_{cr} = 4 mm	28,20	21,5	1905	194,4	0,964	0,560
Nozzle regeneration; r_{cr} = 5 mm (nozzle with elongated throat)	23,00	10,4	2140	218,0	1,085	0,604

we have taken G = 8.8 kg/sec, p_K = 22 kg/cm^2, T_K = 3000°K, R = 30 kg-m/kg deg, k = 1.3, radius of critical section r_{cr} = 10 mm. For the regenerative chamber, at

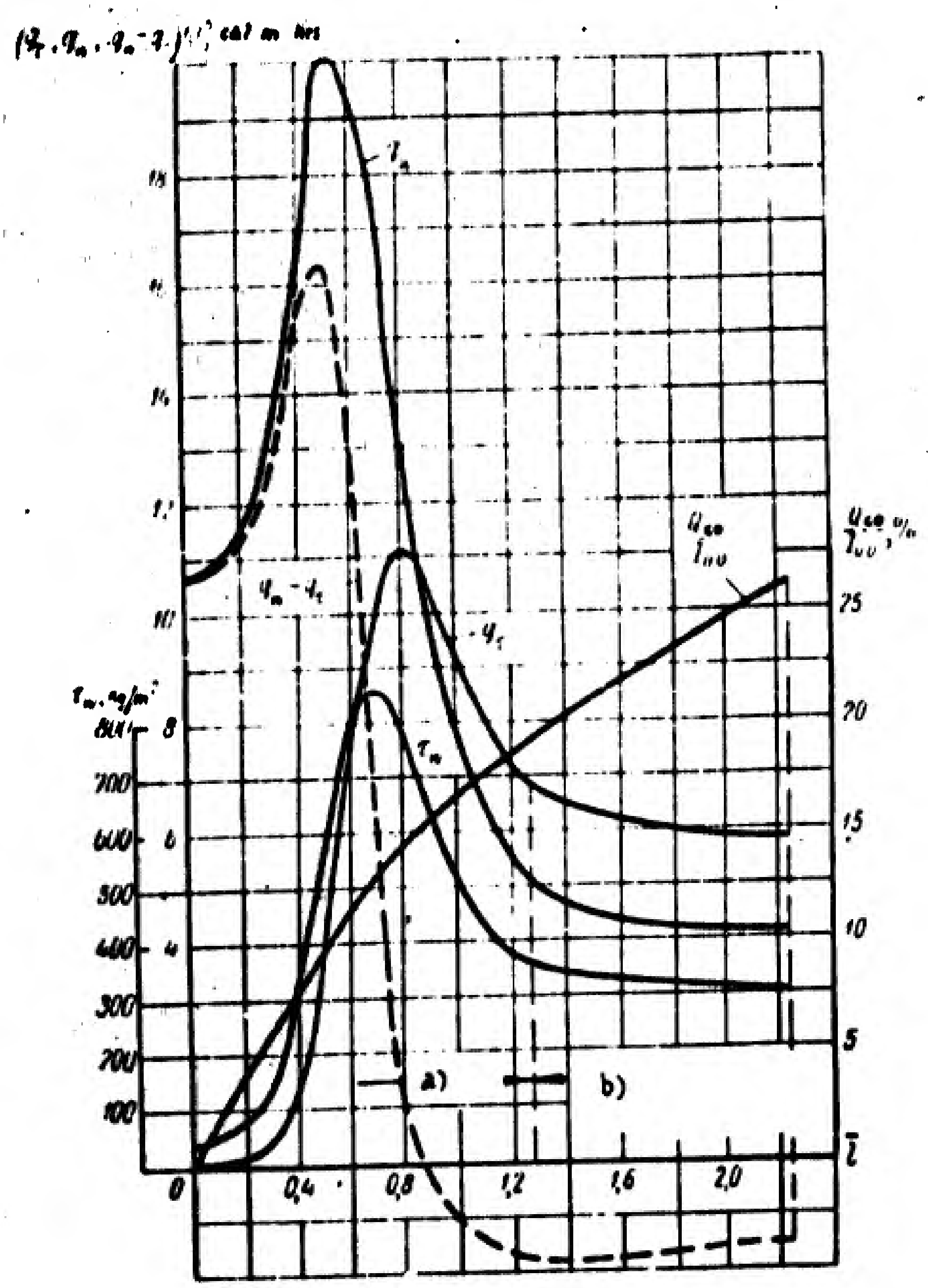

Fig.144 - Thermal Characteristic of Nozzle with Friction and Cooling at External and Nozzle Regeneration

a) Nozzle; b) External regeneration

the same flow rate and the same initial gas parameters, we have 100 nozzles with r_{cr} = 4.0 mm, and 64 nozzles with r_{cr} = 5 mm. The heat is removed from the regenerator by water, which is then introduced into the chamber together with the propellant components.

The second column in Table 21 gives the quantities of heat transferred to the regenerator walls, in percent of the available enthalpy I_0 of the gas before expansion. The third column gives the work of friction in the same units. Nozzle regeneration leads to an increase of 14.7% in specific thrust, while complete regeneration produces a decrease of 3.4%. The thermodynamic efficiency in both cases is increased; the specific fuel consumption, expressed in calories, decreases respectively to 60.5% and 56%.

The specific consumption of the working fluid - in this case the propellant and the water which cools the regenerator walls - varies with the specific thrust.

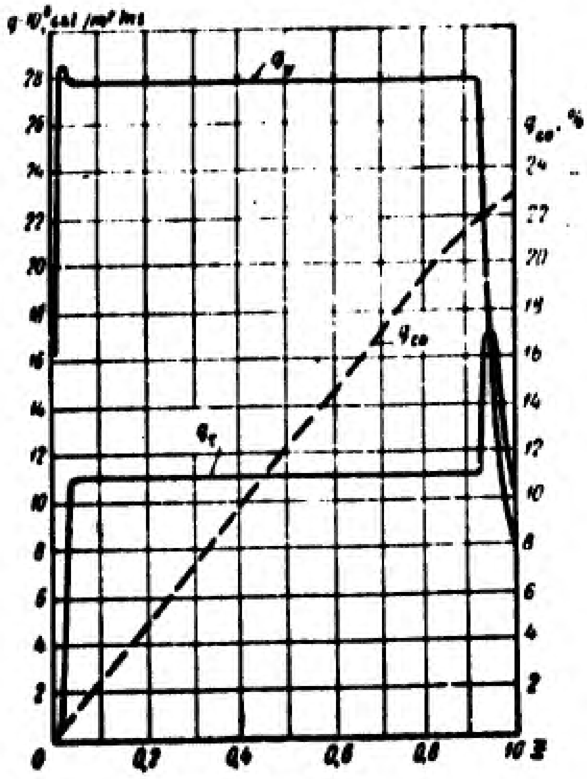

Fig.145 - Heat Characteristic of Nozzle with Friction, when Using Nozzle Regeneration

In special cases, nozzle regeneration may be advantageous; for example, when a rocket moves under water, the energy used in trapping the coolant is slight. The tanks need only carry the propellant, so that the radius of action of the missile increases sharply.

If it is necessary to economize on an especially high-price propellant or on one with a particularly high heat value, nozzle regeneration will help to attain this object. To prevent supersonic velocities from developing in the regenerator, it is possible to restrict the regeneration to the subsonic section of the nozzle; in this case, the surfaces for heat transfer must be those duct surfaces which correspond to high heat loads minimum gas temperature. Figure 145 shows, as a development of the preceding example, the variation of q_w and q_T along the relative axial length of the nozzle, for the case of a regenerative nozzle with r_{cr} = 5 mm having the same length as the original nozzle. The throat occupies most of the length. At the end of the throat in the regenerator, 23.0% of the heat has been transferred from the gas to the coolant, calculated from the initial enthalpy ahead of the nozzle. The exhaust velocity is increased 8.5% over its value in the original nozzle, and the specific consumption of the working fluid is decreased accordingly. The specific consumption of heat decreases to 60.4%, i.e., reaches the same value as in the case of nozzle regeneration at r_{cr} = 4 mm.

These examples demonstrate convincingly that regeneration in a liquid fuel rocket engine may be regarded as a method of increasing economy, and should be checked and studied under practical development conditions.